

**Antibody Array for the Detection of Protein
Phosphorylation & Localization and Application to Dissect
Activities of Different Signaling Pathways**

Dissertation

Zur Erlangung des akademischen Grades

doctor rerum naturalium

(Dr. rer. nat.)

Vorgelegt dem Rat der Biologisch-Pharmazeutischen Fakultät

der Friedrich-Schiller-Universität Jena

Von

Lin Wang

from **Jinan** born **March12,1964**

TABLES OF CONTENTS

1	Introduction.....	1
1.1	Antibody Array Technologies.....	1
1.2	Protein Phosphorylation, Localization and Function.....	2
1.3	Interaction Proteomics and Pathway Building.....	3
1.3.1	BMP2 Signalling	4
1.3.2	The Effect of STI 571 on Cell Signalling	9
1.4	Aim	10
2	Materials and Methods.....	11
2.1	Materials.....	11
2.1.1	Cell Lines.....	11
2.1.2	Chemicals.....	11
2.1.3	Antibodies.....	11
2.1.4	Protein-Molecular Weight Marker.....	11
2.1.5	Apparatus.....	11
2.2	Methods.....	12
2.2.1	Cell Culture.....	12
2.2.2	Cell Numbers and Experimental Format.....	12
2.2.3	Cytoplasmic and Nuclear Protein Extracts.....	12
2.2.4	Determination of Protein Concentration.....	13
2.2.5	Ponceau S Staining	13
2.2.6	Western Analysis	14
2.2.7	Immunoprecipitation.....	14
2.2.8	Cy3 and Cy5 Staining in SDS-PAGE.....	14
2.2.9	Cy3and Cy5 Staining of Microscope-Slide-Size Array.....	14
2.2.10	Cy3 and Cy5 Staining of Mini-Arrayslide.....	15
2.2.11	Silver Staining of Mini-Arrayslide.....	15
2.2.12	Silver Staining in Arraytube.....	15
2.2.12.1	Biotinylation of Cellular Proteins.....	15
2.2.12.2	Incubation of Protein Extracts	15
2.2.12.3	Silver Staining.....	16
2.2.13	Statistical Analysis.....	16
3	Results.....	17
3.1	Antibody Array Technologies.....	17
3.1.1	Cy3 and Cy5 of SDS-PAGE, Microscope-Slide-Size Array, Mini-Arrayslide.....	17
3.1.2	Data Analysis	20
3.2	Modulation of Phosphorylation and Localization in BMP2 Treated U937 Cells.....	26
3.2.1	Total p-Tyrosine and p-p38 Increased: Cytoplasm and Nucleus Increasing.....	29
3.2.2	Total p-ERK and p-JNK Increased: Cytoplasm Increasing and Nucleus Unchanged.....	32
3.2.3	Total p-Akt Increased: Cytoplasm Increasing and Nucleus Decreasing....	34
3.2.4	Total p-Smad1, p-Smad2/3 and c- Myc Unchanged: Cytoplasm Decreasing and Nucleus Increasing.....	35

3.2.5 Total p-p70S6 Unchanged: Cytoplasm Increasing and Nucleus Decreasing.....	39
3.3 Modulation of Phosphorylation and Localization In BMP2 Treated MCF7 Cells	40
3.3.1 Total p-JNK, p-Smad1, p-Smad2/3, p-p38 and p38 Unchanged: Cytoplasm Increasing and Nucleus Decreasing.....	
3.3.2 p-Tyrosine, p-STAT3, p-ERK and p-P70S6 Increased: Cytoplasm Increasing and nucleus unchanged	43
3.3.3 Total c-Myc Unchanged: Nucleus Slightly Increasing and Cytoplasm Slightly Decreasing.....	46
3.3.4 Total p-Akt Unchanged: Nucleus and Cytoplasm unchanged.....	47
3.4 Modulation of Phosphorylation and Localization In STI Treated K562 Cells	47
3.4.1 Total p-Akt and p-p70S6 Decreased: Cytoplasm and Nucleus Decreasing.....	47
3.4.2 Total p-p38, p38, c-Myc, p-Tyrosine, p-Smad1 and p-Smad2/3 Increased: Cytoplasm and Nucleus Increasing.....	48
3.4.3 Total p-STAT3 and p-JNK Increased: Cytoplasm Increasing and Nucleus Unchanged.....	48
3.4.4 Total p-ERK Increased: Cytoplasm Decreasing and Nucleus Increasing..	48
4 Discussion.....	52
4.1 Antibody Array Technologies.....	52
4.2 BMP2 Signalling In U937 Cells.....	54
4.2.1 BMP2 activates Akt, ERK and JNK pathway by increase of cytoplasmic phosphorylation in U937 cells.....	54
4.2.2 BMP2 activates Smad1 and Smad2/3 network, p38 network and c-Myc, Tyrosine network by increase of nuclear phosphorylation in U937 cells.....	55
4.2.3 BMP2 inhibits p70S6 signalling by increase of cytoplasmic phosphorylation and decrease of nucleus in U937 cells.....	57
4.2.4 Possible intracellular relationship in BMP2 treated U937 cells.....	57
4.3 BMP2 Signalling In MCF7 Cells.....	58
4.3.1 BMP2 BMP2 activates p70S6 and ERK signaling, Tyrosine and STAT3 network by increase of cytoplasmic phosphorylation in MCF-7 cells.....	58
4.3.2 BMP2 inhibits p38, JNK and smad signalling by increase of cytoplasmic phosphorylation and decrease of nucleus in MCF-7 cells.....	59
4.3.3 BMP2 activates c-Myc signalling by increase of nuclear phosphorylation in MCF-7 cells..	60
4.3.4 Possible Intracellular relationship in BMP2 treated MCF7 cells.....	60
4.4 STI Signalling In K562 Cells.....	60
4.4.1 STI571 inhibits Akt/p70S6 PI3K signalling by decrease of cytoplasmic and nuclear phosphorylation in K562 cells.....	61
4.4.2 STI571 activates p38 MAPK pathway, c-Myc, Tyrosine and Smad1/Smad2/3 networks by increase of cytoplasmic and nuclear phosphorylation in K562 cells	61
4.4.3 STI571 activates pathway by increase of nuclear phosphorylation and decrease of cytoplasm in K562 cells	61

4.4.4 STI571 activates STAT3 network and JNK/MAPK pathway by increase of cytoplasmic phosphorylation in K562 cells	62
4.4.5 Possible Intracellular Relationship in STI treated K562 cells.....	62
4.5 Models of Signalling Protein and Cellular Response	63
5 Summary.....	68
6 Zusammenfassung.....	70
7 References.....	72

Abbreviations

BSA	Bovin Serum Albumin
bp	Base pair
°C	degree centigrade
IP	Immunoprecipitation
Da	Dalton
DNA	Desoxyribonucleic acid
DTT	Dithiotreitol
EDTA	Ethylendiamine tetraacetic acid
h	hour
k	kilo
μ	micro
M	molar
MW	molecular weight
min	minute
Np-40	Nonidet p-40
PAGE	Polyacrylamide gel electrophoresis
PBS	phosphate-buffered saline
RNA	ribonucleic acid
rpm	rounds per minute
RT	room temperature
SDS	sodium dodecylsulfate
sec	second
p-	phosphorylation
nu	nucleus
cyto	cytoplasm
tyr	tyrosine
con	control
PMSF	phenylmethylsulfonyl fluoride

1 Introduction

1.1 Antibody Array Technologies

Protein array applications have wide fields including protein-protein interaction, protein-RNA interaction, protein-DNA interaction, phosphorylation, dephosphorylation, proteolytic cleavage and dimerization, etc.

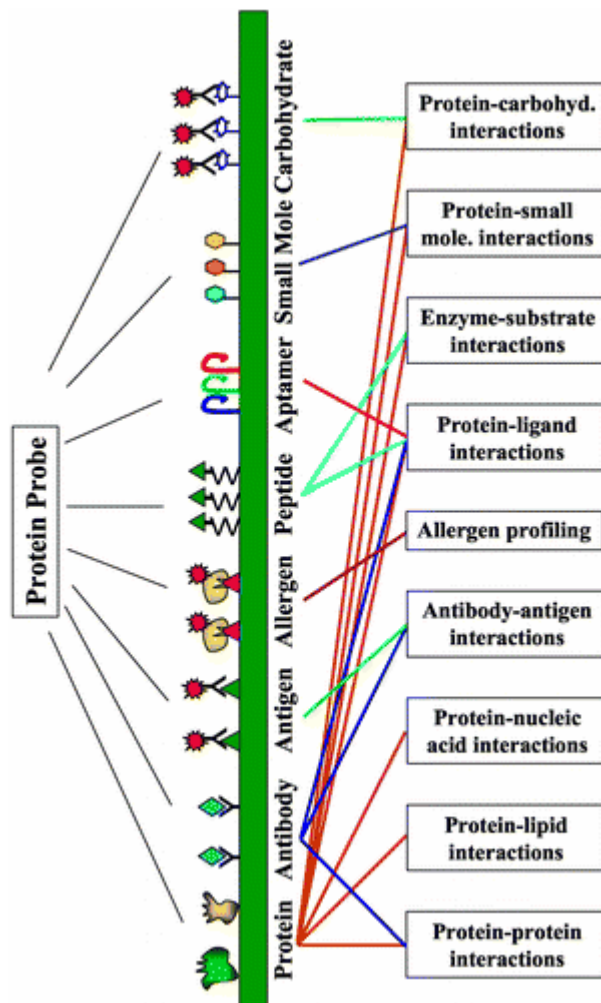


Figure 1.1: Protein microarrays and their applications. Ligands, such as proteins, peptides, antibodies, antigens, allergens, and small molecules, are immobilized in high density on modified surfaces to form functional and analytical protein microarrays. These protein microarrays can also be used for various kinds of biochemical analysis(Zhu et al. 2003).

The number of antibodies, which are specific for proteins and protein modifications, including phosphorylation, is growing at a tremendous speed and it is very likely that good antibodies can be obtained for most proteins and their modifications in the future. To carry out research in a

timely manner it will be required that suitable antibodies combined on micro arrays are used for initial protein expression screening, very similar to the use of gene expression profiling today (Haab et al. 2001; Madoz-Gurpide et al. 2001).

Antibody microarrays hold potential promise for the high-throughput profiling of a smaller number of proteins (Figure 1.1). Briefly, antibodies (or other affinity reagents directed against defined proteins) are spotted onto a surface such as a glass slide; a complex mixture, such as a cell lysate or serum, is passed over the surface to allow the antigens present to bind to their cognate antibodies (or targeted reagents). The bound antigen is detected either by using lysates containing fluorescently tagged or radioactively labelled proteins, or by using a secondary antibodies against each antigen of interest. Low-density antibody arrays have been constructed that measure the levels of several proteins in blood and sera. In high-density arrays constructed recently, Sreekumar et al. spotted 146 distinct antibodies on glass to monitor the changes in quantity of a number of antigens expressed in LoVo colon carcinoma cells (Zhu et al. 2003).

One important issue for antibody array is the matrix or surface used for immobilization. The golden standard in this respect are porous membranes like nitrocellulose or nylon, which are used for a very long time in classical assays and have a very high capacity for protein binding. For application in micro array technology a combination of glass slides and nitrocellulose membranes is commercially available (Schleicher & Schuell) and is used for protein array applications (Knezevic et al. 2001). With a similar idea this group before had developed an activated agarose coating for slides that has a very good binding capacity for antibodies and ensures reliable and highly sensitive detection of protein antigens (Afanassiev et al. 2000). These and other microscope glass slide based technologies require an optimized regime for handling, incubation and washing and a dedicated set up of incubation chambers.

Current methods of detecting protein activity by array require the use of fluorescence and radioisotopes. To date, no protocol for antibody arrays has been setup as standard. Many problems need to be addressed such as storage of antibody, protein purification, incubation and binding to arrays. This work tries to analyse and compare the results under different conditions in details.

This experiment has developed parameters, thresholds, and testing conditions of a novel silver staining system. Antibodies were selected with high specificity for phosphorylated proteins and these antibodies were combined on the micro arrays in the ArrayTube™ platform. Nano-gold particles-mediated silver staining is a suitable technology for the detection of proteomics bound to an antibody array; Quantification is possible using an on-line measurement of the silver precipitation step. The onset of precipitation and the speed of signal accumulation of the silver staining of the process enables quantification whereas end point signals only provide qualitative results; Combination of selective purification, e.g. cytoplasmic extract vs. nuclear extract with the antibody array technology, allows to phosphorylated proteins to defined cellular compartments.

In this study, first setting up the Cy3 and Cy5 staining in SDS-PAGE for the detection of labelling efficiency. Array technologies were developed into four stages from Cy3 and Cy5 staining of Big Glass Arrayslide, Cy3 and Cy5 staining of Mini-Arrayslide, silver staining of Mini-Arrayslide to silver staining of Arraytube including biotinylation of cellular proteins, incubation of protein extracts and silver staining of which has developed parameters, thresholds, and testing conditions of a novel silver staining system for quantitative detection of phosphorylation and localization for function on chip using biotinylation of cellular proteins. Silver staining of antibody microarrays allow for high-throughput identification of protein Phosphorylation. This method is sensitive, specific, reproducible, fast and cheap, presenting obvious advantages and may find wider uses in high-throughput protein screenings, pinciple shown as in Fig. 1.2.

Nano-gold silver Protocol

- . biotin-labeling protein
- . blocking Array-tube
- . hybridization
- . nanogold conjugation
- . enhancer and initiator

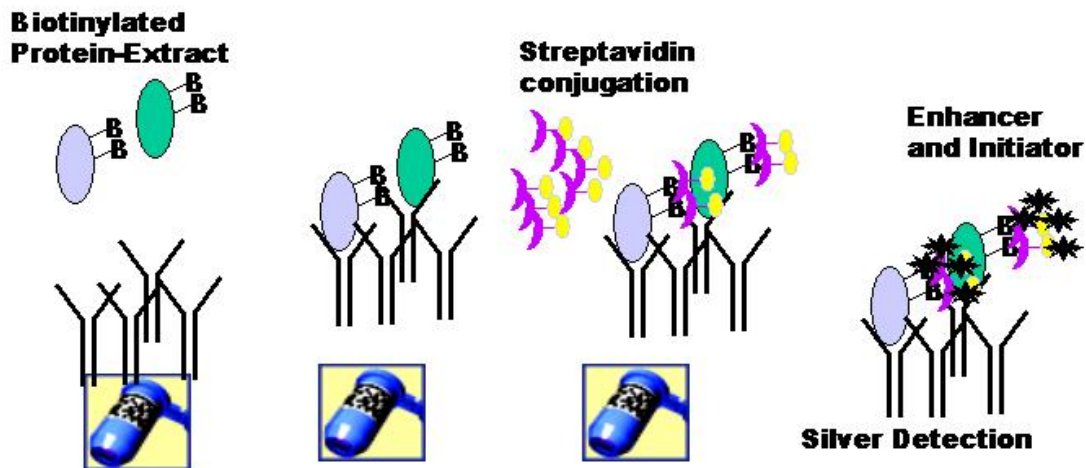


Figure 1.2: Nano-gold silver staining principle, including biotin-labeling protein, blocking Array-tube hybridization, nanogold conjugation, enhancer and initiator.

1.2 Protein Phosphorylation, Localization and Function

With the post-genome era proteomics study for direct analysis of a group of protein become more and more important (James et al. 1997). Identification of the type of modification and its location often provide crucial information for understanding the function or regulation of a given protein in biological pathways(Zhu et al. 2003).

Phosphorylation is one of the most important protein modifications by which many different cellular responses and biological processes are regulated.

Protein localization data provide valuable information in elucidating eukaryotic protein function (Zhu et al. 2003). Protein trafficking between nucleus and cytoplasm fundamentally important to cell regulation. As such, the nuclear import and export are pivotal in orchestrating the activities of the key regulators of the cell cycle (Zhou et al. 2003), such as:

Smad nuclear translocation is a required component of the activin A-induced cell death process in liver cells (Chen et al. 2000).

ERK-1 and -2 nuclear translocation triggers cell proliferation in vitro models from (Tarnawski et al. 1998). ERK activation plays an active role in mediating cisplatin-induced apoptosis of HeLa cells and functions upstream of caspase activation(cyto) to initiate the apoptotic signal(Wang et al. 2000). Lorenzini et al (2002) verified in senescent cells that no ERK are able to phosphorylate efficiently their nuclear targets.

JNK cytoplasmic localization as inhibitor of proliferation from Dickens, et al. (1997) verifying that a murine cytoplasmic protein that binds specifically to JNK [the JNK interacting protein-1 (JIP-1)] and caused cytoplasmic retention of JNK and inhibition of JNK-regulated gene expression.

MKK7-JNK/SAPK and MKK6-p38 pathways to cytoplasmic apoptotic activation induced by Fas (Toyoshima, F. et al. 1997). p38 MAPK induced cytoplasmic domain-dependent cellular migration (differentiation) of alpha 2 integrin subunit (Klekotka et al. 2001).

Phospho-Tyrosine Rak (54 kDa) expressed nuclear and perinuclear regions of the cell in 2 different breast cancer cell lines inhibits growth and causes G(1) arrest of the cell cycle (Meyer et al. 2003).

STAT3 cytoplasmic localization was detected in the pathogenesis of mantle cell lymphoma (MCL) tumours. STAT3 nuclear localization of STAT3 was shown in node-negative breast cancer associated with a better prognosis (differentiation and apoptosis) by tissue microarray analysis (Dolled-Filhart, Camp et al. 2003).

Akt/PKB intranuclear translocation is an important step in signalling pathways that mediate cell proliferation (Borgatti, et al. 2000). No Akt is able to phosphorylate efficiently its nuclear targets in senescent cells (Lorenzini, et al. 2002). p70S6K is localized both in the cytosol and, after cytokine stimulation, also in nucleus in factor-dependent hematopoietic M-07e cells (Fleckenstein et al 2003).

1.3 Interaction Proteomics and Pathway Building

It is widely acknowledged that proteins rarely act as single isolated species when performing their functions in vivo. The analysis of proteins with known functions indicates that proteins involved in the same cellular processes often interact with each other. Following this observation, one valuable approach for elucidating the function of an unknown protein is to identify other proteins with which it interacts, some of which may have known activities. On a large scale, mapping protein-protein interactions has not only provided insight into protein function but facilitated the modeling of functional pathways to elucidate the molecular mechanisms of cellular processes (Zhu, Bilgin et al. 2003)

We are interested to understand some aspects of the regulatory network of signalling pathways and their role in the development of diseases. One of the most prevailing change on the protein level is protein phosphorylation. In many cases it reflects the activation state of the protein. It is controlled by kinase activities leading to phosphorylation and phosphatase activities, which in turn remove the phosphate groups. To understand how a given activation signal growth factor, cytokine, morphogene or drug, activates different signalling pathways. By classical methods, this would require an extremely large number of time consuming experiments. Antibody array potentially allows the identification of all of the proteins that carry those modifications in a single experiment.

1.3.1 BMP2 signalling

BMP2, member of the transforming growth factor- β (TGF β) super-family, is a multifunctional molecule regulating the growth, proliferation, differentiation, invasion and apoptosis in various target cells. Many researchers have shown to play a role in cell proliferation and differentiation in development (Nakamura, et al. 2003; Stoeger, et al. 2002; Tsuda, et al. 2003; Waite, et al. 2003; Pohl, et al. 2003; Bain, et al. 2003; Maguer-Satta, et al. 2003).

BMP2, as other member of the TGF- β family elicits its cellular response through formation of heteromeric complexes of specific type I and type II serine/threonine kinase receptors. Five type II receptors and seven type I receptors, also termed activin receptor-like kinases (ALKs) have thus far been identified. The type II receptor is a constitutively active kinase, which upon ligand-mediated heteromeric complex formation phosphorylates particular serine and threonine residues in the type I receptor juxtamembrane region (also termed the GS-domain). The type I serine/threonine kinase thereby becomes activated and transduces signals downstream; type I acts thus downstream of type II receptor and has been shown to determine signalling specificity within the heteromeric receptor complex (Itoh et al. 2000) as shown in Fig.1.3.

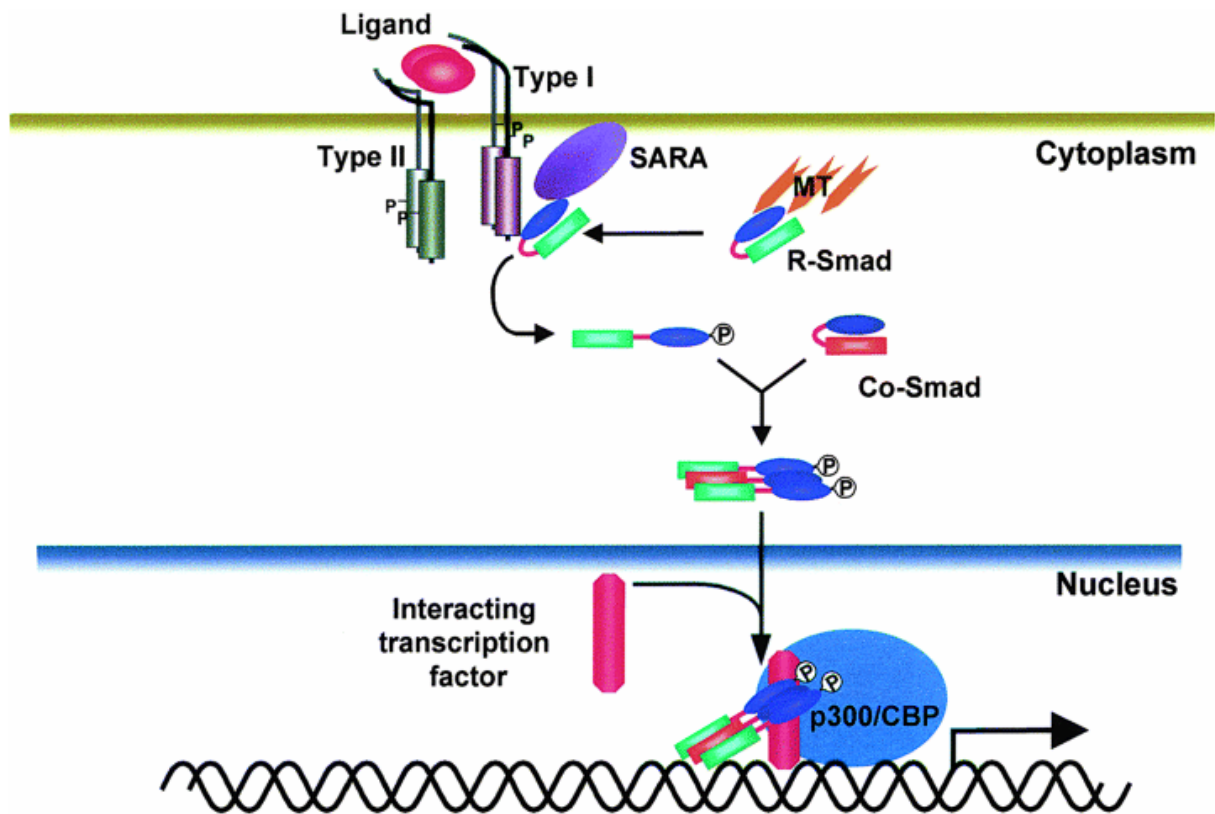


Figure 1.3: Activation of R- and Co-Smads. Upon ligand-induced heteromeric complex formation and activation of type I and type II receptors, R-Smads are phosphorylated and form heteromeric complexes with Co-Smads that translocate into nucleus, where they control the expression of target genes in a cell type specific manner. Nonactivated Smads can be retained in cytoplasm through association with microtubules (MT). The recruitment of Smad2 to the TGF- β receptor complex has been shown to involve a FYVE domain containing protein termed Smad anchor for receptor activation (SARA). Transcriptional modulation by Smads is achieved through complex formation with, e.g. transcriptional coactivators like p300/CBP and interacting transcription factors. R- and Co-Smads appear to form preferentially trimers consisting of one Co-Smad and two R-Smads. However, Smad complexes with other stoichiometry can not be excluded(Itoh et al. 2000).

Smads are pivotal intracellular nuclear effectors of transforming growth factor-beta (TGF-beta) family members. Ligand-induced activation of TGF-beta family receptors with intrinsic serine/threonine kinase activity trigger phosphorylation of receptor-regulated Smads (R-Smads), whereas Smad2 and Smad3 are phosphorylated by TGF-beta, and activin type I receptors, Smad1, Smad5 and Smad8, act downstream of BMP type I receptors. Activated R-Smads form

heteromeric complexes with common-partner Smads (Co-Smads), e.g. Smad4, which translocate efficiently to nucleus, where they regulate, in co-operation with other transcription factors, coactivators and corepressors, the transcription of target genes. Inhibitory Smads act in most cases in an opposite manner from R- and Co-Smads. Like other components in the TGF-beta family signalling cascade, Smad activity is intricately regulated. The multifunctional and context dependency of TGF-beta family responses are reflected in the function of Smads as signal integrators. Certain Smads are somatically mutated at high frequency in particular types of human cancers. Gene ablation of Smads in the mouse has revealed their critical roles during embryonic development, from the following table 1.1 can understand the Binding partners of Smads (Itoh et al. 2000).

Binding proteins	Smad		Functional properties
Membrane component			
ALK-1, - 2, - 3, - 6 ALK-4, - 5, - 7 SARA	Smad1,5, 6, 7, 8 Smad2, 3, 6, 7 Smad2, 3	MH2 MH2 MH2	Serine/threonine kinase Serine/threonine kinase FYVE finger anchor protein
Cytoskelton component Tubulin	Smad2, 3, 4	ND	Microtubule component
Nuclear transport protein Importin β	Smad3	MH1	Nuclear transporter
Cytoplasmic protein β -Catenin Calmodulin Smurf1 STRAP TAK1	Smad4 Smad1, 2, 3, 4 Smad1,5 Smad2, 3, 6, 7 Smad6	ND MH1 PY motif in linker MH2 ND	Wnt signal transducer; linking E-cadherin to the actin cytoskelton protein Calcium binding protein E3 ligase for ubiquitination WD repeat protein MAPKKK
Transcriptional coactivator			
MSG1 p300/CBP	Smad4 Smad1, 2, 3, 4	MH2 MH2	Histone acetyltransferase
Transcriptional repressor Hoxc-8 SIP1 Ski SNIP1 SnoN TGIF	Smad1 Smad6 Smad1, 2, 3, 5 Smad2, 3, 4 Smad1, 2 Smad4 Smad2, 3, 4 Smad2	MH1 linker MH2 MH2 MH2 ND MH2 MH2 MH2	+ Homeodomain containing protein Zinc finger containing protein Nuclear proto-oncogene product Forkhead-associated domain containing nuclear protein product Nuclear proto-oncogene product Homeo-domain containing protein
Transcription factor			
ATF-2 c-Fos c-Jun, JunB, JunD C-terminally truncated Gli3 GR	Smad3, 4 Smad3 Smad3, 4 Smad1, 2, 3, 4 Smad3	MH1 MH2 MH1, linker ND MH2	b-ZIP containing protein Ap-1 family member Ap-1 family member Zinc finger containing protein Glucocorticoid receptor

VDR	Smad3		MH1	Vitamin D receptor
E1A	Smad1, 2, 3		MH2	Adenoviral oncoprotein
Evi1	Smad3		MH2	Zinc finger containing protein
FAST	Smad2, 3		MH2	Winged-helix containing protein
Lef1/Tcf	Smad2,-3		MH1, MH2	HMG box containing protein
Milk	Smad4		MH1	
	Smad2		MH2	Paired-like homeodomain containing protein
Mixer	Smad2		MH2	Paired-like homeodomain containing protein
OAZ	Smad1, 4		MH2	Zinc finger containing protein
PEBP2/CBFA/AML	Smad1, 2, 3, 4		MH2	Runt-domain-containing protein
p52	Smad3		ND	NF- κ B/Rel family
SP1, SP3	Smad2, 3, 4		MH1	Transcription factor
TFE3 (μ E3)	Smad3, 4		MH1	Helix-loop-helix leucine zipper transcription factor

Table 1.1: Binding partners of Smads. Abbreviations: ALK, activin-receptor-like kinase; AML, acute myeloid leukemia; AP, activator protein; ATF, activating transcription factor; CBFA, core-binding factor A; CBP, CREB-binding protein; CREB, cAMP-responsive element-binding protein; E1A; early region 1A; Evi, ecotropic virus integration; FAST, forkhead activin signal transducer; Gli, glioblastoma gene product; HMG, high mobility group; Hoxc-8, homeobox gene c-8; Lef, lymphoid enhancer factor; MH, Mad Homology; MSG, melanocyte-specific gene or mad-supporting gene; ND, not determined; OAZ, Olf1/EBF associated zinc finger; PEBP2, polyomavirus-enhancer-binding protein; PY, PPXY motif; SARA, Smad anchor for activation; SIP, Smad-interacting protein; Ski/SnoN, Sloan-Kettering avian retrovirus/ski-related novel gene; Smurf, Smad ubiquitination regulatory factor; STRAP, serine/threonine kinase receptor-associated protein; TAK, TGF- β ctivated kinase; Tcf, T-cell factor; TFE, transcription factor mu E3; TGIF, 5'TG'-interacting factor; VDR, vitamin D receptor.

TGF- β family members have been shown to activate small GTP-binding proteins and MAP kinases in certain cells, as shown in Fig. 1.4 (Itoh et al. 2000).

Crosstalk with Smad signalling may also result from the ability of TGF- β to activate signalling pathways independently of Smads. TGF- β can activate ERK MAP kinase, p38 MAP kinase and JNK, although the extent and kinetics of activation differ among different cell lines and types. The MAP kinase kinase kinase TAK1, which is rapidly activated by TGF- β but is also involved in other signalling pathways, may initiate these signalling cascades. The activation of p38 MAP kinase and JNK can enhance Smad signalling through either Smad phosphorylation or the phosphorylation of c-Jun and ATF-2, which are transcription factors that cooperate with Smad3, resulting in functional crosstalk with Smad-mediated transcription at defined promoters (Derynck et al. 2001).

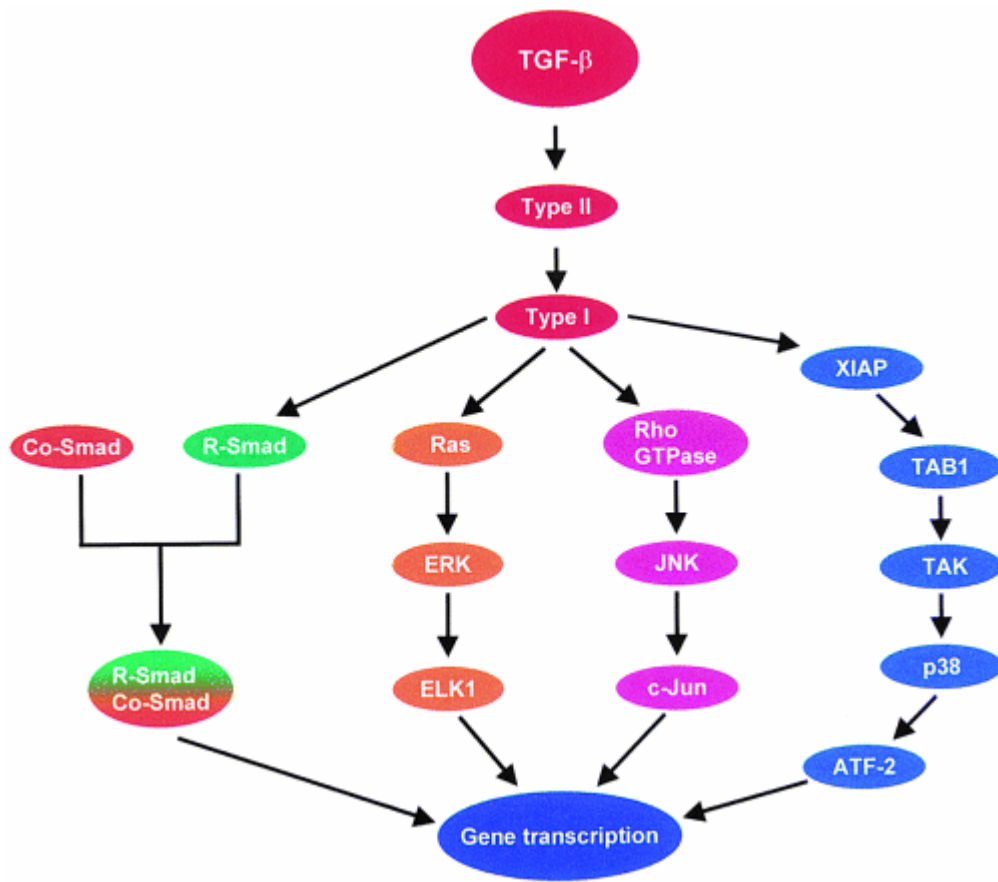


Figure 1.4: TGF- β receptor-initiated signalling cascades. TGF- β activates the Smad pathway as well as other signalling pathways. One example of a downstream transcription factor target for the different activated MAPK are indicated. Possible TGF- β receptor-induced responses that are independent of (Smad-mediated) transcription, as well as cross-talk between different downstream effector pathways are not indicated. Abbreviations: ATF, activating transcription factor; ERK, extracellular regulated kinase; JNK, c-Jun N-terminal kinase; TAB, TAK1-binding protein; TAK, TGF- β activated kinase; TGF- β , transforming growth factor- β ; XIAP, X-linked inhibitor of apoptosis protein(Itoh et al. 2000).

In addition, TGF- β can activate or stabilize the small GTPases RhoA and RhoB; these may in turn have roles in several responses to TGF- β , for example through a requirement of RhoB for activation of JNK. Finally, TGF- β induces an interaction of protein phosphatase 2A with S6 kinase, which regulates protein translation and growth control, decreasing its activity. Although the mechanisms of activation by TGF- β and the roles of these non-Smad signalling cascades remain to be better characterized, these observations indicate that inactivation of the Smad pathways may not leave the cell unresponsive to TGF- β (Derynck et al. 2001), as shown in Fig. 1.4.

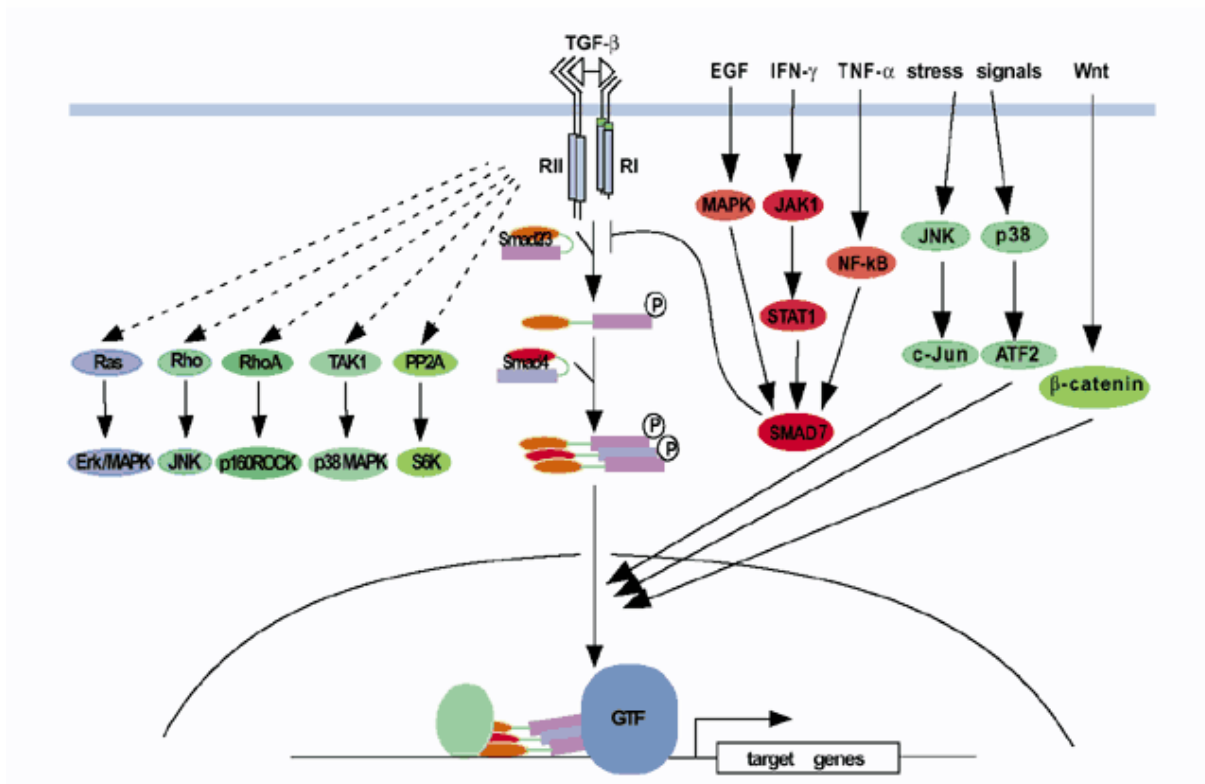


Figure 1.4: TGF-β-induced signalling through Smads, and several non-Smad signalling mechanisms.

After ligand-induced activation of the receptor, Smad2 and/or Smad3 interact transiently with the T_{RI} receptor (RI), and this interaction is stabilized by the FYVE protein SARA. Smad2 and Smad3 are phosphorylated on their C terminals by T_{RI}, and then dissociate from the receptor to form a heterotrimeric complex comprising two receptor-activated Smads and Smad4. This complex then translocates into nucleus, where it interacts at the promoter with transcription factors with sequence-specific DNA binding to regulate gene expression. The heteromeric Smad complex also interacts with the CBP/p300 transcriptional coactivator, which connects the Smad complex with the general transcription factors (GTF). Smad7 inhibits activation of Smad2 and/or Smad3 by the receptors, and Smad7 expression is induced on stimulation of one of several signalling pathways—for example, in response to EGF, interferon-β (IFN-β) or tumor necrosis factor-β (TNF-β). Several other signalling pathways also regulate both signalling by Smads and Smad-mediated gene expression, as exemplified here by the activation of JNK and p38 MAP kinase signalling in response to various stress signals, and β-catenin signalling in response to Wnt proteins. TGF-β also induces activation of Ras, RhoB and RhoA, as well as of TAK1 and protein phosphatase 2A, which leads to the activation of several MAP kinase pathways and the downregulation of S6 kinase activity. The mechanisms of activation of these non-Smad signalling events and how they connect to the heteromeric TGF-β receptor complex remain to be characterized (Derynck et al. 2001).

However, the molecular mechanisms of activation and inhibition of signal transduction from BMP2 to multifunctional positive and negative mediators of cells such as phospho-p70S6 and phospho-Akt (PI3K signalling), phospho-p38 (p38 network), phospho-ERK and phospho-JNK (MAPK pathway), phospho-Tyrosine (tyrosine-kinase network), phospho-STAT3 (Jak/stat network), and phospho-Smad1,2,3 (smad network) in U937 are not well characterized. More importantly, the modulation of phosphorylation and the subcellular localization have not been investigated. And also while the role of BMP in development and bone formation is being well characterized, little information is known about its role in tumor.

This study is to compare two different conditions of BMP2 signalling by using antibody microarray, one long time and high concentration of BMP2 treatment to U937 cells. This first experiment verified the BMP2 induction of apoptosis in U937 cells by observing cell number and FACS, obtaining 2000 ng/ml BMP2 treatment for 3 days as the optimal concentration and incubation time; the other selected short time and lower concentration of BMP2 treatment to MCF7 cells by using the lower concentration of BMP2(100ng/ml) for 4h in MCF-7 cells.

1.3.2 Effect of STI571 on cell signalling

STI571, as an inhibitor of the Bcr/Abl, c-Kit, and platelet-derived growth factor receptor kinases (Buchdunger E et al, 2000) has been shown to inhibit the growth of Bcr/Abl-positive leukemic cells (Druker B. J. et al. 1996). However (Yu, Krystal et al. 2002) indicated the exposure of Bcr/Abl+ cells to STI571 has not in general been associated with down-regulation of the Bcr/Abl protein, they reported that Exposure of K562 cells to concentrations of STI571 that minimally induced apoptosis (200 nM) resulted in early suppression (i.e., at 6 h) of p42/44 MAPK phosphorylation followed at later intervals (larger than or =24 h) by a marked increase in p42/44 MAPK phosphorylation/activation.

Importantly, clinical trials have now demonstrated that STI571, when administered at doses of larger than 300 mg/day, achieves clinical remissions in the large majority of patients with CML (e.g., 96%; Ref. Druker B. J., et al 2001). In addition, preclinical studies have demonstrates that the combination of STI571 with established chemotherapeutic drugs (e.g., ara-C) results in enhanced toxicity in Bcr/Abl-positive leukemias (Thiesing J et al 2000); Fang G., et al (2000) findings raise the possibility that combining STI571 with such agents might lead to enhanced activity in CML and/or circumvention of drug resistance. In this context, Vigneri and Wang (2001) reported recently that coadministration of STI571 with leptomycin, an inhibitor of the nuclear export sequence receptor, resulted in increased killing of cells expressing Bcr/Abl. However, in this study optimal killing occurred in cells exposed to 10 μ M STI571, which is above concentrations obtained in the plasma of patients receiving this agent (Druker B. J., et al. 2001).

In order to overcome problems of STI drug treatment as discussed above, various combination strategies may be possible. To identify important interactions relevant for STI571 treatment, it is interesting how different signal pathways are effected by STI571. I therefore treated the human leukemia cell line K562 with STI571 and studied the changes in signalling protein phosphorylation and localization using the phosphorylation antibody array. As in the other examples cytoplasmic and nuclear extracts were analyzed separately.

1.4 Aim

Development of an optimized antibody array that facilitates the analysis of proteins and their modifications in cellular tracts. With this array system it should be possible to analyse a selection of proteins in parallel and qualitatively and quantitatively compare the phosphorylation state of the selected proteins with a sensitivity and specificity comparable to western blot analysis. After initial experiments with array designs on microscope glass slides, the focus of the technical development was shifted to miniaturized glass chips, that can be mounted on the bottom of standard micro-reaction tubes (ArrayTube, Clondiag, Jena). With this ArrayTube system an optimized antibody array protocol could be developed using nano-gold particle-mediated silver staining for detection of bound antibodies.

After optimization of the system the general applicability of the array system were demonstrated in application examples. The three application models represent signalling processes important in the regulation of cellular proliferation: response of cellular signalling to BMP2 treatment and changes in signalling pathway activation after treatment with STI571. In addition, selective purification of cytoplasmic and nuclear protein extracts were used to assign the proteins to the specific cellular compartment.

The protein analyzed in the application examples included: phospho-p70S6 and phospho-Akt (PI3K signaling), phospho-p38, phospho-ERK and phospho-JNK (MAPK pathway), phospho-Tyrosine (tyrosine-kinase activity), phospho-STAT3 (Jak/stat network), and phospho-Smad1 and phospho-Smad 2,3 (Smad network).

The results obtained are compared with western blot data of selected proteins are discussed.

2 Materials and methods

2.1 Materials

2.1.1 Cell Lines

Leukemia cell line K562 and breast cell line MCF-7 were kindly provided by Dr Joachim Clement. Leukemia cell line U937 provided by Frau Dagmar Haase.

2.1.2 Chemicals

STI571 was kindly provided by Prof. Pachmann and prepared as a 10 mM stock solution in sterile DMSO (Merck Darmstadt, Germany). BMP2 was kindly provided by Dr. Clement stored at -20°C, and dissolved in sterile water as a 1mg/ml stock solution before use. Stock solutions were then diluted in RPMI medium to achieve the desired final concentration. In all of the cases, final concentrations of DMSO were < 0.1% and did not modify responses of cells to STI571.

Biotinamidocaproate N-hydroxysuccinimide ester was purchased from SIGMA D2643; Streptavidin-Gold EM.STP5 and LM/EM Silver Enhancement Kit SEKL15 were purchased from British BioCell; dist.PLANO, Germany. BSA from SIGMA; Milk Powder from Roth GmbH, Germany. Cy 3 and Cy 5 mono-reactive dyes were purchased from Amsham, Germany.

2.1.3 Antibodies

phospho-p70S6 kinase (Thr389), phospho-Akt (Ser473), phospho-STAT3 (Ser727), phospho-Tyrosine (Tyr100), phospho-SAPK/JNK (Thr183/Tyr185), phospho-p42/44 MAPK (Thr202/Tyr204), phospho-p38 (Thr180/Tyr182) and p38 MAPK purchased from Cell Signalling Technology; c-Myc, phospho-Smad1 (Ser463/465) and phospho-Smad2/3 (Ser433/435), β -actin, secondary antibodies antigoat, mouse, rabbit purchased from Santa Cruz Biotechnology.

2.1.4 Protein-molecular weight marker

206 kDa Myosin
124 kDa β -galactosidase
83 kDa BSA
42.3 kDa Carbonic anhydrase
32.2 kDa Soybean trypsin inhibitor
18.8 kDa Lysozyme
7 kDa Aprotinin

2.1.5 Apparatus

ArrayTube™ System

The Clondia ArrayTube™ platform (AT) was selected for the preparation of antibody arrays. In the AT platform the array chip is positioned at the bottom of a standard 1.5 ml micro reaction tube. This allows us to use all the standard laboratory equipment for heating, cooling and shaking, as well as centrifugation of 1.5 ml reaction tubes. Together with conventional microliter pipetors everything needed to perform the experiment. The only additional equipment required is a dedicated ArrayTube™ reader. If, as presented here, silver staining is used for detection, the costs for the reader are fairly low, in particular when compared with fluorescence readers

used for other array platforms with fluorescence labelling. The ArrayTubes™ are prepared and setup by Clondiag. Clondiag offers two choices for chip preparation, spotting of substances or in situ synthesis of oligomers. For the preparation of antibody arrays commercially available antibodies (Cell Signalling Technology, Beverly, MA; Santa Cruz Biotechnology, Santa Cruz, CA) were used and the spotted micro arrays were taken to set up the ArrayTubes™.

Antibody Spotting

For spotting an equal volume of antibody-spotting-buffer (Clondiag) was added to the PBS antibody preparations. All antibodies were obtained at concentrations of at least 1 µg/µl (or higher). We also included a second set of spots containing a 1:5 dilution for each antibody. The antibodies were spotted using a conventional split-pin micro-arrayed (BioRobotics MicroGrid II) onto glass based array substrate containing a three dimensional epoxy activated surface. After spotting, fresh prepared arrays were left in humid environment at room temperature to allow for covalent binding of the antibodies on the activated substrates. The quality of spotting (spots) was monitored by spot size analysis. Arrays were then mounted in ArrayTubes™ and sealed under inert gas atmosphere.

2.2 Methods

2.2.1 Cell Culture

K562, MCF-7 and U937 human cancer cells were cultured in RPMI 1640 supplemented with 10% heat-inactivated FCS (Hyclone, Logan, UT). They were maintained in a 37°C, 5% CO₂, fully humidified incubator, passed twice weekly, and prepared for experimental procedures when in log-phase growth (4×10^5 cells/ml).

2.2.2 Cell numbers and Experimental format

Logarithmically growing cells were placed in sterile plastic T-flasks (Corning, Corning, NY) to which the designated drugs were added and the flasks placed back in the incubator for intervals ranging from 4 to 72 h. 50 µl cell sample was collected and added into 20 ml of 0.9% NaCl tube for counting of cell numbers in cell count reader.

At the end of the incubation period, cells were transferred to sterile centrifuge tubes, pelleted by centrifugation at 400 x g for 10 min at room temperature, and prepared for analysis as described below.

2.2.3 Cytoplasmic and Nuclear protein Extracts

K562, MCF-7 and U937 human cancer cellular proteins were obtained from cell culture cells as cytoplasmic or nuclear fractions using a buffer system that allows lysis of cells in two steps. In the first step only the plasma membrane is lysed, leaving nucleus intact. The nuclei are pelleted by centrifugation. The supernatant contains the cytoplasmic protein lysate. To obtain nuclear proteins, the nuclei are washed repeatedly and then lysed using the nuclear lysis buffer B which described in details as follows:

K562, MCF-7 and U937 human cancer cells (10^5 to 10^6) were collected from culture cells and washed with 10 ml PBS by centrifugation with 1500 x g for 5 min. The cell pellet was resuspended in 1 ml PBS and transferred to 1.5 ml tube by centrifugation for 15 sec, buffer removed. The cell pellet was resuspended in 400 µl ice cold buffer A (cytoplasmic lysis buffer) and left on ice for 15 min (cells should swell). 25 µl of Np-40 (10% solution) was added and vortexed for 10 sec by centrifugation for 30 sec in 9000 rpm. Supernatant in 1.5 ml tube for cytoplasmic proteins was added 0.11 volume of ice cold buffer C and mixed thoroughly by centrifugation for 15 min at maximum speed.

Nuclear pellet was washed in 500 μ l of ice cold buffer A and 20 μ l Np-40 and vortexed for 10 sec followed by a centrifugation with 9000 rpm for 30 sec. The pellet was resuspended in 50 μ l of buffer B and rotated or shaken for 15-20 min at 4°C. Samples were centrifuged for 5 min and supernatants collected and frozen in aliquots of 10 μ l (-70 C).

Buffer A (lysis buffer)

10 mM Hepes pH 7.9
10 mM KCl
0.1 mM EDTA
0.1 mM EGTA
1 mM DTT
0.5 mM PMSF

Buffer B (nuclear extract buffer)

20 mM Hepes pH 7.9
0.4 mM NaCl
1 mM EDTA
1 mM EGTA
1 mM DTT
1 mM PMSF

Buffer C (cytoplasmic extract buffer)

0.3 M Hepes pH7.9
1.4 M KCL
0.03 M MgCl₂

2.2.4 Determination of Protein Concentration

Protein concentration was determined according to Bradford (1976). Several dilutions of protein standards (BSA) containing from 1 to 100 μ g/ml were prepared. 0.1 ml of standard samples and appropriately diluted samples were placed in dry test tubes. 0.1 ml sample buffer was used as a negative control. 1.0 ml diluted dye reagent was added to each tube and mixed several times by gentle inversion. After 15 min, OD₅₉₅ values versus reagent negative control were measured. OD₅₉₅ versus concentration of standard was plotted. The protein of interest was calculated from the standard curve using the Microsoft Excel5 software.

2.2.5 Ponceau S Staining

After PAGE, proteins were visualised by Ponceau.S staining. The proteins were stained by incubation in Ponceau.S solution for 5 min with agitation, followed by incubation in destaining water, until protein bands were visible on a colourless background.

2.2.6 Western Analysis

Equal amounts of protein (20 μ g) were boiled for 10 min, separated by SDS-PAGE (5% stacker and 10% resolving), and electroblotted to nitrocellulose. After blocking in PBS-T (0.05%) and 5% milk for 1h, the blots were incubated in fresh blocking solution with an appropriate dilution of

primary antibody for 4h. The source and dilution of antibodies were as follows: phospho-Akt 1:200, phospho-STAT3 (1:100), phospho-Tyrosine (1:100), phospho-p42/44 MAPK (1:200), phospho-p38 (1:200), phospho-Smad1 (1:100) and β -actin (1:1000). Blots were washed 3 x 5 min in PBS-T and then incubated with a 1:2000 dilution of horseradish peroxidase-conjugated secondary antibody for 1h. Blots were again washed 3 x 5 min in PBS-T and then developed by ECL chemiluminescence.

2.2.7 Immunoprecipitation

The protein G Sepharose beads were equilibrated in TBS for 30 min, pelleted by centrifugation with 2292 x *g* for 3 min and washed twice with TBS. The remainder of protein G Sepharose was stored in TBS with 0.02% NaN₃ at 4°C. 500 μ l (700 μ g/ml) of control cytoplasmic extract in K562 cells incubated with 10 μ l of phospho-Tyrosine specific antibody for 1.5h on a rotator at 4°C. 40 μ l of protein A/G added to the antibody linked antigen for 1h on a rotator at 4°C. The sepharose beads were washed twice by centrifugation with 2500g for 5 min with washing buffer, followed by the addition of loading buffer. Prior to loading on an SDS gel, the samples were boiled for 10 min in loading buffer.

2.2.8 Cy3 and Cy5 Staining in SDS-PAGE

In order to examine the efficiency of antibody labelling, 5 μ l of original anti-goat secondary antibody was incubated with 2 μ l of Cy3 or Cy5 mono-reactive dye on a shaker for 1h at RT. The reaction was stopped by the addition of loading buffer to each sample. Prior to loading on an SDS gel, samples were boiled for 10 min in loading buffer (Figure 61).

2.2.9 Cy3 and Cy5 Staining of Microscope-Slide-Size Array

To compare slide quality and storage conditions of slides at different temperature and time. 20°C for a couple of months or even longer were used between epoxy and aldehyde slide;

To compare protein labelled time and amounts between one kind of protein (or antibody) and the whole protein based on relative fluorescence after labelling proteins: One kind of protein (or antibody), 20ng of protein was needed 0.01 μ l of Cy3 or Cy5 mono-reactive dye, (but usually adding up to Cy3 or Cy5 mono-reactive dye 2 μ l. Therefore, free dye existing). However, the whole protein of cells (more than 1mg/ml) was needed about 50 μ g using 2-3 μ l of Cy3 or Cy5 mono-reactive dye; One kind of protein or antibody labeled half hour and two hours separately. However, the whole protein of cells compared among half, two and four hours. The labelled protein can be stored at -20°C more than one week for reaction later;

To compare stop reagent using and without using stopping reagent. Stopping reagent separately was incubated in SDS-PAGE and microscope-slide-size array for 5 min and 15 min;

To compare protein purification with different methods in order to delete free dye: G25, G50, microcon10, 30 and 50 were used for protein purification which result was checked by protein concentration measure (CCB);

To compare results between deletion and undeletion of free mono-reactive dye Cy3 and Cy5-labelled antibodies, mono-reactive dye Cy3 and Cy5-labelled mixed antibodies were separately incubated and washed completely with each step; Only Cy5 free mono-reactive dye was incubated;

To compare blocking time. Blocking time half to one hour under PBS-0.5%Tween-BSA was used; Blocking slide were stored at -20°C several days afterwards to use for reaction.

To compare reaction volume and time. 7 μ l, 12-15 μ l and 20 μ l of incubation volume under different reaction time 1, 2 and 3 hours were used to react at room temperature and 4°C overnight separately;

To compare washing volume and time. Big volume (30 ml) three times was washed at room temperature or in the dark overnight or shake up and down by hand with vortex several times, or at 4°C overnight.

2.2.10 Cy3 and Cy5 Staining of mini-Arrayslide

Minislide-protein microarray was divided into about 126 minislides in one normal slide, each including different repeating spotted antibodies (each spotting 1.5 μ l) and Cy3 mono-reactive dye markers at four corners.

50 μ g of protein was labelled with 2 μ l of Cy3 or Cy5 mono-reactive dye separately on a shaker for h at RT. The minislide was blocked with 80-100 μ l of 5 % milk powder (fresh) on a shaker for 1.5h. At least 40 μ l volume of 50 ug protein labelled Cy3 and Cy5 mono-reactive dye were mixed together for checking cytoplasm and nucleus at the same time and was reacted with minislide in 96 plate for 1h. The reacted minislide was washed with 300 μ l of PBS-0.5%Tween buffer in 96 plate on a shaker for 30 min twice. Finally the minislide was put on fluorescent image reader for scanning.

2.2.11 Silver staining of mini-Arrayslide

50 μ g of cellular proteins are diluted to a final volume of 25 μ l in buffer (extraction buffer or PBS). For biotinylation 1 μ l of NHS-succinimid-Biotin (SIGMA) (100 μ g/ μ l in ultra pure DMSO; water free) was added and left at room temperature for 1h. Reaction was stopped adding 2% BSA. Finally, the volume was adjusted to 100 μ l with PBS (2% milk powder or 2% BSA).

Arrayslide was blocked with 5% milk powder in PBS for at least 5 minutes at 30° C shaking at 750 rpm (Eppendorf Thermomixer™). Arrays are incubated with the protein extracts for 2h at room temperature. After incubation arrays are washed 3 times for 5 min with 500 μ l PBS-0.5%Tween.

50 μ l of solution A and 50 μ l of solution B from silver enhancement kit were combined immediately before use and added to Arrayslide to reaction.

2.2.12 Silver staining in Arraytube

2.2.12.1 Biotinylation of Cellular Proteins

50 μ g of cellular proteins are diluted to a final volume of 25 μ l in buffer (extraction buffer or PBS). If other buffers than indicated below are used for protein extraction, a change of buffers may be necessary before biotinylation (Tris-based buffers can not be used for biotinylation!). For biotinylation 1 μ l of NHS-succinimid-Biotin (SIGMA) (100 μ g/ μ l in ultra pure DMSO; water free) was added and left at room temperature for 1h. Reaction was stopped adding 2%BSA. Protein preparations were left at room temperature for another 15 minutes to ensure complete consumption of the biotinylation reagent. Finally, the volume was adjusted to 100 μ l with PBS (2% milk powder or 2% BSA). Biotinylated proteins are then ready to add to blocked ArrayTubes™ for binding.

2.2.12.2 Incubation of Protein Extracts

Before incubation with protein extracts, antibody arrays must be blocked. After spotting most of the activated surface is still freely accessible and has a high capacity for protein binding. For

this reason, our arrays were blocked with 5% milk powder in PBS for at least 5 minutes at 30° C shaking at 750 rpm (Eppendorf Thermomixer™). Not all milk powder can be used, so I recommend tests with various milk powders (Sigma). In this case best results were obtained with a milk powder that fully dissolved into a clump free white colored solution at 5% in PBS. Blocking solution is then replaced by the biotinylated protein extract in PBS (supplemented with 2% milk powder or BSA). Arrays are incubated with the protein extracts for 2h at room temperature. Alternatively, I also obtain good results with an overnight incubation at 4°C. After incubation arrays are washed 3 times for 5 min with 500 µl PBS.

2.2.12.3 Silver Staining

The bound biotinylated proteins are detected in a two step detection process. In the first step, streptavidin gold nanoparticles (British BioCell, Plano) are bound to the biotin groups. In the second step, a silver precipitate is formed around the gold particles. This step is monitored online in the ArrayTube™ Reader, which allows to detect the onset of silver precipitation. In this way errors resulting from saturation effects from final point measurements can be avoided.

Before incubation with the streptavidin gold particles tubes are again blocked with PBS (5% milk powder) for 15 min. Blocking solution is replaced by 100 µl of streptavidin gold particles in PBS and tubes are incubated for 30 min at 30° C shaking at 350 rpm. Excess streptavidin gold is removed in 3 wash steps. with 200 µl of PBS-tween (0.1%) for 10 min at 20° C with 750 rpm three times. For silver staining 100 µl silver developing solution is added. The silver developing solutions contains equal amounts of silver enhancer and developer, which are combined directly before use (here I used the reagents from British BioCel, distributed in Germany by Plano. Other reagents may work equally well). Tubes are placed into the ArrayTube™ Reader and recording of pictures is started. Pictures are taken every minute for 40 minutes to 1 h.

50 µl of solution A and 50 µl of solution B from silver enhancement kit were combined immediately before use and added to ArrayTube to start silver development, collect images for 40 min to 1h at 1 min interval and analysis of images with appropriate software e.g. Partisian IconoClust from Clondiag.

2.2.13 Statistical Analysis

For each experiment, 40 exposures are obtained and all are evaluated by the IconoClust software. This software can automatically produce data including mean, background, Sigma etc. To compare results between each experiment, all values are normalized by the median method.

3 Results

3.1 Antibody Array Technologies

3.1.1 Cy3 and Cy5 of SDS-PAGE, Microscope-Slide-Size Array and mini-Arrayslide

One important factor for antibody array is the efficiency of antibody labelling. In order to examine the labelling efficiency, 5 μ l of original anti-goat secondary antibody was incubated with 2 μ l of Cy3 mono-reactive dye or Cy5 mono-reactive dye (taken from a stock dilution to 50 μ l) on a shaker for 1h at RT. Fractionation of the reaction mix by SDS-PAGE was followed by visualization under normal light (because of high Cy5 concentration decided which blue band can be seen in normal light) and revealed two bands, as shown in Fig. 3.1. These bands correspond to the heavy and light chains. This result demonstrates good labelling efficiency and the ability to detect the labelled product on the gel.

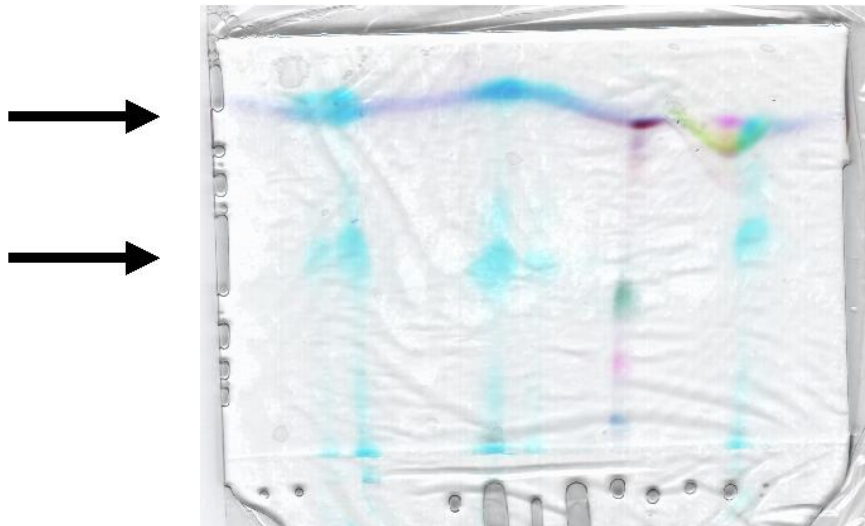
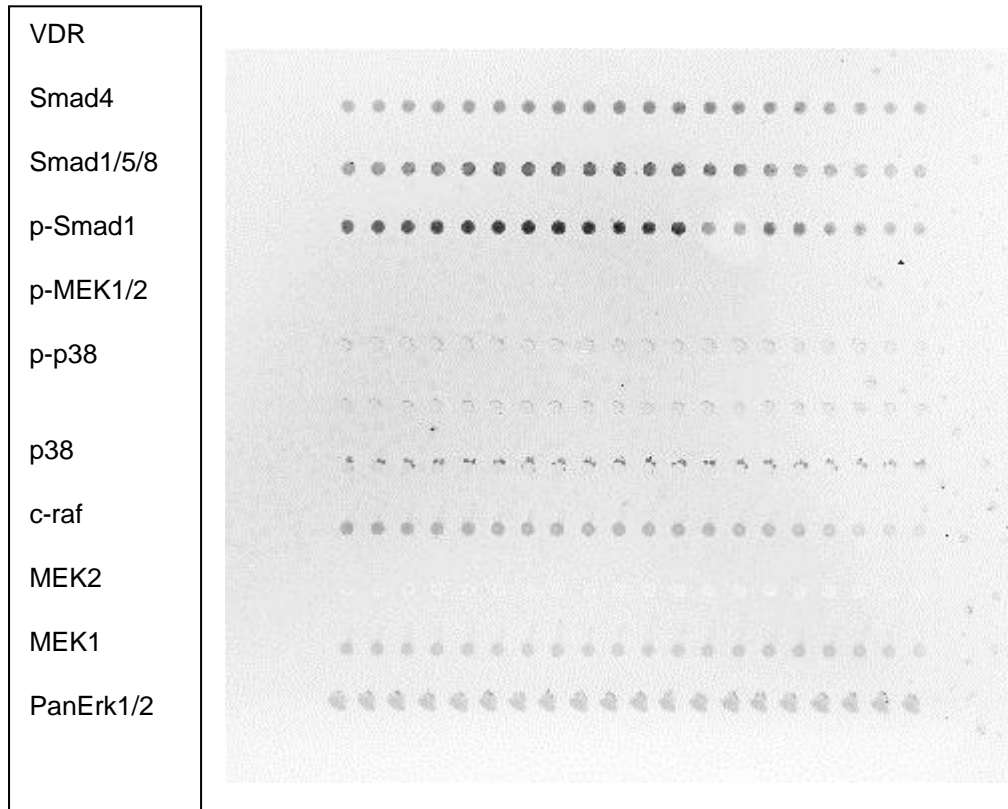


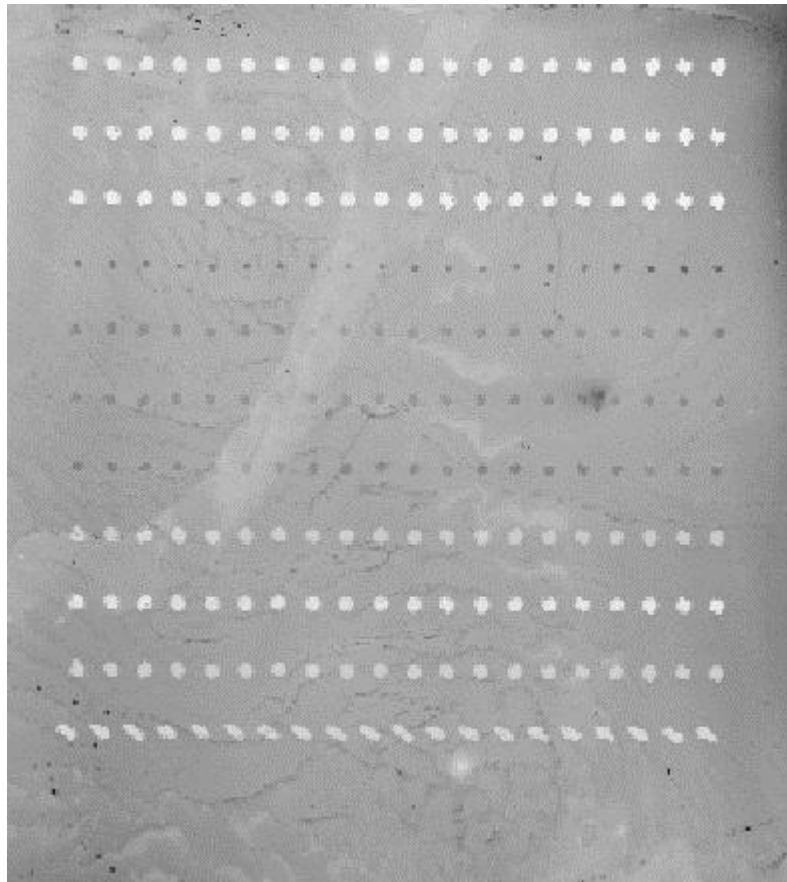
Figure 3.1: Cy5 staining in SDS-PAGE. 5 μ l of original anti-goat secondary antibody was labelled with 2 μ l of Cy5 on a shaker for 1h at RT. Because of the high Cy5 concentration blue bands of labeled proteins can be seen in normal light, upper arrow indicating light chain, lower arrow indicating heavy chain.

At present, most antibody array technologies were used Cy3 and Cy5 staining of microscope-slide-size arrays. Because antibody array is a new technology, standardisation is needed for setting up. This part aim was to summarise the protocol in details under different conditions. One result with Cy5 staining of microscope-slide-size array is shown in Fig. 3.2.

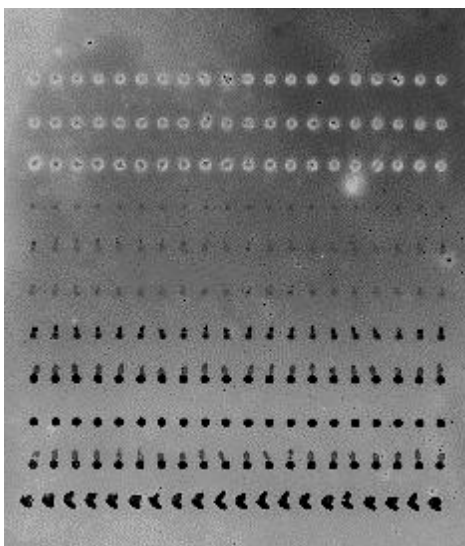


3.2 A

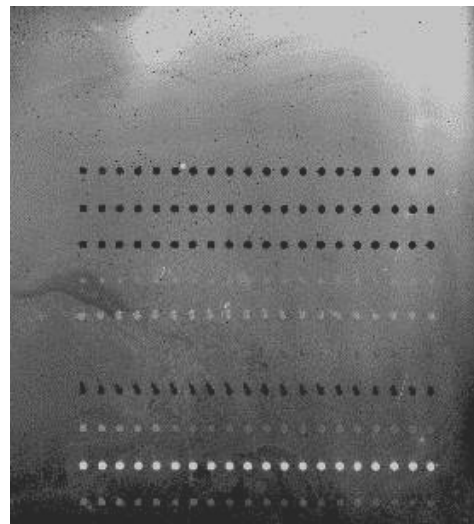
VDR
 Smad4
 Smad1/5/8
 p-Smad1
 p-MEK1/2
 p-p38
 p38
 c-raf
 MEK2
 MEK1
 PanErk1/2



3.2 B



3.2 C



3.2 D

Figure 3.2: Cy3 or Cy5 staining of microscope-slide-size antibody array. Array was spotted by Quantifoil (Jena). Different reaction conditions are shown 3.2 A-D as detailed in the text. Black signals are positive reaction. Each line represented one kind of antibody including PanErk, p-MEK1, p-MEK2, p-p44/42 MAP kinase, p-p38, p-Smad1, p-Smad4, Samd1/5/8, a-Raf and VDR.

To compare slide quality and storage conditions of slides at different temperature and time. 20°C for a couple of months or even longer were used between epoxy and aldehyde slide. The result showed that slides can be stored efficiently at -20°C for a couple of months or even longer and epoxy slides are more sensitive than aldehyde slides for slide quality;

To compare protein labelled time and amounts between one kind of protein (or antibody) and the whole protein based on relative fluorescence after labelling proteins. One kind of protein (or antibody), 20ng of protein was needed 0.01 µl of Cy3 or Cy5 mono-reactive dye, (but usually adding up to Cy3 or Cy5 mono-reactive dye 2µl. Therefore, free dye existing). However, the whole protein of cells (more than 1mg/ml) was needed about 50µg using 2-3µl of Cy3 or Cy5 mono-reactive dye; One kind of protein or antibody labeled half hour and two hours separately. However, the whole protein of cells compared among half, two and four hours. The labelled protein can be stored at -20°C more than one week for reaction later; The results demonstrates the same between labeling time of half hour and two hours. However, the whole protein of cells compared among half, two and four hours. The results demonstrates better for longer time labeling. The labelled protein can be stored at -20°C more than one week later for reaction. The result demonstrated that stored protein reaction is almost the same as before;

To compare stop reagent using and without using stopping reagent. Stopping reagents separately were incubated in SDS-PAGE and microscope-slide-size array for 5 min and 15 min. The result showed that hydroxylamin make dye disappeared under the observation of SDS-PAGE. For stopping time between 5min and 15 min, the result demonstrated that the long time stopping reaction signaling (15 min) is weaker than the short time stopping reaction (5 min); Without using stop reagent, the result demonstrates the same as 5 min stopping and has not appeared a crosstalking reaction (from literature, stopping reagent hydroxylamin easily makes dye disconnected from protein);

To compare protein purification with different methods in order to delete free dye: G25, G50, microcon10, 30 and 50 were used for protein purification checked by protein concentration measure (CCB). The result showed that G25 and G50 make protein dilution, and only microcon10 is the best because of no protein leaking out;

To compare results between deletion and undeletion of free mono-reactive dye Cy3 and Cy5-labelled antibodies, mono-reactive dye Cy3 and Cy5-labelled mixed antibodies were separately incubated and washed completely with each step. The result demonstrates the same as before mixture reaction and indicate no crosstalking reaction between mono-reactive dye Cy3 and Cy5-labelled antibodies. Only Cy5 free mono-reactive dye was incubated. only Cy5 free dye was incubated. The result demonstrates nothing. Therefore, free dye cannot affect the result;

To compare blocking time. Blocking time half to one hour under PBS-0.5%Tween-BSA was used; Blocking slide were stored at -20°C several days afterwards to use for reaction. The result demonstrates the same as before; Some negative-result slide can be repeated to be used;

To compare reaction volume and time. 7µl, 12-15µl and 20 µl of incubation volume under different reaction time 1, 2 and 3 hours were used to react at room temperature and 4°C overnight separately. 7µl of reaction volume makes one spotting line dropping for 18*18cm cover. 12-15µl of reaction volume is very optimal for 18*18cm cover. 20 µl of reaction volume makes cover moving and reaction liquid out for 18*18cm cover; Reaction time used 1, 2 and 3 hours at room temperature and 4°C overnight separately. The results demonstrate the same.

To compare washing volume and time. Big volume (30 ml) three times was washed at room temperature or in the dark overnight or shake up and down by hand with vortex several times, or at 4°C overnight. Washing at room temperature in the dark overnight makes some spots moving; Washing steps can shake up and down by hand and also vortex several times, the result is the same as the big washing volume three times; Washing at 4°C overnight, the result is also good.

Miniarray slide was developed in the next step. One result with Cy3 staining of mini-Arrayslide is shown in Fig. 3.3. The advantage of this technology is that the binding reaction and labelling reaction can be performed in a very small volume and that the handling in tubes and microtitre plates is much easier.

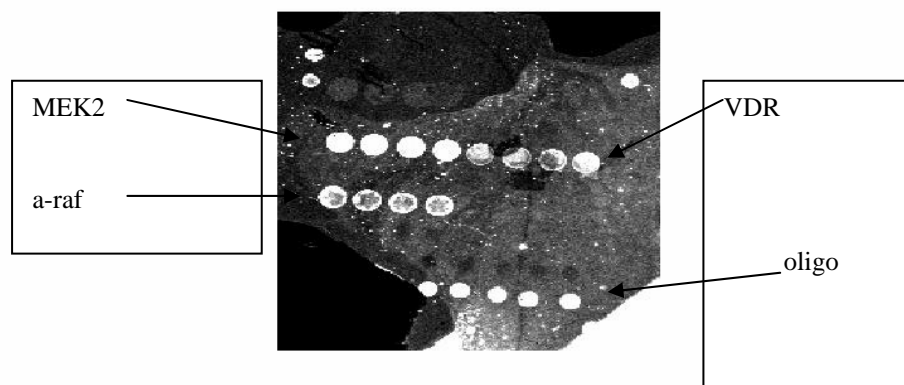


Figure 3.3: Cy3 staining of antibody array in mini-Arrayslide. Control K562 cell protein extraction with labelled Cy3 mono-reactive dye was reacted with minislide. Every four repeating spots represented one kind of antibody including p-MEK1, p-MEK2, p-p44/42 MAP kinase, p-p38, p-Smad1, p-Smad4, a-Raf and VDR. Bright signals are positive results.

Nano-gold particles-mediated silver staining of mini-Arrayslide is an alternative new technology for detection of bound molecules. One example of silver staining in mini-Arrayslide was shown in Fig. 3.4. This technology was used to transfer from mini-Arrayslide to Arraytube.

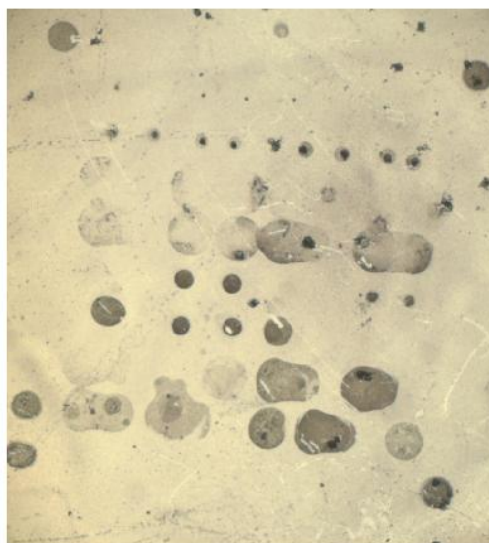


Figure 3.4: Silver staining of mini-Arrayslide. Array was spotted by Quantifoil. This is one example of protein extracts from control K562 cells incubated with mini-arrayslide by visualization under microscope revealing black positive results. Each four repeating spots represented one kind of antibody including p-MEK1, p-MEK2, p-p44/42 MAP kinase, p-p38, p-Smad1, p-Smad4, a-Raf and VDR.

3.1.2 Data Analysis

The pictures obtained were analyzed using the PARTISAN IconoClust image analysis software from Clondiag. This software automatically recognises the arrays and overlays a grid to measure the intensities for each spot. All pictures were combined to generate time curves for the increasing signals of all samples (spots). This time course was then used to assign differences in signal intensities. In comparison with pictures taken after a given period of staining, this procedure eliminates the assignment of the wrong intensity due to saturation effects.

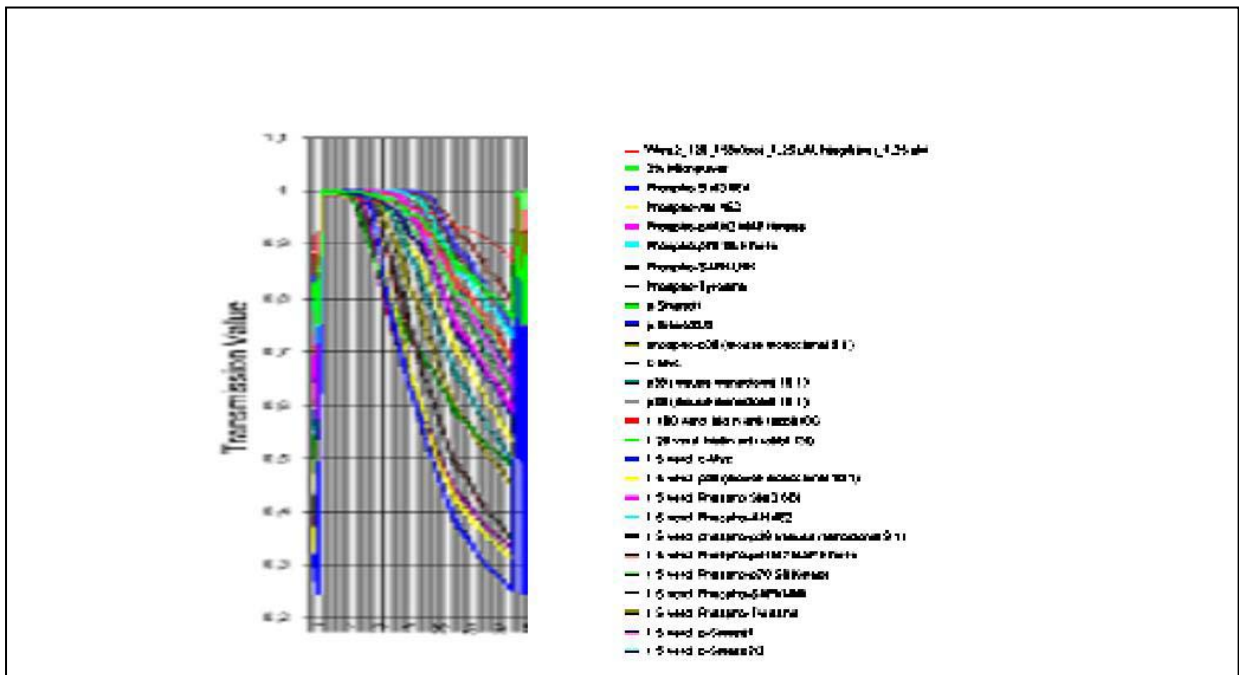
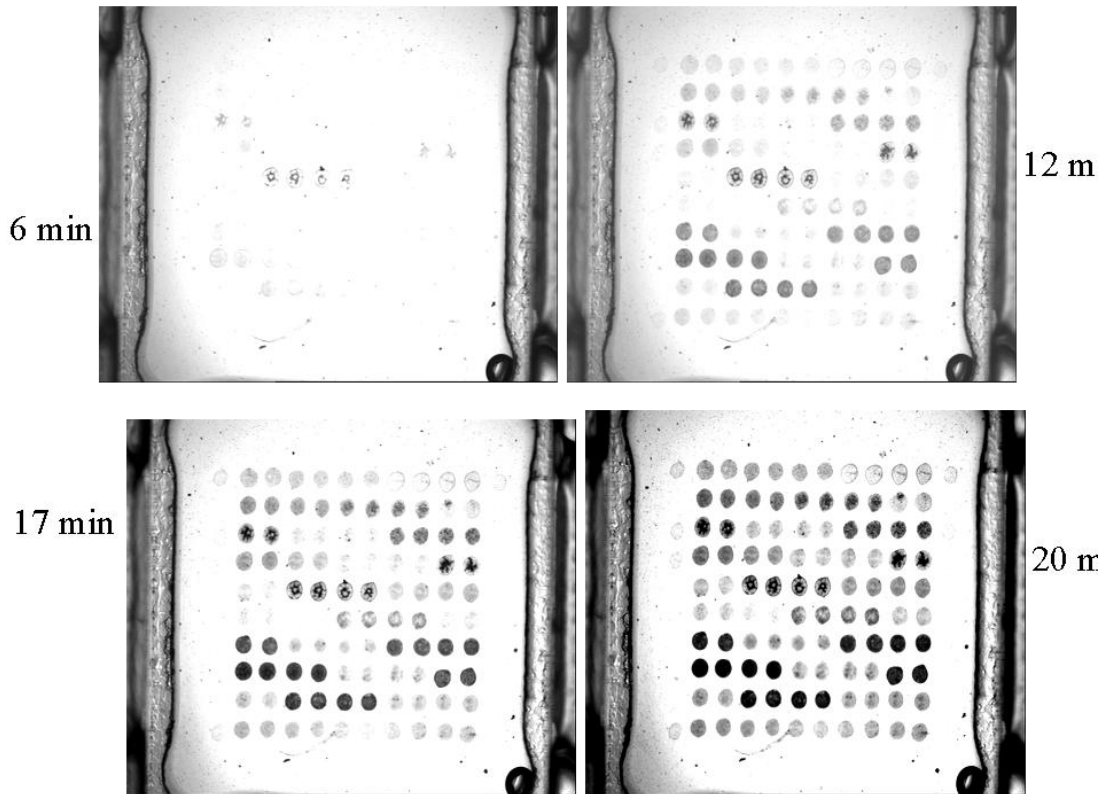


Figure 3.5: Different time point pictures and values. Upper pictures were shown 6,12, 17, and 20 minute points of 2000 ng/ml U937 BMP2 treatment for 3 days. Lower graph dsplays increase of signal during the silver staining measured at different time point for each antibody.

As an example of an ArrayTube™ antibody array were presented. p70S6 kinase, Akt, STAT3, SAPK/JNK, p44/42 MAP kinase, Tyrosine, Smad1 and Smad2/3 are detected only when phosphorylated. For p38 MAP kinase, two antibodies were selected to spot: one phosphorylation specific and one binding the protein independent of phosphorylation. An antibody directed against c-Myc was used total antibody. All antibodies were spotted at two concentrations four times each (undiluted: 1 volume antibody stock + 1 volume spotting buffer; and at a 1:5 dilution). A description of the antibodies with supplier and position on the array is given in Figure 3.5.

SPOT ID	NAME	vendor / concentration
1	phospho-p70 S6 Kinase (1:5 diluted)	CST 0,4
2	phospho-p70 S6 Kinase #9206B	CST 2
3	phospho-Akt 4E2 (1:5 diluted)	CST 0,2
4	phospho-Akt 4E2 #9276B	CST 1
5	phospho Stat3 6E4 (1:5 diluted)	CST 0,2
6	phospho Stat3 6E4 #9136B	CST 1
7	phospho-Tyrosine (1:5 diluted)	CST 0,36
8	phospho-Tyrosine #9411B	CST 1,8
9	phospho-SAPK/JNK (1:5 diluted)	CST 0,2
10	phospho-SAPK/JNK #9255B	CST 1
11	phospho-p44/42 MAPK (1:5 diluted)	CST 0,42
12	phospho-p44/42 MAPK #9106B	CST 2,1
13	phospho-Smad1 (1:5 diluted)	SC 0,4
14	phospho-Smad1 sc12353x	SC 2
15	phospho-Smad2/3 (1:5 diluted)	SC 0,4
16	phospho-Smad2/3 sc11769x	SC 2
17	c-Myc (1:5 diluted)	SC 0,4
18	c-Myc sc42x	SC 2
19	phospho-p38 (1:5 diluted)	CST 0,5
20	phospho-p38 #9216B	CST 2,5
21	p38 MAPK (1:5 diluted)	CST 0,5
22	p38 MAPK #9217B	CST 2,5
23	biotin anti-rabbit IGG (1:20 dil.)	SC
24	biotin anti-rabbit IGG (1:100 dil.)	SC
25	2% milk powder in PBS; 20mM trehalose	
26	biotin-nh2-marker	CCT

Layout of array											
SW AK4 130303											
26	23	23	24	24	24	24	25	25	25	25	26
	21	21	21	21	22	22	22	22	23	23	
26	18	18	19	19	19	19	20	20	20	20	26
26	16	16	16	16	17	17	17	17	18	18	26
	13	13	14	14	14	14	15	15	15	15	26
	11	11	11	11	12	12	12	12	13	13	26
	8	8	9	9	9	9	10	10	10	10	26
	6	6	6	6	7	7	7	7	8	8	26
	3	3	4	4	4	4	5	5	5	5	
26	1	1	1	1	2	2	2	2	3	3	26

Vendor of antibodies used:
CST: Cell Signaling Technology
SC: Santa Cruz Biotechnology

Figure 3.5: A description of the antibodies with supplier and position on the array. p70S6 kinase, Akt, STAT3, SAPK/JNK, p44/42 MAP kinase, Tyrosine, Smad1 and Smad2/3 should be detected only when phosphorylated. For p38 MAP kinase two antibodies were selected to spot one phosphorylation specific and one binding the protein independent of phosphorylation. As reference an antibody directed against c-Myc independent of phosphorylation. All antibodies were spotted at two concentrations four times each (undiluted: 1 volume antibody stock + 1 volume spotting buffer; and at a 1:5 dilution).

One successful enlargement example of silver staining arraytube is shown in Fig. 3.7. The result clearly demonstrates positive, negative signalling and background state.

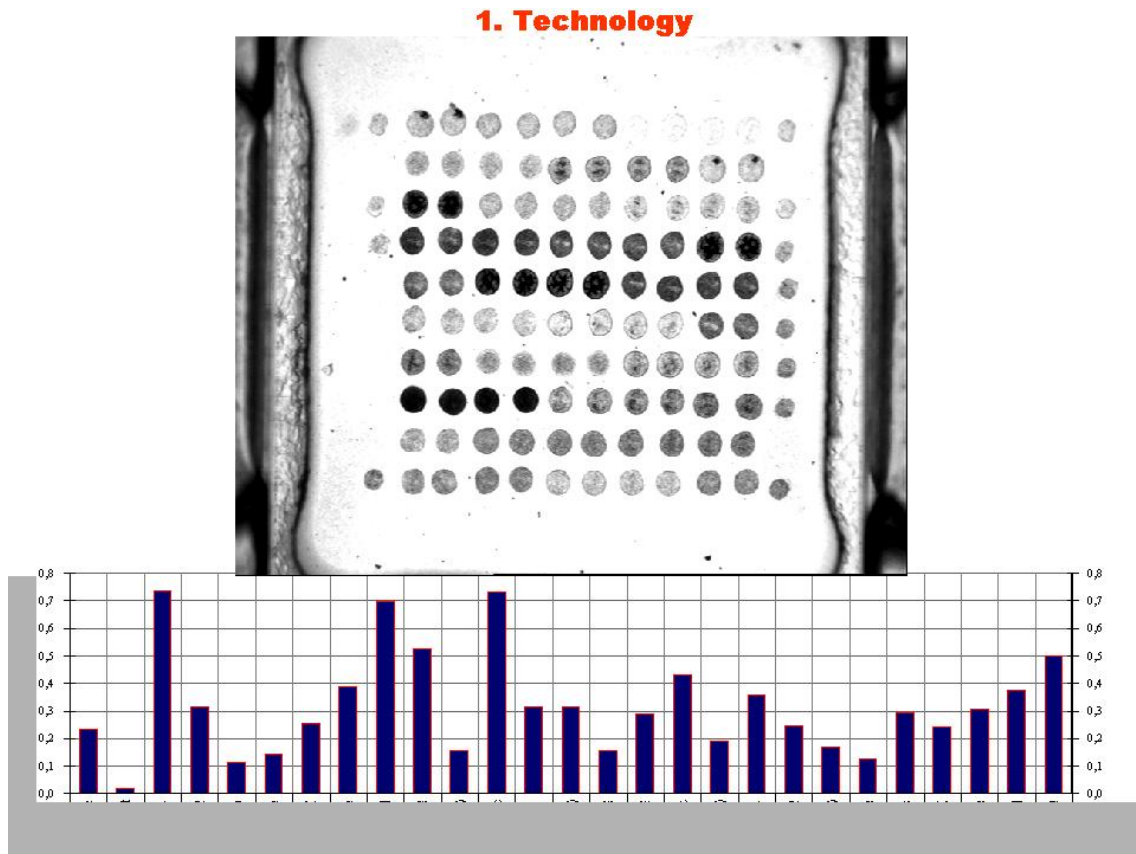
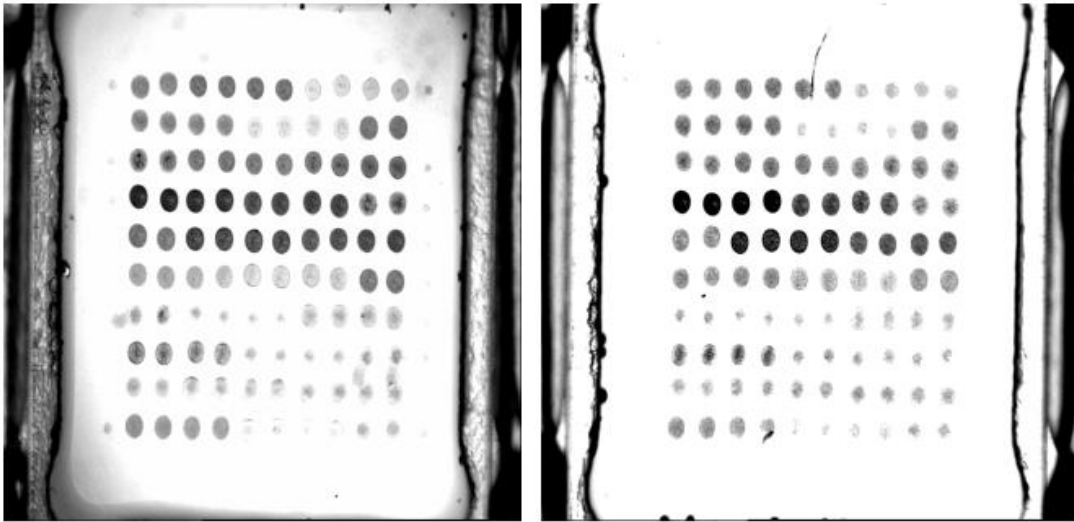


Figure 3.7: One successful picture of silver staining of array-tube. One example of silver staining picture. Protein extracts from the human leukemia cell line U937 using the protocol for the preparation of cytoplasmic protein extracts, the result of silver staining clearly demonstrates positive, negative signalling and background state.

Different parameters were changed for comparison of different protocols, such as change of protein concentration produces the same result, reflecting the technology sensitive and stable. This result was shown in Fig. 3.8



Change of protein concentration

**produces the same result,
reflecting the technology sensitive and stable.**

Figure 3.8 Change different parameters. Change of protein concentration produces the same result, reflecting the technology sensitive and stable.

The same protein (twice amounts) divided into two parts and reacted in 2 tubes, The result of pictures and evaluations are the same, as shown in Fig. 3.9. The experiment demonstrates the technology accurate and robot.

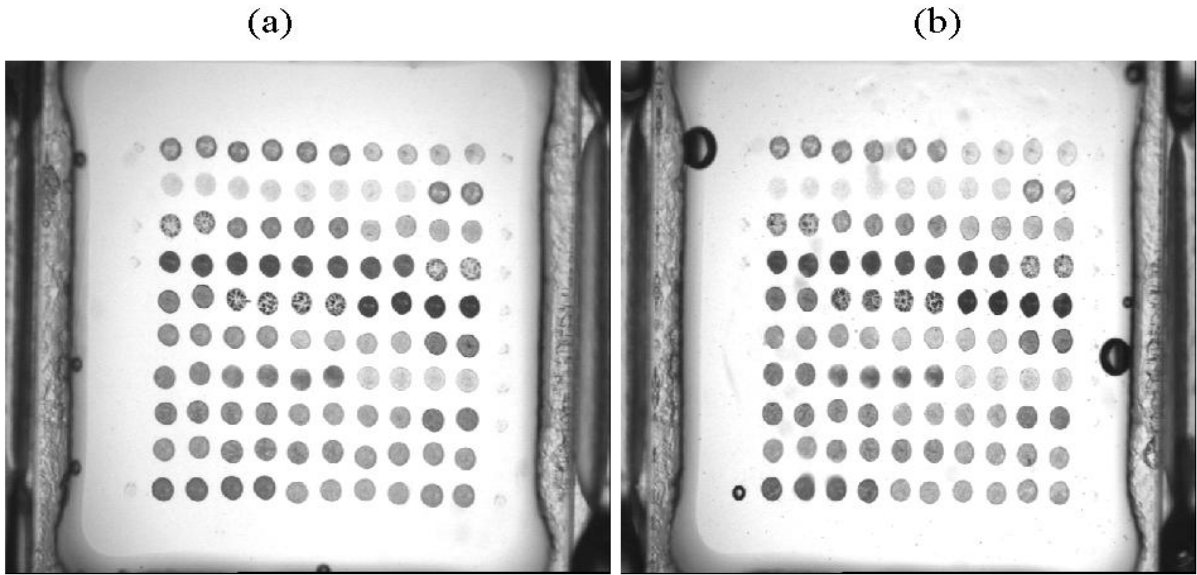


Figure 3.9-a: Pictures on silver staining by array-tube. The same protein (twice amounts) divided into 2 parts and incubated in 2 tubes, showing the results of pictures are the same.

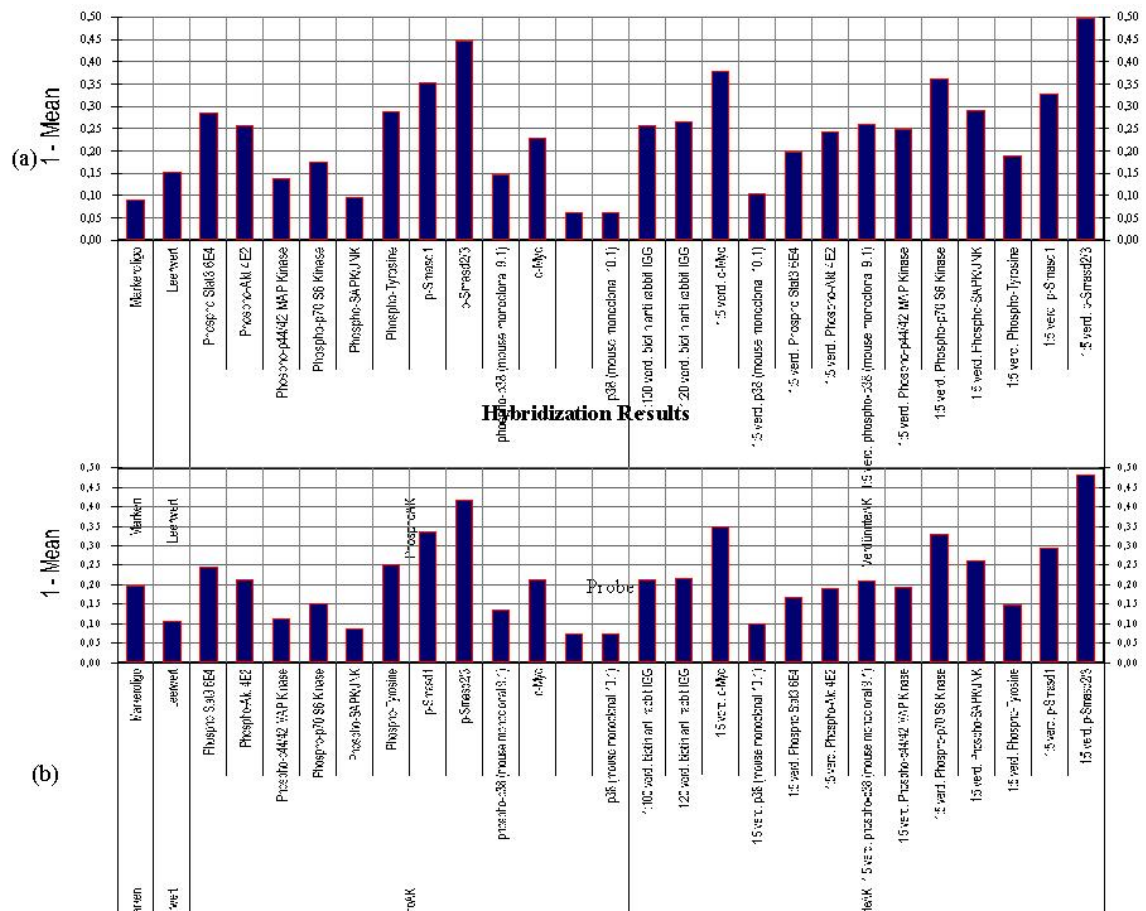


Figure 3.9-b: Evaluation on silver staining by array-tube. The same protein (twice amounts) divided into 2 parts and incubated in 2 tubes, showing the results of evaluation are the same.

The ArrayTube™ platform with small arrays of phosphoprotein specific antibodies were used and spotted in quadruplets on glass chip substrates coated with a three dimensional epoxy activated reactive surface. The ArrayTube™ antibody arrays were incubated with protein extracts from the human leukemia cell line U937. Changes in phosphorylation of signalling proteins were induced by incubation with the bone morphogenetic protein BMP2. After incubation, Smad1, ERK, Akt, STAT3 and Tyrosine phosphorylation could be detected which correlates well with results obtained by western blotting and Cy3/Cy5 staining. In summary, the ArrayTube™ platform can be used for antibody arrays aimed at the detection of intracellular proteins and their respective phosphorylation state.

3.2 Modulation of Phosphorylation and localization in BMP2 treated U937 cells

In order to discover the optimal BMP2 concentration and incubation time in U937 cells, first different BMP2 concentrations were selected from 50 ng/ml, 100 ng/ml, 300 ng/ml, 500 ng/ml, 1000 ng/ml, 1500 ng/ml to 2000 ng/ml under different incubation time from 10 min, 30 min, 2hr, 4h to 24h and examined the cell numbers, this result shows the significant decrease of the cell number is only 2000 ng/ml BMP2 treatment for 24h(data not shown).

Different BMP2 concentrations were selected from 50 ng/ml, 100 ng/ml, 300 ng/ml, 500 ng/ml, 1000 ng/ml, 1500 ng/ml to 2000 ng/ml for 3 days to examine dead cells and cell cycle by FACS. Treatment with high concentrations of the bone morphogenetic protein BMP2 in the human leukemia cell line U937 induces apoptosis, whereas treatment with lower levels of BMP2 lead to differentiation of the cells. This experiment verified that 2000 ng/ml BMP2 treatment is the best condition for the induction of apoptosis in U937 cells from dead cells and cell cycle analysis by FACS (data not shown).

Ponceau S staining of cytoplasmic and nuclear proteins in control U937 cells separated on SDS-PAGE gel. The result of Ponceau S staining shows weaker distribution in nucleus (e) than cytoplasm (g) in control U937 cells the same as antibody arraytube present in both nucleus (b) and cytoplasm (a) in Fig. 3.12. From this result it can be known that antibody microarray technology reflects the global situation.

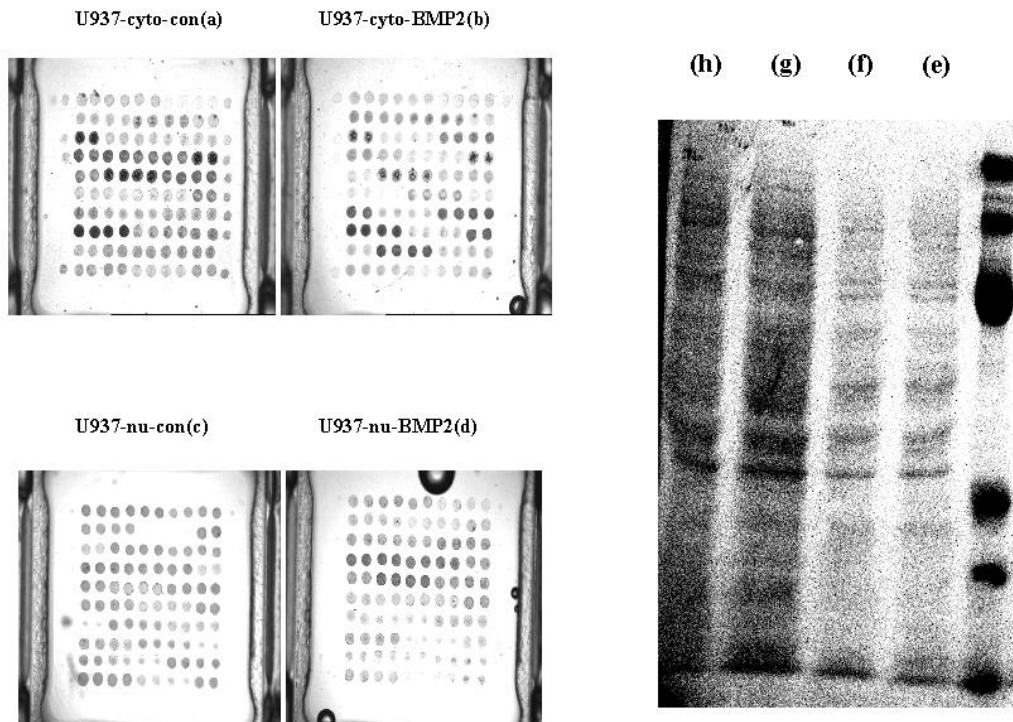


Figure 3.12: Comparison between Ponceau S staining and microarray in U937 cells. Ponceau S staining of cytoplasmic and nuclear proteins of control U937 cells separated on SDS-PAGE gel. The result of Ponceau S staining shows weaker distribution in nucleus (e) than cytoplasm (g) in control U937 cells the same as antibody arraytube present in both nucleus (b) and cytoplasm (a).

3.2.1 Total p-Tyrosine and p-p38, p38 Increased: Cytoplasm and Nucleus Increasing

Phospho-p38 and phospho-Tyrosine displayed increase in cytoplasm and nucleus of 2000 ng/ml BMP2 treated U937 cells for 3 days, when compared with control U937 cells. Total protein (sum of cytoplasm and nucleus) levels of phospho-p38 and phospho-Tyrosine are higher in BMP2 treated U937 cells than in control cells. The cytoplasmic & nuclear change pattern of p38 is similar with that of phospho-p38. This result demonstrates the consistence between protein and phosphorylation expression, as shown in Fig. 3.13, 3.14.

3.2.2 Total p-ERK and p-JNK Increased: Cytoplasm Increasing and Nucleus Unchanged

Phospho-ERK and phospho-JNK displayed increase in cytoplasm and un-changed in nucleus of 2000 ng/ml BMP2 treated U937 cells for 3 days, when compared with control U937 cells. Total protein (sum of cytoplasm and nucleus) levels of phospho-ERK and phospho-JNK are higher in BMP2 treated U937 cells than in control cells, whereas the cytoplasmic activities of ERK and JNK are higher and nuclear activities of ERK and JNK un-changed in BMP2 treated U937 cells than in control cells, as shown in Fig. 3.13, 3.14.

3.2.3 Total p-Akt Increased: Cytoplasm Increasing and Nucleus Decreasing

Phospho-Akt displayed increase in cytoplasm and slightly decrease in nucleus of 2000 ng/ml BMP2 treated U937 cells for 3 days, when compared with control U937 cells. Total protein (sum of cytoplasm and nucleus) level of phospho-Akt is higher in BMP2 treated U937 cells than in control cells, whereas the cytoplasmic activity of akt is higher in BMP2 treated U937 cells than in control cells and nuclear activity is lower in BMP2 treated U937 cells than in control cells, as shown in Fig. 3.13, 3.14.

Western blotting analysis of phosphorylation and localization of BMP2 treated U937 cells with phospho-Akt antibody, the higher phospho-Akt expression in cytoplasm at line 1 and the very lower phospho-Akt expression in nucleus at line 2, as shown in Fig. 3.15(f). This result is consistent with antibody microarray (Figure 3.15b, d). Western blotting analysis of BMP2 treated U937 cells with actin antibody, the same amount of actin expression displayed in cytoplasm at line 1 and in nucleus at line 2, as shown in Fig. 3.15(g).

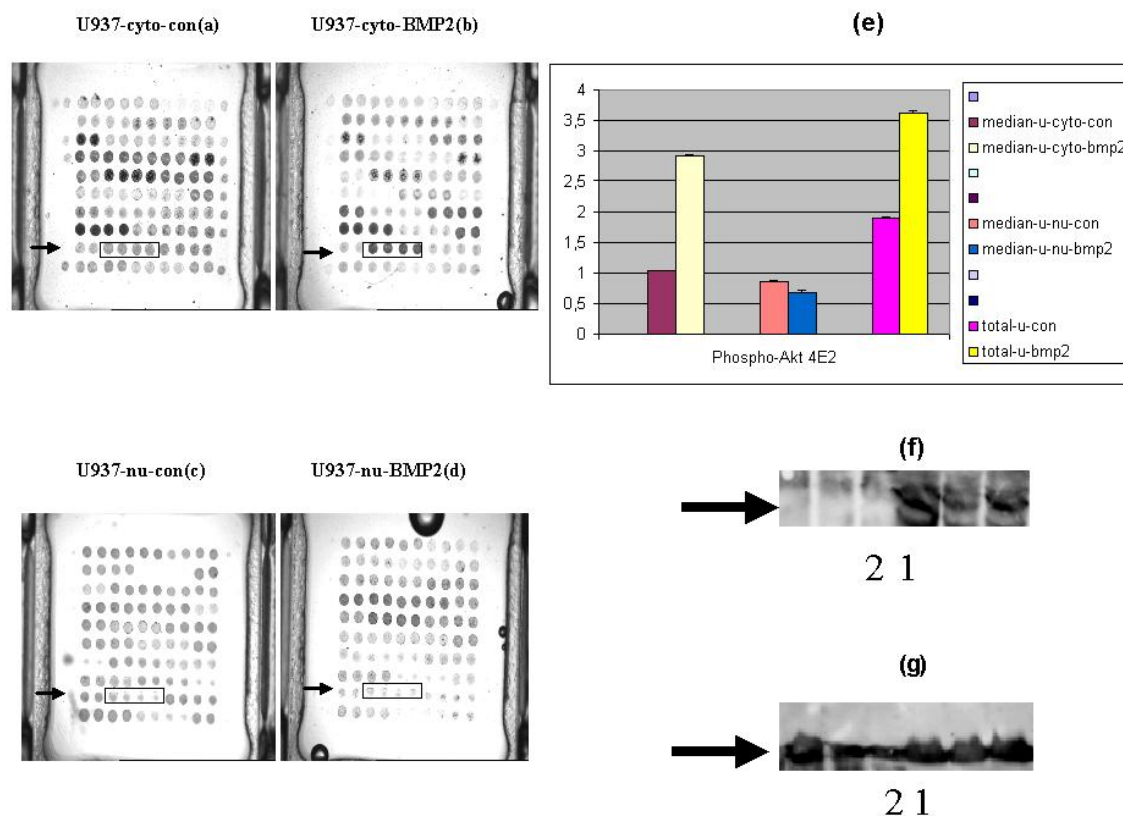


Figure 3.15: p-Akt(ser473) modulation of phosphorylation and localization in BMP2 treated U937 cells. (a-d) Antibody micro-array analysis of p-Akt, untreated (a,c) and treated (b,d) with 2000ng/ml BMP2 for 3 days. (a,b) Cytoplasm; (c,d) Nucleus. Position of p-Akt antibody is marked with frame and arrow. (e) Graphic display of numerical value analysis. BMP2 treated U937 cells displayed the increase in cytoplasm and the slight decrease in nucleus. Total protein (sum of cytoplasm and nucleus) level of phospho-Akt is higher in BMP2 treated U937 cells than in control cells. Each column indicates a mean of four measurements with standard deviations. (f) Western blotting analysis of phosphorylation and localization of BMP2 treated U937 cells with phospho-Akt antibody, the higher phospho-Akt expression in cytoplasm at line 1 and the very lower phospho-Akt expression in nucleus at line 2. This result is consistent with antibody microarray (b, d). (g) Western blotting analysis of BMP2 treated U937 cells with actin antibody, the same amount of actin expression displayed in cytoplasm at line 1 and in nucleus at line 2.

3.2.4 Total p-Smad1, p-Smad2/3, c-Myc and p-STAT3 Unchanged: Cytoplasm Decreasing and Nucleus Increasing

Phospho-Smad1, p-Smad2/3, c-Myc and p-STAT3 displayed decrease in cytoplasm and increase in nucleus of 2000 ng/ml BMP2 treated U937 cells for 3 days, when compared with control U937 cells. Total protein (sum of cytoplasm and nucleus) levels of phospho-Smad1, p-Smad2/3, c-Myc and p-STAT3 were not altered between control and BMP2 treated cells, whereas the nuclear activities of Smad1, Smad2/3, c-Myc and STAT3 are higher in BMP2 treated U937 cells than in control cells and cytoplasmic activities of Smad1, Smad2/3, c-Myc and STAT3 are lower in BMP2 treated U937 cells than in control cells, as shown in Fig. 3.13, 3.14.

Western blotting analysis of phosphorylation and localization of BMP2 treated U937 cells with phospho-smad1 antibody, the similar amount of phospho-smad1 expression displayed in cytoplasm at line 1 and in nucleus at line 2, as shown in Fig. 3.16(f). This result is consistent with antibody microarray (Figure 3.16b, d). Western blotting analysis of BMP2 treated U937

cells with actin antibody, the same amount of actin expression displayed in cytoplasm at line 1 and in nucleus at line 2, as shown in Fig. 3.16(g).

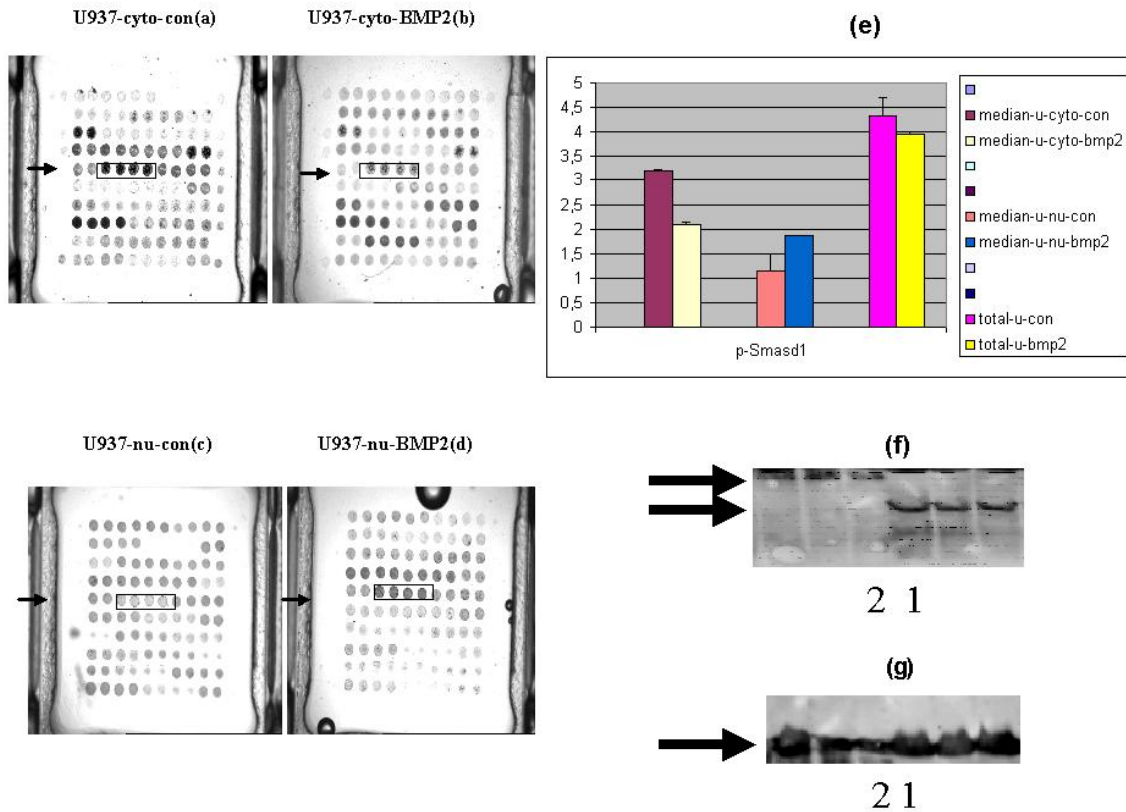


Figure 3.16: p-Smad1(ser 463/465) modulation of phosphorylation and localization in BMP2 treated U937 cells. (a-d) Antibody micro-array analysis of p-Smad1(ser 463/465), untreated (a,c) and treated (b,d) with 2000ng/ml BMP2 for 3 days. (a,b) Cytoplasm; (c,d) Nucleus. Position of p-Smad1(ser 463/465) antibody is marked with frame and arrow. (e) Graphic display of numerical value analysis. BMP2 treated U937 cells displayed the decrease in cytoplasm and the increase in nucleus. Total protein (sum of cytoplasm and nucleus) level of phospho-Smad1 was not altered between control and BMP2 treated cells. Each column indicates a mean of four measurements with standard deviations. (f) Western blotting analysis of phosphorylation and localization of BMP2 treated U937 cells with phospho-smad1 antibody, the similar amount of phospho-smad1 expression displayed in cytoplasm at line 1 and in nucleus at line 2. This result is consistent with antibody microarray (b, d). (g) Western blotting analysis of BMP2 treated U937 cells with actin antibody, the same amount of actin expression displayed in cytoplasm at line 1 and in nucleus at line 2.

Western blotting analysis of phosphorylation and localization of BMP2 treated U937 cells with phospho-STAT3 antibody, the higher amount of phospho-STAT3 expression displayed in cytoplasm at line 1 and the lower amount of phospho-STAT3 expression in nucleus at line 2, as shown in Fig. 3.17(f). This result is consistent with antibody microarray (Figure 3.17b, d). Western blotting analysis of BMP2 treated U937 cells with actin antibody, the same amount of actin expression displayed in cytoplasm at line 1 and in nucleus at line 2, as shown in Fig. 3.17(g).

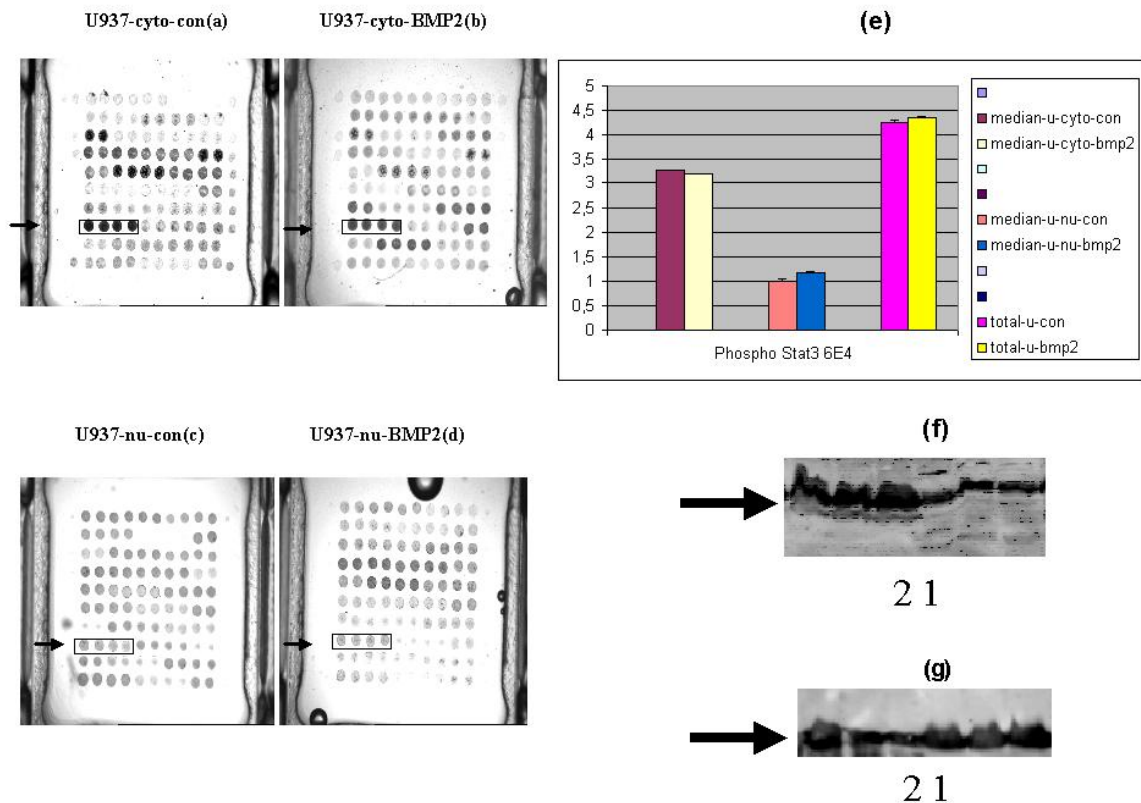


Figure 3.17: p-STAT3 (ser 727) modulation of phosphorylation and localization in BMP2 treated U937 cells. (a-d) Antibody micro-array analysis of p-STAT3, untreated (a,c) and treated (b,d) with 2000ng/ml BMP2 for 3 days. (a,b) Cytoplasm; (c,d) Nucleus. Position of p-STAT3 antibody is marked with frame and arrow. (e) Graphic display of numerical value analysis. BMP2 treated U937 cells displayed the slight decrease in cytoplasm and the slight increase in nucleus. Total protein (sum of cytoplasm and nucleus) level of phospho-STAT3 is almost the same in BMP2 treated U937 cells as in control cells. Each column indicates a mean of four measurements with standard deviations. (f) Western blotting analysis of phosphorylation and localization of BMP2 treated U937 cells with phospho-STAT3 antibody, the higher amount of phospho-STAT3 expression displayed in cytoplasm at line 1 and the lower amount of phospho-STAT3 expression in nucleus at line 2. This result is consistent with antibody microarray (b, d). (g) Western blotting analysis of BMP2 treated U937 cells with actin antibody, the same amount of actin expression displayed in cytoplasm at line 1 and in nucleus at line 2.

3.2.5 Total p-P70S6 Unchanged: Cytoplasm Increasing and Nucleus Decreasing

Phospho-p70S6 displayed increase in cytoplasm and decrease in nucleus of 2000 ng/ml BMP2 treated U937 cells for 3 days, when compared with control U937 cells. Total protein (sum of cytoplasm and nucleus) level of phospho-p70S6 was not altered in control and BMP2 treated cells, as shown in Fig. 3.13-14.

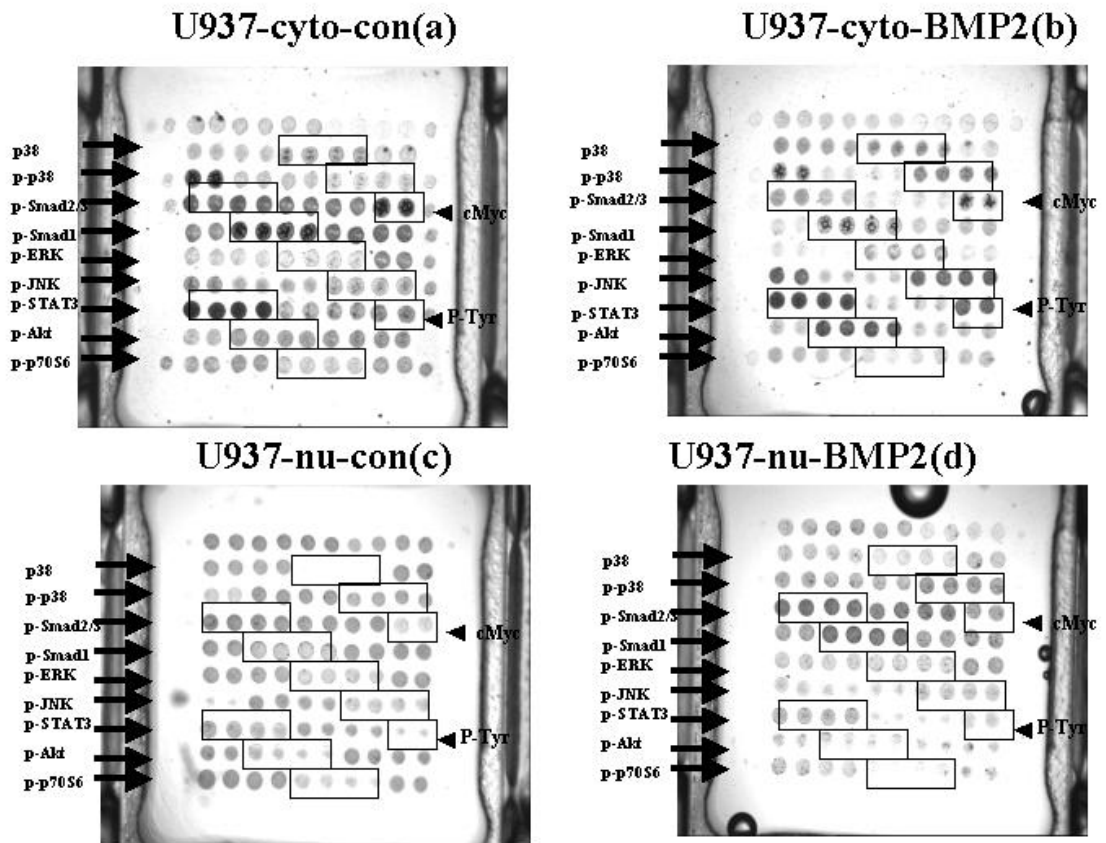
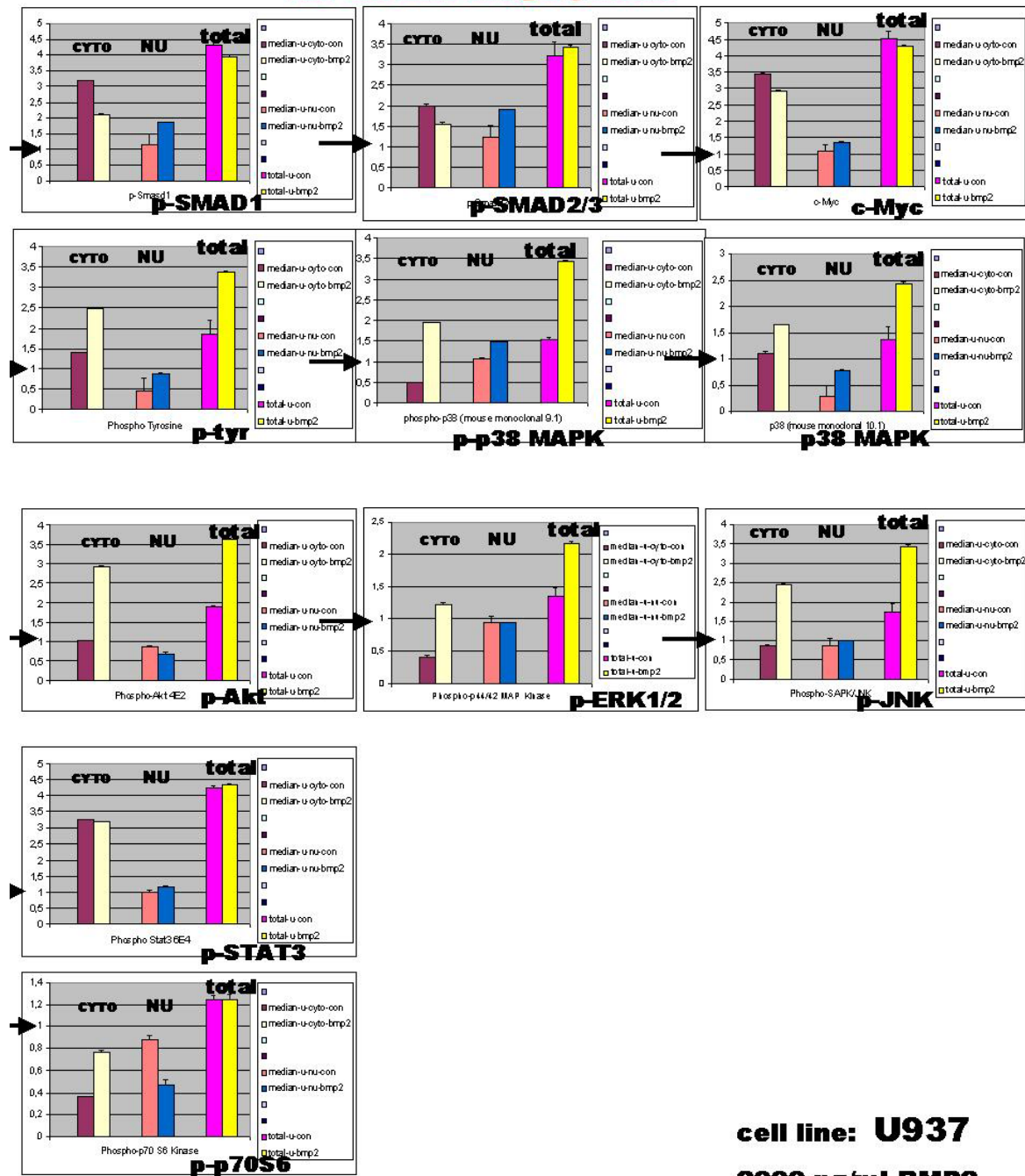


Figure 3.13: Antibody micro-array analysis of phosphorylation and localization in control and BMP2 treated U937 cells. Untreated (a,c) and treated (b,d) with 2000ng/ml BMP2 for 3 days. (a,b) Cytoplasm; (c,d) Nucleus. Positions of p38, p-p38, p-Smad2/3, p-Smad1, p-ERK, p-JNK, p-STAT3, p-Akt and p-p70S6 antibodies are marked with frame and arrow separately.

Five different changed patterns



cell line: **U937**
2000 ng/ml BMP2

Figure 3.14: Graphic numerical value analysis of phosphorylation and localization modulation in BMP2 treated U937 cells. P-p38, p38 and p-Tyr100 displayed the increase in cytoplasm and nucleus of BMP2 treated U937 cells. Total protein (sum of cytoplasm and nucleus) level of p-p38, p38 and phospho-Tyrosine100 are higher in BMP2 treated U937 cells than in control U937 cells. p-ERK (thr202/tyr204) and p-JNK(thr183/tyr185) displayed the increase in cytoplasm and unchanged in nucleus in BMP2 treated U937 cells. Total protein (sum of cytoplasm and nucleus) level of p-ERK and p-JNK are higher in BMP2 treated U937 cells than in control cells. p-Akt(ser473) displayed the increase in cytoplasm and the slight decrease in nucleus in BMP2 treated U937 cells. Total protein (sum of cytoplasm and nucleus) level of phospho-Akt is higher in BMP2 treated U937 cells than in control cells. p-Smad1, p-Smad2/3, c-Myc and p-STAT3 displayed the increase in cytoplasm and the decrease in nucleus in BMP2 treated U937 cells. Total protein (sum of cytoplasm and nucleus) level of p-Smad1, p-Smad2/3, c-Myc and p-STAT3 were not altered between control and BMP2 treated cells. P-p70S6(thr389) displayed the increase in cytoplasm and the decrease in nucleus in BMP2 treated U937 cells. Total protein (sum of cytoplasm and nucleus) levels of phospho-p70S6 was not altered in control and BMP2 treated cells. Each column indicates a mean of four measurements with standard deviations. Different antibodies have different affinities, arrow indicating each antibody quantity value 1 position.

3.3 Modulation of Phosphorylation and localization in BMP2 treated MCF-7 cells

Ponceau S staining of cytoplasmic and nuclear proteins in control MCF-7 cells separated on SDS-PAGE gel. The result of Ponceau S staining shows similar size distribution in nucleus (c) and cytoplasm (d) in control MCF-7 cells. Using the antibody arraytube for phosphorylated proteins, most proteins are present in both nucleus (b) and cytoplasm (a) in Fig. 3.18. From this result it can be known antibody microarray reflecting the global situation.

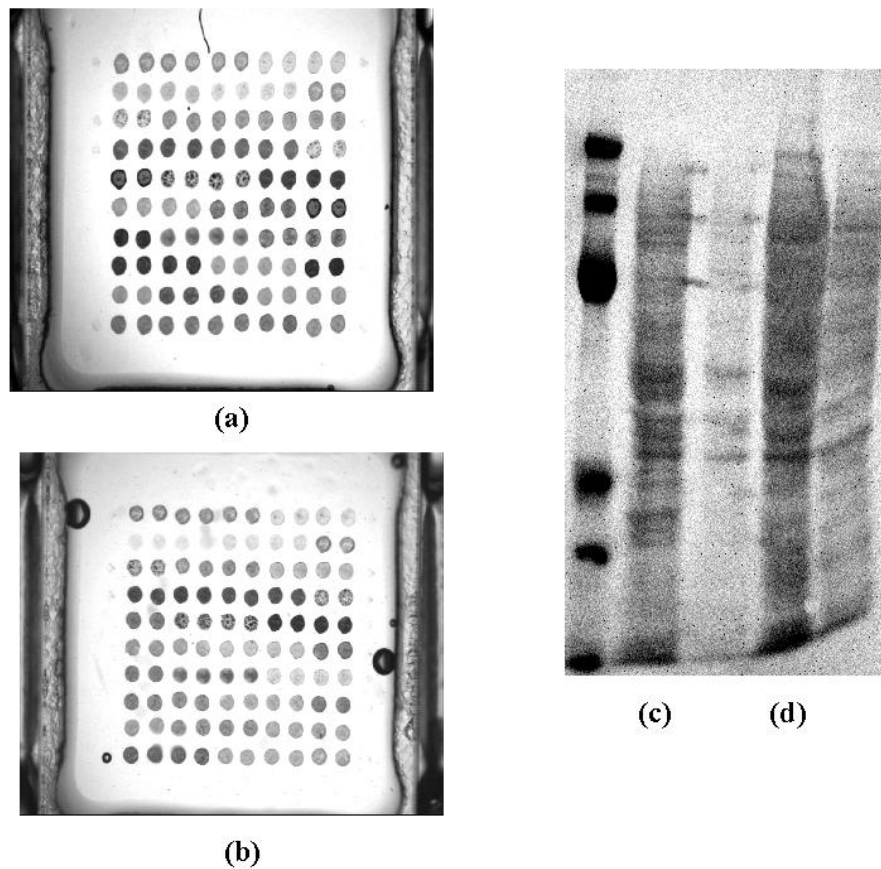


Figure 3.18: Comparison between Ponceau S staining and micorarray in MCF-7 cells. Ponceau S staining of cytoplasmic and nuclear proteins in control MCF-7 cells separated on SDS-PAGE gel. The result of Ponceau S staining shows similar size distribution in nucleus (c) and cytoplasm (d) in control MCF-7 cells. Using the antibody arraytube for phosphorylated proteins, most proteins are present in both nucleus (b) and cytoplasm (a).

3.3.1 Total p-JNK, p-Smad1, p-Smad2/3, p-p38 and p38 Unchanged: Cytoplasm Increasing and Nucleus Decreasing

p-JNK, p-Smad1, p-Smad2/3, p-p38 and p38 displayed increase in cytoplasm and correspondingly decrease in nucleus of 100ng/ml BMP2 treated MCF-7 cells for 4hr, when compared with control MCF-7 cells. Total protein (sum of cytoplasm and nucleus) levels of p-JNK, p-Smad1, p-Smad2/3, p-p38 and p38 are almost the same in BMP2 treated MCF-7 cells as in control cells, shown in Fig. 3.22-23.

Western blotting analysis of phosphorylation and localization of control and BMP2 treated MCF-7 cells with phospho-Smad1 antibody, the similar amount of phospho-Smad1 expression displayed in nucleus of control MCF-7 cells at line 1 and in nucleus of BMP2 treated MCF-7 cells at line 2, as shown in Fig. 3.21(f). This result is consistent with antibody microarray (Figure 3.21c, d). Western blotting analysis of control MCF-7 cells with actin antibody, the same amount appeared in nucleus of control MCF-7 cells at line 1 and in nucleus of BMP2 treated MCF-7 cells at line 2, as shown in Fig. 3.21 (g).

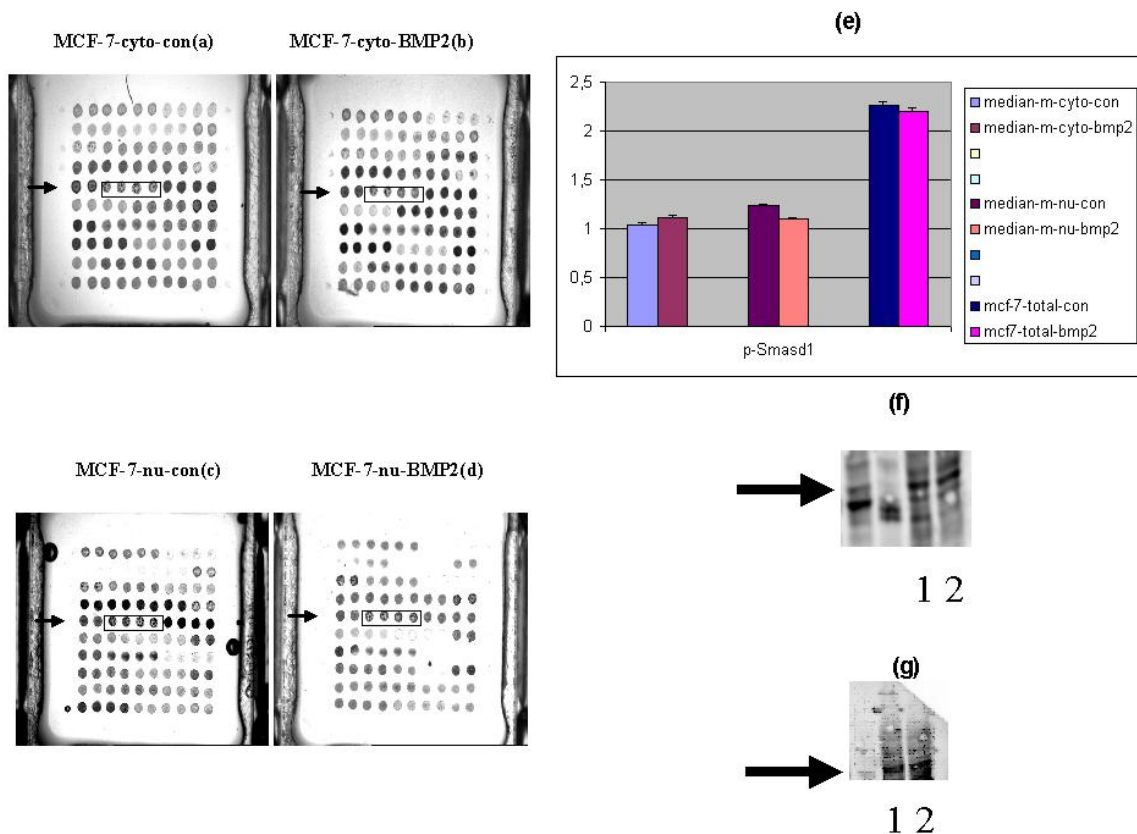


Figure 3.21: p-Smad1(ser 463/465) modulation of phosphorylation and localization in BMP2 treated MCF-7 cells. (a-d) Antibody micro-array analysis of p-Smad1(ser 463/465), untreated (a,c) and treated (b,d) with 100ng/ml BMP2 for 4h. (a,b) Cytoplasm; (c,d) Nucleus. Position of p-Smad1(ser 463/465) antibody is marked with frame and arrow. (e) Graphic display of numerical value analysis. BMP2 treated MCF-7 cells displayed unchanged in cytoplasm and the little decrease in nucleus. Total protein (sum of cytoplasm and nucleus) level of phospho-Smad1 was not significantly altered in BMP2 treated cells compared with control. Each column indicates a mean of four measurements with standard deviations. (f) Western blotting analysis of phosphorylation and localization of control and BMP2 treated MCF-7 cells with phospho-Smad1

antibody, the similar amount of phospho-Smad1 expression displayed in nucleus of control MCF-7 cells at line 1 and in nucleus of BMP2 treated MCF-7 cells at line 2. This result is consistent with antibody microarray (c, d). (g) Western blotting analysis of control MCF-7 cells with actin antibody, the same amount appeared in nucleus of control MCF-7 cells at line 1 and in nucleus of BMP2 treated MCF-7 cells at line 2.

3.3.2 p-Tyrosine, p-STAT3, p-ERK and p-P70S6 Increased: Cytoplasm Increasing and nucleus unchanged

Phospho-Tyrosine, p-STAT3, p-ERK and p-P70S6 displayed increase in cytoplasm and unchanged in nucleus 100ng/ml BMP2 treated MCF-7 cells for 4hr, when compared with control MCF-7 cells. Total protein (sum of cytoplasm and nucleus) levels of p-Tyrosine, p-STAT3, p-ERK and p-P70S6 have increase in BMP2 treated MCF-7 cells compared with control cells, whereas cytoplasmic activities of phospho-p38, p-Tyrosine, p-STAT3, p-ERK and p-P70S6 are higher in BMP2 treated MCF-7 cells than in control cells, the nuclear activities of phospho-p38, p-Tyrosine, p-STAT3, p-ERK and p-P70S6 are unchanged in BMP2 treated MCF-7 cells than in control cells, as shown in Fig. 22-23.

Western blotting analysis of phosphorylation and localization of control and BMP2 treated MCF-7 cells with phospho-Tyrosine specific antibody, the similar amount of phospho-Tyrosine expression displayed in nucleus of control MCF-7 cells at line 1 and in nucleus of BMP2 treated MCF-7 cells at line 2, as shown in Fig. 3.19(f). This result is consistent with antibody microarray (Figure 3.19 c, d). Western blotting analysis of control MCF-7 cells with actin antibody, the same amount appeared in nucleus of control MCF-7 cells at line 1 and in nucleus of BMP2 treated MCF-7 cells at line 2, as shown in Fig. 3.19 (g).

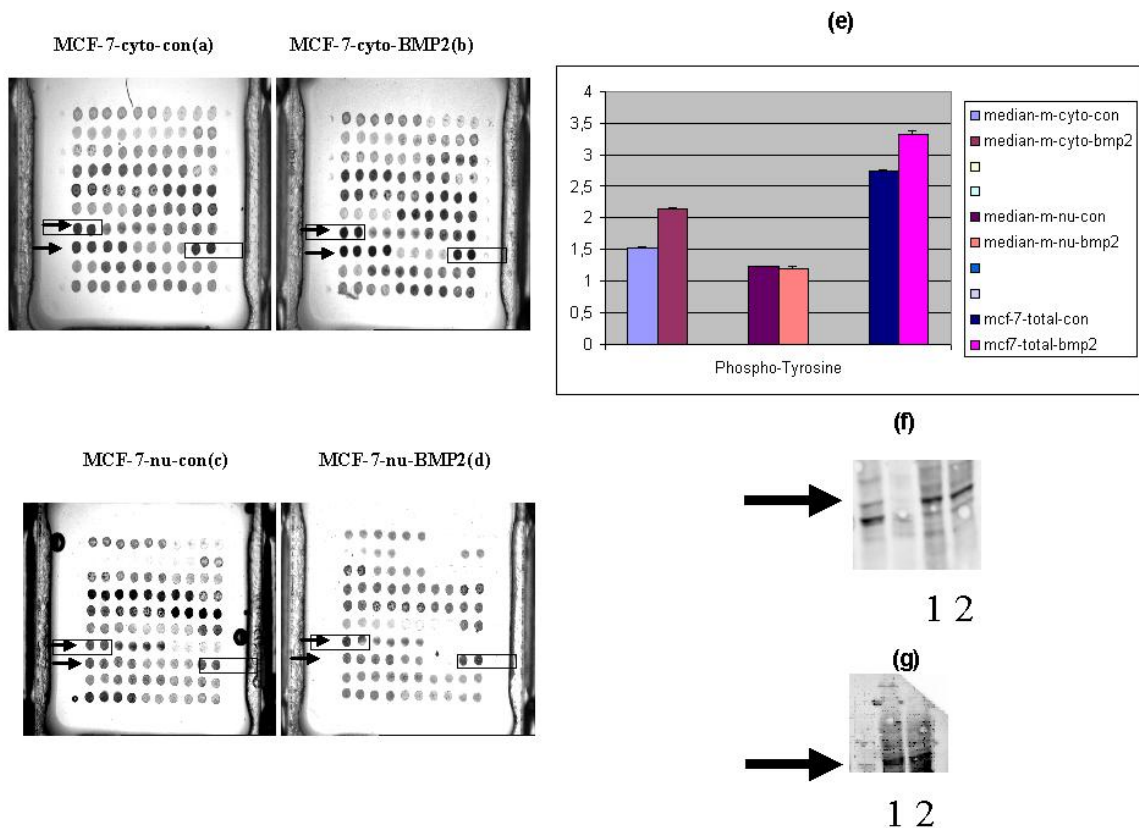


Figure 3.19: p-Tyr100 modulation of phosphorylation and localization in BMP2 treated MCF-7 cells. (a-d) Antibody micro-array analysis of p-Tyr100, untreated (a,c) and treated (b,d) with 100ng/ml BMP2 for 4h. (a,b) Cytoplasm; (c,d) Nucleus. Position of p-Tyr100 antibody is marked with frame and arrow. (e) Graphic display of numerical value analysis. BMP2 treated MCF-7 cells displayed the increase in cytoplasm and unchanged in nucleus. Total protein (sum of cytoplasm and nucleus) level of phospho-Tyrosine was higher in BMP2 treated MCF-7 cells than control cells. Each column indicates a mean of four measurements with standard deviations. (f) Western blotting analysis of phosphorylation and localization of control and BMP2 treated MCF-7 cells with phospho-Tyrosine specific antibody, the similar amount of phospho-Tyrosine expression displayed in nucleus of control MCF-7 cells at line 1 and in nucleus of BMP2 treated MCF-7 cells at line 2. This result is consistent with antibody microarray (c, d). (g) Western blotting analysis of control MCF-7 cells with actin antibody, the same amount appeared in nucleus of control MCF-7 cells at line 1 and in nucleus of BMP2 treated MCF-7 cells at line 2.

Western blotting analysis of phosphorylation and localization of control and BMP2 treated MCF-7 cells with phospho-STAT3 antibody, the similar amount of phospho-STAT3 expression displayed in nucleus of control MCF-7 cells at line 1 and in nucleus of BMP2 treated MCF-7 cells at line 2, as shown in Fig. 3.20(f). This result is consistent with antibody microarray (Figure 3.20c, d). Western blotting analysis of control MCF-7 cells with actin antibody, the same amount appeared in nucleus of control MCF-7 cells at line 1 and in nucleus of BMP2 treated MCF-7 cells at line 2, as shown in Fig. 3.20 (g).

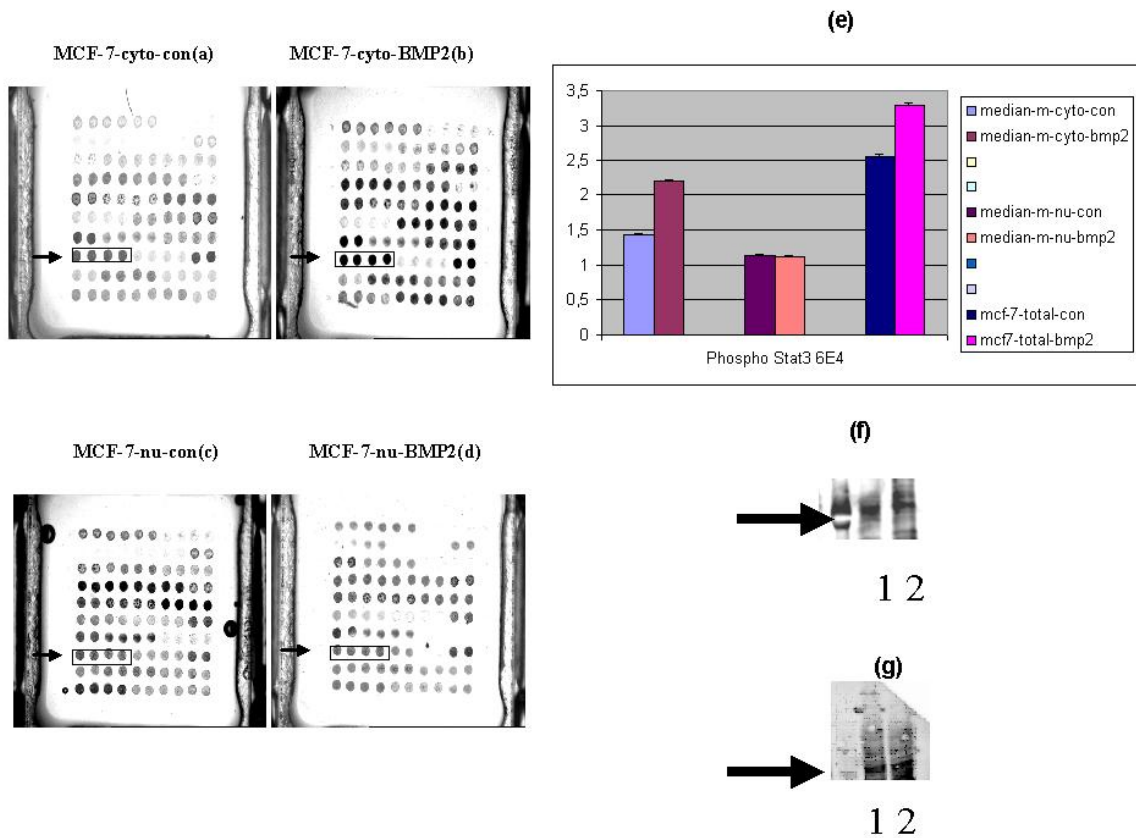


Figure 3.20: p-STAT3 (ser 727) modulation of phosphorylation and localization in BMP2 treated MCF-7 cells. (a-d) Antibody micro-array analysis of p-STAT3, untreated (a,c) and treated (b,d) with 100ng/ml BMP2 for 4h. (a,b) Cytoplasm; (c,d) Nucleus. Position

of p-STAT3 antibody is marked with frame and arrow. (e) Graphic display of numerical value analysis. BMP2 treated MCF-7 cells displayed the decrease in cytoplasm and unchanged in nucleus. Total protein (sum of cytoplasm and nucleus) level of phospho-STAT3 was higher in BMP2 treated MCF-7 cells than control cells. Each column indicates a mean of four measurements with standard deviations. (f) Western blotting analysis of phosphorylation and localization of control and BMP2 treated MCF-7 cells with phospho-STAT3 antibody, the similar amount of phospho-STAT3 expression displayed in nucleus of control MCF-7 cells at line 1 and in nucleus of BMP2 treated MCF-7 cells at line 2. This result is consistent with antibody microarray (c, d). (g) Western blotting analysis of control MCF-7 cells with actin antibody, the same amount appeared in nucleus of control MCF-7 cells at line 1 and in nucleus of BMP2 treated MCF-7 cells at line 2.

3.3.3 Total c-Myc Unchanged: Nucleus Slightly Increasing and Cytoplasm Slightly Decreasing

c-Myc displayed slightly increase in nucleus and slightly decrease in cytoplasm of 100ng/ml BMP2 treated MCF-7 cells for 4hr, when compared with control MCF-7 cells. Total protein (sum of cytoplasm and nucleus) level of c-Myc was not altered between BMP2 treated and control MCF-7 cells, whereas in BMP2 treated MCF-7 cells it was translocated into nucleus, as shown in Fig. 3.22-23.

3.3.4 Total p-Akt Unchanged: Nucleus and Cytoplasm unchanged

p-Akt displayed unchanged in nucleus and cytoplasm, as shown in Fig. 3.22-23.

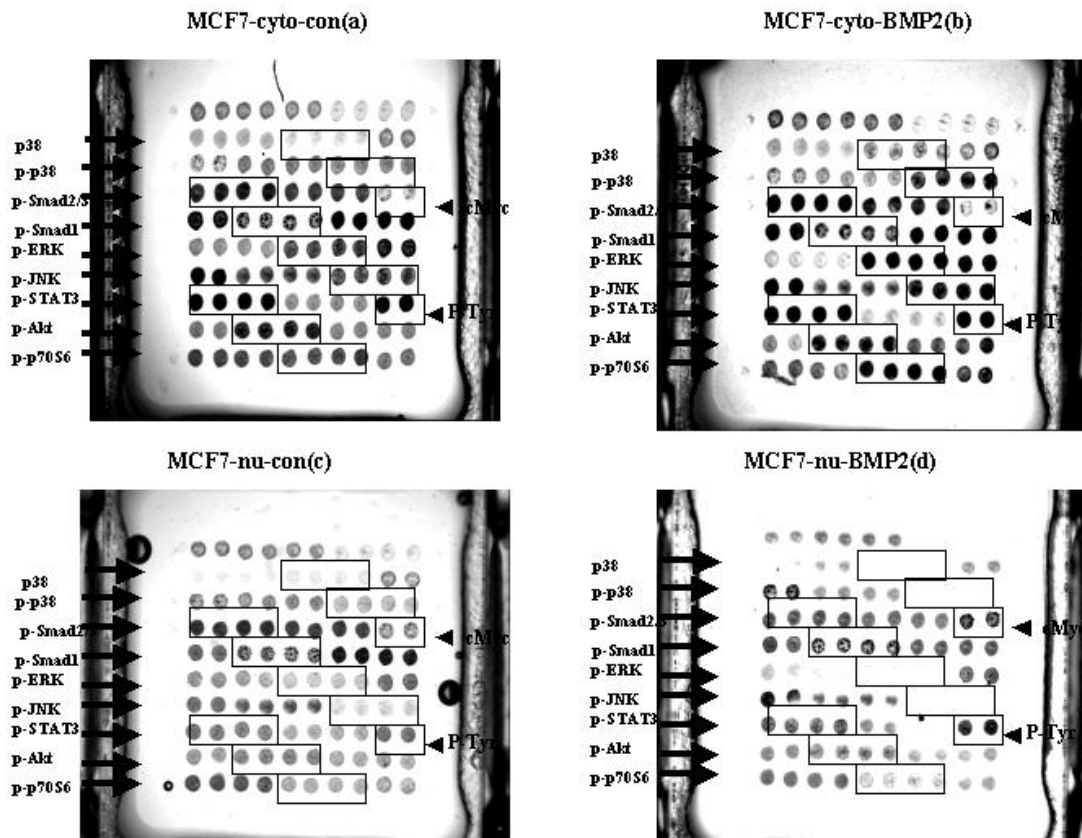
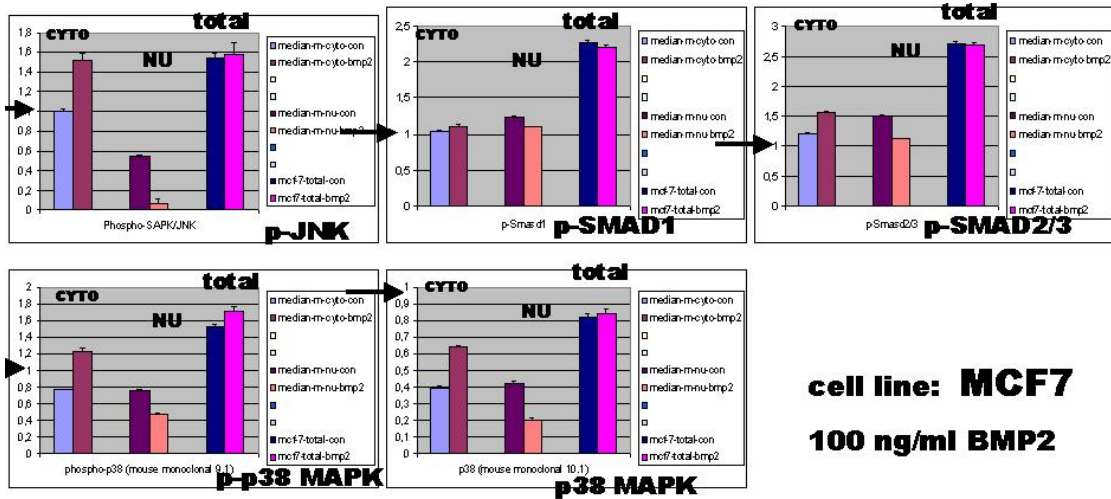


Figure 3.22: Antibody micro-array analysis of phosphorylation and localization in control and BMP2 treated MCF7 cells. Untreated (a,c) and treated (b,d) with 100ng/ml BMP2 for 4h. (a,b) Cytoplasm; (c,d) Nucleus. Positions of p38, p-p38, p-Smad2/3, p-Smad1, p-ERK, p-JNK, p-STAT3, p-Akt and p-p70S6 antibodies are marked with frame and arrow separately.

five different patterns



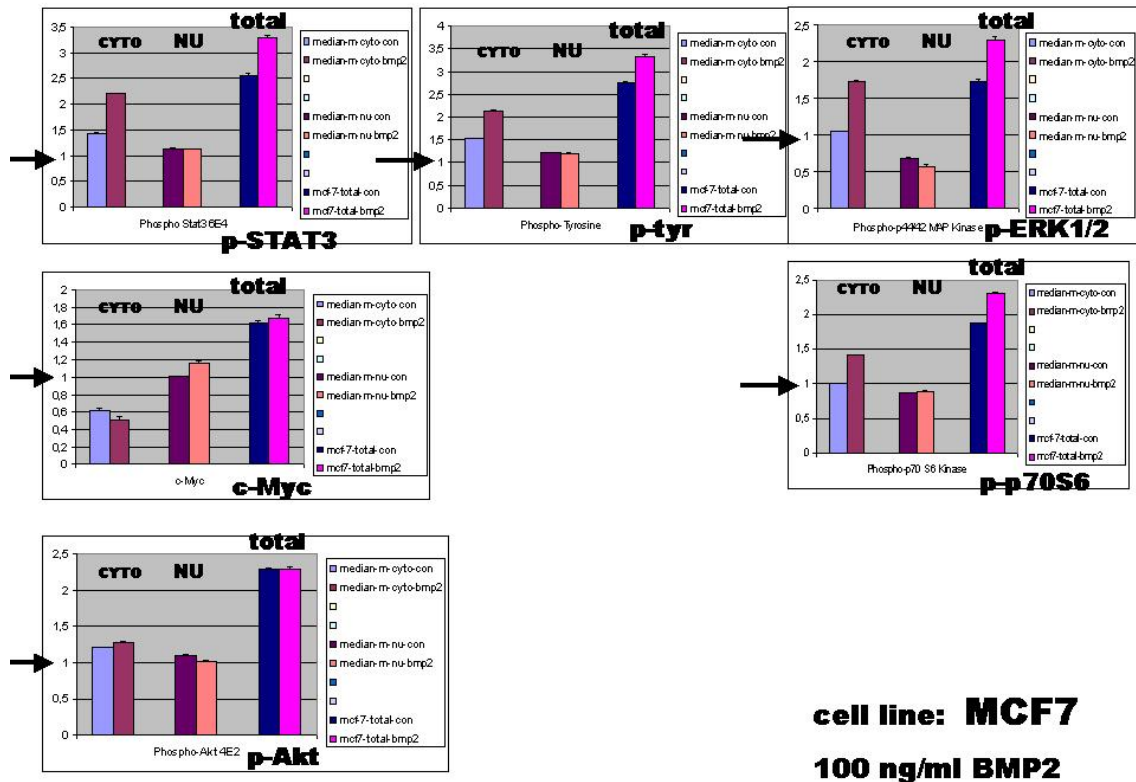


Figure 3.23: Graphic numerical value analysis of phosphorylation and localization modulation in BMP2 treated MCF7 cells. phospho-p38 and p38, p-JNK, p-Smad1, p-Smad2/3 displayed the increase in cytoplasm and the decrease in nucleus of BMP2 treated MCF7 cells. Total protein (sum of cytoplasm and nucleus) level of phospho-p38 and p38, p-JNK, p-Smad1, p-Smad2/3 were not significantly changed in BMP2 treated MCF-7 cells and control cells. c-Myc displayed the slight decrease in cytoplasm and the slight increase in nucleus of BMP2 treated MCF7 cells. Total protein (sum of cytoplasm and nucleus) level of c-Myc was not significantly altered between BMP2 treated MCF-7 cells and control cells. p-Tyrosine, p-STAT3, p-ERK and p-P70S6 displayed the increase in cytoplasm and unchanged in nucleus of BMP2 treated MCF7 cells. Total protein (sum of cytoplasm and nucleus) level of p-p38, p-Tyrosine, p-STAT3, p-ERK and p-P70S6 were increased in BMP2 treated cells. P-Akt displayed unchanged in cytoplasm and nucleus of BMP2 treated MCF7 cells. Each column indicates a mean of four measurements with standard deviations. Different antibodies have different affinities, arrow indicating each antibody quantity value 1 position.

3.4 Modulation of Phosphorylation and localization in STI571 treated K562 cells

3.4.1 Total p-Akt and p-P70S6 Decreased: Cytoplasm and Nucleus Decreasing

Phospho-Akt and phospho-p70S6 displayed decrease in both cytoplasm and nucleus of 0.2 μ M STI571 treated K562 cells for 24hr, when compared with control K562 cells. Total protein (sum of cytoplasm and nucleus) levels of phospho-Akt and phospho-p70S6 are lower in treated K562 cells than control cells, as shown in Fig. 27-28.

3.4.2 Total p-p38, p38, c-Myc, p-Tyrosine, p-Smad1 and p-Smad2/3 Increased: Cytoplasm and Nucleus Increasing

Phospho-p38, p38, c-Myc, phospho-Tyrosine, phospho-Smad1 and phospho-Smad2/3 displayed increase in cytoplasm and nucleus of 0.2 μ M STI571 treated K562 cells for 24hr, when compared with control K562 cells. Total protein (sum of cytoplasm and nucleus) levels of phospho-p38, p38, c-Myc, phospho-Tyrosine, phospho-Smad1 and phospho-Smad2/3 are higher in STI571 treated K562 cells than in control cells, as shown in Fig. 3.27-28.

Western blotting analysis of phosphorylation and localization of control K562 cells with phospho-Tyrosine specific antibody showed not strong phospho-Tyrosine specific expression in nucleus at line 2 and in cytoplasm at line 1 in Fig. 3.24(f). This result is consistent with antibody microarray (Figure 3.24a,c). Immunoprecipitation analysis of phosphorylation in control K562 cells with phospho-Tyrosine specific antibody, three bands in cytoplasm at line 1, as shown in Fig. 3. 25. This result is consistent with western blotting (Figure 24(f)). Western blotting analysis of control K562 cells with actin antibody detected the same amount in nucleus at line 2 and in cytoplasm at line 1, as shown in Fig. 3.24(g).

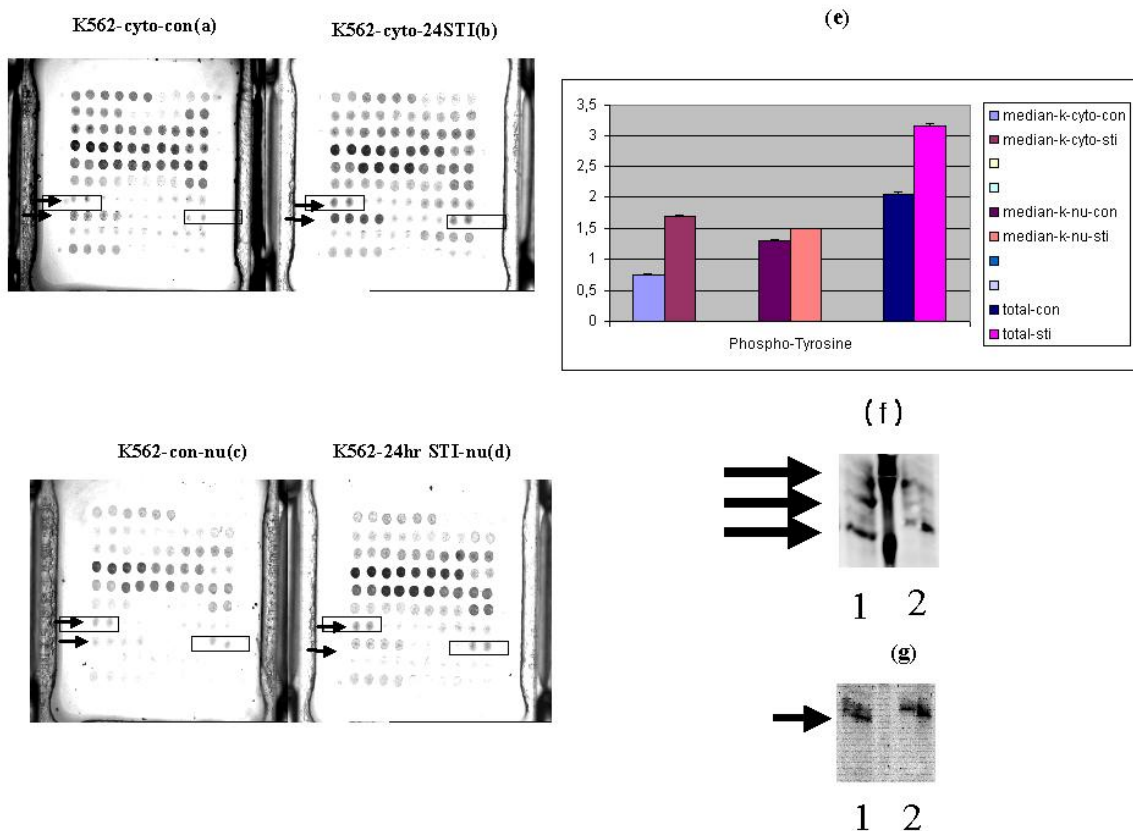


Figure 3.24: p-Tyr100 modulation of phosphorylation and localization in STI571 treated K562 cells. (a-d) Antibody micro-array analysis of p-Tyr100, untreated (a,c) and treated (b,d) with 0.2 μ M STI571 for 24h. (a,b) Cytoplasm; (c,d) Nucleus. Position of p-Tyr100 antibody is marked with frame and arrow. (e) Graphic display of numerical value analysis. STI571 treated K562 cells displayed the increase in cytoplasm and nucleus. Total protein (sum of cytoplasm and nucleus) level of phospho-Tyrosine is higher in STI571 treated cells than in control. Each column indicates a mean of four measurements with standard deviations. (f) Western blotting analysis of phosphorylation and localization of control K562 cells with phospho-Tyrosine specific antibody, showing not strong phospho-

Tyrosine concentration in nucleus at line 2 and in cytoplasm at line 1. The result is consistent with antibody microarray.

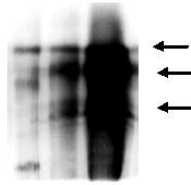


Figure 3.25: phospho-Tyrosine immunoprecipitation analysis of cytoplasm in control K562 cells. Three bands are visible in cytoplasm of control K562 cells at line 1 with phospho-Tyrosine specific antibody (Fig. 41).

Western blotting analysis of phosphorylation and localization of control K562 cells with phospho-p38 antibody showed not strong phospho-p38 expression in nucleus at line 2 and in cytoplasm at line 1 in Fig. 3.26(f). This result is consistent with antibody microarray (Figure 3.26a,c). Western blotting analysis of control K562 cells with actin antibody detected the same amount in nucleus at line 2 and in cytoplasm at line 1, as shown in Fig. 3.26(g).

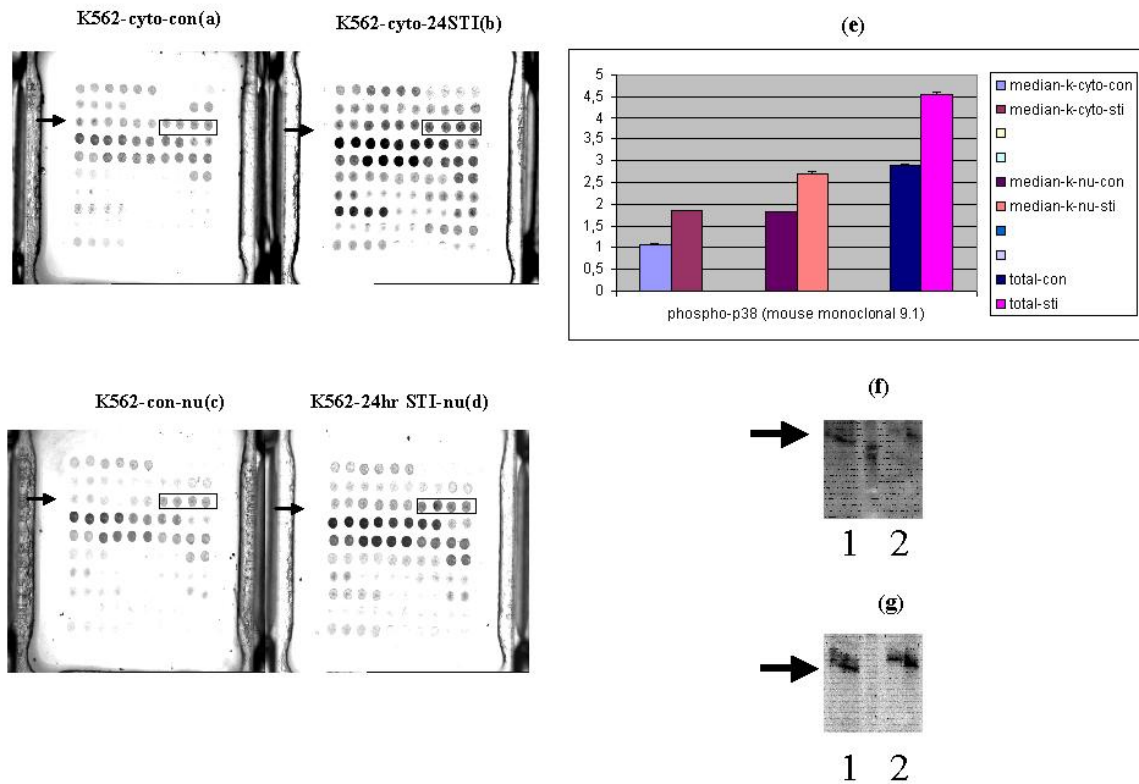


Figure 3.26: p-p38(thr180/tyr182) modulation of phosphorylation and localization in STI571 treated K562 cells. (a-d) Antibody micro-array analysis of p-p38, untreated (a,c) and treated (b,d) with 0.2 μ M STI571 for 24h. (a,b) Cytoplasm; (c,d) Nucleus. Position of p-p38 antibody is marked with frame and arrow. (e) Graphic display of numerical value analysis. STI571 treated K562 cells displayed the increase in cytoplasm and nucleus. Total protein (sum of cytoplasm and nucleus) level of phospho-p38 is higher in STI571 treated cells than in control. Each column indicates a mean of four measurements with standard deviations.

3.4.3 Total p-STAT3 and p-JNK Increased: Cytoplasm Increasing and Nucleus Unchanged

Phospho-STAT3 and p-JNK displayed increase in cytoplasm and un-changed in nucleus of 0.2 μ M STI571 treated K562 cells for 24hr, when compared with control K562 cells. Total protein (sum of cytoplasm and nucleus) levels of phospho-STAT3 and phospho-JNK are higher in STI571 treated K562 cells than in control cells, as shown in Fig. 3. 27-28.

3.4.4 Total p-ERK Increased: Cytoplasm Decreasing and Nucleus Increasing

Phospho-ERK displayed increase in nucleus and little decrease in cytoplasm of 0.2 μ M STI571 treated K562 cells for 24hr, when compared with control K562 cells. Total protein (sum of cytoplasm and nucleus) level of phospho-ERK is higher in STI571 treated K562 cells than in control cells, whereas the nuclear activity of ERK is higher and cytoplasmic activity lower of STI571 treated K562 cells than in control cells, as shown in Fig. 3.27-28.

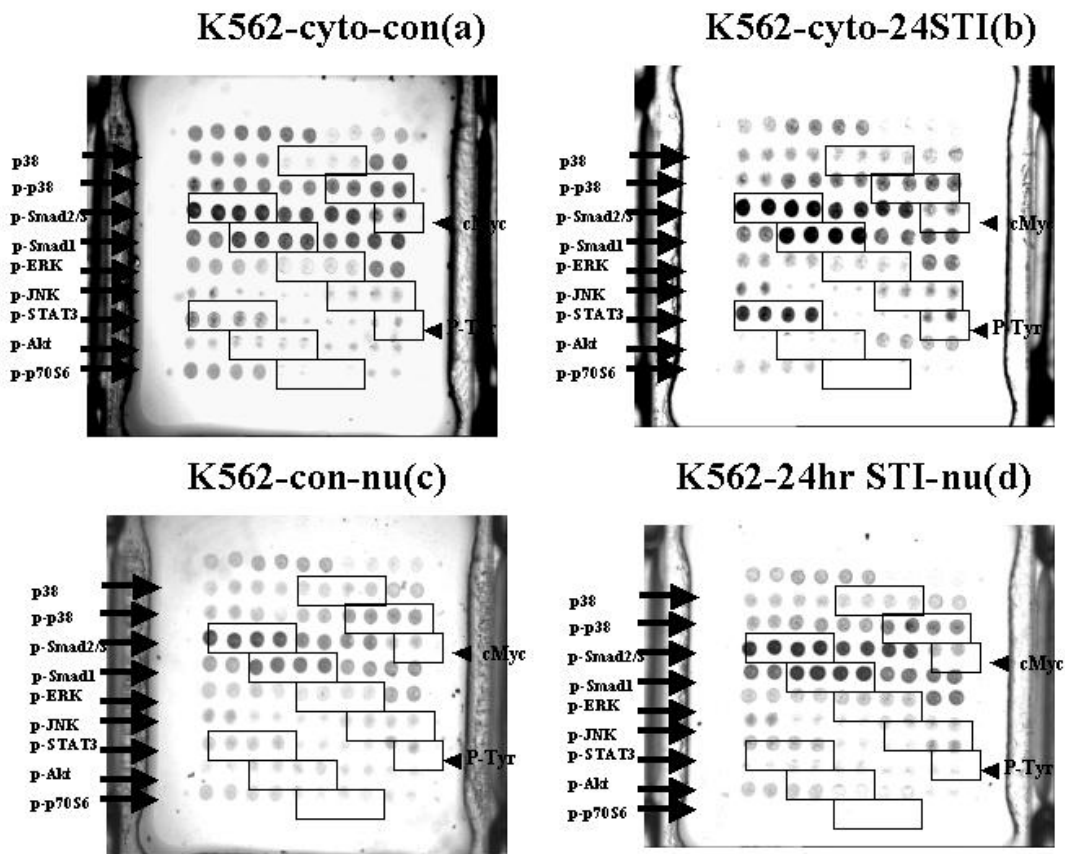
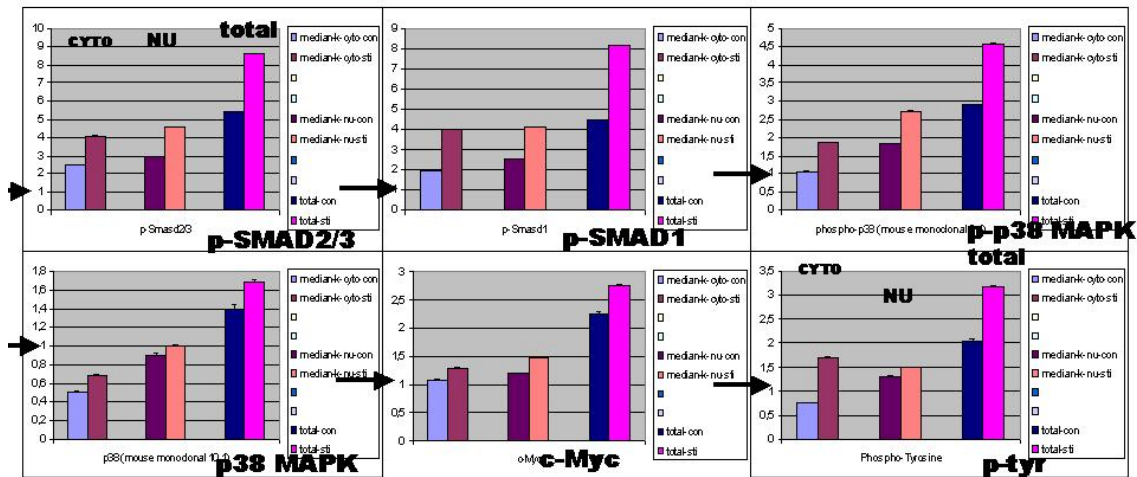


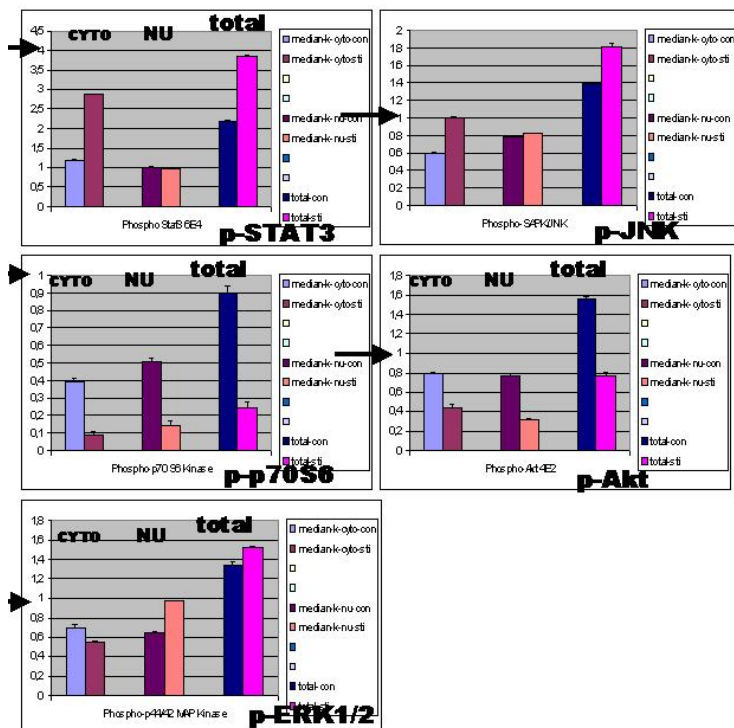
Figure 3.27: Antibody micro-array analysis of phosphorylation and localization in control and STI571 treated K562 cells. Untreated (a,c) and treated (b,d) with 0.2 μ M STI571 for 24h. (a,b) Cytoplasm; (c,d) Nucleus. Positions of p38, p-p38, p-Smad2/3, p-Smad1, p-ERK, p-JNK, p-STAT3, p-Akt and p-p70S6 antibodies are marked with frame and arrow separately.

Five different changed patterns



cell line: K562

STI571



cell line: K562

STI571

Figure 3.28: Graphic numerical value analysis of phosphorylation and localization modulation in STI571 treated K562 cells. p-ERK(thr202/tyr204) displayed the decrease in cytoplasm and the increase in nucleus of STI571 treated K562 cells. Total protein (sum of cytoplasm and nucleus) level of p-ERK is higher in STI571 treated K562 cells than in control cells. p-JNK(thr183/tyr185) and p-STAT3 (ser 727) displayed the increase in cytoplasm and

unchanged in nucleus of STI571 treated K562 cells. Total protein (sum of cytoplasm and nucleus) level of phospho-JNK is higher in STI571 treated K562 cells than in control cells. p-p38, p38, c-Myc, p-Tyrosine, p-Smad1 and p-Smad2/3 displayed the increase in cytoplasm and nucleus of STI571 treated K562 cells. Total protein (sum of cytoplasm and nucleus) level of p-p38, p38, c-Myc, p-Tyrosine, p-Smad1 and p-Smad2/3 are higher in STI571 treated cells than in control. p-Akt(ser473) and p-p70S6(thr389) displayed the decrease in cytoplasm and nucleus of STI571 treated K562 cells. Total protein (sum of cytoplasm and nucleus) level of phospho-Akt and p-P70S6 are lower in STI571 treated K562 cells than in control cells. Each column indicates a mean of four measurements with standard deviations. Different antibodies have different affinities, arrow indicating each antibody quantity value 1 position.

4 Discussion

4.1 Antibody array technologies

“Array technologies that will provide reliable analytical tool on the protein level, will allow us to collect the necessary information on protein modifications and alterations in protein complexes present at given regulatory states of cells for studying the cell signalling and functions. Analysis of gene expression on the protein level and of post-translational protein modifications is essential for understanding different cellular functions of proteins and to follow the time course of signalling processes inside a cell. The increasing number of highly specific antibodies not just for individual proteins but also for protein modifications like site specific phosphorylation provides good tools to analyze this processes in details” (Stefan Wolf, 2003).

To facilitate studies of protein function, we have developed miniaturized assays that accommodate extremely low sample volumes and enable the rapid, simultaneous processing of many antibodies. A high-precision robot designed to manufacture complementary DNA microarrays was used to spot antibodies onto chemically derivatized glass slides at extremely lower and high spatial densities.

Cy3 and Cy5 staining of microscope-slide-size array is suitable for a large of antibody analysis. The protocol already was seen in paper, however, standard of this technology has not been set up.

In this these, to compare slide quality and storage conditions of slides at different temperature and time. 20°C for a couple of months or even longer were used between epoxy and aldehyde slide. The result showed that slides can be stored efficiently at -20°C for a couple of months or even longer. From the point it can be deduced that this technology has very high robotness; epoxy slides are more sensitive than aldehyde slides for slide quality. From the point it can be suggested that epoxy slide is more suitable for reaction.

To compare protein labelled time and amounts between one kind of protein (or antibody) and the whole protein based on relative fluorescence after labelling proteins. One kind of protein (or antibody), 20ng of protein was needed 0.01 µl of Cy3 or Cy5 mono-reactive dye, (but usually adding up to Cy3 or Cy5 mono-reactive dye 2µl. Therefore, free dye existing). However, the whole protein of cells (more than 1mg/ml) was needed about 50µg using 2-3µl of Cy3 or Cy5 mono-reactive dye; One kind of protein or antibody labeled half hour and two hours separately. However, the whole protein of cells compared among half, two and four hours. The labelled protein can be stored at -20°C more than one week for reaction later; The results demonstrates the same between labeling time of half hour and two hours. However, the whole protein of cells compared among half, two and four hours. The results demonstrates better for longer time labeling. The labelled protein can be stored at -20°C more than one week later for reaction. The result demonstrated that stored protein reaction is almost the same as before. From the point it can be indicated the labelling relationship between fluorescence and protein and deduced the labeling time difference between one kind of protein and the whole protein,

To compare stop reagent using and without using stopping reagent. Stopping reagents separately were incubated in SDS-PAGE and microscope-slide-size array for 5 min and 15 min. The result showed that hydroxylamin make dye disappeared under the observation of SDS-PAGE. For stopping time between 5min and 15 min, the result demonstrated that the long time stopping reaction signaling (15 min) is weaker than the short time stopping reaction (5 min); Without using stop reagent, the result demonstrates the same as 5 min stopping and has not appeared a crosstalking reaction (from literature, stopping reagent hydroxylamin easily makes dye disconnected from protein). From this point it can be indicated that stopping reagent hydroxylamin is not necessary and even has bad effect on reaction.

To compare protein purification with different methods in order to delete free dye: G25, G50, microcon10, 30 and 50 were used for protein purification checked by protein concentration

measure (CCB). The result showed that G25 and G50 make protein dilution, and only microcon10 is the best because of no protein leaking out;

To compare results between deletion and undeletion of free mono-reactive dye Cy3 and Cy5-labelled antibodies, mono-reactive dye Cy3 and Cy5-labelled mixed antibodies were separately incubated and washed completely with each step. The result demonstrates the same as before mixture reaction and indicate no crosstalking reaction between mono-reactive dye Cy3 and Cy5-labelled antibodies. Only Cy5 free mono-reactive dye was incubated. only Cy5 free dye was incubated. The result demonstrates nothing. Therefore, free dye cannot affect the result. From this point it can be verified that microcon10 is best for protein purification and free dye has not effect on the result;

To compare blocking time. Blocking time half to one hour under PBS-0.5%Tween-BSA was used; Blocking slide were stored at -20°C several days afterwards to use for reaction. The result demonstrates the same as before; Some negative-result slide can be repeated to be used. From the point it can be deduced that this technology has very high robotness;

To compare reaction volume and time. 7 μl , 12-15 μl and 20 μl of incubation volume under different reaction time 1, 2 and 3 hours were used to react at room temperature and 4°C overnight separately. 7 μl of reaction volume makes one spotting line dropping for 18*18cm cover. 12-15 μl of reaction volume is very optimal for 18*18cm cover. 20 μl of reaction volume makes cover moving and reaction liquid out for 18*18cm cover; Reaction time used 1, 2 and 3 hours at room temperature and 4°C overnight separately. The results demonstrate the same. From the point it can be deduced that the reaction volume is vey critical for microscope-slide-size array;

To compare washing volume and time. Big volume (30 ml) three times was washed at room temperature or in the dark overnight or shake up and down by hand with vortex several times, or at 4°C overnight. Washing at room temperature in the dark overnight makes some spots moving; Washing steps can shake up and down by hand and also vortex several times, the result is the same as the big washing volume three times; Washing at 4°C overnight, the result is also good. From the point it can be deduced that washing for microscope-slide-size array can be used different methods.

Microarray is the best example for scientific research from big to small principle. Antibody arrays builded into the ArrayTube™ platform can be used to set up a relatively low cost system to analyze changes in phosphorylation of cellular proteins. With the ArrayTube™ set up it becomes possible to routinely analyze the phosphorylation of several proteins in parallel in a single experiment. And also, compared with western blotting, the change in Smad1, erk, akt, STAT3 and tyrosine phosphorylation were correlated well with ArrayTube results obtained in BMP2 treatment of the human leukemia cell line U937.

This study has developed parameters, thresholds, and testing conditions of a novel silver staining system for quantitative detection of phosphorylation and localization on chip by labelling biotinylation of cellular proteins. Silver staining technology of antibody microarrays allow for high-throughput identification of protein phosphorylation. This method is sensitive, specific, reproducible, fast and cheap, presenting obvious advantages and may find wider uses in high-throughput protein screenings in details as follows:

Nano-gold-particle mediated silver staining technology of antibody microarray overcomes and avoids the error derived from two fluorescent Cy3 and Cy5 dyes occupying and competing for the same antibody at the same time;

Quantification is possible with an on-line measurement of the silver precipitation step;

1: 5 dilution of antibody not enough to use in array for analysis because of less sensitive, most signalling very weak and only little high, more importantly, which little high signaling compared with that of original antibodies not significant. From this point it can be verified silver staining of arraytube technology specific;

Every sample for repeating experiments, the result of pictures and evaluations are the same. From this point it can be indicated the technology reproducible; Silver staining of arraytube need the lower volume and the less amount of proteins and antibodies and also shorter time for reaction. From this point it can be reflected the technology sensitive, fast and cheap;

The silver staining by labelling biotinylation to direct reaction and overcoming secondary antibody may bring unspecific reaction. From this point it can be indicated the technology specific; All the results in three cell lines are in consistence with cell numbers, FACS, western blotting, IP, Cy3 and Cy5 staining and references. From this point it can be demonstrated the technology accurate;

p38 has the similar cytoplasmic & nuclear change pattern with phospho-p38 in three cell lines. From this point it can be shown the technology verifying the consistence between protein and phosphorylation;

Ponceau S staining was used in comparison with antibody microarray showing the similar change patterns. From this point it can be known antibody microarray reflecting the global situation;

Values of standard deviation in three cell lines all are small. From this point it can be reflected Arraytube technology accurate;

The similar cytoplasmic & nuclear change patterns (such as increasing or decreasing) compared with control often appear in the same signalling in three cell lines (such as pp70S6 and p-Akt appear the same cytoplasmic & nuclear change pattern which all belong to PI3K signalling), the different patterns often appear in the different signalings in three cell lines such as between smad family and PI3K signalling. From this point it can be verified the silver staining of Arraytube technology and median normalization specific and accurate;

Some reverse results obtained between nucleus and cytoplasm of experiment and control under different functions. From this point it can be known the technology reflect not only experimental features and functions but also control situation how to different from experiment;

Here, I need to emphasize that every antibody has very lower signalling in three cell lines. From this point it can be verified silver staining of arraytube no or little unspecific reaction.

It is very surprising that we obtained good results with the three dimensional epoxy activated surface available for the ArrayTube™ platform. Although previously much higher antibody activity and finally signal can be obtained when antibodies are spotted on biopolymer gel surfaces like agarose (Afanassiev et al., 2000) or immobilized nitrocellulose, the optimized combination of 3D surface and antibody preparation used here is of sufficient quality for highly sensitive detection of proteins and protein modifications.

4.2 BMP2 signalling in U937 cells

In the BMP2 signalling, besides most researches in the relationship of smad family as all known, many studies on BMP2 signalling with p21 relationship such as Xing et al. (2002) also confirmed that BMP2 mRNA has been shown to be expressed in the mammary gland and recently BMP2 has been shown to inhibit MCF-7 proliferation as well as induce the expression of p21, and Ghosh-Choudhury N et al.(2000) indicated bone morphogenetic protein-2 induces cyclin kinase inhibitor p21 and hypophosphorylation of retinoblastoma protein in estradiol-treated MCF-7 human breast cancer cells. BMP2 caused cell cycle arrest in the G1 phase which was associated with accumulation of p21CIP1/WAF1 and p27KIP1, and the subsequent apoptosis of myeloma cells (Kawamura, et al. 2002).

Several papers about the relationship of BMP2 signalling with MAPK family as follows: Xing et al.(2002) demonstrates that ERK is involved in BMP2-induced osteoblastic differentiation in mesenchymal progenitor cells and ERK protein level is upphospho-regulated under BMP2

inducement. Ishisaki, A, et al (1999) suggested that BMP2 activate not only the Smad signalling but also the Ras/MAPK/Ap-1 pathway. These two signalling activations converge at the Ap-1 level with Smad proteins regulating Ap-1 activity. Members of the Ap-1 and MAPK family are important mediators in BMP2 regulation of gene expression in osteoblasts. The net effect of BMP2 on gene expression depends on the intricate balance of these two signal transduction pathways. BMP2-induced apoptosis is mediated by activation of the TAK1-p38 kinase pathway that is negatively regulated by Smad6(Kimura, et al 2000).

Recent studies have shown bone morphogenetic protein-2 induces apoptosis in human myeloma cells with modulation of STAT3 and BMP2-induced apoptosis in the mouse hybridomas, showed that BMP2 induced down-regulation of Bcl-X (L) through the inactivation of STAT3, resulting in the induction of apoptosis in myeloma(Kawamura, 2002). About the relationship of BMP2 signalling with PI3K family recently (Waite, et al. 2003) verified that BMP2 exposure results in decreased PTEN protein degradation and increased PTEN levels.

The signalling pathways by which BMP2 induces apoptosis has not been fully elucidated. This experiment first verified a BMP2 induction of apoptosis in U937 cells by observing cell number and FACS, obtaining the optimal concentration and incubation time about BMP2 that is 2000 ng/ml BMP2 treatment for 3 days. The aim is to set up the BMP2 signalling network by the activation and inhibition of phosphorylation with localization and function of several important signalling molecules in U937 cells by antibody microarray.

4.2.1 BMP2 activates Akt, ERK and JNK pathway by increase of cytoplasmic phosphorylation in U937 cells

Phospho-Akt displayed an increase of cytoplasmic phosphorylation and decrease of nucleus in BMP2 treated U937 cells. Total protein (sum of cytoplasm and nucleus) level of phospho-Akt is higher in BMP2 treated U937 cells than in control cells, whereas the cytoplasmic activity of akt is higher in BMP2 treated U937 cells than in control cells and nuclear activity is lower in BMP2 treated U937 cells than in control cells (Figure 3.18). This finding also was verified by other researchers. Lorenzini, et al. (2002) demonstrated that in senescent cells no Akt is able to phosphorylate efficiently their nuclear targets. The nuclear akt induced proliferation which demonstrated by the following paper. An active phosphatidylinositol 3-kinase (PI3K) has been shown in nucleus of different cell types. These findings strongly suggest that the intranuclear translocation of Akt/PKB is an important step in signalling pathways that mediate cell proliferation (Borgatti, et al. 2000). Akt controls cell growth through its effects on the mTOR and p70S6 (in the cytoplasm) kinase pathways, as well as the cell cycle and cell proliferation through its direct action on the CDK inhibitors, p21 and p27 (in the nucleus), and indirectly by affecting the levels of cyclin D1 and p53. Akt is also major mediator of cell survival by directly inhibiting different pro-apoptotic signals such as Bad in the cytoplasm and the Forkhead family of transcription factors in the nucleus, or indirectly by modulating two central regulators of cell death such as p53 and NF- κ B.

Phospho-JNK and phospho-ERK displayed increase in cytoplasm and unchanged in nucleus of BMP2 treated U937 cells, when compared with control U937 cells. Total protein (sum of cytoplasm and nucleus) levels of phospho-ERK and phospho-JNK are higher in BMP2 treated U937 cells than in control cells, whereas the cytoplasmic activities of ERK and JNK are higher and nuclear activities of ERK and JNK unchanged in BMP2 treated U937 cells than in control cells (Figure 3. 13-14). From this result it can be deduced that the BMP2 signalling pathway may be involved in the control of apoptosis most likely through mechanisms involving cytoplasmic activation of ERK/JNK/MAPK pathway in U937 cells.

Phospho-ERK cytoplasmic localization related to apoptosis such as ERK activation plays an active role in mediating cisplatin-induced apoptosis of HeLa cells and functions upstream of caspase activation to initiate the apoptotic signal(Wang, et al. 2000).The nuclear localization for phospho-ERK related to proliferation as follows about Tarnawski, et al. (1998) in vitro models nuclear translocation of Erk-1 and -2 triggers cell proliferation. Some scholars also verified ERK about suppression of growth in cytoplasm such as Blockade of the mitogen-activated protein

(MAP) kinase pathway suppresses growth of colon cancer in vivo, demonstrating a direct link between the extracellular signal-regulated kinase ERK2 and the growth-promoting cell adhesion molecule, integrin α v β 6, in colon cancer cells. Down-regulation of β 6 integrin subunit expression inhibits tumour growth in vivo and MAP kinase activity in response to serum stimulation. In α v β 6-expressing cells ERK2 is bound only to the β 6 subunit. The increase in cytosolic MAP kinase activity upon epidermal growth factor stimulation is all accounted for by β 6-bound ERK. Deletion of the ERK2 binding site on the β 6 cytoplasmic domain inhibits tumour growth and leads to an association between ERK and the β 5 subunit. The physical interaction between integrin α v β 6 and ERK2 defines a novel paradigm of integrin-mediated signalling and provides a therapeutic target for cancer treatment (Ahmed, et al. 2002). About ERK and apoptosis researches such as: ERK activation mediates cell cycle arrest and apoptosis after DNA damage independently of p53 (Tang, et al. 2002). Others also verified ERK apoptosis (Bondar, et al. 2002; Krystal, et al. 2002; Howells, et al. 2002; Kim, et al. 2003; Fujisaki, et al. 2002; Wrede, et al. 2002; Itoh, et al. 2002; Wan, et al. 2002; Chinni, et al. 2002).

JNK cytoplasmic localization functions as inhibitor of proliferation from Dickens, et al. (1997) verifying that a murine cytoplasmic protein that binds specifically to JNK [the JNK interacting protein-1 (JIP-1)] and caused cytoplasmic retention of JNK and inhibition of JNK-regulated gene expression. In addition, JIP-1 suppressed the effects of the JNK signalling pathway on cellular proliferation. Many papers studied about JNK on apoptosis such as Ohtsuka, et al. (2003; Chauhan, et al. 2003; Skutek, et al. 2003; Schroeter, et al. 2003; Tyagi, et al. 2003; Smith, et al. 2003; Lei, et al. 2003; Xu, et al. 2003; Lin, et al. 2003; Kang, et al. 2003; Saeki, et al. 2002).

4.2.2 BMP2 activates Smad1 and Smad2/3 network, p38 network and c-Myc, Tyrosine network by increase of nuclear phosphorylation in U937 cells

4.2.2.1 Smad1 and Smad2/3 network

Phospho-Smad1 and phospho-Smad2/3 displayed decrease in cytoplasm and increase in nucleus of BMP2 treated U937 cells, Total protein (sum of cytoplasm and nucleus) levels of phospho-Smad1 and phospho-Smad2/3 were not altered in BMP2 treated cells compared with in control U937 cells, whereas the nuclear activities of Smad1 and Smad2/3 are higher in BMP2 treated U937 cells than in control cells and cytoplasmic activities of Smad1 and Smad2/3 are lower in BMP2 treated U937 cells than in control cells (Figure 3. 13-14). This data indicated that the smad network induced by BMP2 regulates cell cycle progression of U937 human leukemia cells maybe through the nuclear translocation of phospho-Smad1 and phospho-Smad2/3.

Although little papers about function of Smad1 with localization, Smad1 is multifunctional molecule from Sakae, Nishi et al. (1999) elucidated that Smad1 was highly expressed in proliferating chondrocytes and in those chondrocytes that are undergoing maturation. Smad2 was strongly expressed in proliferating chondrocytes, whereas Smad3 was strongly observed in maturing chondrocytes (Sakou, Onishi et al. 1999). Smad3 related to senescence and tumor suppression that is the inhibition of proliferation from Chen, et al. (2000) studies suggest that signalling from the cell surface to nucleus through Smad3 is a required component of the activin A-induced cell death process in liver cells. Vijayachandra, et al. (2003) indicated that Smad3 regulates senescence and malignant conversion in a mouse multistage skin carcinogenesis model.

The observations here in my work maybe reflected smad3 not smad2 phosphorylation increasing in BMP2 treated U937 cells. Because Smad3 but not Smad2 or Smad4 induced senescence. From Chen et al. (2000) paper can be known that the v-ras (Ha)-transduced Smad3 null keratinocytes underwent rapid conversion from benign papilloma to malignant carcinoma when transplanted to a graft site on nude mice, whereas wild-type keratinocytes predominantly formed papillomas. These results link Smad3-mediated regulation of growth control genes to senescence in vitro and tumor suppression in vivo.

From this experiment displayed higher Smad1 and Smad3 phosphorylation co-expression of nucleus. It can be concluded that the BMP2 signalling pathway may be involved in the control of apoptosis most likely through mechanism involving cooperation of Smad1 and Smad3 by nuclear activation in Smad network in U937 cells.

4.2.2.2 p38 network and c-Myc

Phospho-p38 displayed increase in cytoplasm and nucleus of BMP2 treated U937 cells, when compared with control U937 cells. From this result it can be deduced that the BMP2 signalling pathway may be involved in the control of apoptosis most likely through mechanisms involving cytoplasmic and nuclear activation of p38 network in U937 cells (Figure 3.13-14).

c-Myc displayed slightly decrease in cytoplasm and slightly increase in nucleus of BMP2 treated U937 cells. Total protein (sum of cytoplasm and nucleus) level of c-Myc was not altered between BMP2 treated U937 cells and control cells (Figure 3.13-14). Unfortunately, phospho-c-Myc has not been done for comparison.

This thesis demonstrates higher phospho-p38 and c-Myc co-expression in nucleus. From this result it can be deduced the BMP2 signalling pathway may be involved in the control of apoptosis most likely through mechanisms involving cooperation of c-Myc and p-p38 by nuclear activation in U937 cells. Nuclear localization of p38 kinase as apoptosis and also related to c-Myc, such as Deschesnes, et al. (2001) verifying a strong correlation between activation of p38 and induction of c-Myc-dependent apoptosis in Rat-1 cells.

4.2.2.3 Tyrosine network

Phospho-Tyrosine displayed increase in nucleus and cytoplasm of BMP2 treated U937 cells. From this result it can be deduced that the BMP2 signalling pathway may be involved in the control of apoptosis most likely through mechanisms involving nuclear and cytoplasmic activation of tyrosine network in U937 cells (Figure 3. 13-14).

Phospho-Tyrosine promote tumor cell growth, proliferation and angiogenesis(Shaheen, Davis et al. 1999; Wiener, Nakano et al. 1999; Harashima, Tanaka et al. 2001; Turetschek, Preda et al. 2002). However, recently phospho-Tyrosine also has been shown to play an important role in the inhibition of a variety of human cancer(Meyer, Xu et al. 2003). Phospho-Tyrosine induced apoptosis such as Meyer, et al(2003) studied on Rak is a 54 kDa protein tyrosine kinase originally isolated from breast cancer cells and expressed in epithelial cells. It resembles the protooncogene Src structurally but lacks an amino-terminal myristylation site and localizes to the nuclear and peri nuclear regions of the cell. expression of Rak in 2 different breast cancer cell lines inhibits growth and causes G (1) arrest of the cell cycle. Others indicated phospho-Tyrosine expression inductoin of apoptosis such as (Boudny, et al. 2003; Tomomura, et al. 2003; Luciano, et al. 2003; Belka, et al. 2003; Spiekermann, et al.2003).

4.2.3 BMP2 inhibits p70S6 signalling by increase of cytoplasmic phosphorylation and decrease of nucleus in U937 cells

BMP2 exposure results in decreased PTEN protein degradation and increased PTEN levels in PI3K signalling(Waite, et al. 2003). However, the molecular mechanisms of activation and inhibition of signal transduction from BMP2 to other mediators of PI3K signalling are not confirmed. Both p70S6 kinase (p70S6K) and Akt are kinases downstream of phosphatidylinositol 3 kinase (PI3K) (Miyakawa, et al.2003).

Phospho-p70S6 displayed an increase of cytoplasmic phosphorylation and decrease of nucleus in BMP2 treated U937cells. Total protein (sum of cytoplasm and nucleus) level of phospho-p70S6 was not altered in control and BMP2 treated cells (Figure 3. 13-14). The ribosomal protein S6 kinase (S6K) (one subfamily of ribosomal S6 kinases) belongs to the AGC family of Ser/Thr kinases and is known to be involved in the regulation of protein synthesis and the G (1)/S transition of the cell cycle (Valovka, et al. 2003).Fleckenstein, et al. (2003) shows in factor-

dependent hematopoietic M-07e cells that p70S6K is localized both in the cytosol and, after cytokine stimulation, also in nucleus. Nuclear phospho-p70S6 localization as G1 for growth because of Edlmann, et al (1996) using synchronized Swiss mouse 3T3 fibroblasts that p70 S6 kinase (p70S6k) and mitogen-activated protein kinases (p42MAPK/p44MAPK) are not only activated at the G0/G1 boundary, but also in cells progressing from M into G1. p70S6k activity increases 20-fold in G1 cells released from G0. Throughout G1, S, and G2 it decreases constantly, so that during M phase low kinase activity is measured. The kinase is reactivated 10-fold when cells released from a nocodazole-induced metaphase block enter G1 of the next cell cycle. p70S6k activity is dependent on permanent signalling from growth factors at all stages of the cell cycle. Immunofluorescence studies showed that p70S6k and become concentrated in localized spots in nucleus at certain stages in the cell cycle. Cell cycle-dependent changes in p70S6k activity are associated with alterations in the phosphorylation state of the protein.

From this result, it can be deduced that spatial control of cell cycle is through the retention of p-p70S6 in the cytoplasm, thereby preventing them from physical contact with their substrates or partners. The BMP2 signalling pathway is involved in the control of apoptosis most likely through mechanisms involving the nuclear inhibition by nuclear export in p70S6/Akt PI3K signaling in U937 cells.

In my study shown, the same positive signaling pathway proteins are often observed the same cytoplasmic and nuclear change pattern of phosphorylated proteins such as nucleus increasing, or cytoplasm increasing, or nucleus & cytoplasm increasing or decreasing, etc, whereas total phosphorylated proteins can appear changed or un-changed such as one increasing, the other unchanged, function of these proteins appears the same. For activation and inhibition of specific functions of signaling pathways, it is not sufficient to know overall changes in phosphorylation patterns. Cellular distribution, e.g. cytoplasm or nucleus, is very significant and can show differential regulation and function even when the total amount of phosphorylated protein for one signaling protein is not changed.

4.2.4 Possible intracellular relationship

These findings clearly show that the activation of the p38 MAPK pathway and Smad network are involved in BMP2 signalling and led us to propose a co-operative model whereby BMP2-induced activation stimulates not only a Smad pathway that targets Smad1 and Smad3 for an increase of the nuclear translocation but also a parallel p38 MAPK pathway and enhanced transactivation. The present study shows association and interactions of p38 MAPK with smad in nucleus which function as apoptosis seen in many papers (Watanabe, de Caestecker et al. 2001; Lee, Hong et al. 2002; Takekawa, Tatebayashi et al. 2002; Fu, O'Connor et al. 2003; Hayes, Huang et al. 2003; Jono, Xu et al. 2003; Ohshima and Shimotohno 2003; Ungefroren, Lenschow et al. 2003; Yoo, Ghiassi et al. 2003). Such as: Transforming growth factor-beta (TGF-beta)-dependent apoptosis used GADD45b as an effector of TGF-beta-induced apoptosis that the proximal Gadd45b promoter is activated by TGF-beta through the action of Smad2, Smad3, and Smad4.that ectopic expression of GADD45b in AML12 murine hepatocytes is sufficient to activate p38 and to trigger apoptotic cell death, whereas antisense inhibition of Gadd45b expression blocks TGF-beta-dependent p38 activation and apoptosis (Hata, Nishimura et al. 2003) These results suggest that both Smad and p38 kinase signalling are concomitantly activated and responsible for BMP2-induced adipocytic differentiation by inducing and up-regulating phospho-pARgamma, respectively. Thus, BMP2 controls adipocytic differentiation by using two distinct signalling pathways that play differential roles in this process in C3H10T1/2 cells.

This thesis also show that the BMP2 signalling pathway most likely through mechanisms involving nuclear inhibition of p70S6 signalling in U937 cells which reverse to nuclear activation of Smad1 and Smad2/3 network by nuclear translocation. These results suggest that both Smad and p70S6 signalling are concomitantly activated and responsible for BMP2-induced apoptosis by induction and up-regulation of nuclear and cytoplasmic activities, respectively. Thus, BMP2

controls apoptosis by using two distinct signalling pathways that play differential roles in this process in U937 cells.

In conclude, BMP2 would be useful as a novel therapeutic agent in the treatment of multiple myeloma both by means of its antitumor effect of inducing apoptotis and through its original bone-inducing activity, because bone lesions are frequently seen in myeloma patients (Kawamura, et al. 2000).

4.3 BMP2 Signalling in MCF-7 cells

Most experiments only verify the alteration of Total protein (sum of cytoplasm and nucleus) expression. However, for many proteins, although Total protein (sum of cytoplasm and nucleus) expression appears not or little changed, modulation of phosphorylation and localization inside directly decide on the difference of functions and signalling.

In this study, because the lower concentration (100 ng/ml) of BMP2 treatment and short time (4h) of incubation was selected in MCF-7 cells. Under this condition, most total selective phosphorylated proteins appear not or little changed. However, modulation of phosphorylation and localization inside are big difference. This technology is the best method for analyzing multifunctional proteins and complicated signalling networks. Dr. Clement et al (2000) already tested the similar condition of BMP2 treatment in MCF-7 cells, indicating BMP2 functions under this situation not relating to proliferation and apoptosis.

4.3.1 BMP2 BMP2 activaites p70S6 and ERK signaling, Tyrosine and STAT3 network by increase of cytoplasmic phosphorylation in MCF-7 cells

4.3.1.1 p70S6 and ERK signaling

p70S6 kinase (p70S6K) belong to multifunctional kinases downstream of phosphatidylinositol 3 kinase (PI3K), such as the 70-kDa ribosomal protein S6 kinase (p70S6K) is itself a dual pathway kinase, signalling cell survival as well as growth through differential substrates which include mitochondrial BAD and the ribosomal subunit S6, respectively (Harada, Andersen et al. 2001).

Phospho-p70S6 and ERK displayed increase in cytoplasm in BMP2 treated MCF-7 cells (Figure 3. 22-23).

ERK is involved in BMP2-induced osteoblastic differentiation in mesenchymal progenitor cells and ERK protein level is up-regulated under BMP2 inducement (Xing, et al. 2002). However, this experiment did not verify phospho-ERK localization.

4.3.1.2 Tyrosine and STAT3 network

Phospho-Tyrosine and phospho-STAT3 displayed little increase in cytoplasm and un-changed in nucleus of BMP2 treated MCF-7 cells. Total protein (sum of cytoplasm and nucleus) levels of p-Tyrosine and p-STAT3 have the little increase in BMP2 treated MCF-7 cells compared with control cells, whereas cytoplasmic activities of p-Tyrosine and p-STAT3 are higher in BMP2 treated MCF-7 cells than in control cells, the nuclear activities of phospho-p38, p-Tyrosine and p-STAT3 are lower in BMP2 treated MCF-7 cells than in control cells (Figure 3. 22-23). From this result it can ne concluded that BMP2 signalling pathway may be involved in the control of the cell cycle progression (differentiation) most likely through mechanisms involving cytoplasmic activation of tyrosine and STAT3 networks in MCF-7 cells.

My result also shows that phospho-STAT3 and phospho-Tyrosine regulated by BMP2 signalling in MCF-7 cells have the similar change patterns. Other paper also verified that Activation of STAT3 by receptor tyrosine kinases and cytokines regulates survival in human non-small cell carcinoma cells (Song, et al. 2003). STAT3 functions as inhibition of proliferation such as

Yamanaka, et al (1996) suggesting that STAT3 plays an essential role in the signals for growth arrest and macrophage differentiation through its receptor in a murine myeloid leukaemic cell line, M1.

Based on BMP2 treated U937 cells displaying higher phospho-Tyrosine and phospho-STAT3 co-expression in cytoplasm, the BMP2 signalling pathway may be involved in the control of cell cycle progress most likely through mechanisms involving the cooperation of Tyrosine-STAT network by cytoplasmic activation in MCF-7 cells.

4.3.2 BMP2 inhibits p38, JNK and smad signalling by increase of cytoplasmic phosphorylation and decrease of nucleus in MCF-7 cells

4.3.2.1 p38 and JNK

The c-Jun amino-terminal kinase (JNK) and p38 are a member of mitogen-activated protein (MAP) kinases that are implicated in the control of cell growth, proliferation, differentiation and apoptosis.

Phospho-p38 and phospho-JNK displayed increase in cytoplasm and little decrease in nucleus of BMP2 treated MCF-7 cells. Total protein (sum of cytoplasm and nucleus) levels of phospho-p38 and phospho-JNK are almost the same in BMP2 treated MCF-7 cells as in control cells (Figure 3. 22-23). From this result it can be deduced that spatial control of cell cycle is through the retention of p-JNK and p-p38 in the cytoplasm, thereby preventing them from physical contact with their substrates or partners. BMP2 signalling pathway may be involved in the control of the cell cycle progression (differentiation) most likely through mechanisms involving inhibition of phospho-p38, phospho-ERK and phospho-JNK in MCF-7 cells.

p38 kinase cytoplasmic localization functions as differentiation. Berenbaum, F et al (2003) verified Concomitant recruitment of ERK1/2 and p38 MAPK signalling pathway is required for activation of cytoplasmic phospholipase A2 via ATP in articular chondrocytes. Klekotka (2001) published that alpha 2 integrin subunit cytoplasmic domain-dependent cellular migration requires p38 MAPK. Khurana et al (2003) also verified p38 MAPK interacts with actin and modulates filament assembly during skeletal muscle differentiation.

JNK cytoplasmic localization functions as inhibitor of proliferation from Dickens, et al. (1997) verifying that a murine cytoplasmic protein that binds specifically to JNK [the JNK interacting protein-1 (JIP-1)] and caused cytoplasmic retention of JNK and inhibition of JNK-regulated gene expression. JIP-1 suppressed the effects of the JNK signalling pathway on cellular proliferation.

4.3.2.2 Smad1/Smad2/3 network

Phospho-Smad1, 2/3 displayed little increase in cytoplasm and little decrease in nucleus of BMP2 treated MCF-7 cells, Total protein (sum of cytoplasm and nucleus) levels of phospho-Smad2/3 were not altered in BMP2 treated MCF-7 cells and control cells (Figure 3. 22-23). From this result it can be deduced that the BMP2 signalling pathway may be involved in the control of the cell cycle progression (differentiation) most likely involving nuclear inhibition through cytoplasmic relocalization of phospho-Smad2/3 in MCF-7 cells.

The observations here in my work maybe most smad2 not smad3 in cytoplasm of BMP2 treated MCF-7 cells. Because Smad2 was strongly expressed in proliferating chondrocytes, whereas Smad3 was strongly observed in maturing chondrocytes(Sakou, et al. 1999).

4.3.3 BMP2 activates c-Myc signalling by increase of nuclear phosphorylation in MCF-7 cells

c-Myc displayed increase in nucleus and decrease in cytoplasm of BMP2 treated MCF-7 cells. Total protein (sum of cytoplasm and nucleus) level of c-Myc was not altered between BMP2 treated MCF-7 cells and control cells. From this result it can be deduced that the BMP2

signalling pathway may be involved in the control of the cell cycle progression (differentiation) most likely through mechanisms maybe involving the some activation of c-Myc in MCF-7 cells. Unfortunately, phospho-c-Myc has not been done for comparison (Figure 3. 22-23).

Usually in the differentiation, total c-Myc not changed, however, little information about the alteration of localization in the differentiaon. Here, I showed the nuclear translocation.

4.3.4 Possible intracellular relationship

From all the above it can be concluded that increase co-expression in cytoplasmic phosphorylation of ERK, p70S6, STAT3 and Tyrosine are maybe involved in the cooperative signalings. Subsequent induction of differentiation and led us to propose a co-operative model, which is consistent with other study such as: Lehman et al.(2003) indicated that a kinase from the MEK/MAPK pathway also plays a role in p70S6K activation by GM-CSF in a hematopoietic cell, the neutrophil. Relationships of STAT3 and ERK co-expressed in G1 as follows: Wierenga, et al. (2003) indicated that the EPO-induced STAT3 serine 727 phosphorylation is mediated by a pathway involving MEK, ERK, and MSK1 in the EPO-dependent erythroid cell line ASE2.

4.4 Effects of STI571 on K562 Cells

Yu, Krystal et al. (2002) indicated the exposure of Bcr/Abl+ cells to STI571 has not in general been associated with down-regulation of the Bcr/Abl protein, they reported that Exposure of K562 cells to concentrations of STI571 that minimally induced apoptosis (0.2 μ M) resulted in early suppression (i.e., at 6 h) of p42/44 MAPK phosphorylation followed at later intervals (larger than or =24 h) by a marked increase in p42/44 MAPK phosphorylation/activation. In order to overcome problems of STI571 drug treatment, it is postulated that simultaneous interruption of additional targets in signaltransduction pathways may represent a more effectiive antileukemic therapy strategy. However, modulation of phosphorylation with localization and function from STI571 treatment in K562 cells are not elucidated.

Therefore, in this study, by using antibody microarray and separation of cytoplasm and the nuclear protein, emphasis of differential phosphorylation and localization to multifunctional positive and negative mediators of cellular regulation was given such as phospho-p70S6 and phospho-Akt (PI3K signalling), phospho-p38 (p38 network), phospho-ERK and phospho-JNK (MAPK pathway), phospho-Tyrosine (tyrosine-kinase network), phospho-STAT3 (Jak/STAT network), and phospho-Smad1,2,3 (smad network) in K562 cells.

4.4.1 STI571 inhibits Akt/p70S6 PI3K signalling by decrease of cytoplasmic and nuclear phosphorylation in K562 cells

Phospho-Akt and phospho-p70S6 displayed decrease in cytoplasm and nucleus of STI571 treated K562 cells (Figure 3.27-28). From this result it can be concluded that the STI571 treatment may be involved in the control of growth and proliferation most likely through mechanisms involving nuclear and cytoplasmic inhibition of akt/p70S6 signalling in K562 cells.

Akt controls cell growth through ist effects on the mTOR and p70S6 (in the cytoplasm) kinase pathways, as well as the cell cycle and cell proliferation through its direct action on the CDK inhibitors, p21 and p27 (in the nucleus), and indirectly by affecting the levels of cyclin D1 and p53. Akt is also major mediator of cell survival by directly inhibiting different pro-apoptotic signals such as Bad in the cytoplasm and the Forkhead family of transcription factors in the nucleus, or indirectly by modulating two central regulators of cell death such as p53 anf NF-kB.

From this result, it can be deduced that STI571 reduced growth by the decrease of Akt/p70S6 PI3K signalling in K562 cells.

4.4.2 STI571 activates p38 MAPK pathway, c-Myc, Tyrosine and Smad1/Smad2/3 networks by increase of cytoplasmic and nuclear phosphorylation in K562 cells

Phospho-p38, p38, c-Myc, phospho-Tyrosine, phospho-Smad1 and phospho-Smad2/3 displayed increase in cytoplasm and nucleus of STI571 treated K562 cells (Figure 3. 27-28). From this result it can be deduced that the STI571 treatment may be involved in the control of growth and proliferation most likely through mechanisms involving nuclear and cytoplasmic activation of p38, c-Myc, Tyrosine and Smad1/Smad2/3 networks in K562 cells.

Smad1 was highly expressed in proliferating chondrocytes and in those chondrocytes that are undergoing maturation. Smad2 was strongly expressed in proliferating chondrocytes (Sakou, Onishi et al. 1999), whereas Smad3 was mainly observed in maturing chondrocytes. Therefore, the observations here in my work maybe mostly smad2 not smad3 in nucleus for proliferation. About the relationship of p38 is related to proliferation such as high glucose mediated effects on endothelial cell proliferation occur via p38 MAP kinase (McGinn, Saad et al. 2003).

4.4.3 STI571 activates pathway by increase of nuclear phosphorylation and decrease of cytoplasm in K562 cells

Phospho-ERK displayed increase in nucleus and little decrease in cytoplasm of STI571 treated K562 cells. Total protein (sum of cytoplasm and nucleus) level of phospho-ERK is higher in STI571 treated K562 cells than in control cells, whereas the activity of ERK is higher in nucleus and lower in cytoplasm of STI571 treated K562 cells than in control cells (Figure 3. 27-28). From this result it can be known that the STI571 treatment may be involved in the control of growth and proliferation most likely through mechanisms involving the nuclear activation of ERK in K562 cells.

This result is consistent with other finding that treatment of Bcr-Abl-expressing cells with STI571 elicits a cytoprotective MAPK activation response (Yu, Krystal et al. 2002). However, ERK modulation of phosphorylation with localization and function from STI571 treatment in K562 cells not clear. Phospho-ERK nuclear localization related to proliferation as follows about Tarnawski, Pai et al. (1998) in vitro models nuclear translocation of Erk-1 and -2 triggers cell proliferation.

4.4.4 STI571 activates STAT3 network and JNK/MAPK pathway by increase of cytoplasmic phosphorylation in K562 cells

Phospho-STAT3 and p-JNK displayed increase of cytoplasm and un-changed in nucleus of STI571 treated K562 cells. Total protein (sum of cytoplasm and nucleus) level of phospho-STAT3 and phospho-JNK are higher in STI571 treated K562 cells than in control cells, whereas the activity of STAT3 and phospho-JNK are higher in cytoplasm and un-changed in nucleus of STI571 treated K562 cells than in control cells (Figure 3. 27-28). From this result it can be concluded that the STI571 treatment may be involved in the control of growth and proliferation most likely through mechanisms involving cytoplasmic activation of STAT3 and JNK network in K562 cells.

STAT3 located in cytoplasm which functions as proliferation in STI-treated K562, because Poselova, Evdonin et al. (1998) studied the intracellular distribution of STAT1 and STAT3 transcription factors in normal fibroblasts (REF) and in E1A + Ha-Ras transformed cells by means of indirect immunofluorescence. The obtained data evidence that in REF cells, in response to the growth factor addition, STAT1 and STAT3 proteins are redistributed from cytoplasm to nucleus. In transformants E1A + Ha-Ras, however, significantly different pictures can be seen: while STAT1 is found to be constitutively localized in the cell nucleus, STAT3 is predominantly revealed in the cytoplasm. The data obtained from fractionation of subcellular structures confirm in general the immunofluorescence results on the cytoplasmic localization of STAT3 protein in E1A + Ha-Ras transformants. Thus, transformation of REF cells with E1A +

Ha-Ras oncogenes causes a constitutive activation of STAT1 and STAT3 transcription factors, the proteins, however, being distributed in different cell compartments.

4.4.5 Possible intracellular relationship

Extracellular signal-regulated protein kinase (ERK)-dependent and ERK-independent pathways target STAT3 on serine-727. Here, my observations in this work that STI571 activates STAT3 independently of -ERK and PI-3K signal transduction, which is consistent with other studies as follows: Activation of ERKs or PI-3K are not required for insulin induced STAT3 phosphorylation or transactivation by using utilising the specific MEK inhibitor PD098059 and the PI-3K inhibitor wortmannin, although previous studies have suggested a role for MAP kinases (ERKs) and PI-3K in STAT activation(Coffer, van Puijenbroek et al. 1997). Van Puijenbroek et al. (1999) also indicated regulation of STAT3-mediated transactivation occurs independently of p21ras-ERK signalling.

In this thesis, high levels of c-Myc and phospho-Tyrosine were detected in nucleus and cytoplasm, which is consistent with Minami, Nakagawa et al. (1995) studied on Syk protein tyrosine kinase (PTK) physically associated with IL-2 receptor by -induced proliferative signals in peripheral blood lymphocytes. cDNA expression studies the activation of Syk PTK results in the induction of the c-Myc gene, an event critical for the cell proliferation. Papers about the positive relationships between c-Myc and smad in proliferation as follows: Direct interaction of c-Myc with Smad2 and Smad3 to inhibit TGF-beta-mediated induction of the CDK inhibitor p15 (Ink4B). Others also demonstrated the relationships (Chen, et al. 2002; Kowalik 2002; Yagi, et al. 2002; Baldwin, et al. 2003).

From the result, it can be deduced that the observed phosphorylation suppression of the nuclear Akt and p70S6 PI3K signaling in the presence of activated nuclear p38/ERK pathway, c-Myc, tyrosine and Smad1/ Smad2/3 networks resulted in reduced growth and increased proliferation in response to STI571 treatment in K562 cells, which is consistent with other study such as: Wang, B. et al. also (2002) indicated that a positive p38 mitogen-activated protein kinase pathway and a negative phosphoinositide 3-kinase-Akt pathway induced novel cytoplasmic proteins of nontypeable Haemophilus influenzae up-regulation of human MUC5AC mucin transcription.

It also can be concluded that increase of nuclear phosphorylation of p38/ ERK MAPK pathway, (c-Myc), tyrosine, Smad1/ Smad2/3 networks and increase in cytoplasmic phosphorylation of STAT3 network and JNK MAPK pathway maybe involved in cooperative signalling. Subsequent induction of proliferation and led us to propose a co-operative model.

4.5 Models of Signalling Protein and Cellular Response

This study could demonstrate with the newly developed antibody array, how BMP2 and STI571 influence phosphorylation and localization of signalling proteins. The proteins analyzed included phospho-p70S6 and phospho-Akt (PI3K signalling), phospho-p38 (p38 network), phospho-ERK and phospho-JNK (MAPK pathway), phospho-Tyrosine (tyrosine-kinase network), phospho-STAT3 (Jak/stat network), and phospho-Smad1,2,3 (smad network) in human cancer cell lines.

These findings that the induction of apoptosis in U937 cells under 2000 ng/ml BMP2 treatment for 3 days by using FACS and cell numbers indicates that the BMP2 pathway is involved in the control of apoptosis in U937 cells through multiple mechanisms involving:

- (1) Total phospho-Tyrosine and phospho-p38 increased with cytoplasmic and nuclear phosphorylation increasing;
- (2) Total phospho-ERK and phospho-JNK increased with cytoplasmic phosphorylation increasing and nucleus unchanged;
- (3) Total phospho-Akt increased with cytoplasmic phosphorylation increasing and nuclear phosphorylation decreasing;
- (4) Total phospho-Smad1, phospho-Smad2/3 and c-Myc unchanged with nuclear

phosphorylation increasing and cytoplasmic phosphorylation decreasing;(5) Total phospho-p70S6 unchanged with cytoplasmic phosphorylation increasing and nuclear phosphorylation decreasing. From this I deduce that the BMP2 signalling in response to high doses of BMP2 work most likely through mechanisms involving nuclear activation and cytoplasmic inhibition by the nuclear translocation of phospho-Smad1, phospho-Smad2/3 and c-Myc and also the nuclear inhibition through the cytoplasmic relocation of phospho-p70S6 in U937 cells.

This study indicates that nuclear activation of Smad1/Smad2/3, c-Myc, p38 MAPK and tyrosine networks may be involved in cooperative signalling and subsequent induction of apoptosis. This led to propose a model whereby a BMP2-signal stimulates not only Smad and c-Myc networks, seen by targeting phospho-Smad1 and phospho-Smad2/3, c-Myc by nuclear translocation, but also a parallel activation of the p38 MAPK pathway and tyrosine network with enhancement to nucleus by increase of nuclear and cytoplasmic phosphorylation in BMP2 treated U937 cells. Cytoplasmic activation of ERK/JNK MAPK pathway and Akt signalling may be involved also in the cooperative signalling whereby the BMP2signal stimulates not only the ERK/JNK MAPK pathway increase in cytoplasm and unchange in nucleus of phospho-ERK and phospho-JNK, but also Akt signalling, seen in the enhance of cytoplasmic phosphorylation and decrease of nuclear phosphorylation of Akt in BMP2 treated U937 cells. From this result it can be deduced that negative regulation maybe reflect from a nuclear decrease and unchanged in Akt/p70S6 PI3K and ERK/JNK MAPK activity and a parallel nuclear increase of p38 MAPK pathway, Smad1/Smad2/3, c-Myc, and Tyrosine activity result in a BMP2 induced cell death in U937 cells, as shown in Fig. 4.1.

BMP2-induced apoptosis model in U937 cells

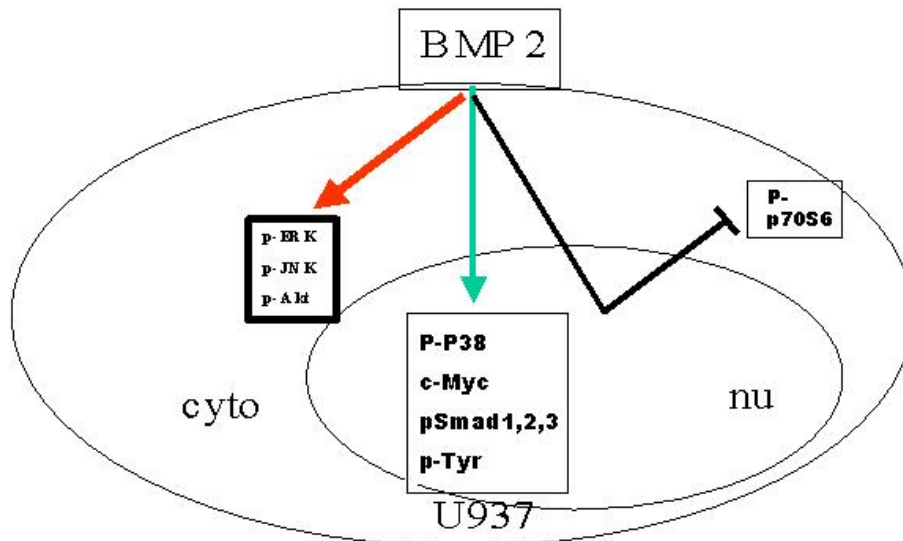


Figure 4.1: BMP2-induced Apoptosis Model in U937 cells. BMP2-induced apoptosis differently activates MAPK pathway by p-ERK and p-JNK cytoplasmic increase and p-p38 nuclear and cytoplasmic increase, activates Smad network by p-Smad1 and p-Smad2/3 nuclear increase, also activates tyrosine network by p-Tyr nuclear and cytoplasmic increase and activates p-Akt signaling by cytoplasmic increase. It inhibits p70S6 signaling by p-p70S6 nuclear export of nuclear decrease and cytoplasmic increase.

In BMP2 signalling of MCF-7 cells under 100 ng/ml BMP2 treatment for 4h, these findings show that the BMP2 signalling pathway may be involved in the control of the cell cycle progression (differentiation) most likely through multiple mechanisms, involving:

Phospho-p38 and p38, p-JNK, p-Smad1, p-Smad2/3 displayed the increase in cytoplasm and the decrease in nucleus of BMP2 treated MCF7 cells. Total protein (sum of cytoplasm and nucleus) level of phospho-p38 and p38, p-JNK, p-Smad1, p-Smad2/3 were not significantly changed in BMP2 treated MCF-7 cells and control cells. c-Myc displayed the slight decrease in cytoplasm and the slight increase in nucleus of BMP2 treated MCF7 cells. Total protein (sum of cytoplasm and nucleus) level of c-Myc was not significantly altered between BMP2 treated MCF-7 cells and control cells. p-Tyrosine, p-STAT3, p-ERK and p-P70S6 displayed the increase in cytoplasm and unchanged in nucleus of BMP2 treated MCF7 cells. Total protein (sum of cytoplasm and nucleus) level of p-p38, p-Tyrosine, p-STAT3, p-ERK and p-P70S6 were increased in BMP2 treated cells. P-Akt displayed unchanged in cytoplasm and nucleus of BMP2 treated MCF7 cells.

From this it can be deduced that BMP2 signalling in response to lower dose and short time of BMP2 treatment most likely through mechanisms involving inhibition by the cytoplasmic relocalization of phospho-JNK, phospho-p38 and phospho-Smad2/3 and also nuclear inhibition by the degradation of phospho-Smad1 in BMP2 treated MCF-7 cells. This result indicated that cytoplasmic activation of ERK/ MAPK pathway, p70S6 signalling, STAT3, and tyrosine are maybe involved in the cooperative signalling and the subsequent induction of differentiation and led to propose a co-operative model whereby BMP2-induced cytoplasmic activation stimulates p70S6 signalling, STAT3 and tyrosine networks that target phospho-p70S6, phospho-STAT3 and phospho-Tyrosine for increase of cytoplasmic phosphorylation, as shown in Fig. 4.2.

BMP2-induced differentiation model in MCF7 cells

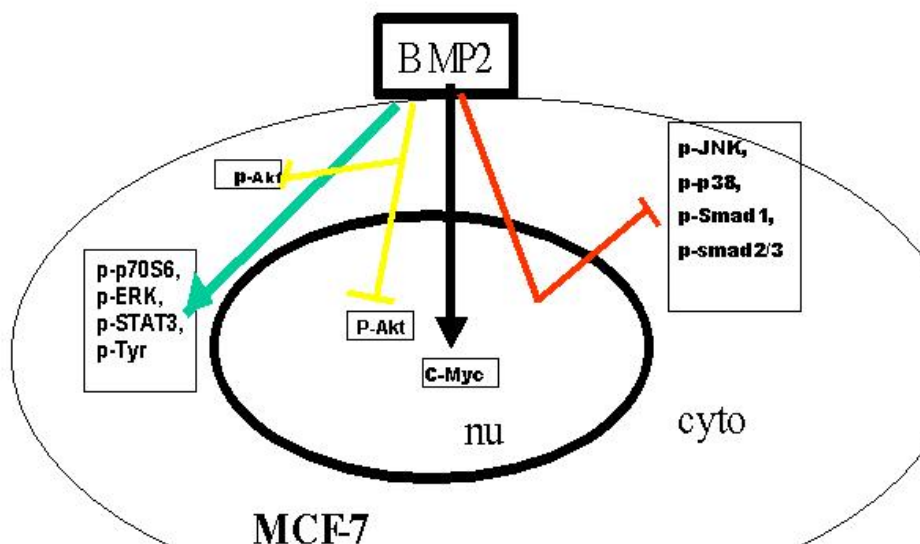


Figure 4.2: BMP2-induced Differentiation Model in MCF7 cells. Short time and lower concentration BMP2 treatment to MCF7 cells (100 ng/ml for 4h) inhibits MAPK pathway and Smad network by p-ERK/p-JNK/p-p38, p-Smad1 and p-Smad2/3 nuclear decrease and cytoplasmic increase, and inhibit Akt signaling by nuclear and cytoplasmic unchange. It activates p70S6 signaling, STAT3 and tyrosine network and c-Myc by p-p70S6, p-STAT3 and p-Tyr cytoplasmic increase and c-Myc nuclear increase.

In 0.2 μ M STI571 treatment of K562 cells for 24h, my findings that the STI571 treatment may be involved in the control of growth and proliferation most likely through multiple mechanisms, involving:

(1) Total phospho-Akt and phospho-p70S6 decreased with cytoplasm and nucleus decreasing; (2) Total phospho-p38, p38, c-Myc, phospho-Tyrosine, phospho-Smad1 and phospho-Smad2/3 increased with cytoplasm and nucleus increasing; (3) Total phospho-STAT3 and phospho-JNK increased with cytoplasm increasing and nucleus un-changed; (4) Total phospho-ERK increased with nucleus increasing and cytoplasm decreasing in STI571 treated K562 cells.

This results indicated that nuclear and cytoplasmic activation of p38/ ERK MAPK pathway, (c-Myc), Tyrosine, Smad1/ Smad2/3 networks and cytoplasmic activation of STAT3 network and JNK MAPK pathway are maybe involved in the cooperative signalling and the subsequent induction of proliferation and led to propose a co-operative model whereby STI-induced activation stimulates not only p38/ERK pathway, c-Myc, tyrosine and smad network that target phospho-p38, phospho-ERK, c-Myc, phospho-Tyrosine, phospho-Smad1 and phospho-Smad2/3 for the increase of nuclear and cytoplasmic phosphorylation but also STAT3 network and JNK/MAPK pathway for increase of cytoplasmic phosphorylation in STI571 treated K562 cells. From this experiment it can be deduced STI571 treatment induced the observed nuclear and cytoplasmic suppression of Akt / p70S6 PI3K signalling target phospho- Akt and phospho-p70S6 by the decrease of nuclear and cytoplasmic phosphorylation in K562 cells. In this thesis it can be deduced the negative nuclear regulation relationship from the observed phosphorylation suppression in nucleus of Akt / p70S6 PI3K signalling in the presence of activated nuclear p38/ERK MAPK pathway, c-Myc, tyrosine and Smad1/Smad2/3 networks resulted in proliferation produced by STI571 treatment in K562 cells, as shown in Fig. 4.3

STI571-inhibited cell growth and induced proliferation model in K562 cells

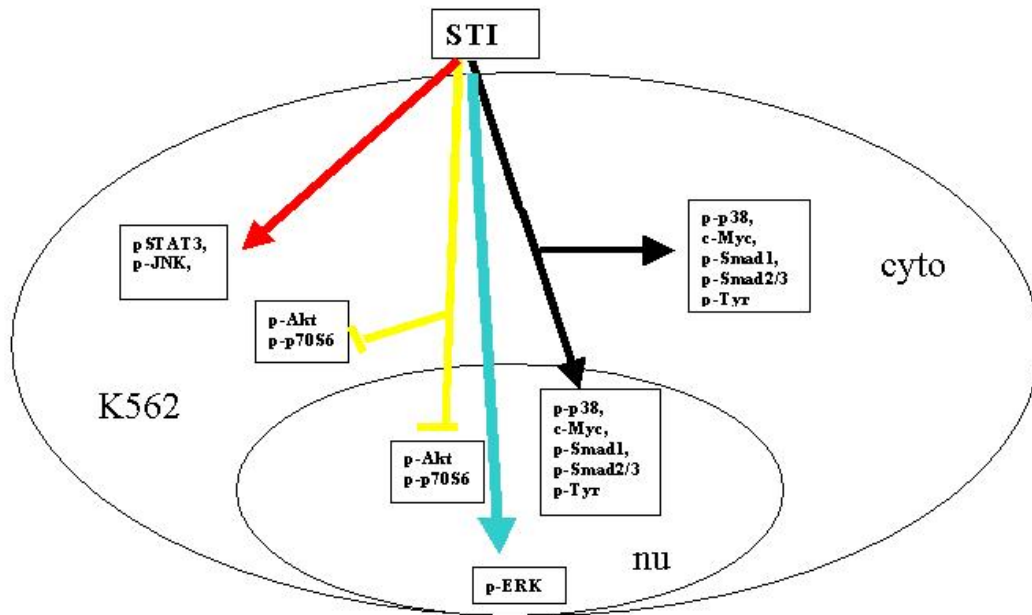


Figure 4.3: STI-inhibited cell growth and induced proliferation Model in K562 cells. 0.2 μ m STI treatment to K562 cells differently activates MAPK pathway by p-ERK nuclear increase, p-JNK cytoplasmic increase and p-p38 nuclear and cytoplasmic increase, and also activates tyrosine network and Smad network by p-Tyr, p-Smad1 and p-Smad2/3 nuclear and cytoplasmic increase, and Jak/STAT pathway by p-STAT3 cytoplasmic increase. It inhibits PI3K signaling by p-Akt and p-p70S6 nuclear and cytoplasmic decrease.

5 Summary

Activity of proteins is not only regulated on the level of gene expression. An additional level for the regulation of protein activity is provided by secondary modifications. One of these modifications is protein phosphorylation. Added through kinases and removed by phosphatases the phosphorylation and thus the activity of proteins can be adjusted to various cellular conditions. In most cases changes in cellular activity are the result of various adjustments regulated and mediated through signaling pathways, in which the activity of many proteins can be changed by phosphorylation. Because the activities of many cellular proteins are changed in biological processes, it is of interest to study the phosphorylation of many proteins in parallel. In this work an antibody array utilizing phosphorylation specific antibodies was developed that allows the simultaneous detection of several phosphoproteins in parallel.

The first part of the work describes the development and optimization of the antibody array technology. After initial experiments in which antibodies were spotted on epoxy activated microscope glass slides and binding of fluorescence labeled protein extracts was measured, the focus was shifted to a more miniaturized format. For this the ArrayTube platform from Clondia (Jena) was chosen. In this system a chip is mounted at the base of a reaction tube and the binding of proteins to the spotted antibody is detected by silver staining. With this system it became possible to establish a reliable assay for protein detection in cellular protein extracts. Crucial points for the system are the quality of the antibody preparation needed for spotting and the labeling of cellular proteins in protein extracts. It could be demonstrated that salt free antibody preparations with a minimal antibody concentration of 1 mg/ml are compatible with the spotting and the Array-Tube chip surface and that N-hydroxy-succinimid-activated biotin is a suitable reagent for labeling of protein extracts.

After successful optimization of the assay system a selection of phosphorylation specific antibodies was used to set up a signaling pathway array system. The proteins analyzed by this system include phospho-p70S6 kinase and phospho-Akt (PI3K/Akt-signaling-pathway), phospho-p38 (p38 map-kinase), phospho-ERK (ERK1,2 map-kinase) and phospho-JNK (SAPK/JNK MAPK-homolog), phospho-Tyrosine, phospho-STAT3 (Jak/Stat-signaling-pathway), and phospho-Smad1 and phospho-Smad2,3 (TGF*/BMP/Smad-signaling-pathway).

This array was used to analyze changes in protein phosphorylation patterns in three application examples: - BMP2 treatment of the leukemia cell line U937 (monocytes), - BMP2 treatment of the breast cancer cell line MCF-7, and - STI571 treatment of the leukemia cell line K562 (BCR-Abl positiv).

The effect of BMP2 treatment on U937 cells is strongly concentration dependent. Using concentrations from 50 ng/ml to 2000 ng/ml BMP2, I demonstrate by measuring cellular proliferation, counting cell numbers, and FACS analysis that at low concentrations BMP2 controls proliferation whereas induction of apoptosis is observed at high concentrations of BMP2.

Using the antibody array, and high dose BMP2 treatment I found: (1) Total phospho-Tyrosine and phospho-p38 increased resulting from parallel increase in cytoplasm and nucleus; (2) Total phospho-ERK and phospho-JNK increased resulting from an increase in cytoplasm whereas phosphorylation in nucleus remained unchanged; (3) Total phospho-Akt increased also resulting from an increase in cytoplasm but was accompanied by a decrease in nucleus; (4) Total phospho-Smad1, phospho-Smad2/3 and c-Myc were unchanged but increased in nucleus and decreased in cytoplasm. (5) Total phospho-p70S6 was unchanged but increased in cytoplasm and decreased in nucleus.

Cytoplasmic activation of ERK/JNK MAPK pathway and Akt signalling may be involved also in the cooperative signalling whereby the BMP2 signal stimulates not only the ERK/JNK MAPK pathway increase in cytoplasm and unchanged in nucleus of phospho-ERK and phospho-JNK, but also Akt signalling, seen in the enhance of cytoplasmic phosphorylation and decrease of nuclear phosphorylation of Akt in BMP2 treated U937 cells. From this result it can be deduced that negative regulation maybe reflect from a nuclear decrease and unchanged in Akt/p70S6

PI3K and ERK/JNK MAPK activity and a parallel nuclear increase of p38 MAPK pathway, Smad1/Smad2/3, c-Myc, and Tyrosine activity result in a BMP2 induced cell death in U937 cells

Treatment of MCF-7 cells with BMP2 (100 ng/ml) for 4h (under this condition BMP2 acts as a survival factor) showed a very different distribution of changes in phosphorylation: phospho-p38 and p38, p-JNK, p-Smad1, p-Smad2/3 displayed the increase in cytoplasm and the decrease in nucleus of BMP2 treated MCF7 cells. Total protein (sum of cytoplasm and nucleus) level of phospho-p38 and p38, p-JNK, p-Smad1, p-Smad2/3 were not significantly changed in BMP2 treated MCF-7 cells and control cells. c-Myc displayed the slight decrease in cytoplasm and the slight increase in nucleus of BMP2 treated MCF7 cells. Total protein (sum of cytoplasm and nucleus) level of c-Myc was not significantly altered between BMP2 treated MCF-7 cells and control cells. p-Tyrosine, p-STAT3, p-ERK and p-P70S6 displayed the increase in cytoplasm and unchanged in nucleus of BMP2 treated MCF7 cells. Total protein (sum of cytoplasm and nucleus) level of p-p38, p-Tyrosine, p-STAT3, p-ERK and p-P70S6 were increased in BMP2 treated cells. P-Akt displayed unchanged in cytoplasm and nucleus of BMP2 treated MCF7 cells.

These changes indicate a cooperative action of the different signaling pathways that is needed to maintain cellular homeostasis, which is only reflected in changes in the distribution of the phosphorylated forms of the proteins analyzed.

In the third example the human leukemia cell line K562 was treated with 0.2 μ M STI571 for 24h. STI571 is a protein tyrosine kinase inhibitor that specifically inhibits the kinase activity of the BCR-Abl fusion protein that is expressed in K562 cells. Treatment with STI571 has an antiproliferative effect on these cells, which leads to the following changes in the phospho-proteins analyzed: (1) Decrease of total phospho-Akt and phospho-p70S6 results from parallel decrease in cytoplasm and nucleus; (2) Increase in total phospho-p38, p38, c-Myc, phospho-Tyrosine, phospho-Smad1 and phospho-Smad2/3 results from parallel increase in cytoplasm and nucleus; (3) Total phospho-STAT3 and phospho-JNK increased resulting from an increase in cytoplasm whereas the concentration in nucleus remained un-changed; (4) Total phospho-ERK increased resulting from an increase in nucleus while in parallel the concentration in cytoplasm decreased.

These changes show that growth inhibition of the phospho-Tyrosine-kinase BCR-Abl by STI571 affects the activity of several signaling pathways. This could be either the result of a direct influence on these signaling pathways but could also reflect an indirect cellular response to the inhibitory effects of STI571.

The results obtained with the phospho-protein-specific antibody array give a global view in the changes of signal-pathway activation reflected in the amount of selected phosphorylated proteins from the pathways analyzed. In combination with the selective purification of protein extracts from different cellular compartments, in this work nucleus or cytoplasm, this technology allows the rapid analysis of changes in concentration and localization of the respective proteins and their phosphorylation state. The information obtained in the application examples was finally used to deduce general regulation models for the different treatments, which are also discussed as part of the work.

6. Zusammenfassung

Die Aktivität von Proteinen ist nicht nur auf der Ebene der Genexpression reguliert. Eine weitere Ebene der Regulation ist durch nachfolgende Modifikationen möglich. Eine dieser Modifikationen ist Proteinphosphorylierung. Hinzugefügt durch Kinasen und entfernt durch Phosphatasen kann die Phosphorylierung und damit die Aktivität der Proteinen an verschiedene zelluläre Konditionen angepasst werden. In den meisten Fällen sind Änderungen in der zellulären Aktivität das Ergebnis verschiedener Anpassungen, die durch Signalwege vermittelt und reguliert werden. Da die Aktivität vieler zellulärer Proteine in biologischen Prozessen verändert wird, ist es von Interesse die Phosphorylierung vieler Proteine nebeneinander zu untersuchen. In dieser Arbeit wurde ein Antikörperarray entwickelt, der phosphorylierungsspezifische Antikörper nutzt und den gleichzeitigen Nachweis mehrerer Signalproteine ermöglicht.

Der erste Teil der Arbeit beschreibt die Entwicklung und die Optimierung der Antikörperarraytechnologie. Nach anfänglichen Experimenten mit Antikörpern, die auf epoxy-Aktivierten Objektträger gespottet wurden, wurde der Schwerpunkt auf ein stark miniaturisiertes Format gelegt. Dafür wurde das Array-Tube-System der Fa. Clondiag CT GmbH Jena gewählt. In diesem System wird der Array-Chip am Boden eines Reaktionsgefäßes angebracht und das Binden der Proteine an die gespotteten Antikörper durch Silberfärbung nachgewiesen. Mit diesem System wurde es möglich eine verlässliche Methode für den Nachweis von Proteinen in Zellextrakten aufzubauen. Entscheidende Punkte für das System sind die Qualität der Antikörperpräparation und die Markierung der zellulären Proteine in den Proteinextrakten. Es konnte gezeigt werden, dass salzfreie Antikörperpräparationen mit einer minimalen Konzentration von 1 mg/ml Antikörper für das Spotten auf die genutzte, epoxy-Aktivierte Oberfläche geeignet sind, bzw. dass N-hydroxy-succinimid-Aktiviertes Biotin ein geeignetes Reagenz für die Markierung der Proteine ist.

Nach der erfolgreichen Optimierung der Methode wurden verschieden phosphorylierungsspezifische Antikörper ausgewählt. Die Proteine die dann nachgewiesen werden konnten waren: phospho-p70S6 Kinase und phospho-Akt (PI3K/Akt-Signalweg), phospho-p38 (p38 MAP-Kinase), phospho-ERK (ERK1,2 MAP-Kinase) und phospho-JNK (SAPK/JNK MAPK-homolog), phospho-Tyrosine, phospho-STAT3 (Jak/Stat-Signalweg), und phospho-Smad1 und phospho-Smad2,3 (TGF-*/BMP/Smad-Signalweg).

Der Array wurde genutzt, um Änderungen in der Proteinphosphorylierung in drei Anwendungsbeispielen zu untersuchen: - BMP2 Behandlung der Leukämie-Zelllinie U937 (Monozyten), BMP2 Behandlung der Brustkrebszelllinie MCF-7 und STI571 Behandlung der Leukämie-Zelllinie K562 (BCR-abl positive Leukämie Zelllinie).

Die BMP2 Wirkung in U937 Zellen ist stark abhängig von der Konzentration. Ich konnte durch Proliferationsmessungen und FACS-Analyse zeigen, dass niedrige BMP2-Konzentrationen zur Proliferation führen, während hohe Konzentrationen von BMP2 Apoptosis in U937 Zellen induzieren.

Mit dem Antikörperarray und hohen Dosen BMP2 ergab sich folgendes Bild: (1) Zunahme von gesamt phospho-Tyrosin und phospho-p38-MAPK und gleichzeitige Zunahme in cytoplasma und Kern; (2) Zunahme von gesamt phospho-ERK und phospho-JNK aufgebaut aus Zunahme im Cytoplasma ohne Änderung im Kern; (3) Zunahme von gesamt phospho-Akt, bei Zunahme im Cytoplasma und Abnahme im Kern; (4) Keine Änderung von gesamt phospho-STAT3, phospho-Smad1, phospho-Smad2/3 und c-Myc, jedoch Zunahme im Kern und Abnahme im

Cytoplasma; (5) Keine Änderung für gesamt phospho-p70S6 Kinase, jedoch Zunahme im Cytoplasma und Abnahme im Kern.

In diesem Beispiel scheint das BMP2 Signal nicht nur STAT3, Smad und Myc-Netzwerke zu aktivieren sondern auch zu einer parallelen Aktivierung des p38 MAPK-Signalwegs und von Phosphotyrosinen zu führen, die mit einer verstärkten Translokation der entsprechenden Proteine in den Kern in BMP2 behandelten U937 Zellen verbunden ist, während phosphoryliertes Akt und p70S6-Kinase überwiegend im Cytoplasma lokalisiert waren. Die Abnahme der Akt/p70S6 Kinasen und der Erk/JNK -Map-Kinasen im Kern und eine parallele Zunahme der Aktivität von p38-Map-Kinase, Smad1/Smad2/3, STAT3 und c-Myc im Kern ist assoziiert mit dem durch BMP2 vermittelten Zelltod.

Behandlung von MCF-7 Zellen mit BMP2 (100ng/ml) für 4h (unter diesen Bedingungen wirkt BMP2 als Überlebensfaktor) zeigt eine sehr unterschiedliche Verteilung der Änderungen in der Phosphorylierung: (1) Nahezu keine Änderung für die gesamt Menge (Cytoplasma und Nukleus) von phospho-p38 MAPK, phospho-ERK, phospho-p70S6, phospho-STAT3 und phospho-Tyrosin, jedoch einen geringfügigen Anstieg dieser phosphorylierten Proteine im Cytoplasma und eine geringfügige Abnahme im Kern; (2) Gesamt c-Myc war unverändert aber geringfügig höher im Kern, ein Hinweis auf eine Translokation des Proteins; (3) Die gesamt Menge an phospho-Akt, phospho-JNK, phospho-Smad2/3 war unverändert, nahm jedoch im Cytoplasma zu, bei gleichzeitiger Abnahme im Kern.

Diese Änderungen weisen auf eine kooperative Anpassung der verschiedenen Signalwege hin, die zur Aufrechterhaltung der zellulären Homöostase erforderlich ist, diese spiegelt sich nur in der Verteilung der phosphorylierten Formen der analysierten Proteine wieder.

Im dritten Anwendungsbeispiel wurde die menschliche Leukemiezelllinie K562 mit 0,2 μ M STI571 für 24h behandelt. STI571 ist ein Tyrosinkinaseinhibitor, der spezifisch die Aktivität der Kinase BCR-Abl hemmt, die in K562 Zellen als Fusionsprotein exprimiert wird. Behandlung mit STI571 hat einen proliferationshemmenden Effekt auf diese Zellen, der zu den folgenden Veränderungen in den untersuchten Phosphoproteinen führt: (1) Abnahme von gesamt phospho-Akt and phospho-p70S6 durch Abnahme in beiden Kompartimenten (Kern und Cytoplasma); (2) Zunahme in gesamt phospho-p38, p38, c-Myc, phospho-Tyrosin, phospho-Smad1 und phospho-Smad2/3 durch Zunahme in Kern und Cytoplasma; (3) Zunahme von gesamt phospho-STAT3 und phospho-JNK durch eine Zunahme im Cytoplasma ohne Änderung im Kern; (4) Zunahme von phospho-ERK durch eine Zunahme im Kern bei gleichzeitiger Abnahme der Konzentration im Cytoplasma.

Diese Änderungen zeigen, dass eine Inhibierung der phospho-Tyrosin-Kinase BCR-abl durch STI571 die Aktivität verschiedener Signalwege beeinflusst. Das kann das Ergebnis einer direkten Beeinflussung dieser Signalwege sein, könnte aber auch eine indirekte zelluläre Anpassung an die Inhibition der BCR-Abl Aktivität durch STI571 sein.

Die Ergebnisse, die mit dem phosphoproteinspezifischen Antikörper erhalten wurden, geben einen Überblick über die Aktivierung verschiedener Signalwege, die sich in der Menge an phosphorylierten Proteinen aus den untersuchten Signalwegen widerspiegelt. In Verbindung mit einer selektiven Aufreinigung der Proteine aus verschiedenen zellulären Kompartimenten, in dieser Arbeit Kern oder Cytoplasma, ermöglicht die Antikörperarray-Technologie die schnelle Untersuchung von Konzentrationsänderungen und der Lokalisierung der phosphorylierten Proteine. Die in den Anwendungsbeispielen erhaltenen Ergebnisse wurden anschließend genutzt, um Regulationsmodelle für die verschiedenen Behandlungen zu erstellen, die auch in der Arbeit diskutiert werden.

7. References

- Afanassiev, V., Hanemann, V., Wolf, S. Preparation of DNA and protein micro arrays on glass slides coated with an agarose film. *Nucleic Acids Res.* 2000. 28: e66.
- Alas, S. and Bonavida, B. Inhibition of Constitutive STAT3 Activity Sensitizes Resistant Non-Hodgkin's Lymphoma and Multiple Myeloma to Chemotherapeutic Drug-mediated Apoptosis. *Clin Cancer Res*, 2003. 9(1): p. 316-26.
- Alkhalaf, M., El-Mowafy, A., Karam, S. Growth inhibition of MCF-7 human breast cancer cells by progesterone is associated with cell differentiation and phosphorylation of Akt protein. *Eur J Cancer Prev*, 2002. 11(5): p. 481-8.
- Angley, C., Kumar, M., Dinsio, K. J., Hall, A. K., Siegel, R. E. Signaling by bone morphogenetic proteins and Smad1 modulates the postnatal differentiation of cerebellar cells. *J Neurosci*, 2003. 23(1): p. 260-8.
- Aoki, Y., Feldman, G.M., Tosato, G. Inhibition of STAT3 signaling induces apoptosis and decreases survivin expression in primary effusion lymphoma. *Blood*, 2003. 101(4): p. 1535-42.
- Bain, G., Muller, T., Wang, X., Papkoff, J. Activated beta-catenin induces osteoblast differentiation of C3H10T1/2 cells and participates in BMP2 mediated signal transduction. *Biochem Biophys Res Commun*, 2003. 301(1): p. 84-91.
- Baldwin, R.L., Tran, H., Karlan, B.Y. Loss of c-Myc repression coincides with ovarian cancer resistance to transforming growth factor beta growth arrest independent of transforming growth factor beta/Smad signaling. *Cancer Res*, 2003. 63(6): p. 1413-9.
- Belka, C., Gruber, C., Jendrossek, V., Wesselborg, S., Budach, W. The tyrosine kinase Lck is involved in regulation of mitochondrial apoptosis pathways. *Oncogene*, 2003. 22(2): p. 176-85.
- Ben-Levy, R., Hooper, S., Wilson, R., Paterson, H. F., Marshall, C. J. Nuclear export of the stress-activated protein kinase p38 mediated by its substrate MAPKAP kinase-2. *Curr Biol*, 1998. 8(19): p. 1049-57.
- Berenbaum, F., Humbert, L., Bereziat, G., Thirion, S. Concomitant recruitment of ERK1/2 and p38 MAPK signalling pathway is required for activation of cytoplasmic phospholipase A2 via ATP in articular chondrocytes. *J Biol Chem*, 2003. 278(16): p. 13680-7.
- Blanchette, F., Rivard, N., Rudd, P., Grondin, F., Attisano, L., Dubois, C. M. Cross-talk between the p42/p44 MAP kinase and Smad pathways in transforming growth factor beta 1-induced furin gene transactivation. *J Biol Chem*, 2001. 276(36): p. 33986-94.
- Borgatti, P., Martelli, A. M., Bellacosa, A., Casto, R., Massari, L., Capitani, S., Neri, L. M. Translocation of Akt/PKB to the nucleus of osteoblast-like MC3T3-E1 cells exposed to proliferative growth factors. *FEBS Lett*, 2000. 477(1-2): p. 27-32.
- Boudny, V. and S. Nakano, Src tyrosine kinase but not activated Ras augments sensitivity to taxanes through apoptosis in human adenocarcinoma cells. *Anticancer Res*, 2003. 23(1A): p. 7-12.
- Buchdunger E., Cioffi C. L., Law N., Stover D., Ohno-Jones S., Druker B. J., Lydon N. B. Abl protein-tyrosine kinase inhibitor STI571 inhibits in vitro signal transduction mediated by c-kit and platelet-derived growth factor receptors. *J. Pharmacol. Exp. Ther.*, 295: 139-145, 2000.
- Calera, M.R., Pilch, P.F. Induction of Akt-2 correlates with differentiation in Sol8 muscle cells. *Biochem Biophys Res Commun*, 1998. 251(3): p. 835-41.
- Calvo, V., Crews, C. M., Vik, T. A., Bierer, B. E. Interleukin 2 stimulation of p70 S6 kinase activity is inhibited by the immunosuppressant rapamycin. *Proc Natl Acad Sci U S A*, 1992. 89(16): p. 7571-5.

- Canicio, J., Gallardo, E., Illa, I., Testar, X., Palacin, M., Zorzano, A., Kaliman, P. p70 S6 kinase activation is not required for insulin-like growth factor-induced differentiation of rat, mouse, or human skeletal muscle cells. *Endocrinology*, 1998. 139(12): p. 5042-9.
- Cappellini, A., Tabellini, G., Zweyer, M., Bortul, R., Tazzari, P. L., Billi, A. M., Fala, F., Cocco, L., Martelli, A. M. The phosphoinositide 3-kinase/Akt pathway regulates cell cycle progression of HL60 human leukemia cells through cytoplasmic relocation of the cyclin-dependent kinase inhibitor p27(Kip1) and control of cyclin D1 expression. *Leukemia*, 2003. 17(11): p. 2157-67.
- Cass, L.A., Meinkoth, J.L. Differential effects of cyclic adenosine 3',5'-monophosphate on p70 ribosomal S6 kinase. *Endocrinology*, 1998. 139(4): p. 1991-8.
- Catlett-Falcone, R., Landowski, T. H. Oshiro, M. M., Turkson, J., Levitzki, A., Savino, R., Ciliberto, G., Moscinski, L., Fernandez-Luna, J. L., Nunez, G., Dalton, W., S. Jove, R. Constitutive activation of STAT3 signaling confers resistance to apoptosis in human U266 myeloma cells. *Immunity*, 1999. 10(1): p. 105-15.
- Chae, H. J., Jeong, B. J., Ha, M. S., Lee, J. K., Byun, J. O., Jung, W. Y., Yun, Y. G., Lee, D. G., Oh, S. H. Chae, S. W. Kwak, Y. G. Kim, H. H. Lee, Z. H. Kim, H. R. ERK MAP Kinase is required in 1,25(OH)2D3-induced differentiation in human osteoblasts. *Immunopharmacol Immunotoxicol*, 2002. 24(1): p. 31-41.
- Chapman, R. S., Lourenco, P., Tonner, E., Flint, D., Selbert, S., Takeda, K., Akira, S., Clarke, A. R., Watson, C. J. The role of STAT3 in apoptosis and mammary gland involution. Conditional deletion of STAT3. *Adv Exp Med Biol*, 2000. 480: p. 129-38.
- Chapman, R. S., Lourenco, P. C., Tonner, E., Flint, D. J., Selbert, S., Takeda, K., Akira, S., Clarke, A. R., Watson, C. J. Suppression of epithelial apoptosis and delayed mammary gland involution in mice with a conditional knockout of STAT3. *Genes Dev*, 1999. 13(19): p. 2604-16.
- Chauhan, D., Li, G., Hideshima, T., Podar, K., Mitsiades, C., Mitsiades, N., Munshi, N., Kharbanda, S., Anderson, K. C. JNK-dependent Release of Mitochondrial Protein, Smac, during Apoptosis in Multiple Myeloma (MM) Cells. *J Biol Chem*, 2003. 278(20): p. 17593-6.
- Chen, C. R., Kang, Y., Siegel, P. M., Massague, J. E2F4/5 and p107 as Smad cofactors linking the TGFbeta receptor to c-Myc repression. *Cell*, 2002. 110(1): p. 19-32.
- Chouinard, N., Valerie, K., Rouabhia, M., Huot, J. UVB-mediated activation of p38 mitogen-activated protein kinase enhances resistance of normal human keratinocytes to apoptosis by stabilizing cytoplasmic p53. *Biochem J*, 2002. 365(Pt 1): p. 133-45.
- Chuenkova, M.V. and M.A. Pereira, The T. cruzi trans-sialidase induces PC12 cell differentiation via MAPK/ERK pathway. *Neuroreport*, 2001. 12(17): p. 3715-8.
- Chung, J., Uchida, E., Grammer, T. C., Blenis, J. STAT3 serine phosphorylation by ERK-dependent and -independent pathways negatively modulates its tyrosine phosphorylation. *Mol Cell Biol*, 1997. 17(11): p. 6508-16.
- Clement, J. H., Marr, N., Meissner, A., Schwalbe, M., Sebald, W., Kliche, K. O., Hoffken, K., Wolf, S. Bone morphogenetic protein 2 (BMP-2) induces sequential changes of Id gene expression in the breast cancer cell line MCF-7. *J Cancer Res Clin Oncol*. 2000.126(5): p. 271-9
- Coffer, P. J., van Puijenbroek, A., Burgering, B. M., Klop-de Jonge, M., Koenderman, L., Bos, J. L., Kruijer, W. Insulin activates STAT3 independently of p21ras-ERK and PI-3K signal transduction. *Oncogene*, 1997. 15(21): p. 2529-39.
- Conejo, R., de Alvaro, C., Benito, M., Cuadrado, A., Lorenzo, M. Insulin restores differentiation of Ras-transformed C2C12 myoblasts by inducing NF-kappaB through an AKT/P70S6K/p38-MAPK pathway. *Oncogene*, 2002. 21(23): p. 3739-53.

Conus, N. M., Hannan, K. M., Cristiano, B. E., Hemmings, B. A., Pearson, R. B. Direct identification of tyrosine 474 as a regulatory phosphorylation site for the Akt protein kinase. *J Biol Chem*, 2002. 277(41): p. 38021-8.

Craig, R. W., Buchan, H. L., Civin, C. I., Kastan, M. B. Altered cytoplasmic/nuclear distribution of the c-Myc protein in differentiating ML-1 human myeloid leukemia cells. *Cell Growth Differ*, 1993. 4(5): p. 349-57.

Crawley, J. B., Williams, L. M., Mander, T., Brennan, F. M., Foxwell, B. M. Interleukin-10 stimulation of phosphatidylinositol 3-kinase and p70 S6 kinase is required for the proliferative but not the antiinflammatory effects of the cytokine. *J Biol Chem*, 1996. 271(27): p. 16357-62.

Daino, H., Matsumura, I., Takada, K., Odajima, J., Tanaka, H., Ueda, S., Shibayama, H., Ikeda, H., Hibi, M., Machii, T., Hirano, T., Kanakura, Y. Induction of apoptosis by extracellular ubiquitin in human hematopoietic cells: possible involvement of STAT3 degradation by proteasome pathway in interleukin 6-dependent hematopoietic cells. *Blood*, 2000. 95(8): p. 2577-85.

Demoulin, J. B., Van Roost, E., Stevens, M., Groner, B., Renauld, J. C. Distinct roles for STAT1, STAT3, and STAT5 in differentiation gene induction and apoptosis inhibition by interleukin-9. *J Biol Chem*, 1999. 274(36): p. 25855-61.

Derynck, R., Akhurst, R.J., Balmain, A. TGF-beta signaling in tumor suppression and cancer progression. *Nat Genet*, 2001. 29(2): p. 117-29.

Deschesnes, R. G., Huot, J., Valerie, K., Landry, J. Involvement of p38 in apoptosis-associated membrane blebbing and nuclear condensation. *Mol Biol Cell*, 2001. 12(6): p. 1569-82.

Dick, A., Risau, W., Drexler, H. Expression of Smad1 and Smad2 during embryogenesis suggests a role in organ development. *Dev Dyn*, 1998. 211(4): p. 293-305.

Dickenson, J.M., Stimulation of protein kinase B and p70 S6 kinase by the histamine H1 receptor in DDT1MF-2 smooth muscle cells. *Br J Pharmacol*, 2002. 135(8): p. 1967-76.

Dickson, L. M., Lingohr, M. K., McCuaig, J., Hugl, S. R., Snow, L., Kahn, B. B., Myers, M. G., Jr. Rhodes, C. J. Differential activation of protein kinase B and p70(S6)K by glucose and insulin-like growth factor 1 in pancreatic beta-cells (INS-1). *J Biol Chem*, 2001. 276(24): p. 21110-20.

Dixon, M., Agius, L., Yeaman, S. J., Day, C. P. Inhibition of rat hepatocyte proliferation by transforming growth factor beta and glucagon is associated with inhibition of ERK2 and p70 S6 kinase. *Hepatology*, 1999. 29(5): p. 1418-24.

Dolled-Filhart, M., Camp, R. L., Kowalski, D. P., Smith, B. L., Rimm, D. L. Tissue Microarray Analysis of Signal Transducers and Activators of Transcription 3 (STAT3) and phospho-STAT3 (Tyr705) in Node-negative Breast Cancer Shows Nuclear Localization Is Associated with a Better Prognosis. *Clin Cancer Res*, 2003. 9(2): p. 594-600.

Druker B. J., Tamura S., Buchdunger E., Ohno S., Segal G. M., Fanning S., Zimmermann J., Lydon N. B. Effects of a selective inhibitor of the Abl tyrosine kinase on the growth of Bcr-Abl positive cells. *Nat. Med.*, 2: 561-566, 1996

Druker B. J., Talpaz M., Resta D. J., Peng B., Buchdunger E., Ford J. M., Lydon N. B., Kantarjian H., Capdeville R., Ohno-Jones S., Sawyers C. L. Efficacy and safety of a specific inhibitor of the BCR-ABL tyrosine kinase in chronic myeloid leukemia. *N. Engl. J. Med.*, 344: 1031-1037, 2001.

Edelmann, H. M., Kuhne, C., Petritsch, C., Ballou, L. M. Cell cycle regulation of p70 S6 kinase and p42/p44 mitogen-activated protein kinases in Swiss mouse 3T3 fibroblasts. *J Biol Chem*, 1996. 271(2): p. 963-71.

Epling-Burnette, P. K., Liu, J. H., Catlett-Falcone, R., Turkson, J., Oshiro, M., Kothapalli, R., et al., Inhibition of STAT3 signaling leads to apoptosis of leukemic large granular lymphocytes and decreased Mcl-1 expression. *J Clin Invest*, 2001. 107(3): p. 351-62.

Fang G., Kim C. N., Perkins C. L., Ramadevi N., Winton E., Wittmann S., Bhalla K. N. CGP57148B (STI-571) induces differentiation and apoptosis and sensitizes Bcr-Abl-positive human leukemia cells to apoptosis due to antileukemic drugs. *Blood*, 96: 2246-2253, 2000.

Feng, L.X., Ravindranath, N., Dym, M. Stem cell factor/c-kit up-regulates cyclin D3 and promotes cell cycle progression via the phosphoinositide 3-kinase/p70 S6 kinase pathway in spermatogonia. *J Biol Chem*, 2000. 275(33): p. 25572-6.

Feng, X. H., Liang, Y. Y., Liang, M., Zhai, W., Lin, X. Direct interaction of c-Myc with Smad2 and Smad3 to inhibit TGF-beta-mediated induction of the CDK inhibitor p15(Ink4B). *Mol Cell*, 2002. 9(1): p. 133-43.

Ferguson, C. M., Schwarz, E. M., Reynolds, P. R., Puzas, J. E., Rosier, R. N., O'Keefe, R. J. Smad2 and 3 mediate transforming growth factor-beta1-induced inhibition of chondrocyte maturation. *Endocrinology*, 2000. 141(12): p. 4728-35.

Fleckenstein, D. S., Dirks, W. G., Drexler, H. G., Quentmeier, H. Tumor necrosis factor receptor-associated factor (TRAF) 4 is a new binding partner for the p70S6 serine/threonine kinase. *Leuk Res*, 2003. 27(8): p. 687-94.

Fu, Y., O'Connor, L. M., Shepherd, T. G., Nachtigal, M. W. The p38 MAPK inhibitor, PD169316, inhibits transforming growth factor beta-induced Smad signaling in human ovarian cancer cells. *Biochem Biophys Res Commun*, 2003. 310(2): p. 391-7.

Fukada, T., Hibi, M., Yamanaka, Y., Takahashi-Tezuka, M., Fujitani, Y., Yamaguchi, T. Two signals are necessary for cell proliferation induced by a cytokine receptor gp130: involvement of STAT3 in anti-apoptosis. *Immunity*, 1996. 5(5): p. 449-60.

Ghosh-Choudhury, N., Abboud, S. L., Nishimura, R., Celeste, A., Mahimainathan, L., Choudhury, G. G. Requirement of BMP2-induced phosphatidylinositol 3-kinase and Akt serine/threonine kinase in osteoblast differentiation and Smad-dependent BMP2 gene transcription. *J Biol Chem*, 2002. 277(36): p. 33361-8.

Grandis, J. R., Drenning, S. D., Zeng, Q., Watkins, S. C., Melhem, M. F., Endo, S., et al., Constitutive activation of STAT3 signaling abrogates apoptosis in squamous cell carcinogenesis in vivo. *Proc Natl Acad Sci U S A*, 2000. 97(8): p. 4227-32.

Grandis, J.R., Zeng, Q., Drenning, S.D. Epidermal growth factor receptor--mediated STAT3 signaling blocks apoptosis in head and neck cancer. *Laryngoscope*, 2000. 110(5 Pt 1): p. 868-74.

Greten, F.R., Weber, C. K., Greten, T. F., Schneider, G., Wagner, M., Adler, G., et al., STAT3 and NF-kappaB activation prevents apoptosis in pancreatic carcinogenesis. *Gastroenterology*, 2002. 123(6): p. 2052-63.

Gruendler, C., Lin, Y., Farley, J., Wang, T. Proteasomal degradation of Smad1 induced by bone morphogenetic proteins. *J Biol Chem*, 2001. 276(49): p. 46533-43.

Gusse, M., Ghysdael, J., Evan, G., Soussi, T., Mechali, M. Translocation of a store of maternal cytoplasmic c-Myc protein into nuclei during early development. *Mol Cell Biol*, 1989. 9(12): p. 5395-403.

Haab BB, Dunham MJ, Brown PO. (2001) Protein microarrays for highly parallel detection and quantitation of specific proteins and antibodies in complex solutions. *Genome Biol*. 2: research0004.

Hannan, K.M., Thomas, G., Pearson, R.B. Activation of S6K1 (p70 ribosomal protein S6 kinase 1) requires an initial calcium-dependent priming event involving formation of a high-molecular-mass signalling complex. *Biochem J*, 2003. 370(Pt 2): p. 469-77.

Harada, H., Andersen, J. S., Mann, M., Terada, N., Korsmeyer, S. J. p70S6 kinase signals cell survival as well as growth, inactivating the pro-apoptotic molecule BAD. *Proc Natl Acad Sci U S A*, 2001. 98(17): p. 9666-70.

Hata, K., Nishimura, R., Ikeda, F., Yamashita, K., Matsubara, T., Nokubi, T., et al., Differential Roles of Smad1 and p38 Kinase in Regulation of Peroxisome Proliferator-activating Receptor gamma during Bone Morphogenetic Protein 2-induced Adipogenesis. *Mol Biol Cell*, 2003. 14(2): p. 545-55.

Hayashi, H., Ishisaki, A., Imamura, T. Smad mediates BMP2-induced upregulation of FGF-evoked PC12 cell differentiation. *FEBS Lett*, 2003. 536(1-3): p. 30-4.

Hayashi, K., Kobayashi, T., Umino, T., Goitsuka, R., Matsui, Y., Kitamura, D. SMAD1 signaling is critical for initial commitment of germ cell lineage from mouse epiblast. *Mech Dev*, 2002. 118(1-2): p. 99-109.

Hayes, S.A., Huang, X., Kambhampati, S., Plataniias, L. C., Bergan, R. C. p38 MAP kinase modulates Smad-dependent changes in human prostate cell adhesion. *Oncogene*, 2003. 22(31): p. 4841-50.

Heliez, C., Baricault, L., Barboule, N., Valette, A. Paclitaxel increases p21 synthesis and accumulation of its AKT-phosphorylated form in the cytoplasm of cancer cells. *Oncogene*, 2003. 22(21): p. 3260-8.

Hirata, Y., Kiuchi, K. Mitogenic effect of glial cell line-derived neurotrophic factor is dependent on the activation of p70S6 kinase, but independent of the activation of ERK and up-regulation of Ret in SH-SY5Y cells. *Brain Res*, 2003. 983(1-2): p. 1-12.

Itoh, S., Itoh, F., Goumans, M. J., Ten Dijke, P. Signaling of transforming growth factor-beta family members through Smad proteins. *Eur J Biochem*, 2000. 267(24): p. 6954-67.

Ivaska, J., Reunanen, H., Westermarck, J., Koivisto, L., Kahari, V. M., Heino, J. Integrin alpha2beta1 mediates isoform-specific activation of p38 and upregulation of collagen gene transcription by a mechanism involving the alpha2 cytoplasmic tail. *J Cell Biol*, 1999. 147(2): p. 401-16.

James, P. "Protein identification in the post-genome era: the rapid rise of proteomics." *Q Rev Biophys*, 1997. 30(4): 279-331.

Jono, H., Xu, H., Kai, H., Lim, D. J., Kim, Y. S., Feng, X. H., et al., Transforming growth factor-beta-Smad signaling pathway negatively regulates nontypeable Haemophilus influenzae-induced MUC5AC mucin transcription via mitogen-activated protein kinase (MAPK) phosphatase-1-dependent inhibition of p38 MAPK. *J Biol Chem*, 2003. 278(30): p. 27811-9.

Ju, W., Hoffmann, A., Verschueren, K., Tylzanowski, P., Kaps, C., Gross, G., et al., The bone morphogenetic protein 2 signaling mediator Smad1 participates predominantly in osteogenic and not in chondrogenic differentiation in mesenchymal progenitors C3H10T1/2. *J Bone Miner Res*, 2000. 15(10): p. 1889-99.

Kageyama, K., Ihara, Y., Goto, S., Urata, Y., Toda, G., Yano, K., et al., Overexpression of calreticulin modulates protein kinase B/Akt signaling to promote apoptosis during cardiac differentiation of cardiomyoblast H9c2 cells. *J Biol Chem*, 2002. 277(22): p. 19255-64.

Kanai, M., Konda, Y., Nakajima, T., Izumi, Y., Kanda, N., Nanakin, A., et al., Differentiation-inducing factor-1 (DIF-1) inhibits STAT3 activity involved in gastric cancer cell proliferation via MEK-ERK-dependent pathway. *Oncogene*, 2003. 22(4): p. 548-54.

- Kanayasu-Toyoda, T., Yamaguchi, T., Oshizawa, T., Kogi, M., Uchida, E., Hayakawa, T. Role of the p70 S6 kinase cascade in neutrophilic differentiation and proliferation of HL-60 cells—a study of transferrin receptor-positive and -negative cells obtained from dimethyl sulfoxide- or retinoic acid-treated HL-60 cells. *Arch Biochem Biophys*, 2002. 405(1): p. 21-31.
- Kanda, S., Hodgkin, M. N., Woodfield, R. J., Wakelam, M. J., Thomas, G., Claesson-Welsh, L. Phosphatidylinositol 3'-kinase-independent p70 S6 kinase activation by fibroblast growth factor receptor-1 is important for proliferation but not differentiation of endothelial cells. *J Biol Chem*, 1997. 272(37): p. 23347-53.
- Kang, H.J., Soh, Y., Kim, M. S., Lee, E. J., Surh, Y. J., Kim, H. R., et al., Roles of JNK-1 and p38 in selective induction of apoptosis by capsaicin in ras-transformed human breast epithelial cells. *Int J Cancer*, 2003. 103(4): p. 475-82.
- Kawamura, C., M. Kizaki, and Y. Ikeda, Bone morphogenetic protein (BMP)-2 induces apoptosis in human myeloma cells. *Leuk Lymphoma*, 2002. 43(3): p. 635-9.
- Kawamura, C., Kizaki, M., Yamato, K., Uchida, H., Fukuchi, Y., Hattori, Y., et al., Bone morphogenetic protein-2 induces apoptosis in human myeloma cells with modulation of STAT3. *Blood*, 2000. 96(6): p. 2005-11.
- Kawashima, K., K. Yamakawa, and J. Arita, Involvement of phosphoinositide-3-kinase and p70 S6 kinase in regulation of proliferation of rat lactotrophs in culture. *Endocrine*, 2000. 13(3): p. 385-92.
- Khurana, A., Dey, C.S. p38 MAPK interacts with actin and modulates filament assembly during skeletal muscle differentiation. *Differentiation*, 2003. 71(1): p. 42-50.
- Kim, J., Adam, R.M., Freeman, M.R. Activation of the ERK mitogen-activated protein kinase pathway stimulates neuroendocrine differentiation in LNCaP cells independently of cell cycle withdrawal and STAT3 phosphorylation. *Cancer Res*, 2002. 62(5): p. 1549-54.
- Kimura, N., Matsuo, R., Shibuya, H., Nakashima, K., Taga, T. BMP2-induced apoptosis is mediated by activation of the TAK1-p38 kinase pathway that is negatively regulated by Smad6. *J Biol Chem*, 2000. 275(23): p. 17647-52.
- Kiuchi, N., Nakajima, K., Ichiba, M., Fukada, T., Narimatsu, M., Mizuno, K., et al., STAT3 is required for the gp130-mediated full activation of the c-Myc gene. *J Exp Med*, 1999. 189(1): p. 63-73.
- Klekotka, P.A., Santoro, S.A., Zutter, M.M. alpha 2 integrin subunit cytoplasmic domain-dependent cellular migration requires p38 MAPK. *J Biol Chem*, 2001. 276(12): p. 9503-11.
- Knezevic V, Leethanakul C, Bichsel VE, Worth JM, Prabhu VV, Gutkind JS, Liotta LA, Munson PJ, Petricoin EF 3rd, Krizman DB. (2001) Proteomic profiling of the cancer microenvironment by antibody arrays. *Proteomics*. 1: 1271-1278.
- Korchynskiy, O., Landstrom, M., Stoika, R., Funa, K., Heldin, C. H., ten Dijke, P., et al., Expression of Smad proteins in human colorectal cancer. *Int J Cancer*, 1999. 82(2): p. 197-202.
- Kowalik, T.F., Smad about E2F. TGFbeta repression of c-Myc via a Smad3/E2F/p107 complex. *Mol Cell*, 2002. 10(1): p. 7-8.
- Kozawa, O., Matsuno, H., Uematsu, T. Involvement of p70 S6 kinase in bone morphogenetic protein signaling: vascular endothelial growth factor synthesis by bone morphogenetic protein-4 in osteoblasts. *J Cell Biochem*, 2001. 81(3): p. 430-6.
- Kretzschmar, M., Doody, J., Massague, J. Opposing BMP and EGF signalling pathways converge on the TGF-beta family mediator Smad1. *Nature*, 1997. 389(6651): p. 618-22.

- Kretzschmar, M., Liu, F., Hata, A., Doody, J., Massague, J. The TGF-beta family mediator Smad1 is phosphorylated directly and activated functionally by the BMP receptor kinase. *Genes Dev*, 1997. 11(8): p. 984-95.
- Kuo, C.J., Chung, J., Fiorentino, D. F., Flanagan, W. M., Blenis, J., Crabtree, G. R. Rapamycin selectively inhibits interleukin-2 activation of p70 S6 kinase. *Nature*, 1992. 358(6381): p. 70-3.
- Lafont, V., Astoul, E., Laurence, A., Liautard, J., Cantrell, D. The T cell antigen receptor activates phosphatidylinositol 3-kinase-regulated serine kinases protein kinase B and ribosomal S6 kinase 1. *FEBS Lett*, 2000. 486(1): p. 38-42.
- Lai, C.F., Chaudhary, L., Fausto, A., Halstead, L. R., Ory, D. S., Avioli, L. V., et al., ERK is essential for growth, differentiation, integrin expression, and cell function in human osteoblastic cells. *J Biol Chem*, 2001. 276(17): p. 14443-50.
- Lai, R., Rassidakis, G. Z., Medeiros, L. J., Leventaki, V., Keating, M., McDonnell, T. J. Expression of STAT3 and its phosphorylated forms in mantle cell lymphoma cell lines and tumours. *J Pathol*, 2003. 199(1): p. 84-9.
- Laprise, P., Chailier, P., Houde, M., Beaulieu, J. F., Boucher, M. J., Rivard, N. Phosphatidylinositol 3-kinase controls human intestinal epithelial cell differentiation by promoting adherens junction assembly and p38 MAPK activation. *J Biol Chem*, 2002. 277(10): p. 8226-34.
- Lee, J.K., Jung, J. C., Chun, J. S., Kang, S. S., Bang, O. S. Expression of p21WAF1 is dependent on the activation of ERK during vitamin E-succinate-induced monocytic differentiation. *Mol Cells*, 2002. 13(1): p. 125-9.
- Lee, K.S., Hong, S.H., Bae, S.C. Both the Smad and p38 MAPK pathways play a crucial role in Runx2 expression following induction by transforming growth factor-beta and bone morphogenetic protein. *Oncogene*, 2002. 21(47): p. 7156-63.
- Lehman, J.A., Calvo, V., Gomez-Cambronero, J. Mechanism of ribosomal p70S6 kinase activation by GM-CSF in neutrophils: Cooperation of a MEK-related, T421/S424-kinase and a rapamycin-sensitive, mTOR-related, T389-kinase. *J Biol Chem*, 2003.
- Lei, K., Davis, R.J. JNK phosphorylation of Bim-related members of the Bcl2 family induces Bax-dependent apoptosis. *Proc Natl Acad Sci U S A*, 2003. 100(5): p. 2432-7.
- Lenormand, P., McMahon, M., Pouyssegur, J. Oncogenic Raf-1 activates p70 S6 kinase via a mitogen-activated protein kinase-independent pathway. *J Biol Chem*, 1996. 271(26): p. 15762-8.
- Li, H.L., Davis, W., Pure, E. Suboptimal cross-linking of antigen receptor induces Syk-dependent activation of p70S6 kinase through protein kinase C and phosphoinositol 3-kinase. *J Biol Chem*, 1999. 274(14): p. 9812-20.
- Li, X., Schwarz, E. M., Zuscik, M. J., Rosier, R. N., Ionescu, A. M., Puzas, J. E., et al., Retinoic acid stimulates chondrocyte differentiation and enhances bone morphogenetic protein effects through induction of Smad1 and Smad5. *Endocrinology*, 2003. 144(6): p. 2514-23.
- Lin, A., Activation of the JNK signaling pathway: breaking the brake on apoptosis. *Bioessays*, 2003. 25(1): p. 17-24.
- Lopez-Carballo, G., Moreno, L., Masia, S., Perez, P., Baretino, D. Activation of the phosphatidylinositol 3-kinase/Akt signaling pathway by retinoic acid is required for neural differentiation of SH-SY5Y human neuroblastoma cells. *J Biol Chem*, 2002. 277(28): p. 25297-304.
- Lopez-Rovira, T., Chalaux, E., Massague, J., Rosa, J. L., Ventura, F. Direct binding of Smad1 and Smad4 to two distinct motifs mediates bone morphogenetic protein-specific transcriptional activation of Id1 gene. *J Biol Chem*, 2002. 277(5): p. 3176-85.

Lorenzini, A., Tresini, M., Mawal-Dewan, M., Frisoni, L., Zhang, H., Allen, R. G., et al., Role of the Raf/MEK/ERK and the PI3K/Akt(PKB) pathways in fibroblast senescence. *Exp Gerontol*, 2002. 37(10-11): p. 1149-56.

Luciano, F., Herrant, M., Jacquet, A., Ricci, J. E., Auburger, P. The p54 cleaved form of the tyrosine kinase Lyn generated by caspases during BCR-induced cell death in B lymphoma acts as a negative regulator of apoptosis. *Faseb J*, 2003. 17(6): p. 711-3.

Madoz-Gurpide J, Wang H, Misek DE, Brichory F, Hanash SM. (2001) Protein based microarrays: a tool for probing the proteome of cancer cells and tissues. *Proteomics*. 1: 1279-1287.

Maguer-Satta, V., Bartholin, L., Jeanpierre, S., Ffrench, M., Martel, S., Magaud, J. P., et al., Regulation of human erythropoiesis by activin A, BMP2, and BMP4, members of the TGFbeta family. *Exp Cell Res*, 2003. 282(2): p. 110-20.

Marte, B.M., Graus-Porta, D., Jeschke, M., Fabbro, D., Hynes, N. E., Taverna, D. NDF/hereregulin activates MAP kinase and p70/p85 S6 kinase during proliferation or differentiation of mammary epithelial cells. *Oncogene*, 1995. 10(1): p. 167-75.

McGinn, S., Saad, S., Poronnik, P., Pollock, C. High glucose mediated effects on endothelial cell proliferation occur via p38 MAP kinase. *Am J Physiol Endocrinol Metab*, 2003.

Milocco, L.H., Haslam, J. A., Rosen, J., Seidel, H. M. Design of conditionally active STATs: insights into STAT activation and gene regulatory function. *Mol Cell Biol*, 1999. 19(4): p. 2913-20.

Minami, Y., Nakagawa, Y., Kawahara, A., Miyazaki, T., Sada, K., Yamamura, H., et al., Protein tyrosine kinase Syk is associated with and activated by the IL-2 receptor: possible link with the c-Myc induction pathway. *Immunity*, 1995. 2(1): p. 89-100.

Miyakawa, M., Tsushima, T., Murakami, H., Wakai, K., Isozaki, O., Takano, K. Increased expression of phosphorylated p70S6 kinase and Akt in papillary thyroid cancer tissues. *Endocr J*, 2003. 50(1): p. 77-83.

Monfar, M., Blenis, J. Inhibition of p70/p85 S6 kinase activities in T cells by dexamethasone. *Mol Endocrinol*, 1996. 10(9): p. 1107-15.

Mora, L.B., Buettner, R., Seigne, J., Diaz, J., Ahmad, N., Garcia, R., et al., Constitutive activation of STAT3 in human prostate tumors and cell lines: direct inhibition of STAT3 signaling induces apoptosis of prostate cancer cells. *Cancer Res*, 2002. 62(22): p. 6659-66.

Nakamura, Y., Ozaki, T., Koseki, H., Nakagawara, A., Sakiyama, S. Accumulation of p27(KIP1) is associated with BMP2-induced growth arrest and neuronal differentiation of human neuroblastoma-derived cell lines. *Biochem Biophys Res Commun*, 2003. 307(1): p. 206-13.

Nakashima, K., Yanagisawa, M., Arakawa, H., Kimura, N., Hisatsune, T., Kawabata, M., et al., Synergistic signaling in fetal brain by STAT3-Smad1 complex bridged by p300. *Science*, 1999. 284(5413): p. 479-82.

Ndubuisi, M.I., Guo, G. G., Fried, V. A., Etlinger, J. D., Sehgal, P. B. Cellular physiology of STAT3: Where's the cytoplasmic monomer? *J Biol Chem*, 1999. 274(36): p. 25499-509.

Nelson, J.M., Fry, D.W. Akt, MAPK (Erk1/2), and p38 act in concert to promote apoptosis in response to ErbB receptor family inhibition. *J Biol Chem*, 2001. 276(18): p. 14842-7.

Nielsen, M., Kaestel, C. G., Eriksen, K. W., Woetmann, A., Stokkedal, T., Kalsoft, K., et al., Inhibition of constitutively activated STAT3 correlates with altered Bcl-2/Bax expression and induction of apoptosis in mycosis fungoides tumor cells. *Leukemia*, 1999. 13(5): p. 735-8.

- Nikitakis, N.G., Siavash, H., Hebert, C., Reynolds, M. A., Hamburger, A. W., Sauk, J. J. 15-PGJ2, but not thiazolidinediones, inhibits cell growth, induces apoptosis, and causes downregulation of STAT3 in human oral SCCa cells. *Br J Cancer*, 2002. 87(12): p. 1396-403.
- Nishimura, R., Hata, K., Harris, S. E., Ikeda, F., Yoneda, T. Core-binding factor alpha 1 (Cbfa1) induces osteoblastic differentiation of C2C12 cells without interactions with Smad1 and Smad5. *Bone*, 2002. 31(2): p. 303-12.
- Ochi, H., Ogino, H., Kageyama, Y., Yasuda, K. The stability of the lens-specific Maf protein is regulated by fibroblast growth factor (FGF)/ERK signaling in lens fiber differentiation. *J Biol Chem*, 2003. 278(1): p. 537-44.
- O'Farrell, A.M., Parry, D. A., Zindy, F., Roussel, M. F., Lees, E., Moore, K. W., et al., STAT3-dependent induction of p19INK4D by IL-10 contributes to inhibition of macrophage proliferation. *J Immunol*, 2000. 164(9): p. 4607-15.
- Ohshima, T., Shimotohno, K. TGF- β mediated signaling via the p38 MAP kinase pathway activates Smad-dependent transcription through SUMO-1 modification of Smad4. *J Biol Chem*, 2003.
- Ohtsuka, T., Buchsbaum, D., Oliver, P., Makhija, S., Kimberly, R., Zhou, T. Synergistic induction of tumor cell apoptosis by death receptor antibody and chemotherapy agent through JNK/p38 and mitochondrial death pathway. *Oncogene*, 2003. 22(13): p. 2034-44.
- Okano, H.J., Park, W. Y., Corradi, J. P., Darnell, R. B. The cytoplasmic Purkinje onconeural antigen cdr2 down-regulates c-Myc function: implications for neuronal and tumor cell survival. *Genes Dev*, 1999. 13(16): p. 2087-97.
- Okuma, E., Inazawa, Y., Saeki, K., Yuo, A. Potential roles of extracellular signal-regulated kinase but not p38 during myeloid differentiation of U937 cells stimulated by cytokines: augmentation of differentiation via prolonged activation of extracellular signal-regulated kinase. *Exp Hematol*, 2002. 30(6): p. 571-81.
- Oritani, K., Tomiyama, Y., Kincade, P. W., Aoyama, K., Yokota, T., Matsumura, I., et al., Both STAT3-activation and STAT3-independent BCL2 downregulation are important for interleukin-6-induced apoptosis of 1A9-M cells. *Blood*, 1999. 93(4): p. 1346-54.
- Ostrowski, J., Woszczyński, M., Kowalczyk, P., Wocial, T., Hennig, E., Trzeciak, L., et al., Increased activity of MAP, p70S6 and p90rs kinases is associated with Ap-1 activation in spontaneous liver tumours, but not in adjacent tissue in mice. *Br J Cancer*, 2000. 82(5): p. 1041-50.
- Park, G.T., Morasso, M.I. Bone morphogenetic protein-2 (BMP2) transactivates Dlx3 through Smad1 and Smad4: alternative mode for Dlx3 induction in mouse keratinocytes. *Nucleic Acids Res*, 2002. 30(2): p. 515-22.
- Phillips-Mason, P.J., R. Goel, and J.J. Baldassare, alpha-Thrombin activates Akt via a nonreceptor tyrosine kinase in IIC9 cells. *Ann N Y Acad Sci*, 2002. 973: p. 142-4.
- Podsypanina, K., Lee, R. T., Politis, C., Hennessy, I., Crane, A., Puc, J., et al., An inhibitor of mTOR reduces neoplasia and normalizes p70/S6 kinase activity in Pten \pm mice. *Proc Natl Acad Sci U S A*, 2001. 98(18): p. 10320-5.
- Pohl, F., Hassel, S., Nohe, A., Flentje, M., Knaus, P., Sebald, W., et al., Radiation-induced suppression of the Bmp2 signal transduction pathway in the pluripotent mesenchymal cell line C2C12: an in vitro model for prevention of heterotopic ossification by radiotherapy. *Radiat Res*, 2003. 159(3): p. 345-50.
- Poselova, T.V., Evdonin, A. L., Medvedeva, N. D., Pospelov, V. A. [Transcription factors STAT1 and STAT3 are localized in different compartments of rat embryo fibroblasts transformed by E1A and Ha-Ras oncogenes]. *Tsitologiya*, 1998. 40(12): p. 1074-9.

Prusty, D., Park, B. H., Davis, K. E., Farmer, S. R. Activation of MEK/ERK signaling promotes adipogenesis by enhancing peroxisome proliferator-activated receptor gamma (PPARgamma) and C/EBPalpha gene expression during the differentiation of 3T3-L1 preadipocytes. *J Biol Chem*, 2002. 277(48): p. 46226-32.

Rahaman, S.O., Harbor, P. C., Chernova, O., Barnett, G. H., Vogelbaum, M. A., Haque, S. J. Inhibition of constitutively active STAT3 suppresses proliferation and induces apoptosis in glioblastoma multiforme cells. *Oncogene*, 2002. 21(55): p. 8404-13.

Rebbaa, A., P.M. Chou, and B.L. Mirkin, Factors secreted by human neuroblastoma mediated doxorubicin resistance by activating STAT3 and inhibiting apoptosis. *Mol Med*, 2001. 7(6): p. 393-400.

Romanelli, A., Martin, K. A., Toker, A., Blenis, J. p70 S6 kinase is regulated by protein kinase Czeta and participates in a phosphoinositide 3-kinase-regulated signalling complex. *Mol Cell Biol*, 1999. 19(4): p. 2921-8.

Ryu, J.K., Choi, H. B., Hatori, K., Heisel, R. L., Pelech, S. L., McLarnon, J. G., et al., Adenosine triphosphate induces proliferation of human neural stem cells: Role of calcium and p70 ribosomal protein S6 kinase. *J Neurosci Res*, 2003. 72(3): p. 352-62.

Saeki, K., Kobayashi, N., Inazawa, Y., Zhang, H., Nishitoh, H., Ichijo, H., et al., Oxidation-triggered c-Jun N-terminal kinase (JNK) and p38 mitogen-activated protein (MAP) kinase pathways for apoptosis in human leukaemic cells stimulated by epigallocatechin-3-gallate (EGCG): a distinct pathway from those of chemically induced and receptor-mediated apoptosis. *Biochem J*, 2002. 368(Pt 3): p. 705-20.

Sakou, T., Onishi, T., Yamamoto, T., Nagamine, T., Sampath, T., Ten Dijke, P. Localization of Smads, the TGF-beta family intracellular signaling components during endochondral ossification. *J Bone Miner Res*, 1999. 14(7): p. 1145-52.

Salh, B., Wagey, R., Marotta, A., Tao, J. S., Pelech, S. Activation of phosphatidylinositol 3-kinase, protein kinase B, and p70 S6 kinases in lipopolysaccharide-stimulated Raw 264.7 cells: differential effects of rapamycin, Ly294002, and wortmannin on nitric oxide production. *J Immunol*, 1998. 161(12): p. 6947-54.

Sanchez-Esteban, J., Wang, Y., Gruppuso, P. A., Rubin, L. P. Mechanical Stretch Induces Fetal Type II Cell Differentiation via an EGFR-ERK Signaling Pathway. *Am J Respir Cell Mol Biol*, 2003.

Sardi, I., Dal Canto, M., Bartoletti, R., Guazzelli, R., Travaglini, F., Montali, E. Molecular genetic alterations of c-Myc oncogene in superficial and locally advanced bladder cancer. *Eur Urol*, 1998. 33(4): p. 424-30.

Sawafuji, K., Miyakawa, Y., Kizaki, M., Ikeda, Y. Cyclosporin A induces erythroid differentiation of K562 cells through p38 MAPK and ERK pathways. *Am J Hematol*, 2003. 72(1): p. 67-9.

Schroeter, H., Boyd, C. S., Ahmed, R., Spencer, J. P., Duncan, R. F., Rice-Evans, C., et al., c-Jun N-terminal kinase (JNK)-mediated modulation of brain mitochondria function: new target proteins for JNK signalling in mitochondrion-dependent apoptosis. *Biochem J*, 2003. 372(Pt 2): p. 359-69.

Scott, P.H., Belham, C. M., al-Hafidh, J., Chilvers, E. R., Peacock, A. J., Gould, G. W., et al., A regulatory role for cAMP in phosphatidylinositol 3-kinase/p70 ribosomal S6 kinase-mediated DNA synthesis in platelet-derived-growth-factor-stimulated bovine airway smooth-muscle cells. *Biochem J*, 1996. 318 (Pt 3): p. 965-71.

Shen, Y., Devgan, G., Darnell, J. E., Jr., Bromberg, J. F. Constitutively activated STAT3 protects fibroblasts from serum withdrawal and UV-induced apoptosis and antagonizes the proapoptotic effects of activated Stat1. *Proc Natl Acad Sci U S A*, 2001. 98(4): p. 1543-8.

Shirogane, T., Fukada, T., Muller, J. M., Shima, D. T., Hibi, M., Hirano, T. Synergistic roles for Pim-1 and c-Myc in STAT3-mediated cell cycle progression and antiapoptosis. *Immunity*, 1999. 11(6): p. 709-19.

Skutek, M., Van Griensven, M., Zeichen, J., Brauer, N., Bosch, U. Cyclic mechanical stretching of human patellar tendon fibroblasts: activation of JNK and modulation of apoptosis. *Knee Surg Sports Traumatol Arthrosc*, 2003. 11(2): p. 122-9.

Slavik, J.M., Lim, D. G., Burakoff, S. J., Hafler, D. A. Uncoupling p70(s6) kinase activation and proliferation: rapamycin-resistant proliferation of human CD8(+) T lymphocytes. *J Immunol*, 2001. 166(5): p. 3201-9.

Smith, W.E., Kane, A. V., Campbell, S. T., Acheson, D. W., Cochran, B. H., Thorpe, C. M. Shiga toxin 1 triggers a ribotoxic stress response leading to p38 and JNK activation and induction of apoptosis in intestinal epithelial cells. *Infect Immun*, 2003. 71(3): p. 1497-504.

Song, L., Turkson, J., Karras, J. G., Jove, R., Haura, E. B. Activation of STAT3 by receptor tyrosine kinases and cytokines regulates survival in human non-small cell carcinoma cells. *Oncogene*, 2003. 22(27): p. 4150-65.

Spiekermann, K., Dirschinger, R. J., Schwab, R., Bagrintseva, K., Faber, F., Buske, C., et al., The protein tyrosine kinase inhibitor SU5614 inhibits FLT3 and induces growth arrest and apoptosis in AML-derived cell lines expressing a constitutively activated FLT3. *Blood*, 2003. 101(4): p. 1494-504.

Stawowy, P., Blaschke, F., Kilimnik, A., Goetze, S., Kallisch, H., Chretien, M., et al., Proprotein convertase PC5 regulation by PDGF-BB involves PI3-kinase/p70(s6)-kinase activation in vascular smooth muscle cells. *Hypertension*, 2002. 39(2 Pt 2): p. 399-404.

Stoeger, T., Proetzel, G. E., Welzel, H., Papadimitriou, A., Dony, C., Balling, R., et al., In situ gene expression analysis during BMP2-induced ectopic bone formation in mice shows simultaneous endochondral and intramembranous ossification. *Growth Factors*, 2002. 20(4): p. 197-210.

Strehlow, I., Schindler, C. Amino-terminal signal transducer and activator of transcription (STAT) domains regulate nuclear translocation and STAT deactivation. *J Biol Chem*, 1998. 273(43): p. 28049-56.

Subramaniam, P.S., Torres, B.A., Johnson, H.M. So many ligands, so few transcription factors: a new paradigm for signaling through the STAT transcription factors. *Cytokine*, 2001. 15(4): p. 175-87.

Suzawa, M., Tamura, Y., Fukumoto, S., Miyazono, K., Fujita, T., Kato, S., et al., Stimulation of Smad1 transcriptional activity by Ras-extracellular signal-regulated kinase pathway: a possible mechanism for collagen-dependent osteoblastic differentiation. *J Bone Miner Res*, 2002. 17(2): p. 240-8.

Takeda, K., Kaisho, T., Yoshida, N., Takeda, J., Kishimoto, T., Akira, S. STAT3 activation is responsible for IL-6-dependent T cell proliferation through preventing apoptosis: generation and characterization of T cell-specific STAT3-deficient mice. *J Immunol*, 1998. 161(9): p. 4652-60.

Takekawa, M., Tatebayashi, K., Itoh, F., Adachi, M., Imai, K., Saito, H. Smad-dependent GADD45beta expression mediates delayed activation of p38 MAP kinase by TGF-beta. *Embo J*, 2002. 21(23): p. 6473-82.

Tamura, Y., Takeuchi, Y., Suzawa, M., Fukumoto, S., Kato, M., Miyazono, K., et al., Focal adhesion kinase activity is required for bone morphogenetic protein--Smad1 signaling and

- osteoblastic differentiation in murine MC3T3-E1 cells. *J Bone Miner Res*, 2001. 16(10): p. 1772-9.
- Tarnawski, A.S., Pai, R., Wang, H., Tomikawa, M. Translocation of MAP (Erk-1 and -2) kinases to cell nuclei and activation of c-fos gene during healing of experimental gastric ulcers. *J Physiol Pharmacol*, 1998. 49(4): p. 479-88.
- Terada, N., Franklin, R. A., Lucas, J. J., Blenis, J., Gelfand, E. W. Failure of rapamycin to block proliferation once resting cells have entered the cell cycle despite inactivation of p70 S6 kinase. *J Biol Chem*, 1993. 268(16): p. 12062-8.
- Terada, N., Lucas, J. J., Szepesi, A., Franklin, R. A., Takase, K., Gelfand, E. W. Rapamycin inhibits the phosphorylation of p70 S6 kinase in IL-2 and mitogen-activated human T cells. *Biochem Biophys Res Commun*, 1992. 186(3): p. 1315-21.
- Tomic, D., Brodie, S. G., Deng, C., Hickey, R. J., Babus, J. K., Malkas, L. H., et al., Smad 3 may regulate follicular growth in the mouse ovary. *Biol Reprod*, 2002. 66(4): p. 917-23.
- Toyoshima, F., T. Moriguchi, and E. Nishida, Fas induces cytoplasmic apoptotic responses and activation of the MKK7-JNK/SAPK and MKK6-p38 pathways independent of CPP32-like proteases. *J Cell Biol*, 1997. 139(4): p. 1005-15.
- Tremblay, K.D., Dunn, N.R., Robertson, E.J. Mouse embryos lacking Smad1 signals display defects in extra-embryonic tissues and germ cell formation. *Development*, 2001. 128(18): p. 3609-21.
- Thiesing J. T., Ohno-Jones S., Kolibaba K. S., Druker B. J. Efficacy of STI571, an abl tyrosine kinase inhibitor, in conjunction with other antileukemic agents against Bcr-Abl-positive cells. *Blood*, 96: 3195-3199, 2000
- Tsai, P.W., Shiah, S. G., Lin, M. T., Wu, C. W., Kuo, M. L. Up-regulation of vascular endothelial growth factor C in breast cancer cells by heregulin-beta 1. A critical role of p38/nuclear factor-kappa B signaling pathway. *J Biol Chem*, 2003. 278(8): p. 5750-9.
- Tsuda, H., Wada, T., Ito, Y., Uchida, H., Dehari, H., Nakamura, K., et al., Efficient BMP2 gene transfer and bone formation of mesenchymal stem cells by a fiber-mutant adenoviral vector. *Mol Ther*, 2003. 7(3): p. 354-65.
- Tyagi, A., Agarwal, R., Agarwal, C. Grape seed extract inhibits EGF-induced and constitutively active mitogenic signaling but activates JNK in human prostate carcinoma DU145 cells: possible role in antiproliferation and apoptosis. *Oncogene*, 2003. 22(9): p. 1302-16.
- Ungefroren, H., Lenschow, W., Chen, W. B., Faendrich, F., Kalthoff, H. Regulation of biglycan gene expression by transforming growth factor-beta requires MKK6-p38 mitogen-activated protein Kinase signaling downstream of Smad signaling. *J Biol Chem*, 2003. 278(13): p. 11041-9.
- Valovka, T., Verdier, F., Cramer, R., Zhyvoloup, A., Fenton, T., Rebholz, H., et al., Protein kinase C phosphorylates ribosomal protein S6 kinase beta11 and regulates its subcellular localization. *Mol Cell Biol*, 2003. 23(3): p. 852-63.
- Van Brocklyn, J.R., Vandenheede, J. R., Fertel, R., Yates, A. J., Rampersaud, A. A. Ganglioside GM1 activates the mitogen-activated protein kinase Erk2 and p70 S6 kinase in U-1242 MG human glioma cells. *J Neurochem*, 1997. 69(1): p. 116-25.
- van Puijenbroek, A.A., P.T. van der Saag, and P.J. Coffey, Cytokine signal transduction in P19 embryonal carcinoma cells: regulation of STAT3-mediated transactivation occurs independently of p21ras-ERK signaling. *Exp Cell Res*, 1999. 251(2): p. 465-76.
- Veyrune, J.L., Campbell, G. P., Wiseman, J., Blanchard, J. M., Hesketh, J. E. A localisation signal in the 3' untranslated region of c-Myc mRNA targets c-Myc mRNA and beta-globin

reporter sequences to the perinuclear cytoplasm and cytoskeletal-bound polysomes. *J Cell Sci*, 1996. 109 (Pt 6): p. 1185-94.

Vigneri P., Wang J. Y. Induction of apoptosis in chronic myelogenous leukemia cells through nuclear entrapment of BCR-ABL tyrosine kinase. *Nat. Med.*, 7: 228-234, 2001

Vijayachandra, K., Lee, J., Glick, A.B. Smad3 regulates senescence and malignant conversion in a mouse multistage skin carcinogenesis model. *Cancer Res*, 2003. 63(13): p. 3447-52.

Vinals, F., Chambard, J.C., Pouyssegur, J. p70 S6 kinase-mediated protein synthesis is a critical step for vascular endothelial cell proliferation. *J Biol Chem*, 1999. 274(38): p. 26776-82.

Vinals, F., Lopez-Rovira, T., Rosa, J. L., Ventura, F. Inhibition of PI3K/p70 S6K and p38 MAPK cascades increases osteoblastic differentiation induced by BMP2. *FEBS Lett*, 2002. 510(1-2): p. 99-104.

Vojtek, A.B., Taylor, J., DeRuiter, S. L., Yu, J. Y., Figueroa, C., Kwok, R. P., et al., Akt regulates basic helix-loop-helix transcription factor-coactivator complex formation and activity during neuronal differentiation. *Mol Cell Biol*, 2003. 23(13): p. 4417-27.

Vriz, S., Lemaitre, J. M., Leibovici, M., Thierry, N., Mechali, M. Comparative analysis of the intracellular localization of c-Myc, c-Fos, and replicative proteins during cell cycle progression. *Mol Cell Biol*, 1992. 12(8): p. 3548-55.

Waite, K.A., Eng, C. BMP2 exposure results in decreased PTEN protein degradation and increased PTEN levels. *Hum Mol Genet*, 2003. 12(6): p. 679-84.

Wan, X., Helman, L.J. Effect of insulin-like growth factor II on protecting myoblast cells against cisplatin-induced apoptosis through p70 S6 kinase pathway. *Neoplasia*, 2002. 4(5): p. 400-8.

Wang, B., Lim, D. J., Han, J., Kim, Y. S., Basbaum, C. B., Li, J. D. Novel cytoplasmic proteins of nontypeable Haemophilus influenzae up-regulate human MUC5AC mucin transcription via a positive p38 mitogen-activated protein kinase pathway and a negative phosphoinositide 3-kinase-Akt pathway. *J Biol Chem*, 2002. 277(2): p. 949-57.

Watanabe, H., M.P. de Caestecker, and Y. Yamada, Transcriptional cross-talk between Smad, ERK1/2, and p38 mitogen-activated protein kinase pathways regulates transforming growth factor-beta-induced aggrecan gene expression in chondrogenic ATDC5 cells. *J Biol Chem*, 2001. 276(17): p. 14466-73.

Watanabe, T., Nakagawa, K., Ohata, S., Kitagawa, D., Nishitai, G., Seo, J., et al., SEK1/MKK4-mediated SAPK/JNK signaling participates in embryonic hepatoblast proliferation via a pathway different from NF-kappaB-induced anti-apoptosis. *Dev Biol*, 2002. 250(2): p. 332-47.

Wierenga, A.T., Vogelzang, I., Eggen, B. J., Vellenga, E. Erythropoietin-induced serine 727 phosphorylation of STAT3 in erythroid cells is mediated by a MEK-, ERK-, and MSK1-dependent pathway. *Exp Hematol*, 2003. 31(5): p. 398-405.

Williams, L., Lali, F., Clarke, C., Brennan, F., Foxwell, B. Interleukin 10 modulation of tumour necrosis factor receptors requires tyrosine kinases but not the PI 3-kinase/p70 S6 kinase pathway. *Cytokine*, 2000. 12(7): p. 934-43.

Wölfel, S., Dummer, A., Pusch, L., Pfalz, M., Wang, L., Clement, J.H., Leube, I., Ehrlich, R. Analyzing Proteins and Protein Modifications with ArrayTube™ Antibody Microarrays. In *Protein Microarrays*(M.Schena,ed), Jones and Bartlett Publishers (Sudbury, MA), 2004.

Xiao, Z., Liu, X., Lodish, H.F. Importin beta mediates nuclear translocation of Smad 3. *J Biol Chem*, 2000. 275(31): p. 23425-8.

Xing, X., Manske, P. R., Li, Y. Y., Lou, J. The role of Sp1 in BMP2-up-regulated Erk2 gene expression. *Biochem Biophys Res Commun*, 2002. 297(1): p. 116-24.

- Xu, G., Kwon, G., Marshall, C. A., Lin, T. A., Lawrence, J. C., Jr., McDaniel, M. L. Branched-chain amino acids are essential in the regulation of PHAS-I and p70 S6 kinase by pancreatic beta-cells. A possible role in protein translation and mitogenic signaling. *J Biol Chem*, 1998. 273(43): p. 28178-84.
- Xu, Z., Kukekov, N.V., Greene, L.A. POSH acts as a scaffold for a multiprotein complex that mediates JNK activation in apoptosis. *Embo J*, 2003. 22(2): p. 252-61.
- Yagi, K., Furuhashi, M., Aoki, H., Goto, D., Kuwano, H., Sugamura, K., et al., c-Myc is a downstream target of the Smad pathway. *J Biol Chem*, 2002. 277(1): p. 854-61.
- Yamamoto, N., Akiyama, S., Katagiri, T., Namiki, M., Kurokawa, T., Suda, T. Smad1 and smad5 act downstream of intracellular signalings of BMP2 that inhibits myogenic differentiation and induces osteoblast differentiation in C2C12 myoblasts. *Biochem Biophys Res Commun*, 1997. 238(2): p. 574-80.
- Yamanaka, Y., Nakajima, K., Fukada, T., Hibi, M., Hirano, T. Differentiation and growth arrest signals are generated through the cytoplasmic region of gp130 that is essential for STAT3 activation. *Embo J*, 1996. 15(7): p. 1557-65.
- Yang, X., Ji, X., Shi, X., Cao, X. Smad1 domains interacting with Hoxc-8 induce osteoblast differentiation. *J Biol Chem*, 2000. 275(2): p. 1065-72.
- Yoo, J., Ghiassi, M., Jirmanova, L., Balliet, A. G., Hoffman, B., Fornace, A. J., Jr., et al., Transforming growth factor-beta-induced apoptosis is mediated by Smad-dependent expression of GADD45b through p38 activation. *J Biol Chem*, 2003. 278(44): p. 43001-7.
- Yoshinari, M., Imaizumi, M., Sato, A., Minegishi, M., Fujii, K., Suzuki, H., et al., G-CSF induces apoptosis of a human acute promyelocytic leukemia cell line, UF-1: possible involvement of STAT3 activation and altered Bax expression. *Tohoku J Exp Med*, 1999. 189(1): p. 71-82.
- Yu, C., Krystal, G., Varticovski, L., McKinstry, R., Rahmani, M., Dent, P., et al., Pharmacologic mitogen-activated protein/extracellular signal-regulated kinase kinase/mitogen-activated protein kinase inhibitors interact synergistically with STI571 to induce apoptosis in Bcr/Abl-expressing human leukemia cells. *Cancer Res*, 2002. 62(1): p. 188-99.
- Yu, Y., Sato, J.D. MAP kinases, phosphatidylinositol 3-kinase, and p70 S6 kinase mediate the mitogenic response of human endothelial cells to vascular endothelial growth factor. *J Cell Physiol*, 1999. 178(2): p. 235-46.
- Zhang, M.Y., Barber, D. L., Alessi, D. R., Bell, L. L., Stine, C., Nguyen, M. H., et al., A minimal cytoplasmic subdomain of the erythropoietin receptor mediates p70 S6 kinase phosphorylation. *Exp Hematol*, 2001. 29(4): p. 432-40.
- Zhou, Y., Ching, Y. P., Chun, A. C., Jin, D. Y. Nuclear localization of the cell cycle regulator CDH1 and its regulation by phosphorylation. *J Biol Chem*, 2003. 278(14): p. 12530-6.
- Zhu, H., M. Bilgin, et al. (2003). "Proteomics." *Annu Rev Biochem* 72: 7

Curriculum Vitae

Name: Wang Lin

Date of birth: 12th of March 1964

Place of birth: Jinan City, Shandong Province, China

Nationality: Chinese

Education and Working experience:

1982.September-1986. July Scientific student. Dept of Biology, Shandong Teacher University obtaining the degree of Bachelor of Science.

1986.September-1989. July Graduate student. Dept of Biology, Shandong Teacher University obtaining the degree of Master on Animal Cell Biology.

1989.September-1995. July Teacher in Dept of Biochemistry, Shandong education University.

1995.September-1998. July Lecturer in Institute of Medicine College, Shandong University.

1998.September-2000. July Lecturer in Institute of life science, Tsinghua University.

2001. December-- Friedrich-Schiller-Universität Jena
Klinik für Innere Medizin II, AG Molekularbiologie

Publications:

From this work:

Book Chapter:

Wölfl, S., Dummer, A., Pusch, L., Pfalz, M., Wang, L., Clement, J.H., Leube, I., Ehrlich, R. Analyzing Proteins and Protein Modifications with ArrayTube™ Antibody Microarrays. In Protein Microarrays(M.Schena,ed), Jones and Bartlett Publishers (Sudbury, MA), 2004.

From previous work:

Full articles:

1. Wang, L., Baihua K., Mingxing, D., Yongzhong, Z., Zengyi, C. "Translocation of p53-Regulated Laminin Receptors in Pro-Apoptotic Microcircumstance of Human Vasculogenesis Inhibition" Cell Biology International, 2000, Vol.24(10): 745-748 (in English).
2. Wang, L., Baihua K., Mingxing, D., Yongzhong, Z., Zengyi, C. Evidence for a role of laminin synthesis to its receptor clustering in tumor invasion Anatomy Transaction, 2000 Vol31.No.2(in Chinese)
3. Wang, L., Baihua K., Mingxing, D., Yongzhong, Z., Zengyi, C. Nuclear translocation of Laminin receptors and Trk A in proliferative trophoblast tumor Anatomy Journal,1999,Vol.22, No.5(in Chinese)
4. Wang, L., Baihua K., Mingxing, D., Yongzhong, Z., Zengyi, C. Different sublocations and possible functions of fibronectin in hematopoietic -phenotype trophoblasts Tsinghua University Transaction 2000,Vol 40 No.26.
5. Wang, L., Baihua K., Mingxing, D., Yongzhong, Z., Zengyi, C. Evidence for ras nuclear posttranscriptional events regulating fibronectin splicings, Chinese histochemistry and cytochemistry Journal, 1999,Vol.8 No.4
6. Wang, L., Baihua K., Mingxing, D., Yongzhong, Z., Zengyi, C. Evidence for TGF-B1 nuclear posttranscriptional events regulating fibronectin splicing in tumor proliferation Chinese Prepotency and heredity journal, 1999, Vol.7, No.2, pp21-22,15
7. Wang, L., Baihua K., Mingxing, D., Yongzhong, Z., Zengyi, C. Evidence for nm23 oncogene nuclear translocation in senescence knots and apoptotic trophoblasts Chinese Prepotency and heredity journal, 1998, Vol.6, No.5, p15
8. Wang, L., Baihua K., Mingxing, D., Yongzhong, Z., Zengyi, C. Relationship between nuclear trasnlocation of Laminin receptors and proliferation of leukocytes and vasculature endothelium Current Advances in Obstetrics and Gynecology,1998,Vol.8, No.2
9. Wang, L., Baihua K., Mingxing, D., Yongzhong, Z., Zengyi, C. Comparison of Laminin & its receptors between endothelial apoptosis of normal term placenta and tumor vasculature Oversea Medicine Tumor Fascicule, 1996, Vol.23
10. Wang, L., Baihua K., Mingxing, D., Yongzhong, Z., Zengyi, C. Ras and TGF-B1 differernt regulation in endothelial apoptosis of normal term placenta and tumor vasculature Shandong Teachers University Transaction,1998,Vol.2

Lecture and Poster Abstracts:

1. Wang, L., Baihua K., Mingxing, D., Yongzhong, Z., Zengyi, C. Comparison of laminin receptors & fibronectin expression between circular and term placental Leukocytes The 14th international morphology congress
2. Wang, L., Baihua K., Mingxing, D., Yongzhong, Z., Zengyi, C. "Study on the relationship of location and function of laminin receptor in normal and abnormal human trophoblast" 10th International Congress on Genes, Gene Families, and Isozymes.Oct. 1999, Beijing
3. Wang, L., Baihua K., Mingxing, D., Yongzhong, Z., Zengyi, C. "Study on function of p16 in normal and abnormal human trophoblast"10th International Congress on Genes, Gene Families, and Isozymes. Oct. 1999, Beijing, P.R.China

4. Wang, L., Baihua K., Mingxing, D., Yongzhong, Z., Zengyi, C. "location and function of laminin receptor(LNR) in normal and abnormal human placenta endothelium" 10th International Congress on Genes, Gene Families, and Isozymes. Oct. 1999, Beijing, P.R.China

Selbständigkeitserklärung

I hereby declare that this thesis was composed by myself and that the work described is my own, unless otherwise stated.

Jena, 15, March 2004

Lin Wang

Acknowledgements

First of all I wish to express my deep gratitude to Professor Dr.Stefan Wolf for providing a good work atmosphere, his instructions and supervision on all the project. Specially, his earnest and strict attitude of doing scholarly research left me very deep expression and will have a great effect on all my life.

My warm thanks to all the colleague of our lab in good cooperation with me.

I am very grateful to Dr. Clement and Prof.Pachmann lab for suppling with cell lines, ST1, BMP2 and equipments; Prof.Wetzker lab for supplying with initial antibodies; Olaf Hoyer at Quantifoil GmbH for help with my initial antibody array spottings; and Ralf Ehricht at Clondiag GmbH for setup of Arraytube.

Many thanks to all the people who ever help me in any aspect.

Most of all, I thank my family: parents, husband and brother supporting me. Specially, with their full love and efforts to take care of my child during his non-mother period.

Substance	Background	Sigma	CoG_y	CoG_x	Mean	mean of 4 - control-u-cyto	mean of 4 u_2000-cyto	STABW-u-2000-cyto	STABW-control-u-cyto
1:100 verd. biotin anti rabbit IGG	0,997042	0,03928	94	290	0,910069	0,919161	0,785725	0,01587229	0,00783776
1:100 verd. biotin anti rabbit IGG	1	0,039062	95	335	0,920462				
1:100 verd. biotin anti rabbit IGG	0,999885	0,036103	92	376	0,928955				
1:100 verd. biotin anti rabbit IGG	0,999885	0,036145	96	422	0,917158				
1:20 verd. biotin anti rabbit IGG	0,999839	0,12985	132	550	0,528564	0,56020475	0,80567	0,02782273	0,22916976
1:20 verd. biotin anti rabbit IGG	1	0,109591	140	589	0,891587				
1:20 verd. biotin anti rabbit IGG	0,998685	0,101298	83	215	0,440488				
1:20 verd. biotin anti rabbit IGG	0,994198	0,099087	81	254	0,38018				
1:5 verd. c-Myc	0,997707	0,080106	221	373	0,671911	0,67885675	0,871129	0,01698127	0,018874
1:5 verd. c-Myc	0,988258	0,070413	222	416	0,671553				
1:5 verd. c-Myc	0,985025	0,062736	224	457	0,665178				
1:5 verd. c-Myc	0,985329	0,066161	222	500	0,706785				
1:5 verd. p38 (mouse monoclonal 10.1)	1	0,033798	135	208	0,871959	0,896291	0,624612	0,03923612	0,02039257
1:5 verd. p38 (mouse monoclonal 10.1)	1	0,038316	136	248	0,886977				
1:5 verd. p38 (mouse monoclonal 10.1)	1	0,034153	138	292	0,914286				
1:5 verd. p38 (mouse monoclonal 10.1)	0,987043	0,038233	139	336	0,911942				
1:5 verd. Phospho Stat3 6E4	0,985369	0,052769	434	453	0,774859	0,749649	0,792632	0,0187861	0,01908075
1:5 verd. Phospho Stat3 6E4	0,996876	0,05335	435	499	0,746157				
1:5 verd. Phospho Stat3 6E4	0,976769	0,049915	435	542	0,749004				
1:5 verd. Phospho Stat3 6E4	0,974269	0,060972	435	580	0,728576				
1:5 verd. Phospho-Akt 4E2	0,986768	0,046955	476	541	0,816968	0,852142	0,805517	0,02920597	0,04022575
1:5 verd.	0,984291	0,03627	477	583	0,81783				

Phospho-Akt 4E2		2			2				
1:5 verd. Phospho-Akt 4E2	1	0,046644	431	203	0,890485				
1:5 verd. Phospho-Akt 4E2	0,999885	0,035537	432	243	0,883283				
1:5 verd. phospho-p38 (mouse monoclonal 9.1)	0,999954	0,04192	180	292	0,91573	0,9182265	0,852665	0,01371255	0,00376608
1:5 verd. phospho-p38 (mouse monoclonal 9.1)	1	0,033116	180	332	0,915971				
1:5 verd. phospho-p38 (mouse monoclonal 9.1)	1	0,035071	182	376	0,917445				
1:5 verd. phospho-p38 (mouse monoclonal 9.1)	1	0,036559	180	417	0,92376				
1:5 verd. Phospho-p44/42 MAP Kinase	0,999862	0,045708	302	204	0,92869	0,93649425	0,863239	0,03965463	0,01607069
1:5 verd. Phospho-p44/42 MAP Kinase	0,998968	0,040483	304	248	0,937856				
1:5 verd. Phospho-p44/42 MAP Kinase	0,998962	0,038546	310	284	0,921124				
1:5 verd. Phospho-p44/42 MAP Kinase	0,996331	0,032839	309	329	0,958307				
1:5 verd. Phospho-p70 S6 Kinase	0,982869	0,043544	475	203	0,841523	0,8192375	0,725097	0,02735028	0,02573533
1:5 verd. Phospho-p70 S6 Kinase	0,982261	0,053633	475	239	0,840213				
1:5 verd. Phospho-p70 S6 Kinase	0,999174	0,038023	474	287	0,790039				
1:5 verd. Phospho-p70 S6 Kinase	0,992019	0,042627	472	327	0,805175				
1:5 verd. Phospho-SAPK/JNK	1	0,044141	348	289	0,859172	0,85235575	0,787044	0,0165096	0,01060456
1:5 verd. Phospho-SAPK/JNK	0,989313	0,049542	349	329	0,847611				
1:5 verd. Phospho-SAPK/JNK	0,982445	0,049182	349	374	0,839782				
1:5 verd. Phospho-SAPK/JNK	0,997225	0,043357	349	415	0,862858				
1:5 verd. Phospho-Tyrosine	0,982548	0,074257	388	372	0,857637	0,798034	0,827435	0,01260046	0,04755448
1:5 verd. Phospho-Tyrosine	0,997225	0,083044	389	416	0,814184				
1:5 verd.	0,993287	0,09503	390	458	0,76728				

Phospho-Tyrosine					8				
1:5 verd. Phospho-Tyrosine	0,960372	0,088054	389	499	0,753027				
1:5 verd. p-Smasd1	0,987543	0,076196	308	543	0,728834	0,74282625	0,891479	0,02324062	0,02202913
1:5 verd. p-Smasd1	0,994106	0,056055	309	583	0,725731				
1:5 verd. p-Smasd1	1	0,0702	265	206	0,742804				
1:5 verd. p-Smasd1	0,995645	0,053797	262	247	0,773936				
1:5 verd. p-Smasd2/3	0,945213	0,074702	264	455	0,631028	0,6128855	0,816376	0,03202448	0,01308037
1:5 verd. p-Smasd2/3	0,959752	0,061842	269	497	0,599928				
1:5 verd. p-Smasd2/3	0,981401	0,049431	266	541	0,611476				
1:5 verd. p-Smasd2/3	0,984498	0,058239	266	583	0,609111				
2% Milchpulver	0,999977	0,005043	98	468	0,999216	0,98324325	0,88098	0,0322537	0,0113329
2% Milchpulver	0,998899	0,016533	83	505	0,978338				
2% Milchpulver	0,999748	0,018178	87	546	0,982446				
2% Milchpulver	0,999931	0,022348	88	591	0,972973				
c-Myc	0,985713	0,149436	225	544	0,325153	0,3015755	0,376046	0,04877382	0,02348665
c-Myc	1	0,110976	225	588	0,269408				
c-Myc	0,976241	0,110052	177	207	0,302174				
c-Myc	0,976102	0,121707	179	247	0,309567				
p38 (mouse monoclonal 10.1)	0,972067	0,129652	141	374	0,722899	0,77766825	0,648293	0,01628248	0,03928393
p38 (mouse monoclonal 10.1)	0,984937	0,099731	140	417	0,776987				
p38 (mouse monoclonal 10.1)	1	0,073088	140	461	0,812182				
p38 (mouse monoclonal 10.1)	0,99984	0,066756	141	505	0,798605				
Phospho Stat3 6E4	0,999354	0,047858	388	204	0,316479	0,34431775	0,318449	0,02689122	0,01933539
Phospho Stat3 6E4	0,999885	0,048923	389	248	0,355724				
Phospho Stat3 6E4	1	0,048109	389	287	0,346152				
Phospho Stat3 6E4	0,99481	0,047455	388	332	0,358916				
Phospho-Akt 4E2	0,998362	0,049088	431	287	0,790351	0,79091625	0,37129	0,01867999	0,00220585
Phospho-Akt 4E2	0,992249	0,047682	433	328	0,78862				
Phospho-Akt 4E2	0,980277	0,044988	434	371	0,793914				
Phospho-Akt 4E2	0,965444	0,043318	435	410	0,79078				
phospho-p38 (mouse monoclonal 9.1)	0,994368	0,081159	181	460	0,915835	0,90225875	0,583527	0,02051781	0,0150344
phospho-p38 (mouse monoclonal 9.1)	0,994368	0,075601	182	505	0,881245				
phospho-p38	0,996955	0,05503	181	545	0,90948				

(mouse monoclonal 9.1)					1				
phospho-p38 (mouse monoclonal 9.1)	1	0,053383	185	586	0,902474				
Phospho-p44/42 MAP Kinase	0,998853	0,056255	306	372	0,963014	0,91739775	0,736188	0,02479355	0,03259717
Phospho-p44/42 MAP Kinase	1	0,0884	308	414	0,887407				
Phospho-p44/42 MAP Kinase	0,99179	0,070376	313	457	0,916118				
Phospho-p44/42 MAP Kinase	0,989267	0,050236	310	499	0,903052				
Phospho-p70 S6 Kinase	0,995024	0,0502	484	367	0,905478	0,926664	0,836557	0,02586311	0,01498335
Phospho-p70 S6 Kinase	0,995736	0,036451	477	410	0,940436				
Phospho-p70 S6 Kinase	0,995322	0,038951	478	454	0,928434				
Phospho-p70 S6 Kinase	0,995548	0,037245	478	495	0,932308				
Phospho-SAPK/JNK	0,975714	0,081156	350	459	0,847059	0,8221825	0,476779	0,03106346	0,02313463
Phospho-SAPK/JNK	0,959839	0,084067	352	499	0,809372				
Phospho-SAPK/JNK	0,989795	0,076625	351	542	0,835513				
Phospho-SAPK/JNK	0,99789	0,080264	352	586	0,796786				
Phospho-Tyrosine	0,982846	0,068524	393	539	0,705345	0,720123	0,466202	0,02197863	0,03154288
Phospho-Tyrosine	0,999931	0,076099	395	587	0,693941				
Phospho-Tyrosine	0,998647	0,083175	347	203	0,715682				
Phospho-Tyrosine	0,999516	0,061716	348	245	0,765524				
p-Smasd1	0,99562	0,150781	262	289	0,347704	0,35535925	0,553927	0,04697691	0,0289699
p-Smasd1	0,951834	0,155113	263	332	0,338233				
p-Smasd1	0,892489	0,176444	263	371	0,398236				
p-Smasd1	0,92299	0,157386	264	414	0,337264				
p-Smasd2/3	0,968189	0,062256	218	202	0,563904	0,59797825	0,672337	0,06211516	0,04376631
p-Smasd2/3	0,963576	0,070177	218	246	0,654605				
p-Smasd2/3	0,969083	0,05137	219	286	0,56299				
p-Smasd2/3	0,99734	0,059482	220	333	0,610414				

Spot ID	Substance	Background	Sigma	CoG_y	CoG_x	Mean	mean-cyto-bmp2
112	1:100 verd. biotin anti rabbit IGG	0.984359	0.024978	91	290	0.785725	0.80916225
113	1:100 verd. biotin anti rabbit IGG	0.996191	0.026507	91	332	0.809046	
114	1:100 verd. biotin anti rabbit IGG	0.998436	0.02776	93	374	0.817763	
115	1:100 verd. biotin anti rabbit IGG	0.991363	0.027247	91	418	0.824115	
106	1:20 verd. biotin anti rabbit IGG	0.987487	0.113089	130	549	0.663171	0.75935025
107	1:20 verd. biotin anti rabbit IGG	0.977417	0.039944	137	590	0.822778	
110	1:20 verd. biotin anti rabbit IGG	0.920843	0.032932	90	209	0.757262	
111	1:20 verd. biotin anti rabbit IGG	0.960558	0.028866	89	250	0.79419	
78	1:5 verd. c-Myc	0.980572	0.032677	221	370	0.870902	0.87181925
79	1:5 verd. c-Myc		1 0.026053	219	415	0.890861	
80	1:5 verd. c-Myc	0.999797	0.035106	221	459	0.849713	
81	1:5 verd. c-Myc	0.989317	0.032038	221	505	0.875801	
98	1:5 verd. p38 (mouse monoclonal 10.1)	0.954347	0.039242	132	207	0.624612	0.6756465
99	1:5 verd. p38 (mouse monoclonal 10.1)	0.994964	0.041737	132	248	0.666418	
100	1:5 verd. p38 (mouse monoclonal 10.1)	0.999615	0.039516	133	292	0.698264	
101	1:5 verd. p38 (mouse monoclonal 10.1)		1 0.048341	135	334	0.713292	
20	1:5 verd. Phospho Stat3 6E4	0.986748	0.055563	434	460	0.787055	0.78278875
21	1:5 verd. Phospho Stat3 6E4	0.980437	0.044136	434	500	0.80489	
22	1:5 verd. Phospho Stat3 6E4	0.982264	0.042203	434	543	0.777134	
23	1:5 verd. Phospho Stat3 6E4	0.999501	0.043582	436	588	0.762076	
10	1:5 verd. Phospho-Akt 4E2	0.979825	0.035753	479	545	0.79709	0.78046425
11	1:5 verd. Phospho-Akt 4E2	0.980687	0.068618	482	584	0.763566	
14	1:5 verd. Phospho-Akt 4E2	0.961438	0.042308	430	200	0.749065	
15	1:5 verd. Phospho-Akt 4E2	0.960376	0.031038	431	245	0.812136	
88	1:5 verd. phospho-p38 (mouse monoclonal 9.1)	0.99295	0.027023	179	292	0.85341	0.85977275
89	1:5 verd. phospho-p38 (mouse monoclonal 9.1)	0.990331	0.029309	178	332	0.860789	
90	1:5 verd. phospho-p38 (mouse monoclonal 9.1)		1 0.074623	179	380	0.84666	
91	1:5 verd. phospho-p38 (mouse monoclonal 9.1)	0.999865	0.037969	178	420	0.878232	
50	1:5 verd. Phospho-p44/42 MAP Kinase	0.947002	0.027578	302	200	0.863239	0.90487675
51	1:5 verd. Phospho-p44/42 MAP Kinase	0.987041	0.029283	302	245	0.880891	
52	1:5 verd. Phospho-p44/42 MAP Kinase	0.992567	0.020414	301	286	0.929279	
53	1:5 verd. Phospho-p44/42 MAP Kinase	0.993569	0.028757	305	331	0.946098	
2	1:5 verd. Phospho-p70 S6 Kinase	0.972937	0.026478	475	197	0.720724	0.7558435
3	1:5 verd. Phospho-p70 S6 Kinase	0.976966	0.021912	474	241	0.753065	
4	1:5 verd. Phospho-p70 S6 Kinase	0.982704	0.026143	476	283	0.760822	
5	1:5 verd. Phospho-p70 S6 Kinase	0.957244	0.027622	474	326	0.788763	

40	1:5 verd. Phospho-SAPK/JNK	0.928691	0.033695	346	288	0.787044	0.79114425
41	1:5 verd. Phospho-SAPK/JNK	0.946811	0.055057	347	330	0.773427	
42	1:5 verd. Phospho-SAPK/JNK	0.991817	0.031262	349	372	0.810901	
43	1:5 verd. Phospho-SAPK/JNK	0.992585	0.039088	348	416	0.793205	
30	1:5 verd. Phospho-Tyrosine	0.970453	0.059724	389	374	0.821944	0.80653375
31	1:5 verd. Phospho-Tyrosine	0.967726	0.05626	391	413	0.809012	
32	1:5 verd. Phospho-Tyrosine	0.978995	0.058647	391	461	0.790752	
33	1:5 verd. Phospho-Tyrosine	0.923971	0.055619	392	499	0.804427	
58	1:5 verd. p-Smasd1	0.996056	0.032432	307	548	0.892845	0.86594775
59	1:5 verd. p-Smasd1	0.987717	0.030149	308	590	0.861278	
62	1:5 verd. p-Smasd1	0.992112	0.040723	265	201	0.835567	
63	1:5 verd. p-Smasd1	0.986711	0.026803	261	245	0.874101	
68	1:5 verd. p-Smasd2/3	0.999933	0.033211	263	460	0.813635	0.776912
69	1:5 verd. p-Smasd2/3		1 0.035798	264	503	0.78753	
70	1:5 verd. p-Smasd2/3	0.999031	0.026614	264	545	0.766614	
71	1:5 verd. p-Smasd2/3	0.999025	0.028572	266	588	0.739869	
116	2% Milchpulver	0.990947	0.054891	94	461	0.88098	0.8461575
117	2% Milchpulver	0.986422	0.052716	95	504	0.86025	
118	2% Milchpulver	0.97185	0.049354	95	548	0.835909	
119	2% Milchpulver	0.94332	0.045811	95	591	0.807491	
82	c-Myc	0.987714	0.144251	223	546	0.384186	0.3909335
83	c-Myc	0.998459	0.131558	224	589	0.347469	
86	c-Myc	0.971445	0.127705	175	205	0.363772	
87	c-Myc	0.979984	0.131303	177	247	0.468307	
102	p38 (mouse monoclonal 10.1)		1 0.078852	135	376	0.648825	0.63437025
103	p38 (mouse monoclonal 10.1)	0.999153	0.08528	137	420	0.624251	
104	p38 (mouse monoclonal 10.1)	0.999932	0.077239	137	464	0.610529	
105	p38 (mouse monoclonal 10.1)	0.994854	0.092581	138	505	0.653876	
26	Phospho Stat3 6E4	0.896605	0.039003	387	200	0.310507	0.342697
27	Phospho Stat3 6E4	0.906513	0.05222	387	241	0.327627	
28	Phospho Stat3 6E4	0.889367	0.037816	387	286	0.357627	
29	Phospho Stat3 6E4	0.899863	0.054408	389	329	0.375027	
16	Phospho-Akt 4E2	0.947274	0.043302	432	284	0.365788	0.39602925
17	Phospho-Akt 4E2	0.937007	0.058226	431	328	0.413066	
18	Phospho-Akt 4E2	0.967959	0.053542	433	373	0.39741	
19	Phospho-Akt 4E2	0.970373	0.046489	433	414	0.407853	
92	phospho-p38 (mouse monoclonal 9.1)	0.999863	0.059662	179	462	0.591882	0.566185
93	phospho-p38 (mouse monoclonal 9.1)	0.999933	0.054265	178	503	0.571201	
94	phospho-p38 (mouse monoclonal 9.1)	0.999391	0.070983	178	547	0.566159	
95	phospho-p38 (mouse monoclonal 9.1)	0.998342	0.065776	179	591	0.535498	
54	Phospho-p44/42 MAP Kinase	0.995806	0.08217	307	372	0.734074	0.7232085
55	Phospho-p44/42 MAP Kinase	0.997824	0.08185	306	414	0.728738	
56	Phospho-p44/42 MAP Kinase	0.997325	0.066059	306	459	0.740848	
57	Phospho-p44/42 MAP Kinase	0.99396	0.069965	308	500	0.689174	
6	Phospho-p70 S6 Kinase	0.960626	0.027716	476	367	0.836557	0.837725
7	Phospho-p70 S6 Kinase	0.977536	0.022415	476	410	0.872658	
8	Phospho-p70 S6 Kinase	0.985283	0.028278	478	455	0.833367	
9	Phospho-p70 S6 Kinase	0.99103	0.033883	477	500	0.808318	
44	Phospho-SAPK/JNK	0.987487	0.039106	349	458	0.4666	0.4567695
45	Phospho-SAPK/JNK	0.988683	0.047176	349	505	0.492369	
46	Phospho-SAPK/JNK	0.99658	0.044002	349	545	0.444741	
47	Phospho-SAPK/JNK	0.988461	0.031866	349	589	0.423368	

34	Phospho-Tyrosine	0.875825	0.044956	396	541	0.467806	0.458722
35	Phospho-Tyrosine	0.946924	0.053715	394	585	0.44746	
38	Phospho-Tyrosine	0.875893	0.041304	345	200	0.435588	
39	Phospho-Tyrosine	0.92107	0.039392	347	245	0.484034	
64	p-Smasd1	0.986838	0.16465	261	287	0.553927	0.56703
65	p-Smasd1	0.992497	0.162088	264	329	0.50966	
66	p-Smasd1	0.97264	0.161341	263	373	0.588911	
67	p-Smasd1	0.990003	0.164266	264	414	0.615622	
74	p-Smasd2/3	0.989385	0.04031	218	201	0.672337	0.71357475
75	p-Smasd2/3	0.97736	0.035808	217	245	0.650868	
76	p-Smasd2/3	0.984695	0.029679	217	289	0.757985	
77	p-Smasd2/3	0.988983	0.029146	217	331	0.773109	
1	Wisp2_129_158r(bio)_1,25 µM, htag4(bio)_1,25 µM	0.900661	0.024438	479	156	0.848796	0.9600825
12	Wisp2_129_158r(bio)_1,25 µM, htag4(bio)_1,25 µM	0.993165	0.007652	494	629	0.996867	
36	Wisp2_129_158r(bio)_1,25 µM, htag4(bio)_1,25 µM	0.99849	0.009208	410	626	0.997098	
48	Wisp2_129_158r(bio)_1,25 µM, htag4(bio)_1,25 µM	0.996349	0.009304	368	626	0.997569	
60	Wisp2_129_158r(bio)_1,25 µM, htag4(bio)_1,25 µM	0.99973	0.008216	321	629	0.997921	0.9739595
72	Wisp2_129_158r(bio)_1,25 µM, htag4(bio)_1,25 µM	0.996303	0.012899	272	635	0.995201	
73	Wisp2_129_158r(bio)_1,25 µM, htag4(bio)_1,25 µM	0.969349	0.027873	224	158	0.907487	
84	Wisp2_129_158r(bio)_1,25 µM, htag4(bio)_1,25 µM	0.995199	0.013235	237	627	0.995229	
85	Wisp2_129_158r(bio)_1,25 µM, htag4(bio)_1,25 µM	0.951702	0.028523	181	160	0.88956	0.8771465
96	Wisp2_129_158r(bio)_1,25 µM, htag4(bio)_1,25 µM	0.981888	0.024969	181	634	0.9413	
109	Wisp2_129_158r(bio)_1,25 µM, htag4(bio)_1,25 µM	0.871036	0.026115	89	160	0.821316	
120	Wisp2_129_158r(bio)_1,25 µM, htag4(bio)_1,25 µM	0.903216	0.030955	97	638	0.85641	

Substance	mean of 4 - control-u-cyto	mean of 4 u_2000-cyto	sd-u-cyto-bmp2	STABW-control-u-cyto	1_mean of 4 - control-u-cyto	1_mean of 4 u_2000-cyto
1:100 verd. biotin anti rabbit IGG	0,919161	0,785725	0,015872286	0,007837761	0,080839	0,214275
1:20 verd. biotin anti rabbit IGG	0,56020475	0,80567	0,027822734	0,229169765	0,43979525	0,19433
1:5 verd. c-Myc	0,67885675	0,871129	0,016981274	0,018873999	0,32114325	0,128871
1:5 verd. p38 (mouse monoclonal 10.1)	0,896291	0,624612	0,039236124	0,020392569	0,103709	0,375388
1:5 verd. Phospho Stat3 6E4	0,749649	0,792632	0,018786098	0,019080754	0,250351	0,207368
1:5 verd. Phospho-Akt 4E2	0,852142	0,805517	0,029205969	0,040225754	0,147858	0,194483
1:5 verd. phospho-p38 (mouse monoclonal 9.1)	0,9182265	0,852665	0,013712552	0,003766084	0,0817735	0,147335
1:5 verd. Phospho-p44/42 MAP Kinase	0,93649425	0,863239	0,03965463	0,016070691	0,06350575	0,136761

1:5 verd. Phospho-p70 S6 Kinase	0,8192375	0,725097	0,027350281	0,025735329	0,1807625	0,274903
1:5 verd. Phospho-SAPK/JNK	0,85235575	0,787044	0,016509598	0,010604564	0,14764425	0,212956
1:5 verd. Phospho-Tyrosine	0,798034	0,827435	0,012600462	0,047554483	0,201966	0,172565
1:5 verd. p-Smasd1	0,74282625	0,891479	0,023240616	0,02202913	0,25717375	0,108521
1:5 verd. p-Smasd2/3	0,6128855	0,816376	0,032024485	0,01308037	0,3871145	0,183624
2% Milchpulver	0,98324325	0,88098	0,032253703	0,0113329	0,01675675	0,11902
c-Myc	0,3015755	0,376046	0,048773822	0,023486655	0,6984245	0,623954
p38 (mouse monoclonal 10.1)	0,77766825	0,648293	0,016282478	0,039283929	0,22233175	0,351707
Phospho Stat3 6E4	0,34431775	0,318449	0,026891219	0,01933539	0,65568225	0,681551
Phospho-Akt 4E2	0,79091625	0,37129	0,018679988	0,002205851	0,20908375	0,62871
phospho-p38 (mouse monoclonal 9.1)	0,90225875	0,583527	0,020517811	0,015034399	0,09774125	0,416473
Phospho-p44/42 MAP Kinase	0,91739775	0,736188	0,024793552	0,032597166	0,08260225	0,263812
Phospho-p70 S6 Kinase	0,926664	0,836557	0,025863105	0,014983349	0,073336	0,163443
Phospho-SAPK/JNK	0,8221825	0,476779	0,031063457	0,023134632	0,1778175	0,523221
Phospho-Tyrosine	0,720123	0,466202	0,021978632	0,031542879	0,279877	0,533798
p-Smasd1	0,35535925	0,553927	0,046976905	0,028969898	0,64464075	0,446073
p-Smasd2/3	0,59797825	0,672337	0,062115159	0,043766307	0,40202175	0,327663
Wis2_129_158 r(bio)_1,25 µM, htag4(bio)_1,25 µM	0,84933142	0,849449	0,063293828	0,07154877	0,15066858	0,150551

	Substance	Valid	Background	QSV	Sigma	Mean
u-nu-bmp2						
1	Wis2_129_158 r(bio)_1,25 µM, htag4(bio)_1,25 µM	0	0.883283	0.160523	0.022645	0.835577
2	1:5 verd. Phospho-p70 S6 Kinase	0	0.934308	0.063669	0.070707	0.663756
3	1:5 verd. Phospho-p70 S6 Kinase	0	0.954087	0.035395	0.072067	0.697226
4	1:5 verd. Phospho-p70 S6 Kinase	0	0.971109	0.017712	0.044577	0.744865
5	1:5 verd. Phospho-p70 S6 Kinase	0	0.977091	0.022932	0.049587	0.741938
6	Phospho-p70 S6 Kinase	0	0.978806	0.004052	0.039759	0.862755
7	Phospho-p70 S6 Kinase	0	0.990251	0.002224	0.029251	0.889446
8	Phospho-p70	0	0.988390	0.003516	0.046638	0.861599

	S6 Kinase					
9	Phospho-p70 S6 Kinase	0	0.977021	0.007295	0.075334	0.807473
10	1:5 verd. Phospho-Akt 4E2	0	0.974465	0.008795	0.095440	0.660651
11	1:5 verd. Phospho-Akt 4E2	0	0.952985	0.026730	0.086435	0.716411
12	Wispi2_129_158 r(bio)_1,25 µM, htag4(bio)_1,25 µM	0	0.925111	0.031428	0.020666	0.861613
14	1:5 verd. Phospho-Akt 4E2	0	0.939906	0.049073	0.065880	0.705860
15	1:5 verd. Phospho-Akt 4E2	0	0.952985	0.026524	0.069745	0.718369
16	Phospho-Akt 4E2	0	0.955348	0.010589	0.087391	0.739315
17	Phospho-Akt 4E2	0	0.968360	0.002566	0.053659	0.806584
18	Phospho-Akt 4E2	0	0.980769	-0.003614	0.062637	0.809666
19	Phospho-Akt 4E2	0	0.992669	-0.002771	0.055269	0.820482
20	1:5 verd. Phospho Stat3 6E4	0	0.996457	0.001492	0.052201	0.765286
21	1:5 verd. Phospho Stat3 6E4	0	0.992954	0.003835	0.097253	0.749638
22	1:5 verd. Phospho Stat3 6E4	0	0.984046	0.017201	0.117177	0.642179
23	1:5 verd. Phospho Stat3 6E4	0	0.962867	0.006400	0.050892	0.737326
26	Phospho Stat3 6E4	0	0.952941	0.030505	0.046483	0.636850
27	Phospho Stat3 6E4	0	0.970187	0.011901	0.050534	0.648158
28	Phospho Stat3 6E4	0	0.979085	-0.001616	0.060102	0.645834
29	Phospho Stat3 6E4	0	0.989299	-0.009356	0.051358	0.639873
30	1:5 verd. Phospho-Tyrosine	0	0.994955	-0.006045	0.053127	0.804049
31	1:5 verd. Phospho-Tyrosine	0	0.996787	-0.004371	0.055007	0.809146
32	1:5 verd. Phospho-Tyrosine	0	0.995680	-0.000702	0.048383	0.812770
33	1:5 verd. Phospho-Tyrosine	0	0.993082	-0.002873	0.042327	0.791766
34	Phospho-Tyrosine	0	0.980702	-0.002846	0.039407	0.754962
35	Phospho-Tyrosine	0	0.964111	0.025074	0.041923	0.735001
36	Wispi2_129_158 r(bio)_1,25 µM, htag4(bio)_1,25 µM	0	0.932779	0.367586	0.040376	0.848272
38	Phospho-Tyrosine	0	0.944810	0.018804	0.042780	0.715435
39	Phospho-Tyrosine	0	0.963975	0.001872	0.043421	0.738442
40	1:5 verd. Phospho-SAPK/JNK	0	0.982397	0.002493	0.060286	0.750750

41	1:5 verd. Phospho-SAPK/JNK	0	0.987121	-0.004765	0.047226	0.779033
42	1:5 verd. Phospho-SAPK/JNK	0	0.982054	-0.010682	0.046081	0.772995
43	1:5 verd. Phospho-SAPK/JNK	0	0.989973	-0.009295	0.062898	0.767762
44	Phospho-SAPK/JNK	0	0.993093	-0.010002	0.062192	0.686150
45	Phospho-SAPK/JNK	0	0.985710	-0.010813	0.050574	0.702899
46	Phospho-SAPK/JNK	0	0.964082	-0.004320	0.044173	0.693636
47	Phospho-SAPK/JNK	0	0.955637	0.365189	0.040415	0.702522
48	Wispl2_129_158 r(bio)_1,25 μM, htag4(bio)_1,25 μM	0	0.948089	0.435342	0.023977	0.879402
50	1:5 verd. Phospho-p44/42 MAP Kinase	0	0.950245	0.016868	0.037525	0.704966
51	1:5 verd. Phospho-p44/42 MAP Kinase	0	0.971546	-0.000086	0.045448	0.697277
52	1:5 verd. Phospho-p44/42 MAP Kinase	0	0.981013	-0.006577	0.033697	0.725097
53	1:5 verd. Phospho-p44/42 MAP Kinase	0	0.986386	-0.004307	0.043860	0.714525
54	Phospho-p44/42 MAP Kinase	0	0.976604	-0.006548	0.064513	0.716186
55	Phospho-p44/42 MAP Kinase	0	0.972816	-0.008286	0.063889	0.714325
56	Phospho-p44/42 MAP Kinase	0	0.982586	-0.009574	0.062965	0.709714
57	Phospho-p44/42 MAP Kinase	0	0.981912	0.000680	0.072895	0.716117
58	1:5 verd. p-Smasd1	0	0.974875	0.062123	0.047582	0.571825
59	1:5 verd. p-Smasd1	0	0.963864	0.404356	0.038833	0.588621
60	Wispl2_129_158 r(bio)_1,25 μM, htag4(bio)_1,25 μM	0	0.947477	0.376623	0.022907	0.877467
62	1:5 verd. p-Smasd1	0	0.947491	0.013368	0.039504	0.592823
63	1:5 verd. p-Smasd1	0	0.966345	-0.003797	0.042664	0.583845
64	p-Smasd1	0	0.975369	-0.020893	0.042859	0.428638
65	p-Smasd1	0	0.979550	-0.012665	0.046945	0.427980
66	p-Smasd1	0	0.980637	-0.021370	0.039839	0.453394
67	p-Smasd1	0	0.973347	-0.031113	0.042367	0.427485
68	1:5 verd. p-Smasd2/3	0	0.968516	-0.019663	0.050772	0.575189
69	1:5 verd. p-Smasd2/3	0	0.974898	0.057925	0.046050	0.580136
70	1:5 verd. p-Smasd2/3	0	0.966221	0.375494	0.064868	0.529146
71	1:5 verd. p-Smasd2/3	0	0.955949	0.338573	0.067019	0.555868
72	Wispl2_129_158 r(bio)_1,25 μM, htag4(bio)_1,25 μM	0	0.942373	0.294895	0.029425	0.867502
73	Wispl2_129_158 r(bio)_1,25 μM, htag4(bio)_1,25 μM	0	0.895890	0.089865	0.018474	0.865939

74	p-Smasd2/3	0	0.910094	-0.011416	0.032167	0.432951
75	p-Smasd2/3	0	0.941087	-0.024621	0.031744	0.415181
76	p-Smasd2/3	0	0.958170	-0.034448	0.038779	0.417864
77	p-Smasd2/3	0	0.962968	-0.014258	0.038667	0.441221
78	1:5 verd. c-Myc	0	0.971747	-0.016393	0.036968	0.485320
79	1:5 verd. c-Myc	0	0.971330	-0.022126	0.047713	0.458623
80	1:5 verd. c-Myc	0	0.948997	0.010019	0.047645	0.455364
81	1:5 verd. c-Myc	0	0.948050	0.301705	0.044392	0.455044
82	c-Myc	0	0.946627	0.418755	0.046383	0.576499
83	c-Myc	0	0.946760	0.290311	0.050037	0.594135
84	Wisp2_129_158 r(bio)_1,25 µM, htag4(bio)_1,25 µM	0	0.925292	0.146231	0.020945	0.872125
85	Wisp2_129_158 r(bio)_1,25 µM, htag4(bio)_1,25 µM	0	0.874709	0.118264	0.028892	0.835233
86	c-Myc	0	0.908857	0.034875	0.036256	0.596192
87	c-Myc	0	0.942417	0.015198	0.061073	0.586479
88	1:5 verd. phospho-p38 (mouse monoclonal 9.1)	0	0.951267	0.004252	0.058470	0.618188
89	1:5 verd. phospho-p38 (mouse monoclonal 9.1)	0	0.963266	0.016900	0.063044	0.619937
90	1:5 verd. phospho-p38 (mouse monoclonal 9.1)	0	0.966722	0.007417	0.052065	0.634981
91	1:5 verd. phospho-p38 (mouse monoclonal 9.1)	0	0.955387	0.017262	0.053166	0.647201
92	phospho-p38 (mouse monoclonal 9.1)	0	0.939050	0.252983	0.051699	0.535298
93	phospho-p38 (mouse monoclonal 9.1)	0	0.928991	0.396642	0.052311	0.540038
94	phospho-p38 (mouse monoclonal 9.1)	0	0.921658	0.362919	0.040743	0.554631
95	phospho-p38 (mouse monoclonal 9.1)	0	0.917380	0.309852	0.053711	0.566270
96	Wisp2_129_158 r(bio)_1,25 µM, htag4(bio)_1,25 µM	0	0.890905	0.134068	0.020863	0.848092
98	1:5 verd. p38 (mouse monoclonal 10.1)	0	0.883793	0.096445	0.048120	0.670540
99	1:5 verd. p38 (mouse monoclonal 10.1)	0	0.912634	0.055709	0.041221	0.686844
100	1:5 verd. p38 (mouse monoclonal 10.1)	0	0.933067	0.035532	0.056914	0.680710
101	1:5 verd. p38 (mouse monoclonal 10.1)	0	0.948797	0.029007	0.073622	0.712186
102	p38 (mouse monoclonal 10.1)	0	0.948685	0.020424	0.030220	0.782124

103	p38 (mouse monoclonal 10.1)	0	0.942528	0.056606	0.037448	0.762721
104	p38 (mouse monoclonal 10.1)	0	0.927518	0.376606	0.032499	0.749060
105	p38 (mouse monoclonal 10.1)	0	0.903298	0.433502	0.034813	0.754216
106	1:20 verd. biotin anti rabbit IGG	0	0.890949	0.354484	0.086923	0.634316
107	1:20 verd. biotin anti rabbit IGG	0	0.871034	0.284821	0.028525	0.689386
109	Wisp2_129_158 r(bio)_1,25 µM, htag4(bio)_1,25 µM	0	0.797727	0.236725	0.022695	0.753143
110	1:20 verd. biotin anti rabbit IGG	0	0.834009	0.153793	0.040588	0.642696
111	1:20 verd. biotin anti rabbit IGG	0	0.869786	0.112697	0.057531	0.627134
112	1:100 verd. biotin anti rabbit IGG	0	0.889161	0.067274	0.049317	0.576831
113	1:100 verd. biotin anti rabbit IGG	0	0.905351	0.049297	0.049817	0.572207
114	1:100 verd. biotin anti rabbit IGG	0	0.910136	0.034584	0.034071	0.615726
115	1:100 verd. biotin anti rabbit IGG	0	0.854043	0.136053	0.040299	0.642343
116	2% Milchpulver	0	0.846749	0.432867	0.031235	0.776015
117	2% Milchpulver	0	0.861394	0.459775	0.068252	0.713116
118	2% Milchpulver	0	0.842366	0.414432	0.028209	0.733470
119	2% Milchpulver	0	0.820693	0.276408	0.020907	0.739336
120	Wisp2_129_158 r(bio)_1,25 µM, htag4(bio)_1,25 µM	0	0.791359	0.255785	0.018287	0.736487

u-nu-con-1-79	Substance	Valid	Background	QSV	Sigma	Mean
1	Wisp2_129_158 r(bio)_1,25 µM, htag4(bio)_1,25 µM	0	0.943342	0.106184	0.022975	0.925612
2	1:5 verd. Phospho-p70 S6 Kinase	0	0.982319	0.083004	0.061894	0.355894
3	1:5 verd. Phospho-p70 S6 Kinase	0	0.995964	0.018995	0.082950	0.387161
4	1:5 verd. Phospho-p70 S6 Kinase	0	0.999864	-0.009098	0.069649	0.420530
5	1:5 verd. Phospho-p70 S6 Kinase	0	1.000.000	-0.017315	0.075168	0.427251
6	Phospho-p70 S6 Kinase	0	0.999111	-0.025715	0.105033	0.540154
7	Phospho-p70 S6 Kinase	0	0.999111	-0.027288	0.105081	0.504882
8	Phospho-p70 S6 Kinase	0	0.999430	-0.027366	0.101319	0.539176
9	Phospho-p70 S6 Kinase	0	0.991908	-0.026396	0.093059	0.529985
10	1:5 verd.	0	0.989238	-0.008643	0.099398	0.403978

	Phospho-Akt 4E2					
11	1:5 verd. Phospho-Akt 4E2	0	0.999365	-0.025639	0.092723	0.450938
12	Wisp2_129_158 r(bio)_1,25 µM, htag4(bio)_1,25 µM	0	0.996170	0.000024	0.005121	0.998613
14	1:5 verd. Phospho-Akt 4E2	0	0.991427	0.042785	0.086978	0.424574
15	1:5 verd. Phospho-Akt 4E2	0	0.999129	-0.009429	0.103157	0.481218
16	Phospho-Akt 4E2	0	0.999954	-0.015220	0.114398	0.518046
17	Phospho-Akt 4E2	0	1.000.000	-0.027229	0.090047	0.517194
18	Phospho-Akt 4E2	0	1.000.000	-0.034021	0.082550	0.568144
19	Phospho-Akt 4E2	0	1.000.000	-0.036500	0.081918	0.593505
20	1:5 verd. Phospho Stat3 6E4	0	1.000.000	-0.032104	0.097934	0.548413
21	1:5 verd. Phospho Stat3 6E4	0	1.000.000	-0.027521	0.089127	0.486331
22	1:5 verd. Phospho Stat3 6E4	0	0.996854	-0.028657	0.099079	0.532413
23	1:5 verd. Phospho Stat3 6E4	0	1.000.000	-0.028008	0.094598	0.551412
26	Phospho Stat3 6E4	0	0.997552	0.001243	0.072626	0.433233
27	Phospho Stat3 6E4	0	0.999932	-0.006704	0.073942	0.454541
28	Phospho Stat3 6E4	0	0.999909	-0.020179	0.062650	0.476876
29	Phospho Stat3 6E4	0	0.999909	-0.024323	0.085500	0.506516
30	1:5 verd. Phospho- Tyrosine	0	1.000.000	-0.030855	0.106380	0.557599
31	1:5 verd. Phospho- Tyrosine	0	1.000.000	-0.036143	0.066390	0.622892
32	1:5 verd. Phospho- Tyrosine	0	1.000.000	-0.023432	0.105397	0.618688
33	1:5 verd. Phospho- Tyrosine	0	0.999954	-0.028051	0.118481	0.503132
34	Phospho- Tyrosine	0	0.997994	-0.024214	0.062417	0.749199
35	Phospho- Tyrosine	0	0.997401	-0.019670	0.095203	0.734027
36	Wisp2_129_158 r(bio)_1,25 µM, htag4(bio)_1,25 µM	0	0.998368	0.000033	0.004610	0.999390
38	Phospho- Tyrosine	0	0.996284	-0.015839	0.056910	0.759533
39	Phospho- Tyrosine	0	1.000.000	-0.019119	0.054082	0.779895
40	1:5 verd. Phospho- SAPK/JNK	0	1.000.000	-0.026566	0.090064	0.530447
41	1:5 verd. Phospho- SAPK/JNK	0	0.998997	-0.025737	0.091427	0.536716
42	1:5 verd. Phospho-	0	1.000.000	-0.035503	0.066407	0.560445

	SAPK/JNK					
43	1:5 verd. Phospho-SAPK/JNK	0	1.000.000	-0.036357	0.071894	0.595146
44	Phospho-SAPK/JNK	0	1.000.000	-0.039642	0.063832	0.543522
45	Phospho-SAPK/JNK	0	0.999977	-0.038145	0.096687	0.539131
46	Phospho-SAPK/JNK	0	0.985583	-0.036449	0.085620	0.549694
47	Phospho-SAPK/JNK	0	0.984656	-0.032455	0.078853	0.519897
48	Wisp2_129_158 r(bio)_1,25 µM, htag4(bio)_1,25 µM	0	0.997620	-0.000000	0.003741	0.999306
50	1:5 verd. Phospho-p44/42 MAP Kinase	0	0.998358	-0.014233	0.078843	0.437307
51	1:5 verd. Phospho-p44/42 MAP Kinase	0	0.999977	-0.021801	0.065083	0.438665
52	1:5 verd. Phospho-p44/42 MAP Kinase	0	1.000.000	-0.023124	0.067952	0.448438
53	1:5 verd. Phospho-p44/42 MAP Kinase	0	0.996781	-0.019659	0.090479	0.463191
54	Phospho-p44/42 MAP Kinase	0	0.999088	-0.032707	0.061147	0.530911
55	Phospho-p44/42 MAP Kinase	0	1.000.000	-0.036277	0.073208	0.496425
56	Phospho-p44/42 MAP Kinase	0	0.999297	-0.033256	0.089048	0.481498
57	Phospho-p44/42 MAP Kinase	0	1.000.000	-0.036136	0.071833	0.486455
58	1:5 verd. p-Smasd1	0	0.997144	-0.044442	0.064103	0.442071
59	1:5 verd. p-Smasd1	0	0.991610	-0.041147	0.067052	0.430867
60	Wisp2_129_158 r(bio)_1,25 µM, htag4(bio)_1,25 µM	0	0.999612	0.000007	0.001488	0.999773
62	1:5 verd. p-Smasd1	0	0.997087	-0.026565	0.059527	0.413834
63	1:5 verd. p-Smasd1	0	0.999819	-0.024796	0.066878	0.434147
64	p-Smasd1	0	0.998951	0.008436	0.064519	0.363755
65	p-Smasd1	0	0.997303	-0.016635	0.052680	0.410466
66	p-Smasd1	0	0.998472	-0.021740	0.044935	0.414387
67	p-Smasd1	0	0.992864	-0.024263	0.056025	0.398829
68	1:5 verd. p-Smasd2/3	0	0.998678	-0.043086	0.051510	0.437469
69	1:5 verd. p-Smasd2/3	0	0.999954	-0.037614	0.064564	0.406286
70	1:5 verd. p-Smasd2/3	0	0.994642	-0.037669	0.066004	0.430146
71	1:5 verd. p-Smasd2/3	0	0.989107	-0.039052	0.074588	0.444517
72	Wisp2_129_158 r(bio)_1,25 µM, htag4(bio)_1,25 µM	0	0.998889	0.000020	0.004757	0.999232
73	Wisp2_129_158 r(bio)_1,25 µM, htag4(bio)_1,25 µM	0	0.959923	0.017397	0.009134	0.956348
74	p-Smasd2/3	0	0.988395	-0.028214	0.053302	0.340455
75	p-Smasd2/3	0	0.995285	-0.026640	0.050510	0.334492
76	p-Smasd2/3	0	0.997948	-0.036934	0.051074	0.380577

77	p-Smasd2/3	0	0.999841	-0.034265	0.055796	0.380781
78	1:5 verd. c-Myc	0	1.000.000	-0.043541	0.064997	0.408156
79	1:5 verd. c-Myc	0	0.987616	-0.048533	0.057601	0.443121
80	1:5 verd. c-Myc	0	0.993789	-0.048076	0.063456	0.432351
81	1:5 verd. c-Myc	0	0.999590	-0.029169	0.087130	0.397386
82	c-Myc	0	0.999547	-0.030073	0.087353	0.466787
83	c-Myc	0	0.998700	-0.022204	0.094424	0.427024
84	Wisp2_129_158 r(bio)_1,25 µM, htag4(bio)_1,25 µM	0	0.995557	0.001578	0.025064	0.994455
85	Wisp2_129_158 r(bio)_1,25 µM, htag4(bio)_1,25 µM	0	0.927644	0.045532	0.010684	0.912593
86	c-Myc	0	0.974361	0.009720	0.085388	0.390786
87	c-Myc	0	0.993844	-0.017802	0.056163	0.427764
88	1:5 verd. phospho-p38 (mouse monoclonal 9.1)	0	0.995212	-0.027146	0.055988	0.499900
89	1:5 verd. phospho-p38 (mouse monoclonal 9.1)	0	0.997294	-0.028764	0.052075	0.474785
90	1:5 verd. phospho-p38 (mouse monoclonal 9.1)	0	0.999773	-0.024711	0.070612	0.400506
91	1:5 verd. phospho-p38 (mouse monoclonal 9.1)	0	0.999612	-0.033475	0.076138	0.439548
92	phospho-p38 (mouse monoclonal 9.1)	0	0.999728	-0.036653	0.070370	0.466715
93	phospho-p38 (mouse monoclonal 9.1)	0	0.999954	-0.036074	0.060385	0.427403
94	phospho-p38 (mouse monoclonal 9.1)	0	0.999932	-0.033832	0.071311	0.453338
95	phospho-p38 (mouse monoclonal 9.1)	0	0.997059	-0.032123	0.062971	0.428923
96	Wisp2_129_158 r(bio)_1,25 µM, htag4(bio)_1,25 µM	0	0.983351	0.002456	0.043374	0.948172
98	1:5 verd. p38 (mouse monoclonal 10.1)	0	0.931565	0.031836	0.083335	0.477463
99	1:5 verd. p38 (mouse monoclonal 10.1)	0	0.969129	0.004225	0.077610	0.440004
100	1:5 verd. p38 (mouse monoclonal 10.1)	0	0.989573	-0.012582	0.064377	0.478203
101	1:5 verd. p38 (mouse monoclonal 10.1)	0	0.997811	-0.010839	0.095573	0.482296
102	p38 (mouse monoclonal 10.1)	0	0.997983	-0.012803	0.036337	0.854758
103	p38 (mouse monoclonal 10.1)	0	0.998313	-0.013576	0.044071	0.842833

104	p38 (mouse monoclonal 10.1)	0	0.997575	-0.011425	0.036330	0.869050
105	p38 (mouse monoclonal 10.1)	0	0.995942	0.011772	0.120904	0.840162
106	1:20 verd. biotin anti rabbit IGG	0	0.997225	-0.024236	0.075575	0.490358
107	1:20 verd. biotin anti rabbit IGG	0	0.982931	-0.024158	0.067453	0.491146
109	Wispi2_129_158 r(bio)_1,25 µM, htag4(bio)_1,25 µM	0	0.842841	0.136250	0.022658	0.821468
110	1:20 verd. biotin anti rabbit IGG	0	0.880812	0.067107	0.058092	0.483869
111	1:20 verd. biotin anti rabbit IGG	0	0.916416	0.038397	0.092995	0.443318
112	1:100 verd. biotin anti rabbit IGG	0	0.951785	0.001047	0.073338	0.436282
113	1:100 verd. biotin anti rabbit IGG	0	0.978374	-0.016944	0.063874	0.416787
114	1:100 verd. biotin anti rabbit IGG	0	0.989170	-0.013452	0.090548	0.398110
115	1:100 verd. biotin anti rabbit IGG	0	0.989466	-0.022049	0.101571	0.468813
116	2% Milchpulver	0	0.989818	-0.017632	0.108079	0.503043
117	2% Milchpulver	0	0.980052	-0.016950	0.085340	0.571915
118	2% Milchpulver	0	0.964478	-0.011922	0.064432	0.575500
119	2% Milchpulver	0	0.936326	0.000359	0.041588	0.626024
120	Wispi2_129_158 r(bio)_1,25 µM, htag4(bio)_1,25 µM	0	0.902918	0.031814	0.018790	0.890743

Substance	Background	Sigma	CoG_y	CoG_x	Mean	mean-m-cyto-con	1-mean-m-cyto-con	sd-m-cyto-con
1:100 verd. Biotin anti rabbit IGG	0,971034	0,04763	80.000.000	331.000.000	0,639272			
1:100 verd. Biotin anti rabbit IGG	0,970521	0,050034	80.000.000	378.000.000	0,65649			
1:100 verd. Biotin anti rabbit IGG	0,985873	0,047545	79.000.000	420.000.000	0,660877			
1:20 verd. Biotin anti rabbit IGG	0,989254	0,053654	124.000.000	554.000.000	0,649577	0,62481375	0,37518625	0,02491483
1:20 verd. biotin anti rabbit IGG	0,976426	0,050608	125.000.000	595.000.000	0,639457			
1:20 verd. biotin anti rabbit IGG	0,886163	0,045571	83.000.000	202.000.000	0,593749			
1:20 verd. biotin anti rabbit IGG	0,924028	0,05055	81.000.000	248.000.000	0,616472			
1:5 verd. c-Myc	1.000.000	0,027716	211.000.000	377.000.000	0,493244	0,499714	0,500286	0,01081141
1:5 verd. c-Myc	0,999889	0,025018	210.000.000	421.000.000	0,493027			
1:5 verd. c-Myc	0,999978	0,025897	211.000.000	463.000.000	0,496871			
1:5 verd. c-Myc	0,999933	0,029648	212.000.000	510.000.000	0,515714			
1:5 verd. p38 (mouse	0,925357	0,024235	124.000.000	200.000.000	0,709251	0,7211055	0,2788945	0,01155259

monoclonal 10.1)								
1:5 verd. p38 (mouse monoclonal 10.1)	0,958534	0,02414	126.000.000	244.000.000	0,714438			
1:5 verd. p38 (mouse monoclonal 10.1)	0,977963	0,025547	124.000.000	287.000.000	0,725683			
1:5 verd. p38 (mouse monoclonal 10.1)	0,980771	0,027615	129.000.000	331.000.000	0,73505			
1:5 verd. Phospho Stat3 6E4	0,994853	0,025404	433.000.000	463.000.000	0,642432	0,636249	0,363751	0,00541902
1:5 verd. Phospho Stat3 6E4	0,997193	0,023942	431.000.000	507.000.000	0,638069			
1:5 verd. Phospho Stat3 6E4	0,994831	0,02379	431.000.000	551.000.000	0,634943			
1:5 verd. Phospho Stat3 6E4	0,988792	0,025497	431.000.000	596.000.000	0,629552			
1:5 verd. Phospho- Akt 4E2	0,984292	0,027571	479.000.000	551.000.000	0,610794	0,6030635	0,3969365	0,01347877
1:5 verd. Phospho- Akt 4E2	0,977094	0,032722	474.000.000	595.000.000	0,593248			
1:5 verd. Phospho- Akt 4E2	0,905993	0,026316	430.000.000	200.000.000	0,5902			
1:5 verd. Phospho- Akt 4E2	0,935748	0,019749	431.000.000	244.000.000	0,618012			
1:5 verd. phospho- p38 (mouse monoclonal 9.1)	0,986995	0,038128	167.000.000	289.000.000	0,617635	0,62093375	0,37906625	0,0085917
1:5 verd. phospho- p38 (mouse monoclonal 9.1)	0,986064	0,032403	170.000.000	333.000.000	0,611375			
1:5 verd. phospho- p38 (mouse monoclonal 9.1)	0,999955	0,040659	168.000.000	379.000.000	0,623088			
1:5 verd. phospho- p38 (mouse monoclonal 9.1)	0,999866	0,035622	166.000.000	422.000.000	0,631637			
1:5 verd. Phospho- p44/42 MAP Kinase	0,965775	0,029758	298.000.000	199.000.000	0,641461	0,669678	0,330322	0,02370452
1:5 verd. Phospho- p44/42 MAP Kinase	0,98652	0,028868	298.000.000	244.000.000	0,664445			
1:5 verd. Phospho- p44/42 MAP Kinase	0,998641	0,025181	298.000.000	289.000.000	0,674101			
1:5 verd. Phospho- p44/42 MAP Kinase	0,998619	0,032998	301.000.000	333.000.000	0,698705			
1:5 verd. Phospho- p70 S6 Kinase	0,849109	0,025299	475.000.000	198.000.000	0,473555	0,50286375	0,49713625	0,02091094
1:5 verd. Phospho- p70 S6 Kinase	0,897308	0,023232	475.000.000	245.000.000	0,505417			
1:5 verd. Phospho- p70 S6 Kinase	0,932248	0,023026	476.000.000	284.000.000	0,509595			
1:5 verd. Phospho- p70 S6 Kinase	0,964283	0,02909	476.000.000	331.000.000	0,522888			
1:5 verd. Phospho- SAPK/JNK	0,990686	0,049546	345.000.000	287.000.000	0,541682	0,5289495	0,4710505	0,01853309
1:5 verd. Phospho- SAPK/JNK	0,996034	0,041128	343.000.000	332.000.000	0,504781			
1:5 verd. Phospho- SAPK/JNK	0,99922	0,052727	343.000.000	376.000.000	0,524208			
1:5 verd. Phospho- SAPK/JNK	0,999513	0,047307	344.000.000	419.000.000	0,545127			
1:5 verd. Phospho- Tyrosine	0,996257	0,029585	386.000.000	378.000.000	0,668391	0,66543525	0,33456475	0,00623859
1:5 verd. Phospho- Tyrosine	0,99971	0,026471	387.000.000	419.000.000	0,668615			
1:5 verd. Phospho- Tyrosine	0,999867	0,022455	387.000.000	463.000.000	0,656079			
1:5 verd. Phospho- Tyrosine	0,982829	0,026824	388.000.000	506.000.000	0,668656			

1:5 verd. p-Smasd1	0,999933	0,077381	299.000.000	551.000.000	0,404387	0,38581325	0,61418675	0,01401415
1:5 verd. p-Smasd1	0,999666	0,085219	300.000.000	596.000.000	0,386246			
1:5 verd. p-Smasd1	0,969006	0,076846	256.000.000	198.000.000	0,37068			
1:5 verd. p-Smasd1	0,987455	0,08811	254.000.000	244.000.000	0,38194			
1:5 verd. p-Smasd2/3	0,998507	0,023758	255.000.000	464.000.000	0,360082	0,3494875	0,6505125	0,00910219
1:5 verd. p-Smasd2/3	0,998485	0,036129	257.000.000	506.000.000	0,354072			
1:5 verd. p-Smasd2/3	0,999889	0,023125	255.000.000	551.000.000	0,342107			
1:5 verd. p-Smasd2/3	0,99971	0,022792	257.000.000	594.000.000	0,341689			
2% Milchpulver	0,988168	0,040773	81.000.000	464.000.000	0,809173	0,78968075	0,21031925	0,01905628
2% Milchpulver	0,982108	0,036584	81.000.000	507.000.000	0,801399			
2% Milchpulver	0,960472	0,035562	82.000.000	553.000.000	0,780599			
2% Milchpulver	0,935784	0,033388	81.000.000	595.000.000	0,767552			
c-Myc	1.000.000	0,09604	212.000.000	551.000.000	0,723886	0,709542	0,290458	0,02319275
c-Myc	0,999621	0,079353	211.000.000	598.000.000	0,734624			
c-Myc	0,952429	0,072673	165.000.000	201.000.000	0,688921			
c-Myc	0,977094	0,100214	166.000.000	243.000.000	0,690737			
p38 (mouse monoclonal 10.1)	0,998351	0,036091	125.000.000	377.000.000	0,812277	0,81369875	0,18630125	0,01226536
p38 (mouse monoclonal 10.1)	0,999889	0,035769	123.000.000	422.000.000	0,826232			
p38 (mouse monoclonal 10.1)	0,998775	0,032261	124.000.000	467.000.000	0,818878			
p38 (mouse monoclonal 10.1)	0,998619	0,040237	123.000.000	508.000.000	0,797408			
Phospho Stat3 6E4	0,937344	0,032529	386.000.000	199.000.000	0,311448	0,32518575	0,67481425	0,00936926
Phospho Stat3 6E4	0,967513	0,031173	386.000.000	243.000.000	0,32881			
Phospho Stat3 6E4	0,984291	0,028202	385.000.000	290.000.000	0,332517			
Phospho Stat3 6E4	0,994318	0,024247	385.000.000	333.000.000	0,327968			
Phospho-Akt 4E2	0,942135	0,032125	431.000.000	285.000.000	0,429151	0,43242825	0,56757175	0,00292649
Phospho-Akt 4E2	0,969029	0,040753	432.000.000	329.000.000	0,436176			
Phospho-Akt 4E2	0,987901	0,039472	429.000.000	376.000.000	0,431562			
Phospho-Akt 4E2	0,990285	0,033311	432.000.000	418.000.000	0,432824			
phospho-p38 (mouse monoclonal 9.1)	0,999844	0,040101	167.000.000	464.000.000	0,651854	0,63993925	0,36006075	0,01279069
phospho-p38 (mouse monoclonal 9.1)	0,999822	0,044014	169.000.000	507.000.000	0,64831			
phospho-p38 (mouse monoclonal 9.1)	0,998797	0,04465	166.000.000	555.000.000	0,635839			
phospho-p38 (mouse monoclonal 9.1)	0,996699	0,041708	168.000.000	595.000.000	0,623754			
Phospho-p44/42 MAP Kinase	0,999978	0,044776	301.000.000	376.000.000	0,529316	0,5086285	0,4913715	0,019392
Phospho-p44/42 MAP Kinase	0,999844	0,041702	302.000.000	419.000.000	0,520887			
Phospho-p44/42 MAP Kinase	0,999109	0,048491	299.000.000	466.000.000	0,494051			
Phospho-p44/42 MAP Kinase	0,998997	0,041227	300.000.000	505.000.000	0,49026			
Phospho-p70 S6 Kinase	0,980994	0,028572	476.000.000	374.000.000	0,546894	0,5228135	0,4771865	0,02793771
Phospho-p70 S6 Kinase	0,989572	0,030864	473.000.000	421.000.000	0,539685			
Phospho-p70 S6 Kinase	0,992335	0,028483	473.000.000	465.000.000	0,520205			

Phospho-p70 S6 Kinase	0,993885	0,025576	474.000.000	508.000.000	0,48447			
Phospho-SAPK/JNK	0,999778	0,049143	345.000.000	465.000.000	0,540511	0,52601275	0,47398725	0,01832057
Phospho-SAPK/JNK	0,99951	0,054168	343.000.000	508.000.000	0,543076			
Phospho-SAPK/JNK	0,998775	0,068958	345.000.000	550.000.000	0,508294			
Phospho-SAPK/JNK	0,997972	0,070124	344.000.000	596.000.000	0,51217			
Phospho-Tyrosine	0,9584	0,024496	390.000.000	548.000.000	0,294526	0,28265175	0,71734825	0,01436544
Phospho-Tyrosine	0,973485	0,019885	388.000.000	592.000.000	0,265015			
Phospho-Tyrosine	0,955971	0,029012	344.000.000	202.000.000	0,27686			
Phospho-Tyrosine	0,976426	0,026826	346.000.000	242.000.000	0,294206			
p-Smasd1	0,997594	0,130823	256.000.000	287.000.000	0,497992	0,51131375	0,48868625	0,01626279
p-Smasd1	0,999443	0,12538	256.000.000	330.000.000	0,524759			
p-Smasd1	0,999513	0,144842	259.000.000	375.000.000	0,496501			
p-Smasd1	1.000.000	0,12337	256.000.000	422.000.000	0,526003			
p-Smasd2/3	0,965575	0,035339	212.000.000	201.000.000	0,464221	0,43330925	0,56669075	0,02135499
p-Smasd2/3	0,980414	0,029469	211.000.000	246.000.000	0,430907			
p-Smasd2/3	0,993226	0,033974	209.000.000	287.000.000	0,419504			
p-Smasd2/3	0,999623	0,027051	210.000.000	335.000.000	0,418605			
Wisp2_129_158r(bio)_1,25 µM, htag4(bio)_1,25 µM	0,761252	0,02856	476.000.000	157.000.000	0,718976	0,88170775	0,11829225	0,11002156
Wisp2_129_158r(bio)_1,25 µM, htag4(bio)_1,25 µM	0,964773	0,027045	479.000.000	642.000.000	0,914559			
Wisp2_129_158r(bio)_1,25 µM, htag4(bio)_1,25 µM	0,981996	0,022077	392.000.000	641.000.000	0,93402			
Wisp2_129_158r(bio)_1,25 µM, htag4(bio)_1,25 µM	0,990307	0,025456	348.000.000	639.000.000	0,959276			
Wisp2_129_158r(bio)_1,25 µM, htag4(bio)_1,25 µM	0,993951	0,021432	305.000.000	643.000.000	0,960754	0,93335475	0,06664525	0,03916843
Wisp2_129_158r(bio)_1,25 µM, htag4(bio)_1,25 µM	0,994602	0,018564	259.000.000	640.000.000	0,953154			
Wisp2_129_158r(bio)_1,25 µM, htag4(bio)_1,25 µM	0,928654	0,021899	212.000.000	156.000.000	0,875507			
Wisp2_129_158r(bio)_1,25 µM, htag4(bio)_1,25 µM	0,991266	0,021385	213.000.000	642.000.000	0,944004			
Wisp2_129_158r(bio)_1,25 µM, htag4(bio)_1,25 µM	0,915441	0,024492	170.000.000	159.000.000	0,852908	0,84069325	0,15930675	0,0553261
Wisp2_129_158r(bio)_1,25 µM, htag4(bio)_1,25 µM	0,975717	0,036937	170.000.000	641.000.000	0,907889			
Wisp2_129_158r(bio)_1,25 µM, htag4(bio)_1,25 µM	0,838102	0,022953	81.000.000	156.000.000	0,774859			
Wisp2_129_158r(bio)_1,25 µM, htag4(bio)_1,25 µM	0,897237	0,031182	81.000.000	641.000.000	0,827117			

Substance	Background	QSV	Sigma	Mean	mean-m-cyto-bmp	sd-m-cyto-bmp	1-m-cyto-bmp
1:100 verd. biotin anti rabbit IGG	0,957429	0,037743	0,056072	0,698753	0,71435075	0,01520994	0,28564925
1:100 verd. biotin anti rabbit IGG	0,973067	0,034792	0,051628	0,703853			
1:100 verd. biotin anti rabbit IGG	0,98233	0,027194	0,046538	0,727246			
1:100 verd. biotin anti rabbit IGG	0,986725	0,027021	0,043333	0,727551			
1:20 verd. biotin anti rabbit IGG	0,994636	0,019338	0,047136	0,798003	0,7102845	0,06576412	0,2897155
1:20 verd. biotin anti rabbit IGG	0,971355	0,050736	0,071598	0,699691			
1:20 verd. biotin anti rabbit IGG	0,898928	0,094754	0,0604	0,638602			
1:20 verd. biotin anti rabbit IGG	0,930187	0,047104	0,055593	0,704842			
1:5 verd. c-Myc	0,998723	0,046631	0,030814	0,621777	0,634799	0,02140388	0,365201
1:5 verd. c-Myc	0,993502	0,035685	0,066459	0,666743			
1:5 verd. c-Myc	1.000.000	0,043264	0,026225	0,6237			
1:5 verd. c-Myc	0,990714	0,043567	0,05908	0,626976			
1:5 verd. p38 (mouse monoclonal 10.1)	0,960604	0,020174	0,021648	0,795908	0,83684125	0,03189102	0,16315875
1:5 verd. p38 (mouse monoclonal 10.1)	0,98182	0,013164	0,020052	0,832936			
1:5 verd. p38 (mouse monoclonal 10.1)	0,994756	0,012229	0,021204	0,845936			
1:5 verd. p38 (mouse monoclonal 10.1)	0,998108	0,009443	0,024921	0,872585			
1:5 verd. Phospho Stat3 6E4	0,977155	0,024825	0,033687	0,722501	0,675519	0,0690048	0,324481
1:5 verd. Phospho Stat3 6E4	0,993434	0,026862	0,039263	0,71495			
1:5 verd. Phospho Stat3 6E4	0,995285	0,030507	0,038227	0,690576			
1:5 verd. Phospho Stat3 6E4	0,981835	0,065421	0,04291	0,574049			
1:5 verd. Phospho-Akt 4E2	0,995622	0,03245	0,055733	0,684005	0,71552	0,11495733	0,28448
1:5 verd. Phospho-Akt 4E2	0,998472	0,067313	0,076127	0,57319			
1:5 verd. Phospho-Akt 4E2	0,963534	0,021766	0,028047	0,761924			
1:5 verd. Phospho-Akt 4E2	0,963061	0,011187	0,023739	0,842961			
1:5 verd. phospho-p38 (mouse monoclonal 9.1)	0,991413	0,016468	0,030951	0,810882	0,82409775	0,0120014	0,17590225
1:5 verd. phospho-p38 (mouse monoclonal 9.1)	0,990895	0,013918	0,026711	0,820225			
1:5 verd. phospho-p38 (mouse monoclonal 9.1)	0,997814	0,012674	0,033667	0,825698			
1:5 verd. phospho-p38 (mouse monoclonal 9.1)	0,994636	0,011998	0,030053	0,839586			
1:5 verd. Phospho-p44/42 MAP Kinase	0,992909	0,01071	0,029962	0,847885	0,8906115	0,03426161	0,1093885
1:5 verd. Phospho-p44/42 MAP Kinase	0,997538	0,007979	0,025909	0,878222			
1:5 verd. Phospho-p44/42 MAP Kinase	0,999407	0,005554	0,024258	0,914732			
1:5 verd. Phospho-p44/42 MAP Kinase	0,99943	0,007873	0,041663	0,921607			
1:5 verd. Phospho-p70 S6 Kinase	0,917077	0,040602	0,037143	0,674029	0,7235675	0,05235058	0,2764325

1:5 verd. Phospho-p70 S6 Kinase	0,929845	0,03234	0,034834	0,69937			
1:5 verd. Phospho-p70 S6 Kinase	0,993744	0,026303	0,033552	0,725338			
1:5 verd. Phospho-p70 S6 Kinase	0,999549	0,015791	0,0378	0,795533			
1:5 verd. Phospho-SAPK/JNK	0,991255	0,024022	0,050872	0,740345	0,73347925	0,01412561	0,26652075
1:5 verd. Phospho-SAPK/JNK	0,939862	0,027363	0,053803	0,72113			
1:5 verd. Phospho-SAPK/JNK	1.000.000	0,025255	0,051722	0,722366			
1:5 verd. Phospho-SAPK/JNK	0,998039	0,021063	0,057971	0,750076			
1:5 verd. Phospho-Tyrosine	0,999775	0,00676	0,018931	0,890499	0,88996075	0,00451533	0,11003925
1:5 verd. Phospho-Tyrosine	0,992202	0,007067	0,031859	0,883416			
1:5 verd. Phospho-Tyrosine	1.000.000	0,006455	0,02356	0,892931			
1:5 verd. Phospho-Tyrosine	0,997295	0,006212	0,031022	0,892997			
1:5 verd. p-Smasd1	1.000.000	0,122971	0,059966	0,492835	0,49537075	0,00466202	0,50462925
1:5 verd. p-Smasd1	0,997461	0,115464	0,058836	0,498239			
1:5 verd. p-Smasd1	0,995126	0,129884	0,05513	0,49018			
1:5 verd. p-Smasd1	0,999977	0,12527	0,060241	0,500229			
1:5 verd. p-Smasd2/3	1.000.000	0,099042	0,038915	0,474643	0,458613	0,01530999	0,541387
1:5 verd. p-Smasd2/3	0,975262	0,110529	0,03021	0,464435			
1:5 verd. p-Smasd2/3	1.000.000	0,112174	0,018928	0,457003			
1:5 verd. p-Smasd2/3	0,995714	0,120932	0,030687	0,438371			
2% Milchpulver	0,983593	0,00828	0,032847	0,909098	0,87075275	0,03225717	0,12924725
2% Milchpulver	0,974974	0,025265	0,050163	0,882032			
2% Milchpulver	0,960648	0,042783	0,044965	0,858038			
2% Milchpulver	0,925011	0,067	0,041049	0,833843			
c-Myc	1.000.000	0,006533	0,063853	0,883587	0,83398825	0,03317877	0,16601175
c-Myc	0,997927	0,012848	0,097295	0,821308			
c-Myc	0,995782	0,013493	0,062145	0,815229			
c-Myc	0,996418	0,012791	0,05275	0,815829			
p38 (mouse monoclonal 10.1)	0,99715	0,018669	0,044036	0,781739	0,792147	0,00934304	0,207853
p38 (mouse monoclonal 10.1)	1.000.000	0,016235	0,05592	0,803922			
p38 (mouse monoclonal 10.1)	0,998837	0,017372	0,058496	0,788821			
p38 (mouse monoclonal 10.1)	0,99329	0,016725	0,052484	0,794106			
Phospho Stat3 6E4	0,994756	0,293675	0,043039	0,276941	0,28968625	0,01418266	0,71031375
Phospho Stat3 6E4	0,99373	0,249154	0,04036	0,307952			
Phospho Stat3 6E4	0,990264	0,282852	0,022657	0,280139			
Phospho Stat3 6E4	0,934648	0,259882	0,028184	0,293713			
Phospho-Akt 4E2	0,992928	0,069526	0,051893	0,569036	0,58299425	0,01254115	0,41700575
Phospho-Akt 4E2	0,993821	0,059559	0,061482	0,598861			
Phospho-Akt 4E2	0,955974	0,061234	0,05649	0,585463			
Phospho-Akt 4E2	0,977109	0,060985	0,069973	0,578617			
phospho-p38 (mouse monoclonal 9.1)	0,999796	0,050829	0,067425	0,641822	0,601079	0,03651183	0,398921
phospho-p38 (mouse monoclonal 9.1)	0,993776	0,058303	0,068461	0,614452			
phospho-p38 (mouse monoclonal 9.1)	0,999635	0,066646	0,076836	0,592679			
phospho-p38 (mouse monoclonal 9.1)	0,995144	0,080521	0,083991	0,555363			
Phospho-p44/42 MAP Kinase	0,999111	0,115178	0,038596	0,453383	0,437403	0,01346586	0,562597
Phospho-p44/42 MAP	0,993109	0,121441	0,061241	0,439755			

Kinase							
Phospho-p44/42 MAP Kinase	0,980527	0,127305	0,035755	0,435822			
Phospho-p44/42 MAP Kinase	0,984832	0,142298	0,044164	0,420652			
Phospho-p70 S6 Kinase	0,956705	0,06321	0,028104	0,571055	0,54188775	0,01963213	0,45811225
Phospho-p70 S6 Kinase	0,98517	0,088094	0,054947	0,533048			
Phospho-p70 S6 Kinase	0,977417	0,071792	0,026509	0,534948			
Phospho-p70 S6 Kinase	0,996192	0,074274	0,025842	0,5285			
Phospho-SAPK/JNK	0,980301	0,072	0,067288	0,56265	0,5077425	0,07008605	0,4922575
Phospho-SAPK/JNK	1.000.000	0,078859	0,064476	0,553872			
Phospho-SAPK/JNK	1.000.000	0,103546	0,063847	0,504601			
Phospho-SAPK/JNK	0,999773	0,157545	0,052741	0,409847			
Phospho-Tyrosine	0,999592	0,20575	0,025326	0,333884	0,3075615	0,02081607	0,6924385
Phospho-Tyrosine	0,982467	0,266907	0,022111	0,285387			
Phospho-Tyrosine	0,993284	0,256995	0,027917	0,298182			
Phospho-Tyrosine	0,992946	0,234181	0,027364	0,312793			
p-Smasd1	0,999617	0,036548	0,097028	0,642025	0,6420925	0,03009513	0,3579075
p-Smasd1	1.000.000	0,045835	0,129663	0,619024			
p-Smasd1	1.000.000	0,046944	0,088005	0,622698			
p-Smasd1	0,996534	0,024952	0,071195	0,684623			
p-Smasd2/3	0,997824	0,107761	0,033248	0,473494	0,49401675	0,01645004	0,50598325
p-Smasd2/3	0,996466	0,099274	0,028439	0,4886			
p-Smasd2/3	0,991154	0,086241	0,03563	0,510512			
p-Smasd2/3	0,991632	0,088377	0,033488	0,503461			
Wisp2_129_158r(bio)_1, 25 µM, htag4(bio)_1,25 µM	0,912905	0,032069	0,02387	0,854355	0,91456425	0,04014776	0,08543575
Wisp2_129_158r(bio)_1, 25 µM, htag4(bio)_1,25 µM	0,997697	0,004158	0,027548	0,934426			
Wisp2_129_158r(bio)_1, 25 µM, htag4(bio)_1,25 µM	0,999134	0,003765	0,041416	0,935719			
Wisp2_129_158r(bio)_1, 25 µM, htag4(bio)_1,25 µM	0,999482	0,004454	0,02829	0,933757			
Wisp2_129_158r(bio)_1, 25 µM, htag4(bio)_1,25 µM	0,99927	0,005589	0,044376	0,910016	0,92134575	0,0101917	0,07865425
Wisp2_129_158r(bio)_1, 25 µM, htag4(bio)_1,25 µM	0,99728	0,004882	0,026497	0,919449			
Wisp2_129_158r(bio)_1, 25 µM, htag4(bio)_1,25 µM	0,975885	0,00538	0,03272	0,92117			
Wisp2_129_158r(bio)_1, 25 µM, htag4(bio)_1,25 µM	0,990706	0,004449	0,027694	0,934748			
Wisp2_129_158r(bio)_1, 25 µM, htag4(bio)_1,25 µM	0,958413	0,007896	0,032357	0,910203	0,8540685	0,0642775	0,1459315
Wisp2_129_158r(bio)_1, 25 µM, htag4(bio)_1,25 µM	0,969106	0,008451	0,039891	0,908753			
Wisp2_129_158r(bio)_1, 25 µM, htag4(bio)_1,25 µM	0,86311	0,096285	0,036594	0,791146			
Wisp2_129_158r(bio)_1, 25 µM, htag4(bio)_1,25 µM	0,887232	0,119346	0,044005	0,806172			

Substance	Background	QSV	Sigma	Mean	mean-m-nu-con	sd-m-nu-con	1-mean-m-nu-con
1:100 verd. biotin anti rabbit IGG	0,976471	1.100.999	0,065448	0,461112	0,489059	0,02278294	0,510941
1:100 verd. biotin anti rabbit IGG	0,951742	0,978392	0,051954	0,480017			
1:100 verd. biotin anti rabbit IGG	0,954432	0,872261	0,079413	0,509823			
1:100 verd. biotin anti rabbit IGG	0,987543	0,937464	0,073373	0,505284			
1:20 verd. biotin anti rabbit IGG	0,992111	0,998337	0,096941	0,491247	0,49475975	0,04195834	0,50524025
1:20 verd. biotin anti rabbit IGG	0,990496	0,767041	0,105174	0,555123			
1:20 verd. biotin anti rabbit IGG	0,922096	1.093.436	0,093823	0,46416			
1:20 verd. biotin anti rabbit IGG	0,933769	1.061.621	0,089214	0,468509			
1:5 verd. c-Myc	0,956724	2.208.622	0,021933	0,262308	0,2583685	0,00638324	0,7416315
1:5 verd. c-Myc	0,999794	2.269.017	0,020389	0,255655			
1:5 verd. c-Myc	0,914325	2.315.702	0,02293	0,250734			
1:5 verd. c-Myc	0,970003	2.228.133	0,024785	0,264777			
1:5 verd. p38 (mouse monoclonal 10.1)	0,969935	0,185911	0,026828	0,839225	0,83689175	0,00388206	0,16310825
1:5 verd. p38 (mouse monoclonal 10.1)	0,984245	0,191746	0,037871	0,834288			
1:5 verd. p38 (mouse monoclonal 10.1)	0,952689	0,186168	0,035218	0,841086			
1:5 verd. p38 (mouse monoclonal 10.1)	0,974925	0,187954	0,031741	0,832968			
1:5 verd. Phospho Stat3 6E4	0,934663	0,802863	0,042294	0,561791	0,5499145	0,03319934	0,4500855
1:5 verd. Phospho Stat3 6E4	0,971811	0,794494	0,046101	0,563234			
1:5 verd. Phospho Stat3 6E4	0,931315	0,976883	0,070875	0,500774			
1:5 verd. Phospho Stat3 6E4	0,965738	0,73598	0,048117	0,573859			
1:5 verd. Phospho-Akt 4E2	0,951596	0,762242	0,065278	0,562664	0,548476	0,0287784	0,451524
1:5 verd. Phospho-Akt 4E2	0,965375	0,73687	0,075522	0,572578			
1:5 verd. Phospho-Akt 4E2	0,919954	0,995093	0,036086	0,507316			
1:5 verd. Phospho-Akt 4E2	0,866369	0,767312	0,050361	0,551346			
1:5 verd. phospho-p38 (mouse monoclonal 9.1)	0,921844	0,922083	0,059981	0,510534	0,47001375	0,02833973	0,52998625
1:5 verd. phospho-p38 (mouse monoclonal 9.1)	0,975581	1.066.327	0,038694	0,468554			
1:5 verd. phospho-p38 (mouse monoclonal 9.1)	0,958101	1.168.672	0,042391	0,449357			
1:5 verd. phospho-p38 (mouse monoclonal 9.1)	0,998234	1.205.739	0,055813	0,45161			
1:5 verd. Phospho-p44/42 MAP Kinase	0,918748	0,971604	0,048388	0,49539	0,526647	0,04876938	0,473353
1:5 verd. Phospho-p44/42 MAP Kinase	0,934302	0,989119	0,041327	0,486515			
1:5 verd. Phospho-p44/42 MAP Kinase	0,920041	0,852619	0,03732	0,530722			
1:5 verd. Phospho-p44/42 MAP Kinase	0,963789	0,710735	0,057031	0,593961			
1:5 verd. Phospho-p70 S6 Kinase	0,930265	2.058.014	0,035936	0,301467	0,31475	0,01307042	0,68525

1:5 verd. Phospho-p70 S6 Kinase	0,918878	1.883.064	0,035337	0,308898			
1:5 verd. Phospho-p70 S6 Kinase	0,92729	1.829.603	0,028783	0,316612			
1:5 verd. Phospho-p70 S6 Kinase	0,975806	1.804.187	0,046281	0,332023			
1:5 verd. Phospho-SAPK/JNK	0,912785	1.521.760	0,065907	0,382988	0,3693005	0,01285257	0,6306995
1:5 verd. Phospho-SAPK/JNK	0,991234	1.546.301	0,082602	0,374904			
1:5 verd. Phospho-SAPK/JNK	0,977342	1.680.293	0,074564	0,352919			
1:5 verd. Phospho-SAPK/JNK	0,936424	1.585.028	0,084529	0,366391			
1:5 verd. Phospho-Tyrosine	0,927348	0,767537	0,044706	0,575303	0,573185	0,00164086	0,426815
1:5 verd. Phospho-Tyrosine	0,911753	0,780675	0,039297	0,572234			
1:5 verd. Phospho-Tyrosine	0,935933	0,770357	0,045212	0,573603			
1:5 verd. Phospho-Tyrosine	0,948584	0,770647	0,052781	0,5716			
1:5 verd. p-Smasd1	0,993556	1.460.478	0,052034	0,387225	0,3724355	0,01388217	0,6275645
1:5 verd. p-Smasd1	0,926015	1.543.375	0,046103	0,366278			
1:5 verd. p-Smasd1	0,930894	1.596.287	0,033023	0,356198			
1:5 verd. p-Smasd1	0,934279	1.438.445	0,042103	0,380041			
1:5 verd. p-Smasd2/3	0,932989	2.965.489	0,022502	0,178958	0,17871375	0,007186	0,82128625
1:5 verd. p-Smasd2/3	0,964683	3.069.012	0,023505	0,171637			
1:5 verd. p-Smasd2/3	0,992664	3.049.379	0,019942	0,175749			
1:5 verd. p-Smasd2/3	0,941016	2.893.775	0,029441	0,188511			
2% Milchpulver	0,992249	0,384987	0,064162	0,750121	0,7548405	0,01578584	0,2451595
2% Milchpulver	0,990473	0,32363	0,061179	0,75084			
2% Milchpulver	0,967009	0,331701	0,061147	0,74088			
2% Milchpulver	0,958478	0,259751	0,061439	0,777521			
c-Myc	0,992065	0,965179	0,112489	0,488023	0,48590425	0,00481375	0,51409575
c-Myc	0,981814	0,992877	0,109312	0,481936			
c-Myc	0,977439	1.014.602	0,098786	0,481952			
c-Myc	0,976631	0,988221	0,110135	0,491706			
p38 (mouse monoclonal 10.1)	0,973956	0,293444	0,034407	0,780069	0,782698	0,00643885	0,217302
p38 (mouse monoclonal 10.1)	0,997492	0,309861	0,033678	0,791084			
p38 (mouse monoclonal 10.1)	0,998267	0,306133	0,039014	0,783729			
p38 (mouse monoclonal 10.1)	0,995184	0,289691	0,032014	0,77591			
Phospho Stat3 6E4	0,940264	1.487.043	0,040513	0,388797	0,42282825	0,02612733	0,57717175
Phospho Stat3 6E4	0,921546	1.351.012	0,047012	0,416389			
Phospho Stat3 6E4	0,895755	1.259.298	0,041487	0,43923			
Phospho Stat3 6E4	0,937026	1.235.161	0,046235	0,446897			
Phospho-Akt 4E2	0,89109	1.184.945	0,043309	0,450093	0,44087325	0,00698436	0,55912675
Phospho-Akt 4E2	0,916986	1.277.849	0,053025	0,438227			
Phospho-Akt 4E2	0,912327	1.291.968	0,045869	0,433541			
Phospho-Akt 4E2	0,934457	1.247.294	0,04258	0,441632			
phospho-p38 (mouse monoclonal 9.1)	0,957463	0,582884	0,049607	0,61948	0,611138	0,01296965	0,388862
phospho-p38 (mouse monoclonal 9.1)	0,996973	0,660735	0,05437	0,593119			
phospho-p38 (mouse monoclonal 9.1)	0,996262	0,624319	0,055386	0,61034			
phospho-p38 (mouse monoclonal 9.1)	0,983878	0,599799	0,042469	0,621613			
Phospho-p44/42 MAP Kinase	0,988258	0,525511	0,042774	0,666745	0,65214425	0,01426587	0,34785575
Phospho-p44/42 MAP	0,93503	0,533233	0,054505	0,660998			

Kinase							
Phospho-p44/42 MAP Kinase	0,947197	0,573497	0,043232	0,645103			
Phospho-p44/42 MAP Kinase	0,976171	0,592828	0,037857	0,635731			
Phospho-p70 S6 Kinase	0,969066	0,840646	0,041345	0,550178	0,5620115	0,00866573	0,4379885
Phospho-p70 S6 Kinase	0,997409	0,805221	0,033118	0,564088			
Phospho-p70 S6 Kinase	0,977024	0,801737	0,038906	0,562807			
Phospho-p70 S6 Kinase	0,999404	0,775553	0,040436	0,570973			
Phospho-SAPK/JNK	0,945648	0,353605	0,051871	0,744224	0,72404475	0,01884331	0,27595525
Phospho-SAPK/JNK	0,962007	0,377237	0,055663	0,733675			
Phospho-SAPK/JNK	0,989808	0,394874	0,059697	0,716917			
Phospho-SAPK/JNK	0,974325	0,423606	0,052582	0,701363			
Phospho-Tyrosine	0,971127	1.630.934	0,034703	0,370527	0,3721625	0,00445518	0,6278375
Phospho-Tyrosine	0,992572	1.634.123	0,04017	0,370774			
Phospho-Tyrosine	0,930719	1.618.757	0,033671	0,368656			
Phospho-Tyrosine	0,937003	1.552.724	0,028666	0,378693			
p-Smasd1	0,90375	1.450.541	0,100056	0,355413	0,3715955	0,01950763	0,6284045
p-Smasd1	0,965761	1.429.725	0,0851	0,367184			
p-Smasd1	0,975709	1.257.509	0,126156	0,399896			
p-Smasd1	0,967328	1.473.151	0,134482	0,363889			
p-Smasd2/3	0,942919	2.388.876	0,025475	0,230148	0,233614	0,01938308	0,766386
p-Smasd2/3	0,930848	1.949.108	0,036246	0,261734			
p-Smasd2/3	0,923599	2.462.358	0,02104	0,218089			
p-Smasd2/3	0,964843	2.371.857	0,019726	0,224485			
Wisp2_129_158r(bio)_1, 25 µM, htag4(bio)_1,25 µM	0,924688	1.119.038	0,187	0,318534	0,76721125	0,30146548	0,23278875
Wisp2_129_158r(bio)_1, 25 µM, htag4(bio)_1,25 µM	0,989965	0,122723	0,049373	0,881399			
Wisp2_129_158r(bio)_1, 25 µM, htag4(bio)_1,25 µM	0,988327	0,104623	0,049053	0,900159			
Wisp2_129_158r(bio)_1, 25 µM, htag4(bio)_1,25 µM	0,878294	0,02191	0,041596	0,968753			
Wisp2_129_158r(bio)_1, 25 µM, htag4(bio)_1,25 µM	0,799794	2.731.872	0,071434	0,169691	0,72696175	0,37643154	0,27303825
Wisp2_129_158r(bio)_1, 25 µM, htag4(bio)_1,25 µM	0,996078	0,00275	0,005866	0,998471			
Wisp2_129_158r(bio)_1, 25 µM, htag4(bio)_1,25 µM	0,973287	0,142601	0,065653	0,868369			
Wisp2_129_158r(bio)_1, 25 µM, htag4(bio)_1,25 µM	0,993418	0,138367	0,06751	0,871316			
Wisp2_129_158r(bio)_1, 25 µM, htag4(bio)_1,25 µM	0,961931	0,144199	0,066105	0,866697	0,8564455	0,02613726	0,1435545
Wisp2_129_158r(bio)_1, 25 µM, htag4(bio)_1,25 µM	0,987209	0,153774	0,059636	0,855416			
Wisp2_129_158r(bio)_1, 25 µM, htag4(bio)_1,25 µM	0,883133	0,1787	0,044824	0,821006			
Wisp2_129_158r(bio)_1, 25 µM, htag4(bio)_1,25 µM	0,932577	0,099296	0,036256	0,882663			

Substance	Background	QSV	Sigma	Mean	mean-m-nu-bmp2	sd-m-nu-bmp2	1-mean-m-nu-bmp2
1:100 verd. biotin anti rabbit IGG	0,910158	1.884.010	0,045124	0,295447	0,293294	0,00433036	0,706706
1:100 verd. biotin anti rabbit IGG	0,910562	1.879.501	0,043082	0,295067			
1:100 verd. biotin anti rabbit IGG	0,909582	1.945.232	0,043499	0,286816			
1:100 verd. biotin anti rabbit IGG	0,913615	1.884.252	0,04661	0,295846			
1:20 verd. biotin anti rabbit IGG	0,911178	1.685.619	0,033228	0,325142	0,33471075	0,01697376	0,66528925
1:20 verd. biotin anti rabbit IGG	0,900178	1.775.375	0,034298	0,315681			
1:20 verd. biotin anti rabbit IGG	0,890728	1.597.172	0,052271	0,348089			
1:20 verd. biotin anti rabbit IGG	0,915143	1.564.510	0,050624	0,349931			
1:5 verd. c-Myc	0,990828	1.940.456	0,021789	0,271509	0,273382	0,01056101	0,726618
1:5 verd. c-Myc	0,997297	2.022.611	0,020974	0,26208			
1:5 verd. c-Myc	0,996123	1.917.309	0,028331	0,272335			
1:5 verd. c-Myc	0,994129	1.822.819	0,02605	0,287604			
1:5 verd. p38 (mouse monoclonal 10.1)	0,987704	0,619277	0,090314	0,617799	0,46282375	0,1170956	0,53717625
1:5 verd. p38 (mouse monoclonal 10.1)	0,990274	0,961432	0,077111	0,487836			
1:5 verd. p38 (mouse monoclonal 10.1)	0,965304	1.370.953	0,048175	0,384943			
1:5 verd. p38 (mouse monoclonal 10.1)	0,949086	1.481.288	0,041685	0,360717			
1:5 verd. Phospho Stat3 6E4	0,974942	1.444.117	0,031653	0,364571	0,371402	0,02146327	0,628598
1:5 verd. Phospho Stat3 6E4	0,966035	1.310.799	0,039042	0,394426			
1:5 verd. Phospho Stat3 6E4	0,960563	1.388.896	0,031622	0,381665			
1:5 verd. Phospho Stat3 6E4	0,991271	1.559.545	0,035809	0,344946			
1:5 verd. Phospho-Akt 4E2	0,931738	1.482.400	0,038276	0,362537	0,32903575	0,02667176	0,67096425
1:5 verd. Phospho-Akt 4E2	0,94142	1.610.982	0,029156	0,336866			
1:5 verd. Phospho-Akt 4E2	0,90781	1.785.662	0,025243	0,301429			
1:5 verd. Phospho-Akt 4E2	0,940157	1.676.246	0,025514	0,315311			
1:5 verd. phospho-p38 (mouse monoclonal 9.1)	0,971242	1.532.283	0,028586	0,341154	0,33159	0,00791372	0,66841
1:5 verd. phospho-p38 (mouse monoclonal 9.1)	0,957527	1.642.090	0,03188	0,324322			
1:5 verd. phospho-p38 (mouse monoclonal 9.1)	0,959366	1.658.889	0,032313	0,325917			
1:5 verd. phospho-p38 (mouse monoclonal 9.1)	0,970677	1.614.310	0,033727	0,334967			

1:5 verd. Phospho-p44/42 MAP Kinase	0,946427	1.363.012	0,03674	0,379293	0,442498	0,05167282	0,557502
1:5 verd. Phospho-p44/42 MAP Kinase	0,974033	1.175.618	0,031455	0,424235			
1:5 verd. Phospho-p44/42 MAP Kinase	0,996433	1.009.352	0,029896	0,469754			
1:5 verd. Phospho-p44/42 MAP Kinase	0,997883	0,890356	0,022517	0,49671			
1:5 verd. Phospho-p70 S6 Kinase	0,856662	1.957.896	0,021703	0,267768	0,26675675	0,00612284	0,73324325
1:5 verd. Phospho-p70 S6 Kinase	0,840279	2.019.500	0,015844	0,266144			
1:5 verd. Phospho-p70 S6 Kinase	0,88962	1.951.758	0,016205	0,274007			
1:5 verd. Phospho-p70 S6 Kinase	0,957771	2.061.182	0,023789	0,259108			
1:5 verd. Phospho-SAPK/JNK	0,997186	1.627.678	0,063699	0,322445	0,30333625	0,03112836	0,69666375
1:5 verd. Phospho-SAPK/JNK	0,987925	1.752.678	0,052897	0,296219			
1:5 verd. Phospho-SAPK/JNK	0,99102	1.975.883	0,045339	0,262561			
1:5 verd. Phospho-SAPK/JNK	0,999712	1.538.824	0,069984	0,33212			
1:5 verd. Phospho-Tyrosine	0,979256	1.608.723	0,03311	0,323354	0,49048175	0,17834084	0,50951825
1:5 verd. Phospho-Tyrosine	0,988213	1.406.409	0,060497	0,361506			
1:5 verd. Phospho-Tyrosine	0,957483	0,472277	0,059922	0,697742			
1:5 verd. Phospho-Tyrosine	0,977711	0,74286	0,043827	0,579325			
1:5 verd. p-Smasd1	0,998173	1.884.289	0,037708	0,285401	0,25531325	0,02942676	0,74468675
1:5 verd. p-Smasd1	0,995325	2.283.454	0,031066	0,23913			
1:5 verd. p-Smasd1	0,965548	2.376.303	0,020248	0,222535			
1:5 verd. p-Smasd1	0,983139	1.958.412	0,029002	0,274187			
1:5 verd. p-Smasd2/3	0,978974	1.975.533	0,028085	0,260314	0,25587025	0,00941325	0,74412975
1:5 verd. p-Smasd2/3	0,983489	1.983.083	0,033456	0,261985			
1:5 verd. p-Smasd2/3	0,995857	2.035.284	0,036276	0,259336			
1:5 verd. p-Smasd2/3	0,993996	2.186.207	0,030079	0,241846			
2% Milchpulver	0,892035	0,60821	0,027294	0,624488	0,597176	0,02278158	0,402824
2% Milchpulver	0,885233	0,639897	0,035453	0,605555			
2% Milchpulver	0,855258	0,681071	0,029	0,586539			
2% Milchpulver	0,841476	0,73084	0,028868	0,572122			
c-Myc	0,995835	2.441.020	0,044077	0,204178	0,22181325	0,01959016	0,77818675
c-Myc	0,999712	2.338.907	0,049758	0,218943			
c-Myc	0,99922	1.998.204	0,088317	0,249699			
c-Myc	0,989277	2.280.564	0,049237	0,214433			
p38 (mouse monoclonal 10.1)	0,940887	0,257724	0,03838	0,87831	0,86441575	0,01689283	0,13558425
p38 (mouse monoclonal 10.1)	0,946006	0,253557	0,030557	0,879708			
p38 (mouse monoclonal 10.1)	0,933444	0,280071	0,058625	0,851102			
p38 (mouse monoclonal 10.1)	0,923784	0,283515	0,056582	0,848543			
Phospho Stat3 6E4	0,948288	2.208.675	0,030527	0,237307	0,25564025	0,01445701	0,74435975
Phospho Stat3 6E4	0,96876	1.931.103	0,042722	0,265233			
Phospho Stat3 6E4	0,949352	1.882.470	0,039319	0,268974			
Phospho Stat3 6E4	0,96249	2.010.034	0,036798	0,251047			
Phospho-Akt 4E2	0,948377	1.586.499	0,034364	0,324189	0,3154635	0,00616246	0,6845365
Phospho-Akt 4E2	0,938606	1.657.542	0,046938	0,315045			
Phospho-Akt 4E2	0,90488	1.658.455	0,055112	0,312558			

Phospho-Akt 4E2	0,927329	1.694.472	0,046898	0,310062			
phospho-p38 (mouse monoclonal 9.1)	0,969403	0,470294	0,059082	0,696482	0,678992	0,01226249	0,321008
phospho-p38 (mouse monoclonal 9.1)	0,97503	0,495699	0,069379	0,676996			
phospho-p38 (mouse monoclonal 9.1)	0,978686	0,510242	0,054682	0,6745			
phospho-p38 (mouse monoclonal 9.1)	0,977689	0,517616	0,059895	0,66799			
Phospho-p44/42 MAP Kinase	0,991377	0,588502	0,047094	0,601215	0,62161775	0,03304709	0,37838225
Phospho-p44/42 MAP Kinase	0,991087	0,613079	0,044718	0,589061			
Phospho-p44/42 MAP Kinase	0,996101	0,542847	0,060759	0,633995			
Phospho-p44/42 MAP Kinase	0,996167	0,52182	0,060948	0,6622			
Phospho-p70 S6 Kinase	0,951944	1.261.705	0,036758	0,395533	0,4011145	0,00610657	0,5988855
Phospho-p70 S6 Kinase	0,946569	1.265.476	0,032618	0,401747			
Phospho-p70 S6 Kinase	0,943348	1.270.341	0,047426	0,397755			
Phospho-p70 S6 Kinase	0,949729	1.219.100	0,04608	0,409423			
Phospho- SAPK/JNK	0,957483	0,026827	0,018664	0,997508	0,9566505	0,0499752	0,0433495
Phospho- SAPK/JNK	1.000.000	0,082061	0,006961	0,998788			
Phospho- SAPK/JNK	1.000.000	0,212901	0,033213	0,932525			
Phospho- SAPK/JNK	1.000.000	0,248385	0,062745	0,897781			
Phospho-Tyrosine	0,969802	2.448.546	0,030465	0,203238	0,20323325	0,04084044	0,79676675
Phospho-Tyrosine	0,991603	2.800.159	0,02925	0,176205			
Phospho-Tyrosine	0,971685	2.884.445	0,029412	0,17254			
Phospho-Tyrosine	0,995968	1.988.042	0,094095	0,26095			
p-Smasd1	0,99844	1.777.349	0,092079	0,28396	0,26628275	0,01613355	0,73371725
p-Smasd1	0,99805	1.789.978	0,080766	0,275773			
p-Smasd1	0,99668	1.961.879	0,064194	0,250544			
p-Smasd1	0,990441	1.937.117	0,067157	0,254854			
p-Smasd2/3	0,987504	2.230.721	0,025368	0,232901	0,2419325	0,008	0,7580675
p-Smasd2/3	0,993605	2.056.766	0,027858	0,252319			
p-Smasd2/3	0,994616	2.140.245	0,024463	0,242159			
p-Smasd2/3	0,98941	2.161.015	0,023396	0,240351			
Wisp2_129_158r(bi o)_1,25 µM, htag4(bio)_1,25 µM	0,873446	0,407053	0,08287	0,740143	0,7921175	0,03756124	0,2078825
Wisp2_129_158r(bi o)_1,25 µM, htag4(bio)_1,25 µM	0,991802	0,303788	0,100747	0,829944			
Wisp2_129_158r(bi o)_1,25 µM, htag4(bio)_1,25 µM	0,999755	0,343884	0,092269	0,798828			
Wisp2_129_158r(bi o)_1,25 µM, htag4(bio)_1,25 µM	0,999601	0,328842	0,152071	0,799555			
Wisp2_129_158r(bi o)_1,25 µM, htag4(bio)_1,25 µM	0,996832	0,401051	0,156956	0,747968	0,7371245	0,05699022	0,2628755
Wisp2_129_158r(bi o)_1,25 µM, htag4(bio)_1,25 µM	0,997541	0,367256	0,138848	0,769691			
Wisp2_129_158r(bi o)_1,25 µM, htag4(bio)_1,25 µM	0,943459	0,523054	0,146818	0,653681			

Wisp2_129_158r(bio)_1,25 µM, htag4(bio)_1,25 µM	0,997807	0,350494	0,13529	0,777158			
Wisp2_129_158r(bio)_1,25 µM, htag4(bio)_1,25 µM	0,953451	0,354918	0,155872	0,7679	0,70263625	0,06405179	0,29736375
Wisp2_129_158r(bio)_1,25 µM, htag4(bio)_1,25 µM	0,984225	0,404414	0,154466	0,729169			
Wisp2_129_158r(bio)_1,25 µM, htag4(bio)_1,25 µM	0,825302	0,63436	0,109225	0,61717			
Wisp2_129_158r(bio)_1,25 µM, htag4(bio)_1,25 µM	0,883151	0,478576	0,144601	0,696306			

Spot ID	Substance	Valid	Background	QSV	Sigma	Mean	mean-k-cyto-con
112	1:100 verd. biotin anti rabbit IGG	0	1.000.000	0,132254	0,031706	0,719467	0,72610625
113	1:100 verd. biotin anti rabbit IGG	0	1.000.000	0,136887	0,031602	0,712933	
114	1:100 verd. biotin anti rabbit IGG	0	0,993979	0,122861	0,064943	0,738309	
115	1:100 verd. biotin anti rabbit IGG	0	1.000.000	0,14789	0,036854	0,733716	
106	1:20 verd. biotin anti rabbit IGG	0	1.000.000	0,107473	0,033034	0,775122	0,7641495
107	1:20 verd. biotin anti rabbit IGG	0	1.000.000	0,104288	0,039178	0,772493	
110	1:20 verd. biotin anti rabbit IGG	0	1.000.000	0,16241	0,03619	0,753705	
111	1:20 verd. biotin anti rabbit IGG	0	1.000.000	0,115968	0,036746	0,755278	
78	1:5 verd. c-Myc	0	1.000.000	0,199298	0,040985	0,622969	0,6360385
79	1:5 verd. c-Myc	0	1.000.000	0,204877	0,038356	0,616271	
80	1:5 verd. c-Myc	0	1.000.000	0,186199	0,044133	0,640108	
81	1:5 verd. c-Myc	0	1.000.000	0,166905	0,043968	0,664806	
98	1:5 verd. p38 (mouse monoclonal 10.1)	0	1.000.000	0,161992	0,04371	0,718748	0,717692
99	1:5 verd. p38 (mouse monoclonal 10.1)	0	1.000.000	0,132957	0,04016	0,718726	
100	1:5 verd. p38 (mouse monoclonal 10.1)	0	1.000.000	0,137273	0,046234	0,709175	
101	1:5 verd. p38 (mouse monoclonal 10.1)	0	1.000.000	0,129048	0,042592	0,724119	
20	1:5 verd. Phospho Stat3 6E4	0	1.000.000	0,083647	0,045255	0,809156	0,82517525
21	1:5 verd. Phospho Stat3 6E4	0	1.000.000	0,080377	0,047519	0,818561	
22	1:5 verd. Phospho Stat3 6E4	0	1.000.000	0,073789	0,035442	0,833733	
23	1:5 verd. Phospho Stat3 6E4	0	1.000.000	0,07181	0,040936	0,839251	
10	1:5 verd. Phospho-Akt 4E2	0	0,999931	0,069696	0,050396	0,847746	0,855057
11	1:5 verd. Phospho-Akt 4E2	0	1.000.000	0,064819	0,037479	0,859555	
14	1:5 verd. Phospho-Akt 4E2	0	1.000.000	0,066349	0,038104	0,850004	
15	1:5 verd. Phospho-Akt 4E2	0	0,999931	0,064009	0,037195	0,862923	
88	1:5 verd. phospho-p38 (mouse monoclonal 9.1)	0	1.000.000	0,135141	0,032353	0,715108	0,72772925
89	1:5 verd. phospho-p38 (mouse monoclonal 9.1)	0	1.000.000	0,134593	0,036922	0,715512	
90	1:5 verd. phospho-p38 (mouse monoclonal 9.1)	0	1.000.000	0,132444	0,0335	0,725603	
91	1:5 verd. phospho-p38 (mouse monoclonal 9.1)	0	1.000.000	0,11113	0,038052	0,754694	
50	1:5 verd. Phospho-p44/42 MAP Kinase	0	1.000.000	0,106788	0,035996	0,762099	0,7671385
51	1:5 verd. Phospho-p44/42 MAP Kinase	0	1.000.000	0,090257	0,0382	0,792561	
52	1:5 verd. Phospho-p44/42 MAP Kinase	0	1.000.000	0,104888	0,035762	0,761605	
53	1:5 verd. Phospho-p44/42 MAP Kinase	0	1.000.000	0,110804	0,032608	0,752289	
2	1:5 verd. Phospho-p70 S6 Kinase	0	0,988097	0,101948	0,036669	0,771976	0,78226925
3	1:5 verd. Phospho-p70 S6 Kinase	0	0,999014	0,098517	0,033309	0,776329	
4	1:5 verd. Phospho-p70 S6 Kinase	0	0,999792	0,083487	0,038589	0,810956	

5	1:5 verd. Phospho-p70 S6 Kinase	0	1.000.000	0,105995	0,12524	0,769816	
40	1:5 verd. Phospho-SAPK/JNK	0	1.000.000	0,058644	0,053921	0,869281	0,878055
41	1:5 verd. Phospho-SAPK/JNK	0	1.000.000	0,059985	0,050689	0,865542	
42	1:5 verd. Phospho-SAPK/JNK	0	1.000.000	0,051287	0,040704	0,892855	
43	1:5 verd. Phospho-SAPK/JNK	0	1.000.000	0,053556	0,039155	0,884542	
30	1:5 verd. Phospho-Tyrosine	0	1.000.000	0,080334	0,042583	0,816446	0,8253
31	1:5 verd. Phospho-Tyrosine	0	1.000.000	0,087749	0,043411	0,801094	
32	1:5 verd. Phospho-Tyrosine	0	1.000.000	0,074606	0,043944	0,831038	
33	1:5 verd. Phospho-Tyrosine	0	1.000.000	0,066315	0,042427	0,852622	
58	1:5 verd. p-Smasd1	0	1.000.000	0,09844	0,031776	0,777468	0,77502025
59	1:5 verd. p-Smasd1	0	1.000.000	0,09295	0,031894	0,793695	
62	1:5 verd. p-Smasd1	0	1.000.000	0,105932	0,040119	0,763282	
63	1:5 verd. p-Smasd1	0	1.000.000	0,102999	0,036519	0,765636	
68	1:5 verd. p-Smasd2/3	0	1.000.000	0,17263	0,033315	0,653756	0,6512855
69	1:5 verd. p-Smasd2/3	0	1.000.000	0,183963	0,029749	0,646576	
70	1:5 verd. p-Smasd2/3	0	1.000.000	0,175455	0,031245	0,651104	
71	1:5 verd. p-Smasd2/3	0	1.000.000	0,191911	0,032168	0,653706	
116	2% Milchpulver	0	1.000.000	0,067579	0,033637	0,860137	0,86017675
117	2% Milchpulver	0	1.000.000	0,069382	0,030508	0,855754	
118	2% Milchpulver	0	1.000.000	0,067401	0,023866	0,856481	
119	2% Milchpulver	0	1.000.000	0,06445	0,028776	0,868335	
82	c-Myc	0	1.000.000	0,100911	0,056148	0,775201	0,758987
83	c-Myc	0	1.000.000	0,102703	0,056161	0,772181	
86	c-Myc	0	1.000.000	0,119775	0,059643	0,738513	
87	c-Myc	0	1.000.000	0,113685	0,051879	0,750053	
102	p38 (mouse monoclonal 10.1)	0	1.000.000	0,055817	0,032197	0,880924	0,88527875
103	p38 (mouse monoclonal 10.1)	0	1.000.000	0,055673	0,037855	0,885606	
104	p38 (mouse monoclonal 10.1)	0	1.000.000	0,059678	0,034436	0,875847	
105	p38 (mouse monoclonal 10.1)	0	1.000.000	0,05072	0,031042	0,898738	
26	Phospho Stat3 6E4	0	1.000.000	0,107867	0,083535	0,759998	0,73236525
27	Phospho Stat3 6E4	0	1.000.000	0,126795	0,098682	0,72491	
28	Phospho Stat3 6E4	0	1.000.000	0,137929	0,078782	0,70928	
29	Phospho Stat3 6E4	0	1.000.000	0,119664	0,077743	0,735273	
16	Phospho-Akt 4E2	0	0,99993	0,073018	0,044928	0,830645	0,82156125
17	Phospho-Akt 4E2	0	1.000.000	0,083907	0,03526	0,806323	
18	Phospho-Akt 4E2	0	1.000.000	0,077711	0,049513	0,821507	
19	Phospho-Akt 4E2	0	1.000.000	0,07481	0,036775	0,82777	
92	phospho-p38 (mouse monoclonal 9.1)	0	1.000.000	0,106853	0,043511	0,763773	0,75769275
93	phospho-p38 (mouse monoclonal 9.1)	0	1.000.000	0,114186	0,057452	0,74857	
94	phospho-p38 (mouse monoclonal 9.1)	0	1.000.000	0,106289	0,051199	0,764184	
95	phospho-p38 (mouse monoclonal 9.1)	0	1.000.000	0,112531	0,050836	0,754244	
54	Phospho-p44/42 MAP Kinase	0	1.000.000	0,075079	0,040533	0,825913	0,8419265
55	Phospho-p44/42 MAP Kinase	0	1.000.000	0,077567	0,040518	0,82069	
56	Phospho-p44/42 MAP Kinase	0	1.000.000	0,065921	0,037003	0,851816	
57	Phospho-p44/42 MAP Kinase	0	1.000.000	0,061014	0,041363	0,869287	
6	Phospho-p70 S6 Kinase	0	1.000.000	0,039284	0,04274	0,93233	0,91163925
7	Phospho-p70 S6 Kinase	0	1.000.000	0,048575	0,037189	0,902486	
8	Phospho-p70 S6 Kinase	0	1.000.000	0,050593	0,034886	0,895425	
9	Phospho-p70 S6 Kinase	0	0,999931	0,044527	0,036814	0,916316	
44	Phospho-SAPK/JNK	0	1.000.000	0,058683	0,049661	0,873498	0,865398
45	Phospho-SAPK/JNK	0	1.000.000	0,059368	0,039445	0,871298	
46	Phospho-SAPK/JNK	0	1.000.000	0,066051	0,041312	0,854228	
47	Phospho-SAPK/JNK	0	1.000.000	0,06265	0,042617	0,862568	
34	Phospho-Tyrosine	0	1.000.000	0,068858	0,040795	0,8456	0,83373775

35	Phospho-Tyrosine	0	1.000.000	0,065515	0,051164	0,854051	
38	Phospho-Tyrosine	0	1.000.000	0,073661	0,046527	0,829397	
39	Phospho-Tyrosine	0	1.000.000	0,08326	0,043709	0,805903	
64	p-Smasd1	0	1.000.000	0,270665	0,037615	0,545155	0,55973425
65	p-Smasd1	0	0,999931	0,260174	0,037256	0,558904	
66	p-Smasd1	0	0,99993	0,247514	0,038147	0,567374	
67	p-Smasd1	0	1.000.000	0,250738	0,033067	0,567504	
74	p-Smasd2/3	0	1.000.000	0,389303	0,044389	0,453497	0,44511475
75	p-Smasd2/3	0	1.000.000	0,399022	0,049981	0,446337	
76	p-Smasd2/3	0	1.000.000	0,40589	0,047047	0,441998	
77	p-Smasd2/3	0	1.000.000	0,412904	0,04029	0,438627	
1	Wisp2_129_158r(bio)_1,25 µM, htag4(bio)_1,25 µM	0	0,988282	0,011125	0,00258	0,999727	750000,25
12	Wisp2_129_158r(bio)_1,25 µM, htag4(bio)_1,25 µM	0	1.000.000	0,000182	0	1.000.000	
36	Wisp2_129_158r(bio)_1,25 µM, htag4(bio)_1,25 µM	0	1.000.000	0,000499	0	1.000.000	
48	Wisp2_129_158r(bio)_1,25 µM, htag4(bio)_1,25 µM	0	1.000.000	0,001278	0	1.000.000	
60	Wisp2_129_158r(bio)_1,25 µM, htag4(bio)_1,25 µM	0	1.000.000	0,000501	0,001431	0,999927	250000,75
72	Wisp2_129_158r(bio)_1,25 µM, htag4(bio)_1,25 µM	0	1.000.000	0,003142	0,001321	0,999934	
73	Wisp2_129_158r(bio)_1,25 µM, htag4(bio)_1,25 µM	0	1.000.000	0,000459	0,00012	0,999996	
84	Wisp2_129_158r(bio)_1,25 µM, htag4(bio)_1,25 µM	0	1.000.000	0,000078	0	1.000.000	
85	Wisp2_129_158r(bio)_1,25 µM, htag4(bio)_1,25 µM	0	1.000.000	0,000684	0	1.000.000	750000,25
96	Wisp2_129_158r(bio)_1,25 µM, htag4(bio)_1,25 µM	0	1.000.000	0,002465	0	1.000.000	
109	Wisp2_129_158r(bio)_1,25 µM, htag4(bio)_1,25 µM	0	1.000.000	0,004421	0	1.000.000	
120	Wisp2_129_158r(bio)_1,25 µM, htag4(bio)_1,25 µM	0	1.000.000	0,006043	0,001404	0,999922	

Substance	QSV	Sigma	Mean	mean-k-cyto-bmp	sd-k-cyto-bmp	1-k-cyto-bmp
1:100 verd. biotin anti rabbit IGG	0,075026	0,047302	0,802564	0,80414425	0,0112371	0,19585575
1:100 verd. biotin anti rabbit IGG	0,079171	0,040207	0,797292			
1:100 verd. biotin anti rabbit IGG	0,082319	0,042039	0,79624			
1:100 verd. biotin anti rabbit IGG	0,077494	0,040499	0,820481			
1:20 verd. biotin anti rabbit IGG	0,047121	0,042619	0,915672	0,89849725	0,02463519	0,10150275
1:20 verd. biotin anti rabbit IGG	0,070511	0,056947	0,862678			
1:20 verd. biotin anti rabbit IGG	0,030033	0,034777	0,913688			
1:20 verd. biotin anti rabbit IGG	0,036632	0,035223	0,901951			
1:5 verd. c-Myc	0,197462	0,04117	0,575572	0,57732125	0,02158108	0,42267875
1:5 verd. c-Myc	0,211504	0,033224	0,562669			
1:5 verd. c-Myc	0,215558	0,037233	0,562664			
1:5 verd. c-Myc	0,181772	0,044257	0,60838			
1:5 verd. p38 (mouse monoclonal 10.1)	0,044894	0,03614	0,851787	0,85584675	0,00798426	0,14415325
1:5 verd. p38 (mouse monoclonal 10.1)	0,049125	0,040559	0,846988			

1:5 verd. p38 (mouse monoclonal 10.1)	0,046084	0,0318	0,859772			
1:5 verd. p38 (mouse monoclonal 10.1)	0,046165	0,036514	0,86484			
1:5 verd. Phospho Stat3 6E4	0,03013	0,037982	0,885836	0,87647525	0,00853775	0,12352475
1:5 verd. Phospho Stat3 6E4	0,036161	0,035144	0,865879			
1:5 verd. Phospho Stat3 6E4	0,033289	0,029056	0,874092			
1:5 verd. Phospho Stat3 6E4	0,032505	0,030885	0,880094			
1:5 verd. Phospho-Akt 4E2	0,015369	0,023544	0,950435	0,955746	0,00521716	0,044254
1:5 verd. Phospho-Akt 4E2	0,013086	0,023058	0,962904			
1:5 verd. Phospho-Akt 4E2	0,012559	0,020393	0,955326			
1:5 verd. Phospho-Akt 4E2	0,013409	0,016059	0,954319			
1:5 verd. phospho-p38 (mouse monoclonal 9.1)	0,088723	0,041432	0,748478	0,7481115	0,01241655	0,2518885
1:5 verd. phospho-p38 (mouse monoclonal 9.1)	0,098484	0,040524	0,732895			
1:5 verd. phospho-p38 (mouse monoclonal 9.1)	0,093378	0,042193	0,747772			
1:5 verd. phospho-p38 (mouse monoclonal 9.1)	0,090136	0,04241	0,763301			
1:5 verd. Phospho-p44/42 MAP Kinase	0,032958	0,030938	0,873048	0,8688755	0,0120979	0,1311245
1:5 verd. Phospho-p44/42 MAP Kinase	0,039728	0,034899	0,851603			
1:5 verd. Phospho-p44/42 MAP Kinase	0,033638	0,036698	0,871094			
1:5 verd. Phospho-p44/42 MAP Kinase	0,031437	0,032247	0,879757			
1:5 verd. Phospho-p70 S6 Kinase	0,021159	0,021327	0,916953	0,913698	0,00385296	0,086302
1:5 verd. Phospho-p70 S6 Kinase	0,0221	0,025342	0,911121			
1:5 verd. Phospho-p70 S6 Kinase	0,021326	0,019114	0,917038			
1:5 verd. Phospho-p70 S6 Kinase	0,022718	0,020472	0,90968			
1:5 verd. Phospho-SAPK/JNK	0,017069	0,027985	0,935597	0,921542	0,01881096	0,078458
1:5 verd. Phospho-SAPK/JNK	0,027107	0,010755	0,894966			
1:5 verd. Phospho-SAPK/JNK	0,020847	0,018097	0,921504			
1:5 verd. Phospho-SAPK/JNK	0,018644	0,031622	0,934101			
1:5 verd. Phospho-Tyrosine	0,0182	0,025542	0,932562	0,93702525	0,00766344	0,06297475
1:5 verd. Phospho-Tyrosine	0,016038	0,014687	0,945658			
1:5 verd. Phospho-Tyrosine	0,019873	0,029342	0,928897			
1:5 verd. Phospho-Tyrosine	0,016958	0,019257	0,940984			
1:5 verd. p-Smasd1	0,089257	0,040926	0,754321	0,7534315	0,01164461	0,2465685
1:5 verd. p-Smasd1	0,086184	0,047034	0,768587			
1:5 verd. p-Smasd1	0,081245	0,041589	0,750287			
1:5 verd. p-Smasd1	0,085946	0,040739	0,740531			
1:5 verd. p-Smasd2/3	0,097572	0,040284	0,731962	0,7228305	0,01429447	0,2771695
1:5 verd. p-Smasd2/3	0,1016	0,052273	0,731852			
1:5 verd. p-Smasd2/3	0,121287	0,038149	0,701849			
1:5 verd. p-Smasd2/3	0,112095	0,037854	0,725659			
2% Milchpulver	0,024594	0,027126	0,979906	0,95031825	0,03973564	0,04968175
2% Milchpulver	0,054523	0,04059	0,901587			
2% Milchpulver	0,048115	0,040933	0,934362			
2% Milchpulver	0,03625	0,022086	0,985418			
c-Myc	0,062361	0,051094	0,837725	0,81898225	0,0182114	0,18101775
c-Myc	0,083086	0,055418	0,798124			
c-Myc	0,058188	0,077801	0,809882			
c-Myc	0,051249	0,050828	0,830198			
p38 (mouse monoclonal 10.1)	0,032228	0,041632	0,920025	0,90443	0,01402079	0,09557
p38 (mouse monoclonal 10.1)	0,044989	0,04177	0,88954			
p38 (mouse monoclonal 10.1)	0,045645	0,037553	0,896185			

p38 (mouse monoclonal 10.1)	0,044938	0,040258	0,91197			
Phospho Stat3 6E4	0,169533	0,031149	0,596734	0,59375625	0,00683154	0,40624375
Phospho Stat3 6E4	0,178717	0,050892	0,584826			
Phospho Stat3 6E4	0,173551	0,038407	0,592629			
Phospho Stat3 6E4	0,169855	0,036978	0,600836			
Phospho-Akt 4E2	0,03007	0,099702	0,889682	0,937451	0,03374369	0,062549
Phospho-Akt 4E2	0,016799	0,019349	0,938739			
Phospho-Akt 4E2	0,011451	0,017207	0,965797			
Phospho-Akt 4E2	0,013081	0,056794	0,955586			
Hospho-p38 (mouse monoclonal 9.1)	0,105468	0,050398	0,738153	0,73888825	0,0177871	0,26111175
Phospho-p38 (mouse monoclonal 9.1)	0,097007	0,053256	0,762778			
Phospho-p38 (mouse monoclonal 9.1)	0,123072	0,053244	0,719901			
phospho-p38 (mouse monoclonal 9.1)	0,118907	0,058185	0,734721			
Phospho-p44/42 MAP Kinase	0,019996	0,036256	0,923541	0,92343825	0,00971648	0,07656175
Phospho-p44/42 MAP Kinase	0,023479	0,031265	0,911893			
Phospho-p44/42 MAP Kinase	0,021612	0,03052	0,922661			
Phospho-p44/42 MAP Kinase	0,01884	0,028785	0,935658			
Phospho-p70 S6 Kinase	0,004942	0,036083	0,984722	0,987013	0,01724115	0,012987
Phospho-p70 S6 Kinase	0,000029	0	1			
Phospho-p70 S6 Kinase	0,000107	0,00235	0,99985			
Phospho-p70 S6 Kinase	0,009271	0,060968	0,96349			
Phospho-SAPK/JNK	0,029855	0,044573	0,89087	0,85879425	0,02236013	0,14120575
Phospho-SAPK/JNK	0,042975	0,042458	0,851802			
Phospho-SAPK/JNK	0,050368	0,046719	0,838918			
Phospho-SAPK/JNK	0,04739	0,057298	0,853587			
Phospho-Tyrosine	0,064429	0,053717	0,794286	0,76183575	0,02204465	0,23816425
Phospho-Tyrosine	0,085373	0,058036	0,753918			
Phospho-Tyrosine	0,08031	0,049828	0,745027			
Phospho-Tyrosine	0,078417	0,057894	0,754112			
p-Smasd1	0,36194	0,042265	0,426577	0,436465	0,00747244	0,563535
p-Smasd1	0,350107	0,039091	0,436096			
p-Smasd1	0,347428	0,036414	0,438678			
p-Smasd1	0,337814	0,03905	0,444509			
p-Smasd2/3	0,387358	0,041287	0,407883	0,425757	0,0190116	0,574243
p-Smasd2/3	0,358008	0,043277	0,426641			
p-Smasd2/3	0,37822	0,035649	0,416649			
p-Smasd2/3	0,327503	0,049132	0,451855			
Wisp2_129_158r(bio)_1,25 µM, htag4(bio)_1,25 µM	0,085689	0,092183	0,781176	0,93627675	0,10472276	0,06372325
Wisp2_129_158r(bio)_1,25 µM, htag4(bio)_1,25 µM	0,010376	0,031243	0,964519			
Wisp2_129_158r(bio)_1,25 µM, htag4(bio)_1,25 µM	0,000267	0,005454	0,999419			
Wisp2_129_158r(bio)_1,25 µM, htag4(bio)_1,25 µM	0,000159	0,000239	0,999993			
Wisp2_129_158r(bio)_1,25 µM, htag4(bio)_1,25 µM	0,000189	0	1.000.000	250000,749	499999,5	-249999,749
Wisp2_129_158r(bio)_1,25 µM, htag4(bio)_1,25 µM	0,000838	0,000779	0,999964			
Wisp2_129_158r(bio)_1,25 µM, htag4(bio)_1,25 µM	0,00008	0,001448	0,999894			
Wisp2_129_158r(bio)_1,25 µM, htag4(bio)_1,25 µM	0,005554	0,013867	0,997721			
Wisp2_129_158r(bio)_1,25 µM, htag4(bio)_1,25 µM	0,019467	0,028646	0,926275	500000,455	577349,744	-499999,455
Wisp2_129_158r(bio)_1,25 µM, htag4(bio)_1,25 µM	0,007406	0	1.000.000			
Wisp2_129_158r(bio)_1,25 µM, htag4(bio)_1,25 µM	0,037702	0,06869	0,893931			

Wisp2_129_158r(bio)_1,25 µM, htag4(bio)_1,25 µM	0,016274	0	1.000.000			
--	----------	---	-----------	--	--	--

k-nu-con	Substance	Valid	Background	QSV	Sigma	Mean
1	Wisp2_129_158r(bio)_1,25 µM, htag4(bio)_1,25 µM	0	0,965675	0,095774	0,036426	0,879483
2	1:5 verd. Phospho-p70 S6 Kinase	0	0,989535	0,194866	0,028543	0,770745
3	1:5 verd. Phospho-p70 S6 Kinase	0	0,999574	0,161068	0,033969	0,79251
4	1:5 verd. Phospho-p70 S6 Kinase	0	0,999686	0,131711	0,026282	0,815641
5	1:5 verd. Phospho-p70 S6 Kinase	0	0,999866	0,120469	0,028898	0,824973
6	Phospho-p70 S6 Kinase	0	0,999865	0,091264	0,036831	0,869682
7	Phospho-p70 S6 Kinase	0	0,999821	0,043279	0,036803	0,916118
8	Phospho-p70 S6 Kinase	0	0,995697	0,098169	0,025459	0,866199
9	Phospho-p70 S6 Kinase	0	0,996056	0,051679	0,025688	0,903309
10	1:5 verd. Phospho-Akt 4E2	0	0,996658	0,089786	0,033465	0,861315
11	1:5 verd. Phospho-Akt 4E2	0	0,996101	0,076295	0,037927	0,870837
12	Wisp2_129_158r(bio)_1,25 µM, htag4(bio)_1,25 µM	0	0,984742	0,07885	0,064834	0,877906
14	1:5 verd. Phospho-Akt 4E2	0	0,995833	0,060852	0,030309	0,894854
15	1:5 verd. Phospho-Akt 4E2	0	0,999888	0,060429	0,044171	0,892914
16	Phospho-Akt 4E2	0	1.000.000	0,141198	0,046255	0,810632
17	Phospho-Akt 4E2	0	1.000.000	0,107183	0,03283	0,850632
18	Phospho-Akt 4E2	0	0,999978	0,128865	0,058135	0,820188
19	Phospho-Akt 4E2	0	0,999978	0,107267	0,033757	0,841823
20	1:5 verd. Phospho Stat3 6E4	0	0,995922	0,096514	0,037235	0,85405
21	1:5 verd. Phospho Stat3 6E4	0	0,998476	0,102178	0,035797	0,85114
22	1:5 verd. Phospho Stat3 6E4	0	1.000.000	0,062148	0,041322	0,888954
23	1:5 verd. Phospho Stat3 6E4	0	0,999978	0,071726	0,035334	0,876462
26	Phospho Stat3 6E4	0	1.000.000	0,20321	0,047164	0,762778
27	Phospho Stat3 6E4	0	0,998355	0,184092	0,046063	0,77704
28	Phospho Stat3 6E4	0	0,998529	0,164392	0,033175	0,797208
29	Phospho Stat3 6E4	0	1.000.000	0,186538	0,045313	0,77328
30	1:5 verd. Phospho-Tyrosine	0	1.000.000	0,048276	0,033531	0,903576
31	1:5 verd. Phospho-Tyrosine	0	1.000.000	0,072239	0,036177	0,879635
32	1:5 verd. Phospho-Tyrosine	0	1.000.000	0,063796	0,026406	0,885103
33	1:5 verd. Phospho-Tyrosine	0	1.000.000	0,066905	0,029163	0,887464
34	Phospho-Tyrosine	0	0,999933	0,278951	0,048708	0,70568
35	Phospho-Tyrosine	0	0,999933	0,264672	0,064188	0,722805
36	Wisp2_129_158r(bio)_1,25 µM, htag4(bio)_1,25 µM	0	0,992788	0,262343	0,080964	0,707563
38	Phospho-Tyrosine	0	0,996056	0,296134	0,054147	0,70132
39	Phospho-Tyrosine	0	0,995588	0,276748	0,050055	0,719512
40	1:5 verd. Phospho-SAPK/JNK	0	0,999978	0,085002	0,037387	0,867559
41	1:5 verd. Phospho-SAPK/JNK	0	0,999977	0,087872	0,045955	0,857315
42	1:5 verd. Phospho-SAPK/JNK	0	1.000.000	0,069609	0,033814	0,87852
43	1:5 verd. Phospho-SAPK/JNK	0	1.000.000	0,072281	0,034369	0,876748
44	Phospho-SAPK/JNK	0	0,998185	0,118126	0,037148	0,830651
45	Phospho-SAPK/JNK	0	1.000.000	0,133068	0,04811	0,824042
46	Phospho-SAPK/JNK	0	1.000.000	0,131241	0,049526	0,819203
47	Phospho-SAPK/JNK	0	0,999866	0,120894	0,040024	0,830328
48	Wisp2_129_158r(bio)_1,25 µM, htag4(bio)_1,25 µM	0	0,99888	0,062026	0,038526	0,904293
50	1:5 verd. Phospho-p44/42 MAP Kinase	0	0,9881	0,192776	0,023412	0,777609
51	1:5 verd. Phospho-p44/42 MAP Kinase	0	0,998588	0,165126	0,024042	0,795068

52	1:5 verd. Phospho-p44/42 MAP Kinase	0	1.000.000	0,184942	0,03342	0,784586
53	1:5 verd. Phospho-p44/42 MAP Kinase	0	1.000.000	0,087114	0,019816	0,860644
54	Phospho-p44/42 MAP Kinase	0	1.000.000	0,078076	0,028977	0,866999
55	Phospho-p44/42 MAP Kinase	0	1.000.000	0,096116	0,048182	0,848422
56	Phospho-p44/42 MAP Kinase	0	0,998185	0,090117	0,028088	0,855856
57	Phospho-p44/42 MAP Kinase	0	0,999617	0,090049	0,040034	0,860931
58	1:5 verd. p-Smasd1	0	0,999597	0,376209	0,035769	0,656995
59	1:5 verd. p-Smasd1	0	0,999532	0,377456	0,050451	0,651446
60	Wisp2_129_158r(bio)_1,25 µM, htag4(bio)_1,25 µM	0	0,998723	0,00222	0,022557	0,995828
62	1:5 verd. p-Smasd1	0	0,996683	0,431257	0,031777	0,629456
63	1:5 verd. p-Smasd1	0	0,999822	0,380165	0,034723	0,65568
64	p-Smasd1	0	1.000.000	1.070.371	0,031798	0,427419
65	p-Smasd1	0	0,99888	0,973937	0,023435	0,450753
66	p-Smasd1	0	0,998873	0,921862	0,02125	0,459726
67	p-Smasd1	0	1.000.000	0,956332	0,024243	0,450116
68	1:5 verd. p-Smasd2/3	0	1.000.000	0,398894	0,031324	0,641533
69	1:5 verd. p-Smasd2/3	0	1.000.000	0,481106	0,03282	0,60097
70	1:5 verd. p-Smasd2/3	0	1.000.000	0,537444	0,055563	0,569726
71	1:5 verd. p-Smasd2/3	0	0,999549	0,545812	0,042663	0,567564
72	Wisp2_129_158r(bio)_1,25 µM, htag4(bio)_1,25 µM	0	1.000.000	0,027987	0,037984	0,944038
73	Wisp2_129_158r(bio)_1,25 µM, htag4(bio)_1,25 µM	0	0,985681	0,063284	0,038021	0,890196
74	p-Smasd2/3	0	0,999059	1.662.937	0,035631	0,326019
75	p-Smasd2/3	0	0,999955	1.555.835	0,037369	0,338888
76	p-Smasd2/3	0	0,999978	1.496.536	0,043581	0,348851
77	p-Smasd2/3	0	0,999978	1.366.563	0,034923	0,370413
78	1:5 verd. c-Myc	0	0,999978	0,667168	0,037603	0,529011
79	1:5 verd. c-Myc	0	0,999776	0,627893	0,033269	0,545122
80	1:5 verd. c-Myc	0	0,999865	0,615928	0,058821	0,540388
81	1:5 verd. c-Myc	0	1.000.000	0,67229	0,045122	0,519432
82	c-Myc	0	1.000.000	0,203893	0,057456	0,752884
83	c-Myc	0	0,997602	0,218818	0,059298	0,742287
84	Wisp2_129_158r(bio)_1,25 µM, htag4(bio)_1,25 µM	0	0,998073	0,048099	0,036304	0,905246
85	Wisp2_129_158r(bio)_1,25 µM, htag4(bio)_1,25 µM	0	0,981266	0,052769	0,025672	0,918071
86	c-Myc	0	0,999552	0,244044	0,047083	0,729086
87	c-Myc	0	0,999843	0,248489	0,043759	0,727931
88	1:5 verd. phospho-p38 (mouse monoclonal 9.1)	0	1.000.000	0,202083	0,046031	0,757603
89	1:5 verd. phospho-p38 (mouse monoclonal 9.1)	0	0,999527	0,084951	0,04706	0,859336
90	1:5 verd. phospho-p38 (mouse monoclonal 9.1)	0	0,999527	0,221067	0,027325	0,741699
91	1:5 verd. phospho-p38 (mouse monoclonal 9.1)	0	0,999777	0,259664	0,041676	0,710269
92	phospho-p38 (mouse monoclonal 9.1)	0	0,999866	0,464326	0,040566	0,600627
93	phospho-p38 (mouse monoclonal 9.1)	0	1.000.000	0,487552	0,045276	0,59248
94	phospho-p38 (mouse monoclonal 9.1)	0	1.000.000	0,478859	0,048764	0,598693
95	phospho-p38 (mouse monoclonal 9.1)	0	0,997138	0,460043	0,044246	0,60401
96	Wisp2_129_158r(bio)_1,25 µM, htag4(bio)_1,25 µM	0	0,998953	0,090628	0,072884	0,865509
98	1:5 verd. p38 (mouse monoclonal 10.1)	0	0,959171	0,156632	0,035912	0,798006
99	1:5 verd. p38 (mouse monoclonal 10.1)	0	0,985008	0,233185	0,035064	0,738334
100	1:5 verd. p38 (mouse monoclonal 10.1)	0	0,996326	0,188337	0,037271	0,773318
101	1:5 verd. p38 (mouse monoclonal 10.1)	0	0,999731	0,140491	0,034871	0,809514
102	p38 (mouse monoclonal 10.1)	0	0,999889	0,112506	0,040782	0,833272
103	p38 (mouse monoclonal 10.1)	0	1.000.000	0,122404	0,037507	0,819798
104	p38 (mouse monoclonal 10.1)	0	0,994456	0,15438	0,062156	0,791157
105	p38 (mouse monoclonal 10.1)	0	0,994375	0,181924	0,037152	0,771987
106	1:20 verd. biotin anti rabbit IGG	0	0,999529	0,190669	0,047954	0,767773
107	1:20 verd. biotin anti rabbit IGG	0	0,997894	0,20797	0,051793	0,754508

109	Wisp2_129_158r(bio)_1,25 µM, htag4(bio)_1,25 µM	0	0,837737	0,211574	0,022305	0,807197
110	1:20 verd. biotin anti rabbit IGG	0	0,882398	0,300576	0,029789	0,706623
111	1:20 verd. biotin anti rabbit IGG	0	0,927585	0,299866	0,026201	0,701375
112	1:100 verd. biotin anti rabbit IGG	0	0,972952	0,376664	0,025672	0,656877
113	1:100 verd. biotin anti rabbit IGG	0	0,998151	0,365525	0,052745	0,649034
114	1:100 verd. biotin anti rabbit IGG	0	0,998648	0,371741	0,045507	0,643631
115	1:100 verd. biotin anti rabbit IGG	0	1.000.000	0,345177	0,047202	0,660827
116	2% Milchpulver	0	0,997928	0,049593	0,036016	0,906703
117	2% Milchpulver	0	0,993681	0,069823	0,042613	0,883587
118	2% Milchpulver	0	0,997356	0,086486	0,039648	0,867566
119	2% Milchpulver	0	0,991216	0,086171	0,034658	0,879115
120	Wisp2_129_158r(bio)_1,25 µM, htag4(bio)_1,25 µM	0	0,973563	0,159964	0,035451	0,810599

k-nu-bmp2	Substance	Valid	Background	QSV	Sigma	Mean
1	Wisp2_129_158r(bio)_1,25 µM, htag4(bio)_1,25 µM	0	1.000.000	0,033192	0,045276	0,918869
2	1:5 verd. Phospho-p70 S6 Kinase	0	0,989945	0,035994	0,0328	0,892598
3	1:5 verd. Phospho-p70 S6 Kinase	0	0,993313	0,039971	0,031828	0,870408
4	1:5 verd. Phospho-p70 S6 Kinase	0	0,996078	0,031928	0,027822	0,897128
5	1:5 verd. Phospho-p70 S6 Kinase	0	0,996808	0,028471	0,035278	0,907029
6	Phospho-p70 S6 Kinase	0	0,997264	0,012178	0,012119	0,994827
7	Phospho-p70 S6 Kinase	0	0,992522	0,014748	0,024078	0,98128
8	Phospho-p70 S6 Kinase	0	0,999772	0,016326	0,028031	0,975933
9	Phospho-p70 S6 Kinase	0	0,999819	0,020701	0,040927	0,950339
10	1:5 verd. Phospho-Akt 4E2	0	1.000.000	0,021489	0,030286	0,947013
11	1:5 verd. Phospho-Akt 4E2	0	1.000.000	0,025543	0,034548	0,927588
12	Wisp2_129_158r(bio)_1,25 µM, htag4(bio)_1,25 µM	0	1.000.000	0,025202	0,019435	0,949338
14	1:5 verd. Phospho-Akt 4E2	0	0,99254	0,030045	0,041333	0,912183
15	1:5 verd. Phospho-Akt 4E2	0	0,995873	0,018876	0,03047	0,960946
16	Phospho-Akt 4E2	0	0,999289	0,019538	0,036772	0,952516
17	Phospho-Akt 4E2	0	0,999772	0,020001	0,038586	0,94995
18	Phospho-Akt 4E2	0	0,997053	0,023076	0,022329	0,937053
19	Phospho-Akt 4E2	0	0,992833	0,020728	0,034992	0,945205
20	1:5 verd. Phospho Stat3 6E4	0	1.000.000	0,025352	0,039749	0,924156
21	1:5 verd. Phospho Stat3 6E4	0	0,999818	0,028323	0,043314	0,910572
22	1:5 verd. Phospho Stat3 6E4	0	1.000.000	0,026478	0,029531	0,930586
23	1:5 verd. Phospho Stat3 6E4	0	1.000.000	0,027695	0,037493	0,937787
26	Phospho Stat3 6E4	0	1.000.000	0,049189	0,055305	0,829654
27	Phospho Stat3 6E4	0	1.000.000	0,045965	0,060594	0,837443
28	Phospho Stat3 6E4	0	1.000.000	0,043082	0,045478	0,846176
29	Phospho Stat3 6E4	0	1.000.000	0,041857	0,048712	0,847306
30	1:5 verd. Phospho-Tyrosine	0	1.000.000	0,020154	0,026519	0,9517
31	1:5 verd. Phospho-Tyrosine	0	1.000.000	0,022931	0,032947	0,938026
32	1:5 verd. Phospho-Tyrosine	0	1.000.000	0,020077	0,021234	0,965466
33	1:5 verd. Phospho-Tyrosine	0	1.000.000	0,023733	0,033449	0,952343
34	Phospho-Tyrosine	0	0,999234	0,068854	0,072168	0,771133
35	Phospho-Tyrosine	0	0,999225	0,078495	0,053391	0,746514
36	Wisp2_129_158r(bio)_1,25 µM, htag4(bio)_1,25 µM	0	0,99429	0,031714	0,020577	0,954425
38	Phospho-Tyrosine	0	0,999658	0,075331	0,058223	0,756098
39	Phospho-Tyrosine	0	0,99966	0,078757	0,055781	0,744617

40	1:5 verd. Phospho-SAPK/JNK	0	1.000.000	0,024393	0,039058	0,926622
41	1:5 verd. Phospho-SAPK/JNK	0	1.000.000	0,029486	0,043288	0,902812
42	1:5 verd. Phospho-SAPK/JNK	0	0,999932	0,02634	0,031367	0,923267
43	1:5 verd. Phospho-SAPK/JNK	0	0,994514	0,026901	0,043579	0,930293
44	Phospho-SAPK/JNK	0	0,994974	0,036697	0,040116	0,87842
45	Phospho-SAPK/JNK	0	0,998141	0,042665	0,057827	0,862464
46	Phospho-SAPK/JNK	0	0,99617	0,048302	0,05493	0,847271
47	Phospho-SAPK/JNK	0	0,998039	0,044979	0,046954	0,870275
48	Wis2_129_158r(bio)_1,25 µM, htag4(bio)_1,25 µM	0	0,992089	0,035912	0,020165	0,943231
50	1:5 verd. Phospho-p44/42 MAP Kinase	0	0,989107	0,039537	0,034564	0,86305
51	1:5 verd. Phospho-p44/42 MAP Kinase	0	1.000.000	0,040053	0,03213	0,857789
52	1:5 verd. Phospho-p44/42 MAP Kinase	0	1.000.000	0,03952	0,033029	0,861598
53	1:5 verd. Phospho-p44/42 MAP Kinase	0	1.000.000	0,034987	0,028911	0,880824
54	Phospho-p44/42 MAP Kinase	0	0,998427	0,041177	0,040381	0,857751
55	Phospho-p44/42 MAP Kinase	0	0,996694	0,048565	0,038215	0,83373
56	Phospho-p44/42 MAP Kinase	0	0,99316	0,051373	0,046716	0,829825
57	Phospho-p44/42 MAP Kinase	0	0,994922	0,051075	0,045056	0,836785
58	1:5 verd. p-Smasd1	0	0,999887	0,195648	0,045321	0,549156
59	1:5 verd. p-Smasd1	0	0,999184	0,191665	0,05323	0,5523
60	Wis2_129_158r(bio)_1,25 µM, htag4(bio)_1,25 µM	0	0,99388	0,042822	0,047632	0,927612
62	1:5 verd. p-Smasd1	0	1.000.000	0,211062	0,048489	0,532379
63	1:5 verd. p-Smasd1	0	1.000.000	0,213422	0,047151	0,528441
64	p-Smasd1	0	0,931543	0,592337	0,033878	0,306177
65	p-Smasd1	0	0,880692	0,562753	0,032643	0,316622
66	p-Smasd1	0	0,910328	0,541884	0,033636	0,322916
67	p-Smasd1	0	0,955933	0,54772	0,031649	0,32067
68	1:5 verd. p-Smasd2/3	0	0,958846	0,166756	0,049486	0,585469
69	1:5 verd. p-Smasd2/3	0	0,961924	0,189203	0,039754	0,556406
70	1:5 verd. p-Smasd2/3	0	0,955326	0,192322	0,048073	0,549252
71	1:5 verd. p-Smasd2/3	0	0,95187	0,183307	0,042096	0,559188
72	Wis2_129_158r(bio)_1,25 µM, htag4(bio)_1,25 µM	0	0,979485	0,049904	0,036634	0,903551
73	Wis2_129_158r(bio)_1,25 µM, htag4(bio)_1,25 µM	0	0,959923	0,017942	0,010452	0,997947
74	p-Smasd2/3	0	0,959371	0,750033	0,048739	0,259152
75	p-Smasd2/3	0	0,999681	0,811915	0,037367	0,245369
76	p-Smasd2/3	0	0,99984	0,791279	0,038466	0,250451
77	p-Smasd2/3	0	1.000.000	0,769245	0,040147	0,255006
78	1:5 verd. c-Myc	0	0,99991	0,393578	0,038484	0,389855
79	1:5 verd. c-Myc	0	0,999683	0,4453	0,032023	0,363082
80	1:5 verd. c-Myc	0	0,997019	0,461601	0,029911	0,353701
81	1:5 verd. c-Myc	0	0,996147	0,403977	0,043207	0,380326
82	c-Myc	0	0,996532	0,082666	0,041035	0,751261
83	c-Myc	0	0,985486	0,089735	0,041518	0,729583
84	Wis2_129_158r(bio)_1,25 µM, htag4(bio)_1,25 µM	0	0,955457	0,055883	0,022998	0,898168
85	Wis2_129_158r(bio)_1,25 µM, htag4(bio)_1,25 µM	0	1.000.000	0,020692	0,003246	0,99951
86	c-Myc	0	1.000.000	0,06791	0,053312	0,779746
87	c-Myc	0	0,992134	0,070836	0,040858	0,77192
88	1:5 verd. phospho-p38 (mouse monoclonal 9.1)	0	0,992088	0,091941	0,049162	0,720781
89	1:5 verd. phospho-p38 (mouse monoclonal 9.1)	0	1.000.000	0,098674	0,040951	0,702739
90	1:5 verd. phospho-p38 (mouse monoclonal 9.1)	0	0,999863	0,099816	0,04166	0,704563
91	1:5 verd. phospho-p38 (mouse monoclonal 9.1)	0	0,985288	0,088143	0,04176	0,727174
92	phospho-p38 (mouse monoclonal 9.1)	0	0,978363	0,159678	0,045047	0,588976
93	phospho-p38 (mouse monoclonal 9.1)	0	0,97771	0,270824	0,090716	0,465926
94	phospho-p38 (mouse monoclonal 9.1)	0	0,965726	0,168757	0,052797	0,575882
95	phospho-p38 (mouse monoclonal 9.1)	0	0,949612	0,1562	0,052175	0,59303

96	Wisp2_129_158r(bio)_1,25 µM, htag4(bio)_1,25 µM	0	0,917349	0,067416	0,022122	0,876374
98	1:5 verd. p38 (mouse monoclonal 10.1)	0	0,997036	0,052082	0,041966	0,833272
99	1:5 verd. p38 (mouse monoclonal 10.1)	0	0,999404	0,054757	0,036756	0,829417
100	1:5 verd. p38 (mouse monoclonal 10.1)	0	0,999818	0,055893	0,04221	0,826473
101	1:5 verd. p38 (mouse monoclonal 10.1)	0	0,999048	0,055233	0,045608	0,832294
102	p38 (mouse monoclonal 10.1)	0	0,999098	0,051762	0,031048	0,852917
103	p38 (mouse monoclonal 10.1)	0	0,996945	0,055494	0,039243	0,841675
104	p38 (mouse monoclonal 10.1)	0	0,984956	0,061661	0,038407	0,828109
105	p38 (mouse monoclonal 10.1)	0	0,970109	0,067175	0,038578	0,816392
106	1:20 verd. biotin anti rabbit IGG	0	0,945121	0,084959	0,043317	0,759397
107	1:20 verd. biotin anti rabbit IGG	0	0,914474	0,090284	0,039037	0,755387
109	Wisp2_129_158r(bio)_1,25 µM, htag4(bio)_1,25 µM	0	0,999339	0,027704	0,006264	0,998936
110	1:20 verd. biotin anti rabbit IGG	0	0,998385	0,056274	0,046865	0,817836
111	1:20 verd. biotin anti rabbit IGG	0	0,997348	0,058916	0,045095	0,807872
112	1:100 verd. biotin anti rabbit IGG	0	0,997724	0,093257	0,054097	0,710381
113	1:100 verd. biotin anti rabbit IGG	0	0,994242	0,087625	0,055573	0,725153
114	1:100 verd. biotin anti rabbit IGG	0	0,99046	0,097779	0,043869	0,701116
115	1:100 verd. biotin anti rabbit IGG	0	0,977388	0,093	0,0487	0,716346
116	2% Milchpulver	0	0,953327	0,057491	0,032666	0,903339
117	2% Milchpulver	0	0,930336	0,066474	0,03147	0,875633
118	2% Milchpulver	0	0,902981	0,076635	0,026875	0,847851
119	2% Milchpulver	0	0,87534	0,088302	0,028278	0,824548
120	Wisp2_129_158r(bio)_1,25 µM, htag4(bio)_1,25 µM	0	0,837939	0,106843	0,03679	0,756541

Substance	MCF-7-cyto-control	MCF-7-cyto-100ng/ml bmp2	median-m-cyto-con	median-m-cyto-bmp2	Median-m-nu-con	Median-	mcf-7-total-con	mcf7-total-bmp2
1:100 verd. biotin anti rabbit IGG	0,356185	0,28564925	0,756150349	0,880326583	1	1,053269232	1,75615035	1,93359581
1:20 verd. biotin anti rabbit IGG	0,37518625	0,2897155	0,796488381	0,892858133	0,98884265	0,991542023	1,78533103	1,88440016
1:5 verd. c-Myc	0,500286	0,365201	1,062064471	1,12549271	1,45150125	1,082945924	2,51356572	2,20843863
1:5 verd. p38 (mouse monoclonal 10.1)	0,2788945	0,16315875	0,592069216	0,502829904	0,31923109	0,800603385	0,9113003	1,30343329
1:5 verd. Phospho Stat3 6E4	0,363751	0,324481	0,772212321	1	0,88089525	0,936857664	1,65310757	1,93685766
1:5 verd. Phospho-Akt 4E2	0,3969365	0,28448	0,842662305	0,876723136	0,88371064	1	1,72637295	1,87672314
1:5 verd. phospho-p38 (mouse monoclonal 9.1)	0,37906625	0,17590225	0,80472529	0,54210339	1,03727485	0,996193165	1,84200014	1,53829656
1:5 verd. Phospho-p44/42 MAP Kinase	0,330322	0,1093885	0,701245408	0,337118352	0,92643378	0,830896728	1,62767918	1,16801508
1:5 verd. Phospho-p70 S6 Kinase	0,49713625	0,2764325	1,05537782	0,851921992	1,34115289	1,092820147	2,39653071	1,94474214
1:5 verd. Phospho-SAPK/JNK	0,4710505	0,26652075	1	0,82137552	1,23438812	1,038302339	2,23438812	1,85967786
1:5 verd. Phospho-Tyrosine	0,33456475	0,11003925	0,710252404	0,339123862	0,83535085	0,759382113	1,54560326	1,09850598

1:5 verd. p-Smasd1	0,61418675	0,50462925	1,30386604	1,555188902	1,22825238	1,109875452	2,53211842	2,66506435
1:5 verd. p-Smasd2/3	0,6505125	0,541387	1,380982506	1,668470573	1,60739939	1,109045303	2,98838189	2,77751588
2% Milchpulver	0,21031925	0,12924725	0,446489814	0,398319932	0,47981959	0,600365817	0,9263094	0,99868575
c-Myc	0,290458	0,16601175	0,616617539	0,511622406	1,00617439	1,159803596	1,62279193	1,671426
p38 (mouse monoclonal 10.1)	0,18630125	0,207853	0,39550165	0,640570634	0,42529764	0,202073732	0,82079929	0,84264437
Phospho Stat3 6E4	0,67481425	0,71031375	1,432573047	2,189076556	1,12962504	1,109388093	2,56219809	3,29846465
Phospho-Akt 4E2	0,56757175	0,41700575	1,204906374	1,285146896	1,09430786	1,020227978	2,29921423	2,30537487
phospho-p38 (mouse monoclonal 9.1)	0,36006075	0,398921	0,764378235	1,229412508	0,76107026	0,478427875	1,5254485	1,70784038
Phospho-p44/42 MAP Kinase	0,4913715	0,562597	1,043139748	1,733836496	0,68081393	0,563938019	1,72395368	2,29777451
Phospho-p70 S6 Kinase	0,4771865	0,45811225	1,013026204	1,411830739	0,85721933	0,892574381	1,87024553	2,30440512
Phospho-SAPK/JNK	0,47398725	0,4922575	1,00623447	1,517061091	0,5400922	0,064607764	1,54632667	1,58166886
Phospho-Tyrosine	0,71734825	0,6924385	1,522869098	2,133987814	1,22878669	1,187495086	2,75165579	3,3214829
p-Smasd1	0,48868625	0,3579075	1,037439192	1,103015277	1,22989641	1,093526593	2,2673356	2,19654187
p-Smasd2/3	0,56669075	0,50598325	1,203036086	1,559361719	1,49995009	1,129818019	2,70298618	2,68917974

1000ng/ml-1	#DIV/0!					
0	1007000	1042000	944000	1035000		16
10	979600	967000	996800	975000		16
30	564200	538000	585000	569600		16
160	99333,3333	109000	100000	89000		16
285	189000	182000	188000	197000		16
1450	459666,667	430000	476000	473000		16
	#DIV/0!					
	#DIV/0!					
1000ng/ml-2	#DIV/0!					17
0	464000	472800	427200	492000		17
10	481666,667	72000	664000	709000		17
30	479933,333	451200	481600	507000		
160	477200	455000	491000	485600		
285	313600	332800	301600	306400		
1450	435000	428000	429000	448000		
	#DIV/0!					18
	#DIV/0!					18
1000ng/ml-3	#DIV/0!					18
0	452000	463200	471200	421600		18
10	1059000	1058000	1073000	1046000		18
30	382666,667	368000	372800	407200		18
160	502000	487000	501000	518000		18
285	168400	173600	158000	173600		
1450	396333,333	388000	387000	414000		
	#DIV/0!					19

160	445666,667	475000	436000	426000	20
285	459333,333	465000	431000	482000	
1450	820000	808000	828000	824000	
	#DIV/0!				21
1500ng/ml-3	#DIV/0!				21
0	841866,667	892800	838400	794400	21
10	471666,667	479000	468000	468000	21
30	1280000	1270000	1290000	1280000	21
160	380666,667	404000	342000	396000	
285	356666,667	381000	370000	319000	
1450	464666,667	483000	463000	448000	
	#DIV/0!				
2000ng/ml-1	#DIV/0!				
0	817866,667	800000	846400	807200	22
10	122866,667	133600	116000	119000	22
30	489600	453000	516800	499000	22
160	334666,667	352000	320000	332000	22
285	1313333,33	1360000	1280000	1300000	22
1450	445600	436800	450000	450000	22
	#DIV/0!				
2000ng/ml-2	#DIV/0!				
0	1312666,67	1298000	1282000	1358000	23
10	792266,667	796000	796000	784800	23
30	812533,333	836800	824800	776000	23
160	360000	384000	348000	348000	23
285	2247666,67	2359000	2250000	2134000	23
1450	341733,333	354400	332800	338000	23

experiment	average				1	
control 1					1	
	0	267200	258400	269600	273600	1
	160	451133,333	446400	483000	424000	1
	285	403066,667	391200	420000	398000	1
	1450	407000	405000	420000	396000	1
experiment control 2						2
	0	355733,333	355200	349600	362400	2
	30	392800	534400	484000	160000	2
	160	495000	476000	487000	522000	2
	285	521000	539000	513000	511000	2
	1450	412333,333	411000	402000	424000	
experiment control 3						3
	0	314133,333	308000	307200	327200	3
	160	1053666,67	1019000	1102000	1040000	3
	285	328666,667	337000	289000	360000	3

	1450	362333,333	378000	350000	359000	
50ng/ml-1						4
	0	271333,333	288000	268000	258000	4
	30	820333,333	848000	867000	746000	4
	160	386266,667	409000	364800	385000	4
	285	239333,333	245000	224000	249000	4
	1450	341333,333	332000	344800	347200	
		#DIV/0!				
50ng/ml-2						5
	0	365066,667	359200	390400	345600	5
	30	2285000	2310000	2258000	2287000	5
	160	1834000	1802000	1850000	1850000	5
	285	418333,333	436000	414000	405000	5
	1450	307600	320000	312800	290000	
		#DIV/0!				
50ng/ml-3						6
	0	419466,667	410400	434400	413600	6
	30	1126333,33	1193000	1100000	1086000	6
	160	495400	496000	483200	507000	6
	285	991000	986000	1007000	980000	6
	1450	377600	396000	364000	372800	
		#DIV/0!				
		#DIV/0!				
100ng/ml-1						7
	0	654400	626400	666400	670400	7
	30	598066,667	598400	603000	592800	
	160	238866,667	260000	225600	231000	7
	285	1053666,67	1055000	1026000	1080000	7
	1450	393066,667	408800	384800	385600	7
						7
100ng/ml-2						8
	0	439200	447200	437600	432800	8
	30	1215000	1205000	1238000	1202000	8
	160	720600	620000	897000	644800	8
	285	1028666,67	1026000	1030000	1030000	8
	1450	365533,333	365600	351000	380000	
100ng/ml-3						9
	0	368800	324000	398400	384000	9
	30	1019400	1046000	1013000	999200	9
	160	725000	723000	662000	790000	9
	285	1008000	1042000	970000	1012000	9
	1450	488266,667	468800	523200	472800	9
		#DIV/0!				
		#DIV/0!				
300-1						10
	0	100800	116000	174400	12000	10
	10	30133,3333	33600	28800	28000	10
	30	28533,3333	43200	23200	19200	10
	160	422666,667	439000	441000	388000	10
	285	365000	377000	370000	348000	10
	1450	443600	452800	440000	438000	
		#DIV/0!				

		#DIV/0!				
300-2		#DIV/0!				11
	0	628266,667	653600	607200	624000	11
	30	709000	723000	696000	708000	11
	160	501866,667	472800	520800	512000	11
	285	678000	657000	670000	707000	11
	1450	412000	409000	420000	407000	
		#DIV/0!				
		#DIV/0!				
300-3		#DIV/0!				
	0	692533,333	696800	690400	690400	12
	30	1449333,33	1335000	1273000	1740000	12
	160	1294666,67	1242000	1287000	1355000	12
	285	1315333,33	1339000	1289000	1318000	12
	1450	788333,333	762000	800000	803000	12
		#DIV/0!				12
500ng/ml-1		#DIV/0!				
	0	618933,333	604800	632800	619200	
	10	142400	144000	148000	135200	13
	30	1720000	1717000	1699000	1744000	13
	160	366400	372800	340800	385600	13
	285	604666,667	616000	618000	580000	13
	1450	538666,667	560000	566000	490000	13
		#DIV/0!				
		#DIV/0!				
500ng/ml-2		#DIV/0!				
	0	654400	644800	683200	635200	14
	10	43466,6667	47200	42400	40800	14
	30	31733,3333	44000	30400	20800	14
	160	665666,667	667000	660000	670000	14
	285	271933,333	275000	276800	264000	14
	1450	436333,333	433000	437000	439000	
		#DIV/0!				
500ng/ml-3		#DIV/0!				15
	0	1018600	1066000	1005000	984800	15
	10	1286333,33	1294000	1298000	1267000	15
	30	1188000	1193000	1237000	1134000	15
	160	421866,667	436000	421600	408000	15
	285	372666,667	354000	400000	364000	
	1450	387666,667	384000	392000	387000	
		#DIV/0!				
		#DIV/0!				
1000ng/ml-1		#DIV/0!				
	0	1007000	1042000	944000	1035000	16
	10	979600	967000	996800	975000	16
	30	564200	538000	585000	569600	16
	160	99333,3333	109000	100000	89000	16
	285	189000	182000	188000	197000	16
	1450	459666,667	430000	476000	473000	16
		#DIV/0!				
		#DIV/0!				
1000ng/ml-2		#DIV/0!				17
	0	464000	472800	427200	492000	17
	10	481666,667	72000	664000	709000	17
	30	479933,333	451200	481600	507000	
	160	477200	455000	491000	485600	
	285	313600	332800	301600	306400	

	1450	435000	428000	429000	448000	
		#DIV/0!				18
1000ng/ml-3		#DIV/0!				18
	0	452000	463200	471200	421600	18
	10	1059000	1058000	1073000	1046000	18
	30	382666,667	368000	372800	407200	18
	160	502000	487000	501000	518000	18
	285	168400	173600	158000	173600	
	1450	396333,333	388000	387000	414000	
		#DIV/0!				19
1500ng/ml-1		#DIV/0!				19
	0	977800	1058000	922400	953000	19
	10	305866,667	446000	50000	421600	19
	30	706866,667	724000	683000	713600	19
	160	1007666,67	1173000	920000	930000	19
	285	1264333,33	1245000	1278000	1270000	
	1450	589333,333	612000	596000	560000	
		#DIV/0!				20
		#DIV/0!				20
1500ng/ml-2		#DIV/0!				20
	0	915466,667	880000	926400	940000	20
	10	128466,667	127000	121600	136800	20
	30	261333,333	280000	264000	240000	20
	160	445666,667	475000	436000	426000	20
	285	459333,333	465000	431000	482000	
	1450	820000	808000	828000	824000	
		#DIV/0!				21
1500ng/ml-3		#DIV/0!				21
	0	841866,667	892800	838400	794400	21
	10	471666,667	479000	468000	468000	21
	30	1280000	1270000	1290000	1280000	21
	160	380666,667	404000	342000	396000	
	285	356666,667	381000	370000	319000	
	1450	464666,667	483000	463000	448000	
		#DIV/0!				22
2000ng/ml-1		#DIV/0!				22
	0	817866,667	800000	846400	807200	22
	10	122866,667	133600	116000	119000	22
	30	489600	453000	516800	499000	22
	160	334666,667	352000	320000	332000	22
	285	1313333,33	1360000	1280000	1300000	22
	1450	445600	436800	450000	450000	22
		#DIV/0!				23
2000ng/ml-2		#DIV/0!				23
	0	1312666,67	1298000	1282000	1358000	23
	10	792266,667	796000	796000	784800	23
	30	812533,333	836800	824800	776000	23
	160	360000	384000	348000	348000	23
	285	2247666,67	2359000	2250000	2134000	23
	1450	341733,333	354400	332800	338000	23
		#DIV/0!				24
2000ng/ml-3		#DIV/0!				24
	0	295400	320800	298400	267000	
	30	1747333,33	1726000	1706000	1810000	24
	160	1081666,67	1057000	1094000	1094000	24
	285	1164666,67	1212000	1141000	1141000	24

1450	360133,333	357600	346000	376800	24
					24
					24
					24

